



THE UNIVERSITY *of* EDINBURGH

This thesis has been submitted in fulfilment of the requirements for a postgraduate degree (e.g. PhD, MPhil, DClinPsychol) at the University of Edinburgh. Please note the following terms and conditions of use:

This work is protected by copyright and other intellectual property rights, which are retained by the thesis author, unless otherwise stated.

A copy can be downloaded for personal non-commercial research or study, without prior permission or charge.

This thesis cannot be reproduced or quoted extensively from without first obtaining permission in writing from the author.

The content must not be changed in any way or sold commercially in any format or medium without the formal permission of the author.

When referring to this work, full bibliographic details including the author, title, awarding institution and date of the thesis must be given.

**Formation and subsequent metabolism
of ascorbate oxidation products *in vitro*
and in plant cells**

Rebecca A. Dewhirst



Doctor of Philosophy - Cell and Molecular Biology

University of Edinburgh

2015

Declaration

This thesis has been composed by myself and the work, of which it is a record, has been carried out by myself. All sources of information have been specifically acknowledged by means of a reference.

Rebecca Alice Dewhirst

Acknowledgements

The research in this thesis was funded by a BBSRC (Biotechnology and Biological Sciences Research Council) industrial CASE (Collaborative Award in Science and Engineering) studentship in collaboration with Vitacress Salads Ltd.

Firstly, I would like to thank my supervisor, Stephen Fry, I really appreciate the time and guidance he has given to me over the years. I must also thank all the members, past and present, of the Fry lab for all the help and support over the last four years; it's been great being a member of the lab.

Thank you to both Graham Clarkson and Steve Rothwell from Vitacress for valuable input throughout my PhD project. I'm especially grateful for all the people at Vitacress who helped me so much during my summer visit to Hampshire.

I'd also like to thank my lovely flatmates, Suzy Howat and Pumi Perera, as well as all the other friends that have made my time in Edinburgh immensely enjoyable.

I'm very grateful to my family, especially Mum and Dad for providing respite in Sri Lanka numerous times over the past few years; the sun, beach and cocktails were very welcome.

Finally I'd like to thank all members of IMPS for countless enjoyable lunchtimes and cake clubs; I've thoroughly enjoyed being a part of the department.

List of abbreviations

AA: L-ascorbate	GlcN: glucosamine
ABTS: 2,2'azino-bis(3-ethylbenzthiazoline-6-sulfonic acid)	GlcUA: D-glucuronic acid
AG: arabinogalactan	GPD-Gal: guanosine diphosphate galactose
AIR: alcohol-insoluble residue	GPD-Gul: guanosine diphosphate gulose
AO: ascorbate oxidase	GPD-Man: guanosine diphosphate mannose
APX: ascorbate peroxidase	GR: glutathione reductase
Ara: L-arabinose	GSH: glutathione
BuOH: butan-1-ol	GSL: glucosinolate
CB: cellobiose	GSSG: glutathione disulphide
cOxT: cyclic oxalyl-L-threonate	Gul: L-gulose
CPM: counts per minutes	Gul-1-P: L-gulose-1-phosphate
DCPIP: dichlorophenolindophenol	GulA: L-gulonic acid
DHA: L-dehydroascorbic acid	HG: homogalacturonan
DHAR: dehydroascorbic acid reductase	HOAc: acetic acid
DKG: diketo-L-gulonate	HPLC: high-pressure liquid chromatography
DMF: dimethylformate	HVPE: high-voltage paper electrophoresis
EDTA: ethylenediaminetetraacetic acid	Lb acid: lactobionic acid
EPG: endo-polygalacturonase	L-Tar: L-tartrate
EtOH: ethanol	Mal: maltose
Fru: D-fructose	Man: D-mannose
Fru-6-P: D-fructose-6-phosphate	Man-1-P: D-mannose-1-phosphate
Gal: L-galactose	Man-6-P: D-mannose-6-phosphate
Gal-1-P: L-galactose-1-phosphate	MDHAR: monodehydroascorbate reductase
GalA: L-galactonic acid	MeOH: methanol
GalUA: L-galacturonic acid	m_{og} : mobility relative to orange G
Glc: D-glucose	MPA: meta-phosphoric acid
Glc-1-P: D-glucose-1-phosphate	
Glc-6-P: D-glucose-6-phosphate	

MS: mass spectrometry	Raf: raffinose
<i>m</i> -Tar: <i>meso</i> -tartrate	RG-I: rhamnogalacturonan I
NADP ⁺ : nicotinamide adenine dinucleotide phosphate	RG-II: rhamnogalacturonan II
NADPH: reduced nicotinamide dinucleotide phosphate	ROS: reactive oxygen species
NMR: nuclear magnetic resonance	SOD: superoxide dismutase
OxA: oxalate	Spd: spermidine
OxG: oxalyl glucose	Spn: spermine
OxT: oxalyl-L-threonate	Suc: sucrose
P.His: poly-histidine	TFA: trifluoroacetic acid
P.Lys: poly-lysine	ThrO: L-threonate
PIPES: piperazine-N, N'-bis(2-ethanesulfonic acid)	TLC: thin-layer chromatography
PrOH: propanol	WCx: watercress compound
Put: putrescine	XG: xyloglucan
PxI: peroxidase inhibitor	XGOs: xyloglucan oligosaccharides
	Xyl: D-xylose

Abstract

Vitamin C (ascorbate and dehydroascorbic acid) is vital for plants and found throughout the plant cell including in the apoplast. The structure of ascorbate was determined eighty years ago; however, many of its degradation pathways remain unclear. Numerous degradation products of ascorbate have been reported to occur in the apoplast but many still remained unidentified^{1,2}.

Ascorbate is well known as an antioxidant, and acts to quench reactive oxygen species (ROS), such as hydrogen peroxide and ozone in the plant apoplast. The immediate oxidation product of ascorbate is dehydroascorbic acid (DHA), which may be quickly hydrolysed to diketogulonic acid (DKG). The further reactions of radiolabelled and non-radiolabelled DHA and DKG with various ROS have been investigated. Differences were observed in the products formed from the various ROS, allowing a unique fingerprint of oxidation products to be described for each ROS. Equally, different compounds were produced depending on the starting substrate; for example cyclic oxalyl threonate was only observed in the reactions of DHA and not DKG.

A major oxidation product of DHA is OxT. A novel enzyme activity involving the transfer of the oxalyl group from OxT to an acceptor substrate such as a sugar has been detected. This enzyme activity could have potential cell wall modification roles, in the formation of oxalate cross-linkages between cell wall components. This would provide a novel role for ascorbate derivatives in cell growth.

Vitamin C is also a vital component of the human diet, and most dietary ascorbate comes from plants such as salads. The degradation of ascorbate during post-harvest processing and storage of salad leaves has been investigated. Spinach leaves were found to be particularly prone to losing ascorbate during the industrial washing process. The use of radiolabelled ascorbate has allowed the determination that the major degradation product formed from ascorbate during spinach washing was oxalate.

M.A. Green and S.C. Fry (2005) *Nature*, **433**, 83-87

² H.T. Parsons *et al.* (2011) *Biochem. J.*, **440**, 375-383

Lay summary

Vitamin C (made up of ascorbate and dehydroascorbic acid) is a vital component of the human diet. The majority of dietary vitamin C comes from plants. Vitamin C is a fairly unstable compound, and understanding more about the degradation pathways of vitamin C may help to prevent the degradation of vitamin C in crop plants, such as salads.

A major role of vitamin C, in both plants and people, is as an antioxidant, acting to quench reactive oxygen species that may otherwise cause damage within cells. The reaction of vitamin C derivatives with reactive oxygen species was studied, and it was found that different reactive oxygen species lead to the formation of different degradation products of vitamin C.

One of the products of the oxidation of vitamin C is oxalyl threonate. This compound was hypothesised to have a role in plant growth. Plant cells are surrounded by a cell wall which provides structural support and shape to the cell. Plant growth involves the loosening and restructuring of the cell wall. A novel enzyme which transfers the oxalyl group from oxalyl threonate to an acceptor substrate, such as a cell wall component, was discovered. This newly described enzyme activity could provide a role for vitamin C derivatives in plant growth. Further novel products (oxalyl sugars) of this enzyme were discovered, and found to be stable in plant cell cultures, suggesting they may have a biological role within plants, perhaps as compounds which protect the plant by deterring herbivores.

Salads are an important source of dietary vitamin C. The vitamin C content of several species of salad leaves were monitored during the commercial washing and packaging process and during post-harvest storage. The vitamin C content varied widely between different salad species but all the species tested lost vitamin C during the 10-day storage time, with rocket leaves retaining the most vitamin C. Spinach leaves were found to lose a significant proportion of vitamin C during the commercial washing and packaging process, the major product formed from vitamin C during this washing process was oxalic acid.

This project has added valuable knowledge about the many complex degradation pathways of vitamin C, including characterising novel compounds and novel enzyme activities involving vitamin C derivatives. Important information about the vitamin C turnover in salads throughout the washing process has also been obtained, and consequently improvements can now be made to the commercial washing process.

Table of contents

Declaration.....	i
Acknowledgements	ii
List of abbreviations	iii
Abstract	v
Lay summary	vi
Table of contents	vii
List of figures.....	xii
Introduction	1
1.1 Overview of ascorbate	1
1.2 History of ascorbate	2
1.3 Chemistry of ascorbate	3
1.4 Biosynthesis of ascorbate	6
1.5 Degradation of ascorbate	10
1.5.1 Oxidation of DHA.....	10
1.5.2 Degradation of DKG.....	13
1.6 Reactive oxygen species	15
1.6.1 Hydrogen peroxide.....	15
1.6.2 Superoxide anion	16
1.6.3 Hydroxyl radical	17
1.6.4 Singlet oxygen	18
1.7 Ascorbate as an antioxidant	19
1.7.1 Apoplastic ascorbate	19
1.7.2 Ascorbate–glutathione pathway.....	21
1.8 Ascorbate in plant growth	22
1.9 Ascorbate as a biosynthetic precursor	24

1.10	The primary plant cell wall	24
1.10.1	Structure of the plant cell wall	25
1.10.2	Cross-linking within the cell wall	26
1.11	Acyltransferases	27
1.12	Ascorbate in salad plants	28
1.13	Outline of project	31
	Materials and methods	33
2.1	Materials and chemicals	33
2.2	Plant cell suspension culture	33
2.2.1	<i>Arabidopsis</i> cell culture media.....	33
2.2.2	Spinach cell culture media.....	33
2.2.3	Rose cell culture media	33
2.2.4	Maintenance of cell suspension cultures	33
2.3	Salad leaves growth conditions	34
2.3.1	Salad leaves grown at Vitacress, Hampshire	34
2.3.2	Salad leaves grown in University of Edinburgh facilities	34
2.4	High-voltage paper electrophoresis	34
2.4.1	One dimensional HVPE at pH 2.0 and pH 6.5.....	34
2.4.2	Two dimensional HVPE.....	36
2.5	High-pressure liquid chromatography	36
2.6	Thin-layer chromatography	36
2.7	Anion-exchange column chromatography	37
2.7.1	Purification of [¹⁴ C]DHA by anion-exchange column chromatography	37
2.7.2	Purification of DKG-derivatives C and E by anion-exchange column chromatography.....	37
2.8	Detection of non-radiolabelled compounds	38
2.8.1	Staining of sugars on paper with silver nitrate.....	38
2.8.2	Staining of phosphates on paper with molybdate	38

2.8.3	Staining of reducing sugars on paper with Wilson's dip (aniline hydrogen-phthalate).....	38
2.8.4	Staining of acidic compounds on paper with bromophenol blue	38
2.8.5	Staining of amines on paper in ninhydrin.....	39
2.8.6	Staining of sugars on TLC with thymol	39
2.8.7	Staining of compounds on TLC with molybdate	39
2.8.8	Staining of compounds on TLC with ninhydrin	39
2.9	Detection of radiolabelled compounds	40
2.9.1	Detection of radiolabelled compounds by autoradiography	40
2.9.2	Quantification of radiolabelled compounds by scintillation counting.....	40
2.10	Elution of ascorbate derivatives from paper.....	40
2.11	Preparation of diketogulonate.....	41
2.11.1	Preparation of diketogulonate from dehydroascorbic acid: method 1	41
2.11.2	Preparation of diketogulonate from dehydroascorbic acid: method 2.....	41
2.11.3	Preparation of diketogulonate from ascorbic acid: method 3	41
2.12	Mass spectrometry of ascorbate derivatives	41
2.13	Nuclear magnetic resonance spectroscopy of ascorbate derivatives	42
2.14	<i>In vitro</i> oxidation of ascorbate derivatives by reactive oxygen species.....	42
2.14.1	Conditions used for the ROS reactions	42
2.14.2	Generation of ROS.....	42
2.15	Alkali treatment of ascorbate derivatives C and E.....	43
2.16	The fate of radiolabelled ascorbate derivatives to plant cell suspension cultures.....	43
2.16.1	The fate of [¹⁴ C]AA derivatives in live plant cell suspension cultures	43
2.16.2	The fate of [¹⁴ C]AA derivatives in frozen/thawed or boiled cell cultures	44
2.16.3	Alkali hydrolysis of radiolabelled AIR	44
2.16.4	Enzyme treatment of radiolabelled AIR.....	45
2.17	Acyltransferase purification and assay	45

2.17.1	Eluting cell wall enzymes from plant cell-suspension cultures	45
2.17.2	Acyltransferase assay with cell cultures	46
2.17.3	Acyltransferase assay with enzyme extracts.....	46
2.17.4	Acyl transferase assay with polysaccharide-impregnated paper.....	47
2.18	Determination of ascorbate content of salad leaves using the DCPIP assay	47
2.19	Determination of ascorbate content of salad leaves during the washing process	48
2.19.1	Monitoring the ascorbate content of salad leaves during washing and storage on site at the Vitacress premises	48
2.19.2	Simulating the washing process in the laboratory.....	49
2.19.3	The effect of chlorine on the retention of ascorbate during washing	49
2.19.4	Monitoring degradation product formation during the washing process with [¹⁴ C]AA.....	49
	Results	51
3.1	Purification and identification of ascorbate degradation products C and E	51
3.1.1	Introduction to compounds C and E.....	51
3.1.2	Purification of C and E.....	51
3.1.3	C and E interconvert.....	53
3.1.4	Further characterisation of compounds C and E using HVPE.....	55
3.1.5	Identification of novel DKG hydrolysis products	57
3.1.6	The structures of C and E are supported by MS and NMR data	62
3.2	Purification of an ascorbate-derived peroxidase-inhibitor.....	70
3.2.1	Introduction to an ascorbate-derived peroxidase-inhibitor	70
3.2.2	Purification of peroxidase inhibitor using HPLC.....	70
3.2.3	The characterisation of the peroxidase inhibitor using HVPE was inconclusive... ..	74
3.2.4	The peroxidase inhibitor is not compound C or E	75
3.2.5	Analysis of purified peroxidase inhibitor by NMR.....	77
3.3	The <i>in-vitro</i> reaction of DHA and DKG with reactive oxygen species	80
3.3.1	Introduction to the reaction of DHA and DKG with reactive oxygen species	80

3.3.2	The <i>in-vitro</i> reaction of DHA with different reactive oxygen species	80
3.3.3	The <i>in-vitro</i> reaction of DKG with different reactive oxygen species	90
3.3.4	Purification of [¹⁴ C]DHA	97
3.3.5	The reaction of radiolabelled DHA with reactive oxygen species	99
3.3.6	Summary of the oxidation of DHA and DKG by various ROS	103
3.4	The fate of radiolabelled ascorbate degradation products in plant cell suspension cultures	107
3.4.1	Introduction to ascorbate and plant cell suspension cultures	107
3.4.2	Fate of [¹⁴ C]DHA in spinach, rose and <i>Arabidopsis</i> cell cultures.....	109
3.4.3	Fate of [¹⁴ C]OxT in spinach and <i>Arabidopsis</i> cell cultures	110
3.4.4	Radiolabeled oxalate is released from radiolabelled AIR produced from spinach cells incubated with [¹⁴ C]OxT	113
3.4.5	The incorporation of radioactivity into the cell wall material of spinach cells requires an enzyme	115
3.4.6	Treatment of the radiolabeled spinach AIR with cell wall degrading enzymes.....	119
3.5	A novel enzyme catalysing a reaction between ascorbate derivatives and cell wall components.....	123
3.5.1	Introduction to the reaction of ascorbate derivatives with cell wall components... ..	123
3.5.2	Plant cell cultures incubated with radiolabeled OxT and non-radiolabeled sugars produce novel oxalyl sugars	123
3.5.3	The putative acyltransferase can be eluted from the cell walls of plant cell cultures.....	129
3.5.4	The reaction of [¹⁴ C]OxT with various acceptor substrates catalysed by an acyltransferase.....	133
3.5.5	The activity of acyltransferase with different donor substrates	144
3.5.6	Investigating the fate of oxalyl glucose <i>in vivo</i>	149
3.6	Ascorbate degradation in harvested salad leaves	154
3.6.1	Introduction to ascorbate in salad leaves	154

3.6.2	Ascorbate content of a selection of salad leaves during cold storage	154
3.6.3	Effect of washing on ascorbate content of salad leaves	155
3.6.4	Ascorbate retention in different ages of salad leaves	166
3.6.5	Degradation of ascorbate in watercress	167
3.6.6	Characterisation of WCx, a compound from watercress that indicates freshness.....	173
	Discussion	184
4.1	Overview	184
4.2	The oxidation of DHA and DKG	186
4.3	Characterisation of non-oxidative derivatives of DKG	189
4.4	The fate of ascorbate oxidation products <i>in vitro</i> and <i>in vivo</i>	191
4.5	The degradation of ascorbate in salad leaves	194
4.6	Compound from watercress that serves as an indicator of freshness	196
4.7	Summary	199
	References	200

List of figures

Figure 1: Chemical structures of ascorbic acid, ascorbate and DHA.....	1
Figure 2: Chemical species associated with reducing properties of vitamin C.	4
Figure 3: The biosynthetic pathways of ascorbic acid in plants.	7
Figure 4: Oxidation pathway of DHA as proposed by Parsons and Fry..	11
Figure 5: Formation of tartaric acid from DHA in Vitaceae.	12
Figure 6: Degradation of DKG..	14
Figure 7: Ascorbate–glutathione cycle..	21
Figure 8: Diagram of HVPE apparatus.....	35
Figure 9: Sampling leaf discs from [¹⁴ C]AA-fed spinach.....	50
Figure 10: DKG, C and E are formed from NaOH treatment of DHA.....	52

Figure 11: Purification of C and E by HVPE.....	53
Figure 12: C and E interconvert.....	54
Figure 13: HVPE at pH 2.0 reveals that preparations of compound E contain numerous compounds..	55
Figure 14: Purification of five C and E-related compounds.....	56
Figure 15: 2D HVPE of C and E-related compounds.	58
Figure 16: Alkali and acid treatment of individual C and E-related compounds.....	59
Figure 17: C* co-migrates with xylonic acid by HVPE at pH 6.5..	60
Figure 18: Purification and interconversion of [¹⁴ C]E and C.....	61
Figure 19: H ⁺ NMR analysis of compound C.....	63
Figure 20: ¹³ C NMR spectroscopy analysis of compound C.	64
Figure 21: Mass spectrometry analysis of compound C purified by anion-exchange column chromatography.....	65
Figure 22: MS analysis of compounds E, C, C' and C*.....	67
Figure 23: The hydrolysis pathway of DHA.....	69
Figure 24: HPLC profile of DKG aged for 24 hours on ice.....	71
Figure 25: HPLC profile of pooled and neutralised fractions containing Pxl.	72
Figure 26: Pxl eluted from HPLC column in TFA.	73
Figure 27: Analysis of peroxidase inhibitor by HVPE.	74
Figure 28: Pxl is not compound C or compound E.....	76
Figure 29: Purification of Pxl from 200 mM DKG for NMR.....	77
Figure 30: ¹ H NMR analysis of Pxl.....	78
Figure 31: Reaction of DHA with H ₂ O ₂ :	81
Figure 32: Reaction of DHA with superoxide radical.	82
Figure 33: Reaction of DHA with the hydroxyl radical analysed by HVPE at pH 6.5.	84
Figure 34: Reaction of DHA with the hydroxyl radical analysed by HVPE at pH 2.0.	85
Figure 35: Reaction of DHA with singlet oxygen.....	88
Figure 36: Compounds formed during the degradation of riboflavin by singlet oxygen.....	89
Figure 37: Reaction of DKG with H ₂ O ₂	90
Figure 38: Reaction of DKG with superoxide.	92
Figure 39: Reaction of DKG with H ₂ O ₂ and O ₂ ⁻	93
Figure 40: Reaction of DKG with hydroxyl radical.....	95
Figure 41: Reaction of DKG with singlet oxygen.....	96
Figure 42: Purification of [¹⁴ C]DHA by anion-exchange column chromatography.....	98
Figure 43: Reaction of [¹⁴ C]DHA with H ₂ O ₂ and O ₂ ⁻	99

Figure 44: Structures of OxT isomers..	100
Figure 45: Quantification of products formed from the reaction of [¹⁴ C]DHA with H ₂ O ₂ and O ₂ ⁻ ..	101
Figure 46: The reaction of [¹⁴ C]DHA with various concentrations of hydroxyl radical.	102
Figure 47: Oxidation pathways of ascorbate.	104
Figure 48: Summary of products formed from DKG and DHA by different ROS.	106
Figure 49: Schematic of potential oxalate cross-link formation in the cell wall.	108
Figure 50: [¹⁴ C]DHA enters the cells of <i>Arabidopsis</i> , rose and spinach cell cultures.	109
Figure 51: Fate of [¹⁴ C]OxT in <i>Arabidopsis</i> and spinach cell culture.	111
Figure 52: Radioactivity accumulates in AIR of spinach cell cultures incubated with [¹⁴ C]OxT	112
Figure 53: NaOH hydrolysis of radiolabelled spinach AIR releases free oxalate.	114
Figure 54: Incorporation of radioactivity from [¹⁴ C]OxT into the AIR of spinach cells over time.	114
Figure 55: Boiled, frozen/thawed and untreated spinach cells incubated with [¹⁴ C]OxT.	115
Figure 56: The fate of [¹⁴ C]OxT in untreated and frozen/thawed spinach cell cultures.	117
Figure 57: AIR produced from spinach cells incubated with [¹⁴ C]OxT after washing in EtOH and EDTA.	118
Figure 58: Oxalyl esterase activity of commercial cell wall-cleaving enzymes.	120
Figure 59: The treatment of radiolabelled spinach AIR with cell wall-degrading enzymes.	121
Figure 60: Formation of oxalyl sugars in spinach cell cultures with [¹⁴ C]OxT and sugars.	124
Figure 61: Oxalyl sugars are not formed in the absence of cells.	125
Figure 62: Oxalyl sugars were formed in the presence of <i>Arabidopsis</i> and spinach cells of increasing ages.	126
Figure 63: Oxalyl glucose production is greater in higher pH value buffers.	127
Figure 64: OxG formation over time at different pH values.	128
Figure 65: Acyltransferase activity was present in <i>Arabidopsis</i> and spinach cell wall extracts.	130
Figure 66: Acyltransferase time course <i>Arabidopsis</i> and spinach.	132
Figure 67: Oxalyl glucose production increases with glucose concentration.	133
Figure 68: The reaction of acyltransferase activity with [¹⁴ C]OxT and oligosaccharides.	135
Figure 69: The reaction of [¹⁴ C]OxT and polyamines catalysed by acyltransferase.	136
Figure 70: [¹⁴ C]OxT reaction with acyltransferase and polysaccharides.	138
Figure 71: The formation of oxalyl esters with polysaccharide–cellulose complexes and [¹⁴ C]OxT catalysed by an acyltransferase.	139
Figure 72: [¹⁴ C]OxA becomes trapped in the cellulose-polysaccharide complex.	141
Figure 73: Radioactivity bound to paper incubated with acyltransferase and [¹⁴ C]OxT or [¹⁴ C]OxA after prolonged washing.	143
Figure 74: OxG is formed from cOxT and OxT but not OxA.	145

Figure 75: Formation of reactive intermediates during the oxidation of AA.....	146
Figure 76: The reaction of [¹⁴ C]AA with acyltransferase extract and glucose and H ₂ O ₂	148
Figure 77: Purification of OxG.	149
Figure 78: [¹⁴ C]OxG is stable in spinach cell culture.....	150
Figure 79: Washing of cells fed [¹⁴ C]OxG, [¹⁴ C]OxT or [¹⁴ C]OxA.	152
Figure 80: The ascorbic acid content of salad leaves during storage at 4°C.	155
Figure 81: The ascorbic acid content of salad leaves before and after the washing process.....	156
Figure 82: Ascorbic acid content of washed and unwashed salad leaves during storage.	157
Figure 83: Effect of vacuum cooling on ascorbic acid content of spinach leaves.	158
Figure 84: Ascorbic acid content of spinach leaves throughout washing.	159
Figure 85: HVPE analysis of washed spinach was inconclusive.....	161
Figure 86: Ascorbic acid content during washing of spinach leaf discs.....	162
Figure 87: The degradation of [¹⁴ C]AA fed to spinach leaves throughout washing.	164
Figure 88: The effect of chlorine on the ascorbic acid content of spinach leaves.	165
Figure 89: Ascorbic acid content in spinach at different growth stages.....	166
Figure 90: Ascorbic acid content of watercress at different growth stages.	168
Figure 91: HVPE analysis of extracts from various growth stages of watercress.	169
Figure 92: The compound co-migrating with Glc-6-P does not diminish upon phosphatase treatment..	170
Figure 93: Analysis of a watercress extract by HVPE at pH 6.5.	171
Figure 94: 2D HVPE of a watercress extract.....	172
Figure 95: WCx is present in UK-grown watercress extracts but not Portuguese-grown watercress extracts.....	174
Figure 96: HVPE of purified WCx.....	175
Figure 97: Wilson's dip staining of WCx.....	176
Figure 98: WCx separates into two compounds after HVPE at pH 6.5.	177
Figure 99: Saponification of WCx.....	178
Figure 100: TLC analysis of WCx stained in thymol, molybdate and ninhydrin.	179
Figure 101: MS analysis of purified WCx.....	180
Figure 102: Structures of glucosinolates.	181
Figure 103: Proposed degradation pathways of ascorbate <i>in vitro</i>	188
Figure 104: Example of oxalyl sugar formation via acyltransferase activity.	191
Figure 105: Structure of glucosinolates.	196

Introduction

1.1 Overview of ascorbate

Vitamin C consists of L-ascorbic acid, commonly found in the ionised form L-ascorbate (referred to as ascorbate, or AA, throughout) as well as dehydro-L-ascorbic acid (DHA) (Figure 1). Vitamin C is chemically the simplest of the vitamins, essential nutrients in the human diet. Humans lack the ability to synthesise the compound owing to the absence of the final enzyme in the mammalian biosynthetic pathway (10). Plants, however, can synthesise vitamin C and it can accumulate to millimolar concentrations in plant cells and account for up to 10% of the total water-soluble carbohydrates (11).

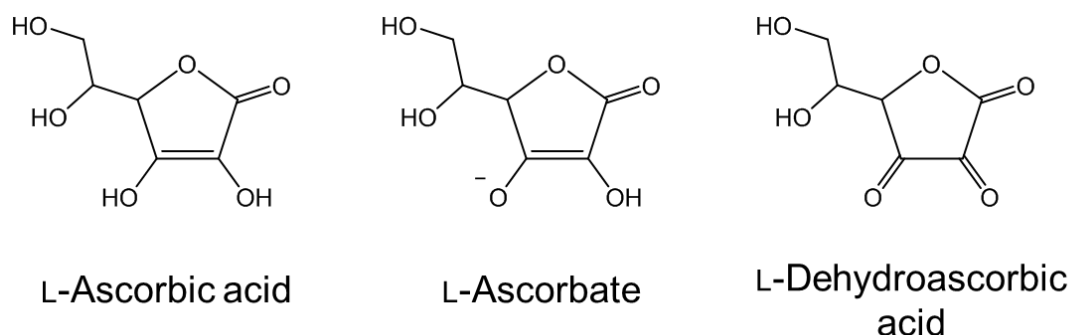


Figure 1: Chemical structures of ascorbic acid, ascorbate and DHA. Ascorbate is the ionised form of ascorbic acid, and the most common form in physiological conditions. DHA (dehydroascorbic acid) is the first oxidation product of ascorbate. DHA is not a true acid as it cannot be ionised at physiological pH values.

Although vitamin C can be synthesised commercially, and indeed is the most widely produced vitamin in industry (12,13), our primary dietary source of this compound remains plants. As plants are such important sources of ascorbate, in-depth knowledge of the metabolism of ascorbate *in planta* is vital. Though the major biosynthetic pathway has been elucidated (14), many questions surrounding ascorbate degradation remain, and this report will aim to answer some of them.

The benefits of vitamin C are widely publicised, and as a result it is not uncommon for foods to be supplemented with ascorbate. Vitamin C has a vital role in collagen synthesis, and a deficiency of vitamin C leads to scurvy, the symptoms of which relate to the loss of collagen

(15,16). As well as preventing scurvy, the vitamin has many other reported health benefits, such as in the treatment or prevention of diabetes, cardiovascular disorders, age-related diseases and even cancer (17). Ascorbate is well known as an antioxidant, but also has numerous other roles *in planta* including as an enzyme co-factor, and in the regulation of the cell cycle (18).

1.2 History of ascorbate

Scurvy has afflicted many sailors throughout history, and was described by the ancient Greeks, Egyptians and Romans (19). The importance of citrus fruits in the prevention of scurvy was reported by Edinburgh surgeon James Lind (20) in the mid-1700s in what is regarded as the first study which controlled for population, although the practice of eating fresh fruit and vegetables to stave off scurvy was already used among some populations (21). However, it was not until almost two centuries later that the compound responsible for this anti-scorbutic (scurvy-preventing) activity was isolated, the chemical structure determined and the name of ascorbic acid given (22,23).

The compound was classified as a vitamin prior to the elucidation of its chemical structure. The concept of vitamins as essential micronutrients was established in 1912 by Casimir Funk (24). He proposed that diseases caused by the deficiencies of certain foods were in fact due to the deficiency of specific compounds within those foods. The word vitamin is a portmanteau word deriving from 'vital' and 'amine', as the first vitamin discovered (vitamin B₃, niacin) contained an amine group (24). It was assumed that other compounds, a lack of which would manifest as a disease, would also necessarily contain amine groups. This is now understood not to be the case, as several of the 13 recognised vitamins, including vitamin C, do not contain an amine group.

A reducing factor was isolated by Albert Szent-Györgyi from numerous sources (22,25) including the adrenal cortex of oxen, as well as plant samples such as turnip roots, tomato and citrus fruits. It was then several years until the structure of this reducing factor, determined as having the formula C₆H₈O₆ (22), was identified as vitamin C. The identity of this compound as vitamin C was confirmed by its scurvy-preventing properties when fed to guinea pigs having an otherwise vitamin C-free diet (26). The use of guinea pigs in this study was fortuitous, as they are one of only a very small number of animals which do not synthesise vitamin C themselves. Other animals that have lost the ability to synthesise vitamin C include some species of primates (including humans), teleost fish, some passerine birds and most species of bats (27).

Further confirmation that the so-called hexuronic acid was in fact vitamin C was provided by the successful synthesis of the compound (28). With this confirmation vitamin C was then named ascorbic acid, in recognition of its anti-scorbutic properties.

Since the discovery of the structure of vitamin C, a huge amount of research into ascorbate has been carried out, but there is still much more to learn about this small but very important molecule.

1.3 Chemistry of ascorbate

Ascorbic acid (AA) is the trivial name for the compound *L-threo*-hex-2-enono-1,4-lactone, and is a very effective reducing agent. AA is a sugar acid lactone containing an ene-diol group (8) and has a molecular weight of 176.1. AA is weakly acidic owing to the presence of two hydroxyl groups at C2 and C3 (Figure 2).

The hydroxyl group at C3 is very readily ionisable at a physiological pH, having a pK_a value of 4.25 (8) (Figure 2). This leads to the mono-anion of ascorbate (commonly defined as *L*-ascorbate) being the predominant form of AA in most biological systems. The second hydroxyl group at C2 has a much higher pK_a of 11.8, meaning it is only weakly acidic.

The reducing properties of AA, and thus its vitamin activity, are due to this ene-diol group. As an antioxidant a major role of ascorbate is to detoxify reactive oxygen species (ROS). This can occur via the donation of one or two electrons from ascorbate to the ROS, thereby preventing further oxidative reactions (6). These reactions occur via numerous reactive intermediates (Figure 2).

The donation of the first electron, from the mono-anion of ascorbate (AA^-), results in the formation of the ascorbyl radical (AA^\bullet , also known as the ascorbate free radical or monodehydroascorbate), which is unusually long-lived for a free radical species. This ascorbyl radical is very acidic and under apoplasmic physiological conditions (pH values between 2 and 5) is likely to convert to the semi-dehydroascorbate anion radical (8). A second electron can then be donated to form dehydroascorbic acid (DHA; Figure 2). DHA is commonly found in the bicyclic form and can also occur in the dihydrated form (HDHA), which has a pK_a of approximately 8-9 (6,29). 'Dehydroascorbic acid' is perhaps a misnomer, as DHA does not contain any readily ionisable hydroxyl groups, and so cannot truly be classified as an acid.

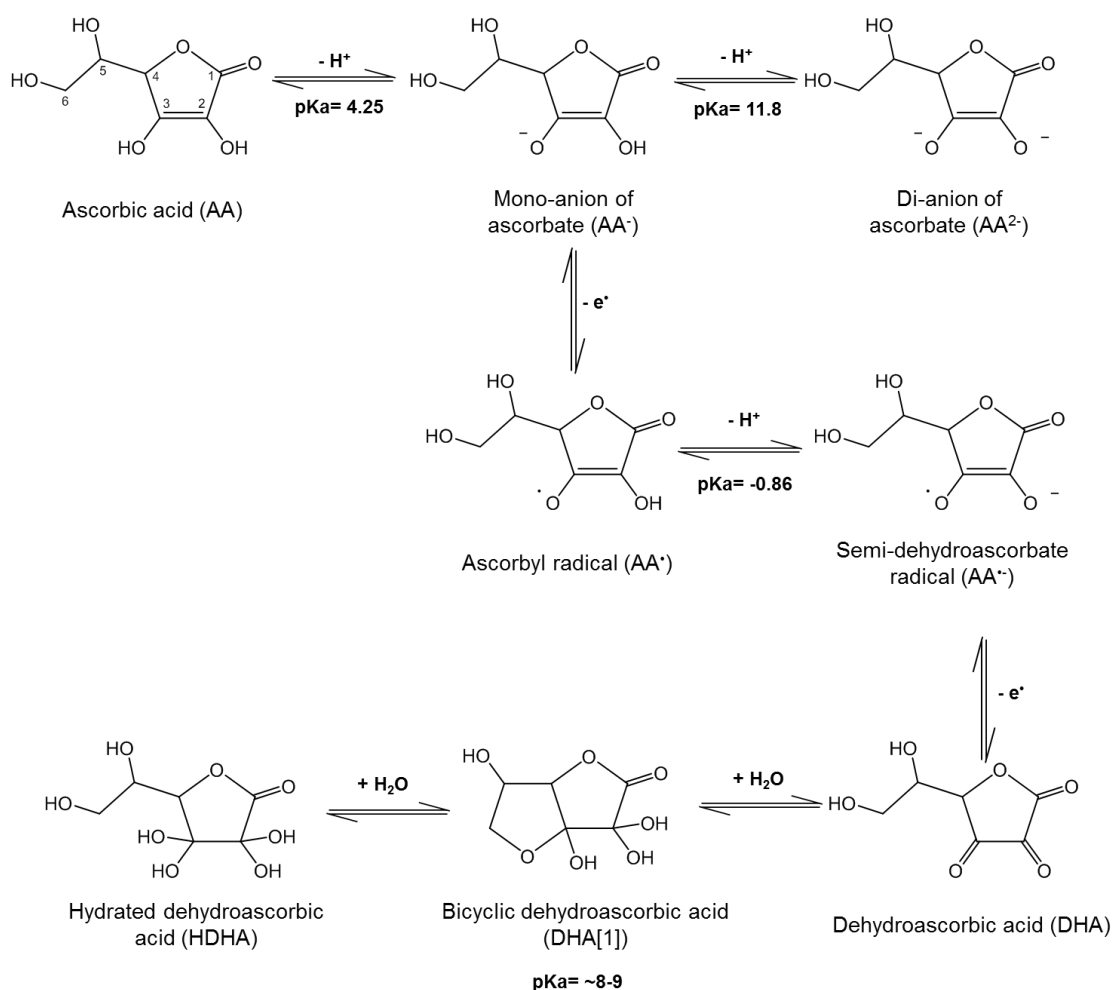


Figure 2: Chemical species associated with reducing properties of vitamin C. The structures of AA compounds associated with its reducing properties are shown, along with the pK_a values if known. The carbon atoms are numbered on AA, and should be assumed to be the same on the other chemical species. Adapted from Du et al 2012 (6) and Bradshaw et al 2011 (8)

The autoxidation of AA describes the reaction of AA with molecular oxygen (O₂), forming DHA and H₂O₂. This reaction, while thermodynamically viable, is kinetically forbidden owing to the different electron spin states of AA[·] (containing one unpaired electron so in singlet state) and O₂ (containing two unpaired electrons so in triplet state) (8). Autoxidation of ascorbate is relatively slow, as governed by the fact that this must occur (to avoid the conflicting electron spin states) via the di-anion of ascorbate (AA²⁻), which is not readily formed at physiological pH values as suggested by its high pK_a of 11.8 (6). However, the oxidation of AA catalysed by transition metal ions (often present under physiological conditions) is very rapid (30), and can occur via AA[·], avoiding the conflicting spin restrictions.

Metal ions of Fe^{3+} and Cu^{2+} are known to be particularly efficient catalysts of the oxidation of AA (30). There are two proposed mechanisms by which these ions act to catalyse the oxidation of AA. One theory is that the initial electron transfer results in the metal ion being reduced and the AA being oxidised, as the metal ion interacts directly with AA. The metal ion is then re-oxidised to its original state by O_2 . Alternatively, electron transfer between AA and O_2 could occur in one step with the metal ion acting as a bridge (8).

The relative stability of AA^\bullet as a free radical allows the possibility of this compound being reduced back to AA^- with the addition of an electron. This can be catalysed by monodehydroascorbate reductase (MDHAR) (31), which is an integral part of the ascorbate–glutathione cycle (discussed further in section 1.7.2), allowing the quenching of H_2O_2 without the loss of ascorbate. Non-enzymic disproportionation of AA^\bullet leads to the formation of DHA, which can also be reduced back to AA in the ascorbate–glutathione cycle, by the action of DHA reductase (DHAR) (11).

The most common reactions that AA undergoes are oxidation reactions, whereas DHA can undergo oxidation, reduction and hydrolysis. The oxidation of DHA produces oxalyl-L-threonate (OxT), cyclic oxalyl-L-threonate (cOxT), oxalic acid (OxA) and L-threonate (ThrO) (2,32). These oxidation reactions will be discussed further in section 1.5.1. The hydrolysis of DHA involves breaking the lactone bond, thus opening the ring, resulting in the formation of 2,3-diketo-L-gulonic acid (DKG). This reaction occurs relatively slowly at low pH values (below pH 4), but happens much more quickly at higher pH values, which are more common in intraprotoplasmic biological systems. It is this hydrolysis reaction which causes DHA to be unstable in aqueous solutions, and this reaction is thought to be irreversible *in vivo* (33).

The stereoisomer of AA, D-isoascorbic acid (known also as erythorbic acid) is not widely produced naturally although it has been reported to be formed by *Penicillium cyaneo-fulvum* (34), and has been synthesised (35). This compound shows reduced anti-scorbutic properties compared with L-AA (36), potentially because of the inability of cells to transport and absorb this isomer of ascorbate. Fungi and yeast cells contain a C_5 analogue of ascorbate, D-erythroascorbic acid (D-*glycero*-pent-2-enono-1,4-lactone) (37,38). This compound has very similar pK_a values as AA (pK_a of 4.0 and 11.6) and has been shown to have similar anti-scorbutic properties in insect models, but not necessarily in humans (39).

1.4 Biosynthesis of ascorbate

Initial studies on the biosynthesis of ascorbate in rats showed that ascorbate is produced from glucose (40). Further work involving the feeding of specifically labelled [6-¹⁴C]glucose or [1-¹⁴C]glucose demonstrated that this conversion of glucose to ascorbate involves an inversion of the carbon chain, i.e. [1-¹⁴C]glucose produced [6-¹⁴C]AA (41), owing to reduction at C-1 of glucose, and oxidation at C-6. This conversion was determined to occur via intermediates of D-glucuronic acid, L-gulonic acid and L-gulono-1,4-lactone (42).

As mentioned previously, humans, along with a select group of other species, are unable to synthesise ascorbate and thus require vitamin C in their diet. The inability to synthesise ascorbate is due to a mutation in the final enzyme (L-gulono-lactone oxidase) in the mammalian biosynthetic pathway (10,43). This enzyme, catalysing the oxidation of L-gulono-1,4-lactone to L-ascorbate, is present in the liver of ascorbate-synthesising mammals (43), and in the kidney of ascorbate-synthesising fish, amphibians and reptiles (44).

The biosynthetic pathway of ascorbate in plants proved much more difficult to pin down than the mammalian biosynthetic pathway. In fact it was not until 1998 that the major pathway in plants was elucidated (14). It has since been reported that at least three other pathways, occurring via various intermediates, are also present in plants (9) (Figure 3).

The pathway in plants was originally proposed to follow the same steps as in rats (42) from D-glucose to L-ascorbic acid, via the intermediates of D-glucuronic acid and L-gulonic acid. The feeding of the lactones of both D-glucuronic acid and L-gulonic acid (intermediate compounds in the mammalian biosynthetic pathway) to cress seedlings, as well as rats, also resulted in the formation of ascorbic acid (42). However, tracer studies carried out in plants with glucose labelled in the C-1 and C-6 positions showed that inversion of the carbon skeleton does not occur in plants, as it does in mammals (45,46), providing evidence for an alternative ascorbate biosynthetic pathway in plants.

A breakthrough occurred in 1998 with the proposal of a pathway that did not require the inversion of the carbon backbone (14) occurring via intermediates of L-galactose and L-galactono-1,4-lactone (Figure 3, L-galactose pathway). The most effective precursor of ascorbate in plants had been shown to be L-galactono-1,4-lactone (46), the production of which is catalysed by L-galactose dehydrogenase (enzyme 8 in figure 3) (47), but the occurrence of this compound *in planta* was disputed (48). However, it was shown that L-galactono-1,4-lactone can be produced by the oxidation of C-1 of L-galactose. L-Galactose supplied to various plant tissues (*Arabidopsis thaliana* leaves and germinating pea seedlings)

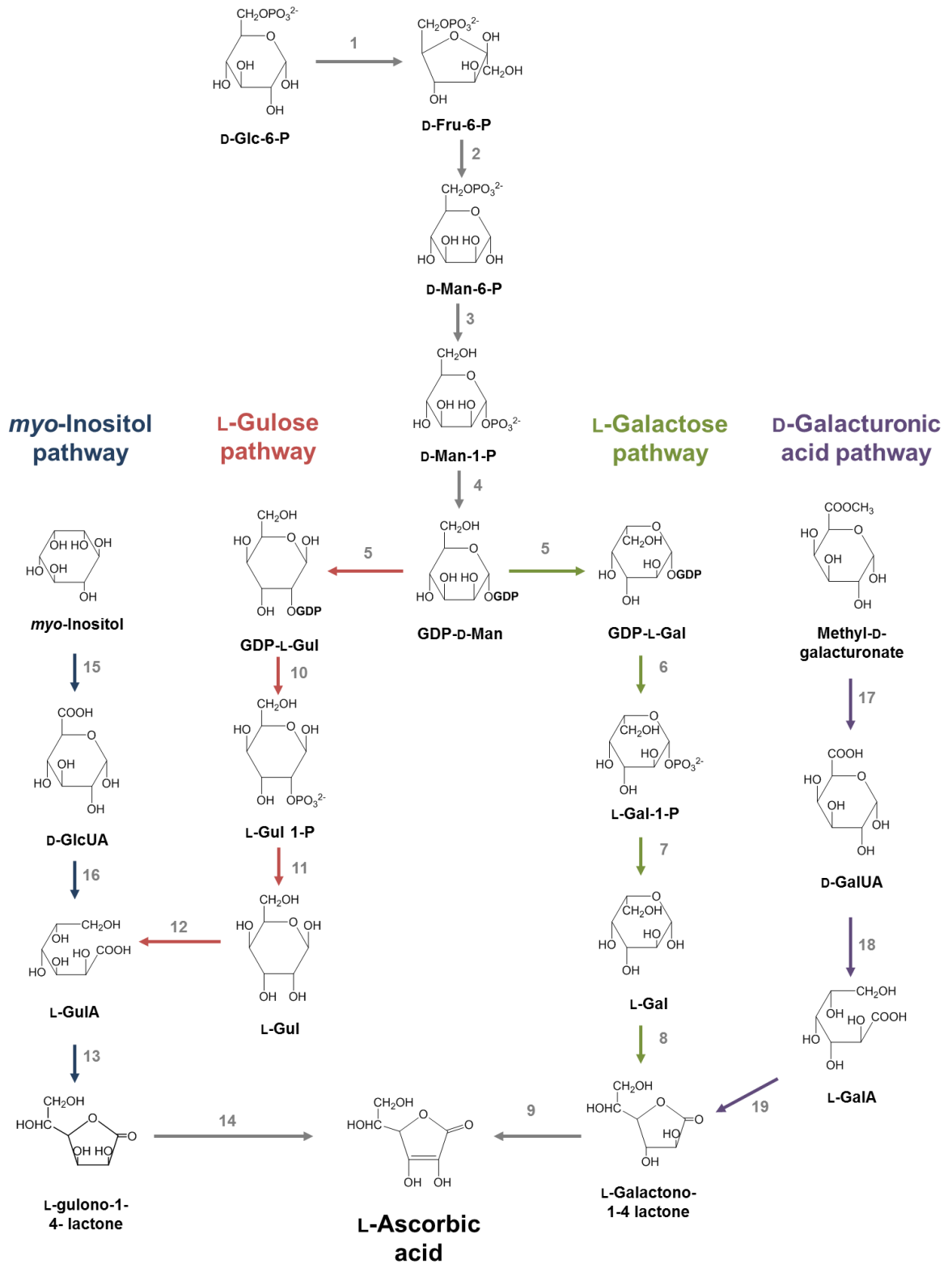


Figure 3: The biosynthetic pathways of ascorbic acid in plants. The four known pathways to ascorbate in plants are shown in different colours. The enzymes involved are: 1, glucose-6-phosphate isomerase; 2, mannose-6-phosphate isomerase; 3, phosphomannomutase; 4, GDP-mannose pyrophosphorylase; 5, GDP-mannose-3',5' epimerase; 6, phosphodiesterase; 7, sugar phosphatase; 8, L-galactose dehydrogenase; 9, L-galactono-1,4-lactone dehydrogenase; 10, phosphodiesterase; 11, sugar phosphatase; 12, L-gulose dehydrogenase; 13, aldono-lactonase; 14, gulono-1,4-lactone dehydrogenase; 15, *myo*-inositol oxygenase; 16, glucuronate reductase; 17, methylesterase; 18, D-galacturonate reductase; 19, aldono-lactonase. Adapted from (3) and (9)

led to a rapid increase in ascorbate levels (14), demonstrating that L-galactose is an effective precursor of ascorbate. L-Galactose residues are found in the cell wall (49), demonstrating that plants are capable of synthesising the L-isomer of galactose (D-galactose is more abundant in plants), providing the opportunity for this compound to be an intermediate in ascorbate biosynthesis (18,50). The production of ascorbate from L-galactono-1,4-lactone is catalysed by the plant mitochondrial enzyme L-galactono lactone dehydrogenase (enzyme 9 in figure 3)

Mutants of *Arabidopsis thaliana* deficient in ascorbate metabolism have allowed the identification of key enzymes within this pathway. One of the most studied of these mutants is *vitamin C-1 (vtc1)* which was originally named *soz1* owing to its sensitivity to ozone. The *VTC1* locus encodes GDP-mannose pyrophosphorylase (51) (enzyme 4 in Figure 3), and the mutant plants show a 70% reduction in ascorbate (52). The *vtc1* mutants did not completely lack GDP-mannose pyrophosphorylase, but rather the enzyme showed a deficiency in its activity of about 35%. It was predicted that a null mutant with a complete lack of GDP-mannose pyrophosphorylase would be embryo-lethal, owing to the numerous functions of GDP-mannose in plants, and indeed a different (null) mutation (*cyt1*) in the same gene proved to be embryo-lethal (53). The *vtc1* mutant showed numerous phenotypes, in addition to sensitivity to ozone, related to ascorbate deficiency, including early senescence, late flowering and slower growth (52,54). A related mutant (*vtc4*) was also found to have reduced ascorbate levels; the *VTC4* locus was found to encode L-galactose-1-P phosphatase (55) (enzyme 7 in Figure 3). *VTC2* was the final enzyme in this pathway to be characterised (all are named in Figure 3) and encodes GDP-L-galactose phosphorylase (56) (enzyme 6 in Figure 3). *VTC5* also encodes a GDP-L-galactose phosphorylase (57). The *vtc2* mutant had approximately 20% ascorbate, whereas *vtc5* mutants had approximately 90% ascorbate levels, but a double mutant of *vtc2* and *vtc5* was not viable (57). The different expression patterns of *VTC2* and *VTC5* are thought to relate to varying diurnal rhythms (58).

All these mutants of the Smirnoff–Wheeler pathway show marked reductions in ascorbate levels, but not a complete lack of ascorbate. The mutants in the pathway showed a reduction rather than a complete lack of the enzyme activities, which would explain the low levels of ascorbate that remain in these mutants. Alternatively, the presence of low levels of ascorbate in the mutants of the Smirnoff–Wheeler biosynthetic pathway could suggest that alternative biosynthetic pathways may also exist in plants. Although this pathway, via L-galactose, has been found to be the dominant pathway in numerous plants (59), it is now generally accepted

that there are at least three other distinct pathways of ascorbate biosynthesis in plants (Figure 3).

An alternative pathway was defined in ripening tomato fruits (60), in which it was found that the previously described genes involved in the Smirnoff–Wheeler pathway were down-regulated, but ascorbate levels increased. This alternative pathway was found to proceed via D-galacturonate (D-galacturonic acid pathway in Figure 3), presumably from pectin in the cell wall.

The third pathway utilises *myo*-inositol as the substrate (61) (*myo*-inositol pathway in figure 3). Over-expression of a *myo*-inositol oxygenase gene (*miox4*) in *Arabidopsis* led to a significant increase in the ascorbic acid content (61). The spatial expression of the gene also correlates with tissues containing high levels of ascorbate, such as flowers and leaves. This pathway involves L-gulono-1,4-lactone as the immediate precursor to ascorbate, as in the mammalian pathway. Previous work using radiolabelled *myo*-inositol fed to parsley (*Petroselinum*) leaves and strawberry (*Fragaria*) fruits showed negligible radiolabelled ascorbate (44), suggesting that this substrate provides only a minor contribution for ascorbate biosynthesis.

Another pathway that uses part of the mammalian biosynthetic pathway utilises phosphorylated derivatives of L-gulose (L-gulose pathway in Figure 3) generated by GDP-mannose epimerase (62) (enzyme 5 in Figure 3). This enzyme is implicated in the dominant Smirnoff–Wheeler (L-galactose) pathway, converting GDP-mannose to GDP-galactose, but it was discovered that this enzyme could also catalyse the conversion of GDP-mannose to GDP-gulose. This GDP-gulose is hypothesised to go on to form ascorbate via intermediates of L-gulose-1-P and L-gulose, before feeding into the last stages of the *myo*-inositol and mammalian pathways via L-gulonic acid and L-gulono-1,4,-lactone.

The major biosynthetic pathway of ascorbate in plants is the Smirnoff-Wheeler pathway, as demonstrated by the loss of the majority of ascorbate in plants with mutations in key enzymes in this pathway. The D-galacturonic acid pathway is thought to be organ specific, having been discovered in tomato fruits. The *myo*-inositol pathway makes only a very small contribution to the overall ascorbate pool within the plant, and the L-gulose pathway has not been verified *in planta* as yet, so would similarly only be expected to contribute as a very minor pathway.

1.5 Degradation of ascorbate

Although several biosynthetic pathways of ascorbate are now well characterised, many of the degradation pathways have yet to be fully elucidated. The current study will report on various aspects of ascorbate degradation pathways.

Ascorbate is unstable in aqueous solutions at a physiological pH. Under aerobic conditions, the first oxidation product of ascorbate is the ascorbate free radical (AA^{\cdot} ; section 1.3) which can convert back to ascorbate, or oxidise further to produce dehydro-L-ascorbic acid (DHA) (63). DHA is important as it has been shown to have anti-scorbutic properties in guinea pigs (64); this could be due in part to the conversion of DHA back to AA, which is dependent on glutathione, and occurs in human blood cells (65). DHA and its hydrolysis product 2,3-diketo-L-gulonic acid (DKG) have been shown to be more susceptible to degradation by H_2O_2 than AA itself, suggesting that DKG and DHA preferentially react with H_2O_2 above AA (32). DHA also provides greater protection than AA in the presence of transition metal ions against the oxidation of low density lipoproteins by inhibiting lipid peroxidation and Cu^{2+} uptake (66).

The oxidation of ascorbate to DHA is reversible in plant cells, and partly enzymatically controlled (33). Dehydroascorbic acid reductase (DHAR) catalyses the reduction of DHA to ascorbate (67). This enzyme is integral to the ascorbate–glutathione pathway (discussed further in section 1.7.2), allowing the recycling of ascorbate and preventing it from being lost from the cell. The proportion of vitamin C present in the form of either ascorbate or DHA is important for the redox state of the cell (68,69), which in turn governs the vulnerability of cells to infection. DHA represents a branch point in ascorbate catabolism and can undergo further degradation, either oxidation or hydrolysis, which is irreversible and results in a loss of vitamin C from the cell.

1.5.1 Oxidation of DHA

DHA can be hydrolysed to 2,3-diketo-L-gulonate (DKG) (70,71), or alternatively oxidised to a range of products. Well-documented end products of the oxidation of DHA are L-threonic acid (ThrO) and oxalic acid (OxA) (32). These are known to be formed largely via intermediates of oxalyl-L-threonate (OxT) and cyclic oxalyl-L-threonate (cOxT) (1,2,72). This pathway was originally identified in rose cell-suspension culture supplied with [1- ^{14}C]AA. All the compounds were formed non-enzymically, but some steps were enhanced in the presence of enzymes (72). Further investigation into the fate of DHA under oxidising

conditions revealed the theoretical possibility of highly reactive intermediate compounds which then go on to form cOxT, OxT and OxA (necessarily with ThrO) simultaneously in a 6:1:1 ratio (2) (Figure 4).

Mass spectrometry analyses of oxidised AA and DHA showed that they both produced ThrO, via a 6-carbon intermediate, as determined by mass spectrometry (32). The 6-carbon intermediate was proposed to be 2,3-diketo-4,5,5,6-tetrahydroxyhexanoic acid and was found to be produced during hydrogen peroxide oxidation of AA, but not significantly with cupric ion oxidation, which instead produces *threo*-hexa-2,4-dienoic acid lactone (73). AA has been demonstrated to form hydroxyl radicals and H₂O₂ in solutions containing metal ions via the Fenton reaction (74). This difference in intermediate compounds demonstrate that

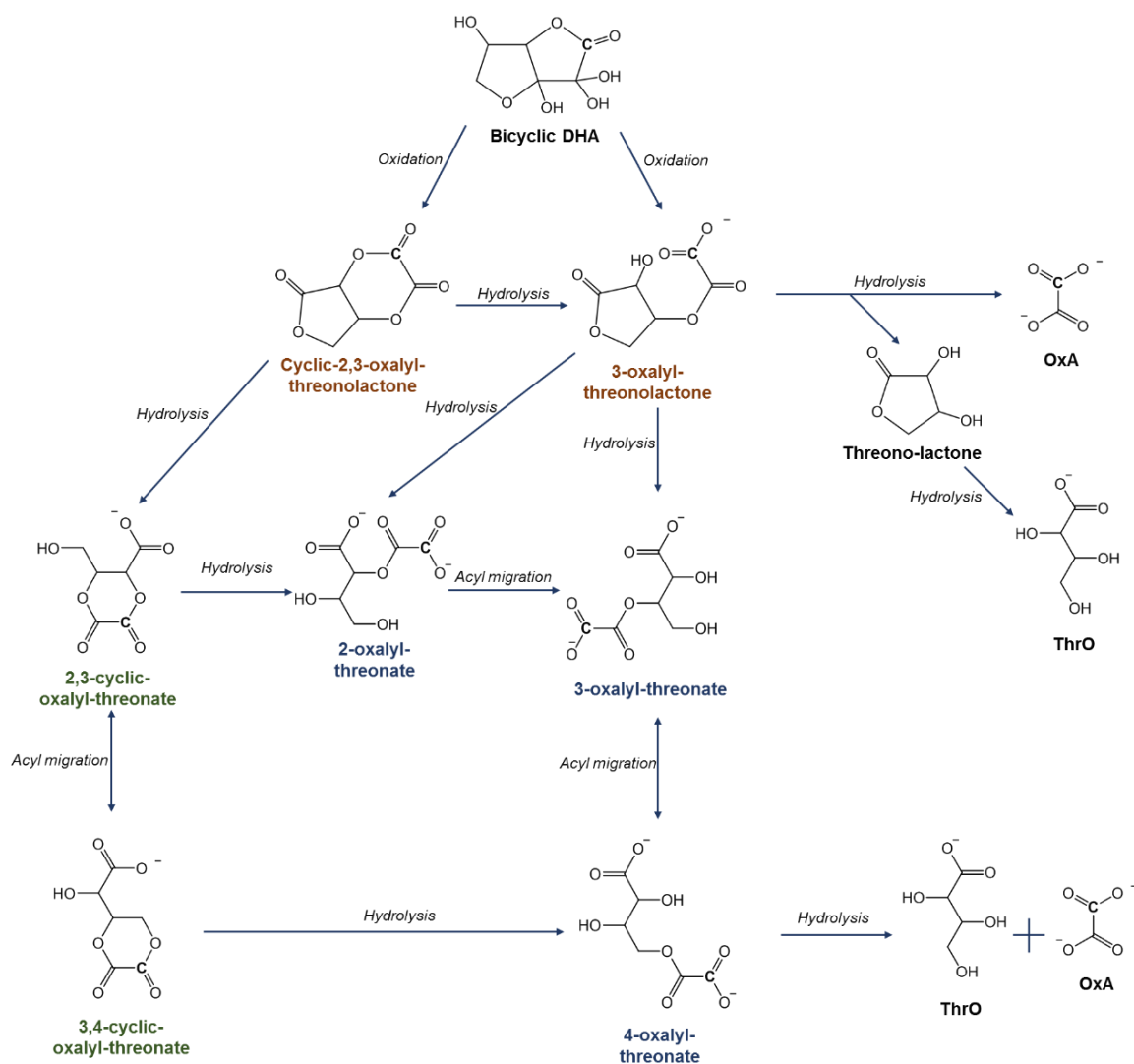


Figure 4: Oxidation pathway of DHA as proposed by Parsons and Fry. Isomers of cOxT are shown in green, isomers of OxT are shown in blue and reactive intermediates are shown in orange. Adapted from (1) and (2).

different ROS can form different oxidation products from AA.

Some compounds in the oxidation pathway of DHA, namely cOxT and OxT, have theoretical isomers. The two isomers of cOxT (Figure 4) are 2,3-cOxT and 3,4-cOxT. These compounds are proposed to originate from a highly reactive intermediate (cyclic-2,3-oxalyl-L-threonolactone) formed during the oxidation of DHA with H₂O₂ (1). This intermediate compound would be very short-lived, rapidly undergoing hydrolysis of either the lactone ring (producing the relatively stable 2,3-cOxT, which itself can produce 3,4-cOxT by acyl migration) or one of the oxalyl ester bonds (producing the second highly reactive intermediate 3-oxalyl-L-threonolactone). *In vivo* the formation of 3-oxalyl-L-threonolactone appears to be favoured (1). This second highly reactive intermediate compound can undergo hydrolysis of the lactone ring, forming either 2-oxalyl-L-threonate or 3-oxalyl-L-threonate. 2-OxT is proposed to be fairly unstable, forming 3-OxT by acyl migration. OxT is reported to be composed of three isomers, of which 4-OxT is thought to be the most stable, owing to this isomer having its two negative charges furthest apart (75). Interconversion between 3-OxT and 4-OxT is reported to occur *in vivo* (1).

Alternatively, 3-oxalyl-threonolactone could undergo hydrolysis of the oxalyl ester bond, producing L-threonolactone and OxA. In turn, threonolactone itself would be likely to be hydrolysed, producing free ThrO. ThrO and OxA could also be produced from 4-OxT, by hydrolysis of the remaining oxalyl bond (Figure 4).

Although these oxidation products can be formed *in vitro*, some of the steps are catalysed by enzymes *in vivo* (72,75). An oxalyl esterase is proposed to catalyse the reaction of OxT to ThrO and OxA. OxT appeared relatively stable in non-enzymatic conditions (in fresh culture medium and boiled spent culture medium) but depleted in conditions with plant enzymes present (both in rose cell-suspension culture and cell-free spent medium), resulting in an increase in OxA (72). Esterases have also been proposed to act during the conversion of

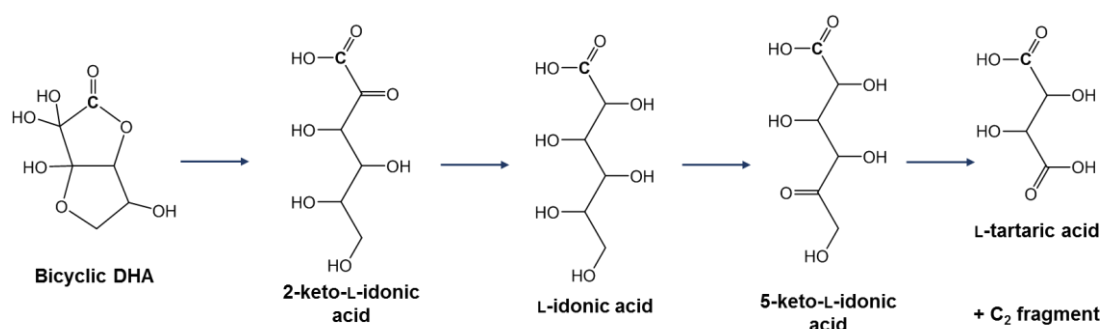


Figure 5: Formation of tartaric acid from DHA in Vitaceae. The C-1 of the original ascorbate molecule is indicated with C. DHA is shown in the bicyclic form. Adapted from Hancock and Viola (2005) (3)

cOxT to OxT in rose cell-suspension cultures (1).

Different plant families are known to exhibit different ascorbate oxidation pathways, with plants in the Vitaceae (such as grapes) forming tartrate via L-idonate derivatives (Figure 5). A gene encoding L-idonate dehydrogenase was identified in a grape species (*Vitis vinifera*). This enzyme catalyses the formation of 5-keto-L-idonic acid from L-idonic acid (figure 5); the subsequent formation of tartaric acid is thought to be non-enzymic. A species (*Ampelopsis aconitifolia*) known to accumulate ascorbate was found to have a deletion of the L-idonate dehydrogenase gene (76). Plants in the Geraniaceae, however, form OxA and ThrO via OxT-related compounds (77) (Figure 4). Tartrate can also be produced from the oxidation of ThrO (78).

1.5.2 Degradation of DKG

If oxidation is limited, DHA undergoes hydrolysis to form DKG (Figure 6). This hydrolysis is thought to be irreversible *in vivo*, in mammalian cells (33,79), as DKG has been shown to have no anti-scorbutic properties (80). However, there is some evidence that DHA can be formed from DKG *in vitro* using stronger agents than are present *in vivo*, such as aqueous hydrogen iodide (80) or mercaptoethanol (81).

DKG itself can be further degraded into numerous, incompletely characterised, compounds (Figure 6). The oxidation of DKG ultimately produces ThrO and OxA (2). An alternative pathway for the production of ThrO from DKG has also been reported to occur via an unidentified intermediate product, known as compound H, hypothesised to be a C₅ compound (2). This reaction would presumably also produce CO₂, rather than OxA (a C₂ compound), therefore OxA is most likely not formed via compound H.

An alternative degradation pathway of DKG produces compounds C and E (72) (Figure 6). The nature of the reaction yielding these products remains unknown. These compounds are interconvertible, and C is proposed to be the lactone of E. The chemical structures of C and E remain uncertain, but C is hypothesised to be a mixture of two epimers: 2-carboxy-L-xylonolactone (pictured in Figure 6) and 2-carboxy-L-lyxonolactone, whereas E is suggested to be 2-carboxy-L-xylionate, more correctly termed 2-carboxy-L-*threo*-pentonate (1). *In vivo*, C was found to be produced before E, with the yield of both increasing in moderately oxidising conditions favouring the production of DKG. Compound C is thought to be a stable end point of ascorbate catabolism. This could be due to C being formed before E, or

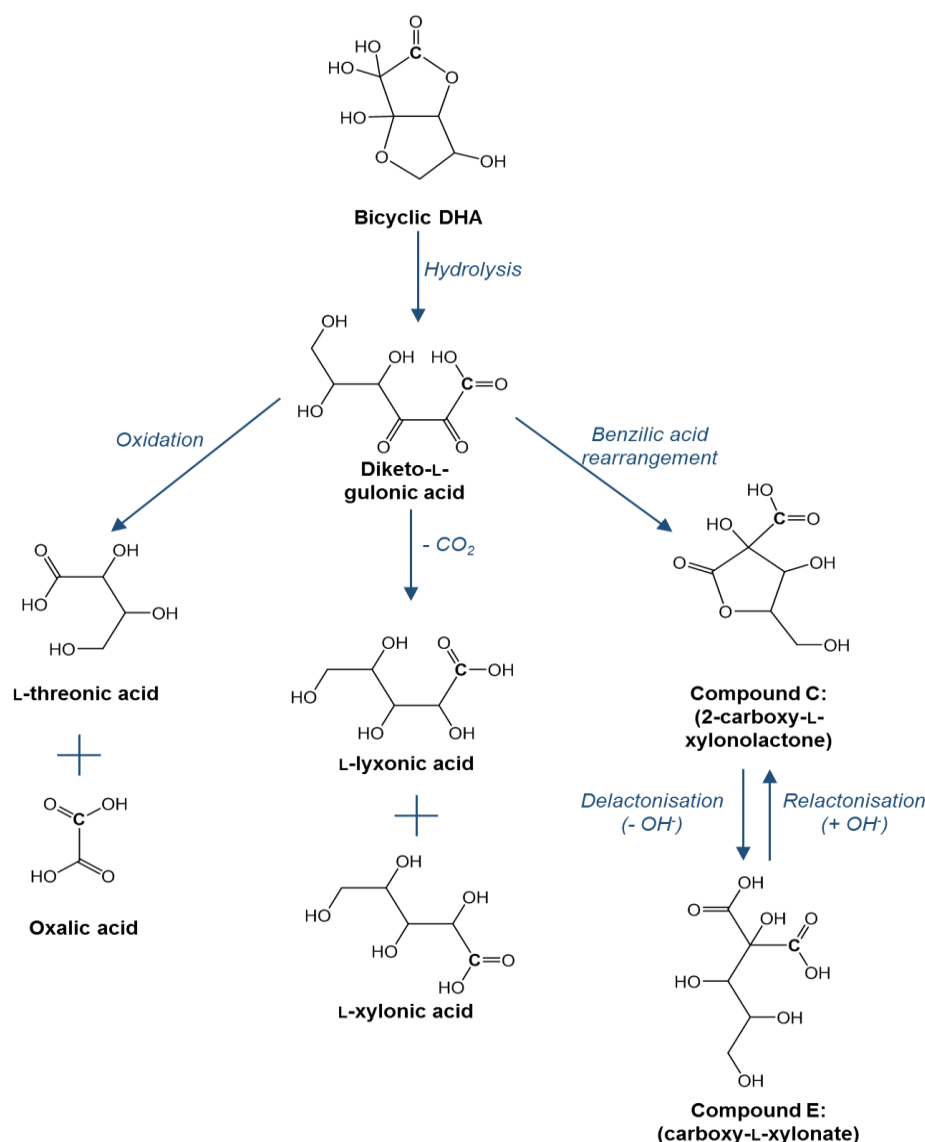


Figure 6: Degradation of DKG. The original C-1 of ascorbate is indicated with a **C**. The proposed identities of compound C and E are written in brackets (1). Adapted from (1) and (4).

because the equilibrium favours the production of C (1). Further characterisation of these compounds will be reported on in the current study.

In animal cells DKG has been shown to undergo non-oxidative decarboxylation to form xylonic acid and lyxonic acid (4,82). These compounds can then enter the pentose phosphate pathway, ultimately resulting in the formation of Glc-6-P and lactic acid (83). The production of xylonic acid and lyxonic acid has not been documented to occur in plants. Experiments carried out with [1-¹⁴C]AA, such as those described in the current study, would be unable to detect the formation of xylonic or lyxonic acid as the ¹⁴C would be lost as CO₂.

Preparations of DKG, containing several unidentified compounds, caused an increase in H₂O₂ production in *Picea abies* (Norway spruce) cell-suspension culture and in fresh culture medium (84). This increase in H₂O₂ was thought to be due to a DKG-related compound producing H₂O₂ itself, or a DKG-related compound that acts to inhibit peroxidase activity (84). An increase in a peroxidase-inhibitory compound would lead to an increase in H₂O₂ as there would be a reduction in the peroxidase-catalysed scavenging of H₂O₂, allowing H₂O₂ to accumulate. Numerous currently unidentified catabolites of DKG were observed after separation of DKG preparations by both by high-voltage paper electrophoresis (HVPE) and high pressure liquid chromatography (HPLC) (84). Aged preparations of DKG were shown to contain a particular compound, isolated after fractionation by HPLC, which acts to inhibit peroxidase activity (A. Kärkönen and S.C Fry, unpublished). The nature of this compound will be discussed further in section 3.2.

1.6 Reactive oxygen species

Reactive oxygen species (ROS) are important signalling molecules within the plant (85). They have vital roles in plant immunity and in growth and development (86). However, an excess of ROS can lead to oxidative stress and cause damage within the plant, including oxidation of proteins, and the damaging of DNA and membranes. Ascorbate, in its role as an antioxidant, acts to quench reactive oxygen species, therefore protecting the plant cells from oxidative stress. Numerous different ROS are found within plant cells, and are often produced as part of normal metabolic processes; several of these species will be discussed individually.

1.6.1 Hydrogen peroxide

H₂O₂ (hydrogen peroxide) is the most well-known ROS generated in the plant, and different ROS often react with H₂O to produce H₂O₂ (87). H₂O₂ is generated during various metabolic processes including photosynthesis, in photosystem I. It is also produced from the oxidation of glycollate in the peroxisome (88).

The synthesis of lignin in secondary cell walls has been shown to require the action of peroxidases (89), in turn necessitating the formation of H₂O₂ as a substrate for these enzymes. It was subsequently determined that H₂O₂ is formed by the action of NADH oxidase (a further peroxidase) in isolated horseradish cell walls (90), providing an important substrate for enzymes involved in lignin synthesis. Several peroxidases (91) and other

enzymes such as amine oxidases (92) also contribute to the formation of H_2O_2 in the cell wall.

As well as being the most abundant, H_2O_2 is also the most long-lived of the ROS. This longevity also allows the possibility of H_2O_2 having a role as a cell signalling molecule (87,93,94). The relative stability of H_2O_2 would allow the molecule to participate in long-range signalling events.

H_2O_2 and $\text{O}_2^{\cdot-}$ (superoxide) have roles as antimicrobial agents as a part of the oxidative burst (95). This is known to occur when plants are infected by a pathogen. $\text{O}_2^{\cdot-}$ has been shown to be generated in response to infection in potato tubers (96), and in cell-suspension cultures (95,97). This $\text{O}_2^{\cdot-}$ disproportionates to H_2O_2 and O_2 *in vivo*. The role of the oxidative burst is thought to primarily be to damage the invading pathogen (98) both directly, and by inducing signalling pathways for cell death and protective responses in neighbouring cells (99). A further protective role of H_2O_2 from the oxidative burst has been reported (100), in which H_2O_2 is able to cross-link proteins into the cell wall, thus strengthening the cell wall and preventing the pathogen from gaining access into the cell.

NADPH oxidases, also known as respiratory burst oxidase homologues are key enzymes involved in generating reactive oxygen species in the apoplast. NADPH oxidases are localised to the extracellular membrane and produce the superoxide anion, which quickly goes on to form H_2O_2 in the apoplast, and so is a key source of ROS in the apoplast (101,102).

NADPH oxidases have been implicated in plant immunity (103), serving a role in response to pathogen attack, as well as in connection with various other biotic and abiotic stresses. NADPH oxidases produce ROS immediately upon infection, the enzyme has then been shown to undergo S-nitrosylation, which diminishes the production of ROS, limiting the hypersensitive response, reducing excessive cell death (104). They have also been found to have a key role in cell expansion, producing ROS which go on to regulate the activation of calcium channels (105). This suggests a role for NADPH oxidases in plant growth. Barley germination was delayed by treatment with an NADPH oxidase inhibitor, which was demonstrated to reduce superoxide production (106).

1.6.2 Superoxide anion

The superoxide anion ($\text{O}_2^{\cdot-}$) is produced by the one-electron reduction of molecular O_2 (107). $\text{O}_2^{\cdot-}$ is produced in the mitochondria, where up to 4% of O_2 is reduced to $\text{O}_2^{\cdot-}$ (107,108). It is also produced in the chloroplast, in PSI (109). $\text{O}_2^{\cdot-}$ is very short-lived, having a half-life of

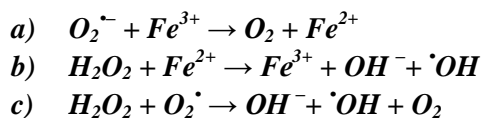
just 4 μ s in the presence of enzymes, and up to 0.5 s at pH 6.5 without enzymes (107,110,111).

Superoxide has also been reported to form at cell surfaces, by the action of plasma membrane-associated NADPH oxidases (112). These enzymes reduces O_2 to $O_2^{\cdot-}$, utilising NADPH as an electron donor.

During pathogen infection an oxidative burst is known to occur, as mentioned in the previous section (96,113). This oxidative burst involves the production of large amount of $O_2^{\cdot-}$, which quickly disproportionates to H_2O_2 and O_2 (113). This disproportionation is catalysed *in vivo* by superoxide dismutase, which converts the very reactive $O_2^{\cdot-}$ to the less damaging and more stable H_2O_2 and O_2 (114).

1.6.3 Hydroxyl radical

The hydroxyl radical ($\cdot OH$) has been reported to be the most potent but most short-lived of the ROS (115). $\cdot OH$ is generated from the reaction of H_2O_2 with reduced metal ions, such as Fe^{2+} or Cu^+ . This occurs via the Haber–Weiss reactions shown below. $O_2^{\cdot-}$ transfers an electron to Fe^{3+} , resulting in the formation of O_2 (reaction a). H_2O_2 on the other hand oxidises Fe^{2+} to Fe^{3+} , producing OH^- and $\cdot OH$ (reaction b). The overall reaction (reaction c) shows the formation of $\cdot OH$ from H_2O_2 and $O_2^{\cdot-}$ (110).



An alternative route of $\cdot OH$ generation that does not require $O_2^{\cdot-}$ occurs via the reaction of ascorbate with Cu^{2+} or Fe^{3+} and O_2 . Ascorbate can facilitate the reduction of O_2 to H_2O_2 , as well as the reduction of Cu^{2+} to Cu^+ (or Fe^{3+} to Fe^{2+}) non-enzymically. $\cdot OH$ is then produced from the reaction of H_2O_2 and the metal ions in the classical Fenton reaction (116,117).

As $\cdot OH$ is the most reactive of the ROS, mechanisms to control this ROS may involve the elimination of the precursors of $\cdot OH$ rather than $\cdot OH$ itself, as it is too reactive to be controlled directly, and there are no known scavengers of $\cdot OH$ (110,113). The precursor, $O_2^{\cdot-}$, is removed by the action of superoxide dismutase (118), and H_2O_2 is removed by the action of catalases and peroxidases. The production of $\cdot OH$ from H_2O_2 is also catalysed by horseradish peroxidase (119).

A major site of $\cdot OH$ generation within the plant cell is thought to be photosystem II in the chloroplast, due to the presence of H_2O_2 and $O_2^{\cdot-}$, and metal ions such as Fe^{3+} and Mn^{2+}

(120,121). $\cdot\text{OH}$ is also generated in the mitochondria, formed from H_2O_2 and $\text{O}_2^{\cdot-}$ in the presence of metal ions such as Mn^{2+} or Fe^{3+} present in the electron transfer chains (121,122). A further site of $\cdot\text{OH}$ production is in the cell walls, where it is also formed from H_2O_2 and Cu^{2+} or Fe^{3+} . Within the cell wall $\cdot\text{OH}$ is thought to contribute to cell wall loosening and thus plant growth by oxidative scission of polysaccharides (123). This ascorbate-dependent production of $\cdot\text{OH}$ within the cell wall has been proposed to have a role in fruit softening (124).

1.6.4 Singlet oxygen

Singlet oxygen ($^1\text{O}_2$) is the excited state of molecular (triplet) oxygen. This ROS is the primary cause of lipid peroxidation in leaves (125). $^1\text{O}_2$ is the predominant ROS generated in PSII, from molecular (triplet) oxygen in the presence of chlorophyll (109). Singlet oxygen is produced by photo-activation, which occurs in leaves owing to the presence of chlorophyll, which acts as a photosensitiser (126). *In vitro*, $^1\text{O}_2$ can be produced from photosensitiser dyes such as eosin, rose Bengal and riboflavin (127).

Singlet oxygen is known to have roles in various cell-signalling pathways, including in programmed cell death (128,129). It also plays a role in plant-pathogen interactions, with some plants producing $^1\text{O}_2$ as a response to pathogen infection (130). Some plants produce secondary metabolites that are photosensitisers (also known as phototoxins), such as phytoalexins, rapidly in response to infection (131). These compounds accumulate at the point of infection and produce toxic $^1\text{O}_2$ in light, thus defending the plant from pathogens (132,133). Phototoxins including furanocoumarins and furanoquinoline are found in prickly ash (*Zanthoxylum americanum*) and wild parsnip (*Pastinaca sativa*) (134). Leaves of these two species were shown to produce $^1\text{O}_2$ at the adaxial leaf surface when incubated under light. This singlet oxygen, which is more stable in gas than in aqueous solutions was shown to be able to travel up to 2 mm, allowing it to act as a defence mechanism against pathogens and herbivores at the leaf surface, with minimal damage to the healthy plant cells (134).

1.7 Ascorbate as an antioxidant

ROS, discussed in the previous section, are potentially damaging and may require detoxification within the plant cell. One of the most abundant antioxidants in plants is ascorbate (135). Ascorbate can react directly with $\cdot\text{OH}$, $\text{O}_2^{\cdot-}$ and $^1\text{O}_2$, and can reduce H_2O_2 via the ascorbate–glutathione pathway (11) (discussed in section 1.7.2).

1.7.1 Apoplastic ascorbate

Ascorbate is found throughout the plant cell, and has been detected in all cell compartments (136). The majority of a plant's ascorbate is found in the cytosol and the peroxisomes, as measured by immunocytochemical labelling of *Arabidopsis thaliana* cells, along with smaller proportions accumulating in the other cell compartments including plastids and the apoplast (136). In *Arabidopsis thaliana* the apoplast was found to contain ~10% the total ascorbate (AA and DHA, at a concentration of 200-300 nmol g⁻¹ fresh weight) and this decreased upon pathogen infection (137). The apoplastic ascorbate levels vary between species, with the spinach (*Spinacia oleracea*) apoplast containing ascorbate at a level of ~50 nmol g⁻¹ fresh weight (138) and the wheat (*Triticum aestivum*) apoplast having levels of 70-140 nmol g⁻¹ fresh weight (139). The ascorbate levels also vary between tissues; the apoplast of *Kalanchoé daigremontiana* stems were shown to contain ascorbate at levels of ~15 nmol g⁻¹ fresh weight, compared to leaves which contained ~80 nmol g⁻¹ fresh weight (140). The apoplastic ascorbate was shown to be increased in snap beans (*Phaseolus vulgaris*) with increased tolerance to ozone (141).

Ascorbate has been shown to be exported to the apoplast during oxidative stress and apoplastic ascorbate represents the first defence of a plant cell to exogenous oxidative stresses such as ozone (142-144). Indeed, the apoplastic ascorbate of Norway spruce (*Picea abies*) was found to decrease by 30% upon ozone treatment, suggesting that ascorbate was being consumed during the defence against oxidative stress (145).

The level of ascorbate present in a plant cell greatly influences its tolerance to oxidative stress. In fact a key enzyme in the ascorbate biosynthetic pathway was originally identified through a mutant found because of its sensitivity to ozone (146). A major cause of oxidative stress in plants is ozone. The apoplastic ascorbate levels of several populations of *Plantago major* were found to be correlated with their ozone tolerance (147). Equally, applying exogenous ascorbate to the plants' leaves increased the ozone resistance of a less resistant population.

Ascorbate also quenches singlet oxygen in plant cells (148). Ascorbate and DHA levels were found to significantly decrease in the presence of singlet oxygen (149), whereas glutathione levels were found to markedly increase, potentially in order to maintain the redox potential within the cell; equally, further studies have demonstrated an increase in glutathione synthesis upon oxidative stress (150,151). The products formed from the reaction of ascorbate and DHA with $^1\text{O}_2$ have not been defined, but will be reported on in the current study.

The actions of these ROS are interconnected, with many ROS degrading to form H_2O_2 . Ozone has also been reported to yield singlet oxygen during the reaction of ozone with biological molecules such as NADH, NADPH, methionine and ascorbate; these compounds incorporate one atom from ozone into the oxidised compound, and the two remaining atoms go on to form $^1\text{O}_2$ (152).

Ascorbate oxidase (AO) is an apoplastic enzyme that facilitates the oxidation of AA to MDHA using molecular oxygen. In turn, MDHA disproportionates to form DHA and AA. The expression of AO has been demonstrated to correlate with growth, with increased mRNA in rapidly dividing tissues of pumpkin seedlings (153) and the highest AO activity in zucchini squash was reported to occur in the exponential growth phase (154). AO expression is induced by growth hormones, such as auxin (153,155), which further supports the role of AO in plant growth and cell expansion. Equally, AO is suppressed by salicylic acid, corresponding with an inhibition of the growth of tobacco seedlings (155). Furthermore, AO has been demonstrated to catalyse the decarboxylation of auxin, potentially serving a role in the regulation of auxin in root meristems (156).

AO is also key for maintaining the redox state of the apoplast. The AA pool in the apoplast is highly oxidised. An alteration in the redox state of the apoplast can be triggered by pathogen attack and ozone stress, among others, which cause an oxidative burst, which in turn acts as a signal to initiate a defence response. As there is no NADPH or glutathione in the apoplast, AA serves as the major apoplastic antioxidant and AO regulates the ratio of AA to DHA, which is vital for maintaining the redox state of the apoplast (157). Overexpression of AO was shown to reduce AA in the apoplast and to reduce auxin-mediated responses (158). Tobacco plants overexpressing AO were found to be more sensitive to oxidative stress and more susceptible to fungal infection (159), further demonstrating the importance of this enzyme.

1.7.2 Ascorbate–glutathione pathway

The major H_2O_2 scavenging pathway in plant cells is the ascorbate–glutathione pathway (Halliwell–Foyer–Asada cycle) (11,160). This pathway occurs within the cytosol, chloroplasts and mitochondria (161).

The scavenging of H_2O_2 in this pathway occurs via the action of four enzymes (11,162) (Figure 7): ascorbate peroxidase (163) (APX), monodehydroascorbate reductase (31) (MDHAR), DHA reductase (67) (DHAR) and glutathione reductase (164) (GR). These enzymes, along with ascorbate, glutathione and NADPH allow the conversion of H_2O_2 to H_2O and regulate the redox state of the cell.

Glutathione (GSH), a tripeptide containing a thiol group, is present in the plant cell at relatively high concentrations and is an important antioxidant (165,166). Reduced glutathione (GSH) can be oxidised to glutathione disulphide (GSSG) by the action of GR (Figure 7).

APX reduces H_2O_2 with the use of AA as a reductant (163,167). Two molecules of AA are required to reduce one molecule of H_2O_2 to H_2O (11). This reaction yields two molecules of unstable MDHA, which can either disproportionate to DHA and AA non-enzymically or alternatively can be reduced back to AA by MDHAR (31). The reduction of MDHA back to AA requires NADPH as a reductant. DHA can also be reduced back to AA and this occurs via the action of DHAR (67). The reduction of DHA by DHAR is coupled to the oxidation of GSH to GSSG. In turn, GSSG itself can be reduced back to GSH by GR, which requires NADPH as an electron donor (168). This complete pathway allows the scavenging of both AA, by MDHAR and DHAR, and GSH, by GR. This in principle results in the quenching of

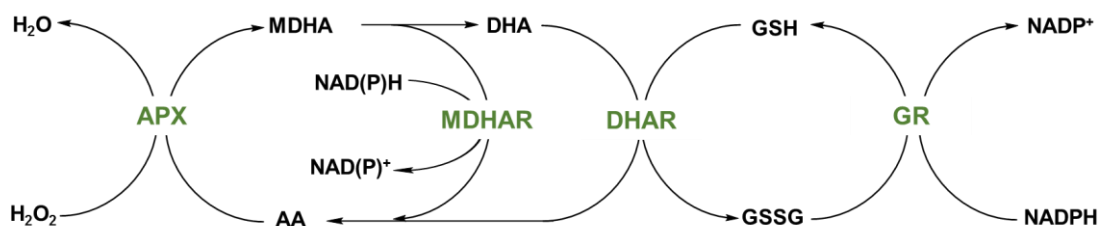


Figure 7: Ascorbate–glutathione cycle. Enzymes in the pathway are in green; APX (ascorbate peroxidase); MDHAR (MDHA reductase); DHAR (DHA reductase); GR (glutathione reductase). Adapted from (7).

H₂O₂ with no net loss of AA or GSH (Figure 7).

In contrast, the current work will be reporting on experiments investigating the permanent loss of AA and DHA, and the subsequent formation of oxidation products arising from ROS, including H₂O₂, reactions with AA and DHA.

An increase in the expression levels of DHAR, resulting in an increase in AA levels, in turn led to an increased tolerance to ozone (169). Similarly, decreasing the expression of DHAR resulted in tobacco (*Nicotiana tabacum*) with a decreased tolerance to ozone (169). The APX enzymes are especially important in conferring oxidative stress resistance. Genetic studies have demonstrated that overexpression of APX as well as superoxide dismutase (SOD), which removes the potentially toxic superoxide ion, led to an increased tolerance of a variety of oxidative stresses (170).

1.8 Ascorbate in plant growth

Ascorbate is known to have a role in plant growth, as illustrated by *Arabidopsis* mutants deficient in ascorbate biosynthesis (*vtc1*) which exhibit slow growth phenotypes (52). As well as slow growth, *vtc1* mutants showed further growth and developmental phenotypes such as smaller cells, late flowering and early senescence (52,171).

Levels of ascorbate measured in shoot segments of pea plants (*Pisum sativum*) showed that the highest levels are found in rapidly dividing meristematic cells. The ascorbate levels decreased with the rate of cell division (172). As rapidly dividing cells are found in young growing plant tissues this provides evidence for a role for ascorbate in plant growth.

Although ascorbate is established as an antioxidant, under certain conditions it can also act as a pro-oxidant (123). Ascorbate can enhance the production of the reagents of the classical Fenton reaction, producing $\cdot\text{OH}$ from H₂O₂ and reducing metal ions such Cu²⁺. H₂O₂ can be produced from the reduction of oxygen, and Cu⁺ can be produced from the reduction of Cu²⁺. Ascorbate facilitates both these reactions non-enzymically. The hydroxyl radicals produced can then react with cell wall polysaccharides, and potentially contribute to cell wall loosening, and thus plant growth (123). Ascorbate, by promoting the production of these hydroxyl radicals, has also been proposed to have a role in fruit softening (124).

Cell expansion was found to be induced by exogenous MDHA in onion root meristems (173). The addition of DHA to tobacco cell cultures was shown to introduce a delay in the cell cycle (174), particularly if the DHA was introduced during the G1 phase. This has been suggested to be linked to the increase in ascorbate oxidation in the apoplast resulting in increasing levels of DHA during oxidative stress. The increase in DHA is proposed to delay the cell cycle until conditions are more favourable for division. The redox state of the cells, as measured by the ratio of AA to DHA, appeared unaltered by the addition of either DHA or ascorbate, suggesting that either of these alone is not the factor influencing the cell cycle (174).

Genetic studies into the apoplastic enzyme ascorbate oxidase (AO) have demonstrated a role for ascorbate in plant cell expansion. The oxidation of ascorbate produces MDHA and is catalysed by AO which requires oxygen. MDHA rapidly degrades to DHA, which is then transported into the cell via transporters. For cell expansion to occur the cell wall must be loosened. AO was over-expressed in tobacco cells derived from protoplasts. These cells were grown in elongation culture medium and the rate of elongation was increased in the cells over-expressing AO (175). This was suggested to occur via MDHA, formed by ascorbate oxidase, activating a proton pump. This increases the osmotic pressure, by increasing the uptake of cellular ions and nutrients, thus promoting elongation. This elongation could occur *in vivo* if the cell wall is loosened. AO activity was found to be highest in fastest growing regions of zucchini squash (*Cucurbita pepo*) leaves, and the activity was demonstrated to be localised to the fruit epidermis (154). This localisation to cells that are under increased tension suggests a role for AO in cell wall loosening. This was proposed to occur via the action of the end product of AO, DHA, and several mechanisms were suggested for this. These include the possibility that DHA could modify lysine or histidine side-chains within the cell wall, thus preventing protein cross-linking with cell wall polysaccharides (154). A further proposed mechanism for the action of DHA in cell wall loosening involves the removal of calcium from the cell wall, which would result in a less rigid structure, more amenable to cell growth (154). This would occur via the action of OxA, produced from DHA in several plant species (176), which in turn could sequester calcium from the pectin in the cell walls, promoting cell wall loosening. AO activity is induced by auxin, a hormone that triggers plant growth, providing further evidence for the role of ascorbate oxidase in plant growth (144).

1.9 Ascorbate as a biosynthetic precursor

A further role of ascorbate in plants is as a biosynthetic precursor of compounds such as OxA and tartrate. OxA, as discussed in section 1.5, is formed during ascorbate catabolism. The cleavage of the carbon backbone of ascorbate between C2 and C3 ultimately results in the formation of OxA and ThrO. Several plants, such as spinach, are known to accumulate OxA, formed via this pathway (176). OxA has been proposed to have a protective role in the plant, protecting it from herbivores (177).

Tracer labelling studies in cell cultures of *Pistia stratiotes* showed that L-[1-¹⁴C]ascorbate led to the formation of labelled OxA (178). Feeding the cell cultures with L[1-¹⁴C]galactose, a major intermediate in the biosynthesis of ascorbic acid, also resulted in labelled OxA (178). As well as demonstrating that ascorbate is a biosynthetic precursor of OxA this study also supported the then newly proposed Wheeler–Smirnoff–Jones biosynthetic pathway of ascorbate itself.

Some plants are known to accumulate tartrate; for instance tartrate is the major organic acid present in grapes (78). It can be formed directly by the cleavage of ascorbate at the C4–C5 bond (179) or from the oxidation of ThrO, originating from C3–C6 of ascorbate (38). The tartrate level in grapes is important for wine making, but the *in planta* role of tartrate is not clear. Plants, such as *Ampelopsis aconitifolia*, that do not accumulate tartrate were found to have up to four times as much ascorbate as tartrate-accumulating plants, suggesting some plants preferentially metabolise AA to form tartrate (76).

1.10 The primary plant cell wall

Ascorbate has been demonstrated to be present in the apoplast (136), and ascorbate oxidase, which produces DHA, is localised to the cell wall (154). It has previously been shown that oxalyl-containing ascorbate oxidation products are generated in the apoplast of rose cell-suspension culture (72). Experiments investigating the hypothesis that these oxidation products (namely OxT and cOxT) could have a role in cell wall cross-linking, and thus plant growth, by formation of an oxalate-bridge between cell wall components will be reported (discussed further in section 3.4 and 3.5).

Plant cell walls are of utmost importance in providing structural strength and shape to the cells. They also provide a barrier to environmental stresses and pathogens (180). Although

the plant cell wall must be a strong, sometimes inextensible, structure, it is also dynamic and has the capability to continually remodel during cell growth (181).

1.10.1 Structure of the plant cell wall

The primary plant cell wall is made up of cellulose microfibrils embedded in a matrix of hemicellulose and pectin. The cellulose microfibrils are tethered by hemicelluloses. Traditionally the pectins and the hemicelluloses were distinguished by their ability to be extracted from plant material. Pectins are soluble in hot mild acid or chelating agents, and contain many galacturonic acid residues, whereas hemicelluloses are soluble in alkali (182,183).

Cellulose is the most defined of the three groups of polysaccharides comprising the cell wall. Cellulose consists of β -1-4 linked glucan chains, which are made by CESA (cellulose synthase) proteins (184). Several of these chains are then packed into bundles, forming crystallised microfibrils (183).

Hemicelluloses are a class of polysaccharides that contain β -1-4 linked backbones (182). The major hemicellulose in primary plant cell walls is xyloglucan (apart from in the Poales, for instance mixed-linkage-glucan is the major hemicellulose in *Equisetum* (185)). Xyloglucan consists of a β -1-4 glucan backbone, with α -1-6-xylosyl sidechains (186). These xylosyl side-chains can also be substituted with other sugar residues such as galactose and fucose (187).

Other hemicellulosic polysaccharides include xylans, comprising of β -1-4 linked xylose residues. Xylans can be modified to form glucuronoxylans (by substitution of xylose residues with α -linked glucuronosyl groups). The glucuronoxylans can in turn be modified to contain arabinose residues, forming arabinoxylans or glucuronoarabinoxylans (182).

Pectins make up approximately 35% of the primary cell walls of dicots and non-poalean monocots and often consist of approximately 70% galacturonic acid (188). Pectins are comprised of acidic polysaccharides; homogalacturonan and rhamnogalacturonan I and II. Homogalacturonan is a linear polysaccharide that consists of α -1-4 linked galacturonic acid. Homogalacturonan can be partially methyl-esterified, and acetylated (189). It can also form cross-links with other pectic polysaccharides, e.g. rhamnogalacturonans, or potentially hemicelluloses such as xyloglucan (190).

The potentially enzyme-mediated interactions between cell wall polysaccharides and ascorbate oxidation products will be reported on.

1.10.2 Cross-linking within the cell wall

The primary plant cell wall is a dynamic structure which is continuously being modified, allowing the cell to expand and divide, which is vital for plant growth.

The matrix of the cell wall consists of hemicelluloses, pectins and glycoproteins which are held in place by cross-links (191). Cross-linking between polymers of adjacent cell walls would lead to cell adherence, and cross-linking between components within the cell wall leads to an decrease in cell wall extensibility (192). Cellulose microfibrils have been proposed to be cross-linked by xyloglucan, as shown by the decrease in immunogold labelling of cross-links and epitopes of xyloglucan upon endoglucanase treatment (193). These cross-links were found to be dynamic during the elongation of epidermal cells (193).

Pectins are often linked by borate or calcium. Cell–cell adhesion has been demonstrated to rely on both calcium and ester cross-linking of pectic polysaccharides (194). Rhamnogalacturonan II is found as a dimer in cell walls, covalently cross-linked by a borate bridge (195). This borate cross-link occurs via apiose residues of RG II. These borate bridges are thought to be vital for cell wall strength, and for decreasing the porosity of the cell wall (196,197). Rose cell cultures were able to be grown in the absence of boron, so the dimer of RG II is not necessary for these cells, but these cells did exhibit diminished biophysical properties (198,199). This dimerization of RG II by borate bridging was found to occur during synthesis and secretion, but not after the RG II had been secreted into the apoplast (199).

Ferulic acid commonly occurs cross-linked to arabinoxylan polymers in the Poaceae family. Oxidative coupling of two feruloyl groups attached to adjacent arabinoxylan chains forms a covalent cross-link acting to tighten the cell wall (200,201). Feruloyl cross-links also occur within the secondary plant cell wall, cross-linking polysaccharides with lignin (202). These cross-links reduce the degradability of the cell walls (203). Feruloyl cross-links are also thought to increase resistance to pathogens and insect herbivores (204).

The current study will report on experiments conducted to investigate the potential for a novel cell wall cross-linking mechanism via oxalate bridges, derived from ascorbate oxidation products.

1.11 Acyltransferases

Derivatives of ascorbate, namely OxT and cOxT (section 1.5.1) contain oxalyl groups which have the potential to act as acyl donors for an acyltransferase reaction. These oxalyl groups could theoretically form oxalyl esters with cell wall components by transacylation. A cross-linking oxalate bridge could be formed within the cell wall from cOxT, due to the presence of two oxalyl ester groups in this compound. This could provide a novel mechanism for cross-linking in the cell wall, and is potentially mediated by an acyltransferase. This hypothesis will be discussed further in sections 3.4 and 3.5.

Many plant secondary metabolites undergo modifications, such as methylation, glycosylation and acylation, all of which are governed by various enzymes (205). The transfer of acyl groups from a donor molecule onto a hydroxyl, thiol or amino group of an acceptor molecule produces an acyl ester derivative. These reactions are catalysed by acyltransferases (206).

A major superfamily of plant acyltransferases is the BAHD superfamily (206). This superfamily is named after the first four enzymes characterised in this family: BEAT (benzylalcohol-*O*-acetyltransferase (207)), AHCT (anthocyanin-*O*-hydroxycinnamoyl transferase (208)), HCBT (anthranilate *N*-hydroxycinnamoyl/benzoyltransferase (209)) and DAT (deacetylindoline-4-*O*-acetyltransferase (210)). The members of this class of proteins share significant gene sequence similarity, suggesting an evolutionary link between the enzymes, thus constituting a superfamily.

All the proteins in the BAHD superfamily are monomeric enzymes and use CoA thioesters as donor substrates (205). Not all acyltransferases use CoA thioesters as substrates, for instance cutin synthase (CD1) transfers the hydroxyacyl group from the substrate 2-mono(10,16-dihydroxy hexadecanoyl)glycerol (2-MHG) either to another 2-MHG or to the cutin polymer (211). The acyltransferase reported in section 3.5 in the current study utilises OxT and cOxT as substrates, transferring the oxalyl group from these compounds onto acceptors such as sugar molecules.

Acyltransferases have a wide range of functions within the plant, including in the modification of phenolic compounds (212). The modification of anthocyanins by the addition of aromatic acyl groups (usually coumaroyl or sinapoyl groups) stabilises the blue colour of flowers (213). The modification of anthocyanins by the addition of aliphatic acyl groups, often malonoyl groups, increases their water solubility and stability. The addition of another aliphatic acyl group, palmitate, to cysteine residues of proteins associated with the tonoplast is thought to contribute to increased resistance to salt stress (214).

Acyl sugars, produced from the esterification of sugars with fatty acids, are thought to protect plants from predation by insects (215,216). These acyl sugars are exuded from trichomes, and are especially common in the Solanaceae family (217).

Acyltransferases also play a role in plant growth. Plants lacking in an S-acyltransferase (known as AtPAT10, which acts to transfer an acyl group such as palmitate to a cysteine residue of an acceptor protein) were found to show reduced cell expansion and cell division, resulting in a dwarf phenotype (218). The growth of root hairs was found to be regulated by an S-acyltransferase (called TIP GROWTH DEFECTIVE, TIP1), responsible for controlling cell shape and growth (219).

Acyltransferases have also been reported to play a role in cell wall modifications, including in the incorporation of hydroxycinnamate into rice cell walls (220) and in the feruloylation of arabinoxylan of the cell walls of grasses, discussed in section 1.10.2 (221). Furthermore, cell wall components cutin and suberin, which act as barriers for pathogens and water, were found to require acyltransferases during their synthesis (211,222). A tomato mutant with a cutin deficiency was found to be lacking in the CD1 (*cutin-deficient 1*) gene, which was subsequently demonstrated to encode an extracellular acyltransferase, cutin synthase (211).

1.12 Ascorbate in salad plants

Vitamin C is the most widely synthesised vitamin, but the majority, up to 90%, of our dietary vitamin C is plant-derived (223). Fresh fruit and vegetables are an important source of vitamin C. As ascorbate is the least stable of the vitamins, cooking generally destroys much of the ascorbate in the food (223). For this reason salads are an invaluable source of ascorbate, as salad leaves are generally eaten raw. There is also evidence to suggest that it is much more beneficial to eat fruit and vegetables rather than rely on vitamin supplements (224). This is likely to be due to the complex synergistic effects of numerous other compounds in the fruit or vegetables, an example of which would be the ability of ascorbate to aid uptake of iron into cells (225).

The ascorbate content of salad plants varies hugely, with some species having up to 110 mg ascorbate per 100 g fresh weight (curly kale (226)) and some as little as 3 mg per 100 g fresh weight (iceberg lettuce (226)). The ascorbate content can also vary between cultivars of the same species (227,228).

As well as this genetic variation, growth conditions can also lead to variation in the ascorbate content of salads. The growth stage at which spinach is harvested has been shown to affect the ascorbate levels, with younger leaves having greater levels of ascorbate (229). This could be due to the role of ascorbate in plant growth, so faster growing plants are more likely to have higher levels of ascorbate. Equally, younger leaves have higher rates of photosynthesis, and ascorbate has a role in the protection of photosynthesis, so the higher levels of ascorbate could be due to this.

Plants grown in higher light levels have been reported to have higher ascorbate content (230). The post-harvest storage of spinach in the light compared to the dark was also shown to increase the ascorbate levels (231). It has been suggested that light/dark cycles during postharvest storage of spinach leaves increased the nutritional quality (232). This increase in nutritional quality could include an improvement in the retention of ascorbate, as it has been demonstrated that intracellular ascorbate levels in spinach follow a circadian rhythm, with the peak level occurring around midday (233). This in turn would suggest that the time of harvest would be important for the ascorbate content, especially if the harvested leaves were then stored in the dark.

Post-harvest treatments of salads are also known to affect ascorbate levels. Storage temperature is especially important (223), and most commercial salad processing plants aim to keep the temperature as low as possible to avoid the loss of ascorbate. Carrots (234) and a selection of vegetables including spinach and kale (235), as well as iceberg lettuce (236), all showed considerable increases in the loss of ascorbate with an increase in post-harvest storage temperature.

In order to increase the shelf life, salads would ideally be cooled quickly after harvesting. This can be achieved with vacuum cooling, which allows rapid cooling of leaves by evaporating some of the moisture from them (237). Vacuum cooling has been shown to increase the retention of ascorbic acid in iceberg lettuce during postharvest storage (238). It has also been reported to improve the sensory and nutritional qualities of spinach, but the effect on ascorbate specifically was not tested (239). The effect of vacuum cooling on the ascorbate content of spinach leaves will be reported on in the current study.

The washing process of pre-packaged salads is also a potential source of ascorbate loss. An important aspect of the washing process is to remove potentially pathogenic micro-organisms e.g. fungi. This can be achieved using various sanitizers, including chlorine or ozone-based sanitizers. Ozone treatment was found to significantly decrease the ascorbate

content of rocket leaves during storage (240). This loss of ascorbate is likely to be due to the oxidising nature of ozone, acting to degrade the ascorbate. Equally, iceberg lettuce washed in chlorinated water showed a marked decrease in ascorbate content after just one day of storage compared with lettuce washed in non-chlorinated water (241). Spinach leaves washed in chlorinated water also showed lower ascorbate content immediately after washing, when compared with washing in water alone (242). The ascorbate retention in spinach leaves during storage was considerably lower after washing with chlorine-based sanitizers compared with peroxyacetic acid-based sanitizers. (243). As with ozone, this loss of ascorbate could be due to the oxidising nature of chlorine.

Other steps in the processing of pre-packaged salads could also lead to a loss of ascorbate. The method of slicing used on iceberg lettuce influences the ascorbate content throughout shelf life, with hand-torn leaves showing a considerable increase in the retention of ascorbate compared with blade-cut leaves (236). This could be due to more severe wounds being incurred with hand-torn leaves, leading to an increase in ascorbate as a wound response.

The packaging atmosphere also influences the nutritional quality of processed salads. Flushing bags of shredded iceberg lettuce with nitrogen was shown to increase the retention of ascorbate throughout shelf-life (236). This is presumably due to the lack of oxidation occurring in the nitrogen atmosphere. Other modified atmosphere packaging (MAP) techniques, such as increasing CO₂ and decreasing O₂ levels, led to an increase in ascorbate retention in spinach (244). However, this effect does not occur in all species, with several fruits (245) as well as Swiss chard (246) showing a decrease in ascorbate content when stored in MAP compared with air.

There is much interest in increasing the ascorbate content of food (247). The benefit of this would potentially be two-fold, as this would create more nutritious crops, as well as making the crops themselves more tolerant of stress, such as oxidative stress (147,169,248,249). Although ascorbate can be easily synthesised chemically and then added to food there is a general trend away from adding additives to food, creating a market for ascorbate-enriched crops. The increase of ascorbate in crop plants could be achieved by either increasing the biosynthesis or decreasing the degradation. Either of these could be done genetically, or by altering growth conditions and postharvest treatment practices. This project has focussed on the postharvest processing of salad leaves as potential areas in which the loss of ascorbate could be avoided.

1.13 Outline of project

This PhD project aims to expand on the knowledge of vitamin C degradation *in vitro*, in plant cell-suspension cultures and in harvested salad leaves.

Ascorbate has a well-established role as an important antioxidant, but the fate of ascorbate itself during these reactions is little known. The fate of ascorbate derivatives *in vitro* (both radiolabelled and non-radiolabelled) has been investigated in reactions with various ROS, including hydrogen peroxide, superoxide, hydroxyl radical and singlet oxygen. Studying the degradation products formed from these different ROS may provide a tool which would identify the oxidative stress that a plant was currently undergoing. As well as this, the oxidation products themselves may serve roles in the plant, and so information about their formation would be invaluable.

The fate of oxidation products of AA, namely OxT and cOxT, has been studied in cell-suspension cultures. In particular the potential of cOxT to form oxalyl cross-links between cell wall components has been investigated. These investigations led to the discovery of a novel acyltransferase enzyme activity, which produces novel products of oxalyl sugar esters, which remain stable in plant cell-suspension cultures. Evidence for the formation of oxalyl esters with cell wall components of cell-suspension cultures, as well as free sugars, has also been found. This could provide a novel function for ascorbate-oxidation products in cell growth. An acyltransferase could act to transfer an oxalyl group from cOxT to cell wall components, forming an oxalate bridge, which would potentially have a role in remodelling the cell wall.

As well as oxidation, DHA can also be hydrolysed. Previous work has detected two further degradation products of the DHA hydrolysis product DKG, named compounds C and E. Further work has been undertaken to purify and characterise these compounds, using MS and NMR techniques. Another catabolite of DKG has been demonstrated to inhibit peroxidase activity (84). Further work has been carried out in an attempt to purify and characterise this ascorbate-derived peroxidase inhibitor (PxI).

The ascorbate content of postharvest salad leaves has also been studied. The ascorbate content of numerous salad species throughout storage has been monitored, as well as the ascorbate content throughout the commercial washing process of spinach leaves, which proved to be the most susceptible of the species tested to the loss of ascorbate. There is commercial interest in increasing the ascorbate content of pre-packaged salads, particularly from a nutritional perspective, as ascorbate is known to have various health benefits.

Therefore, it would be valuable to ascertain whether the washing process is contributing to post-harvest losses of ascorbate, which could be avoided by altering the washing procedure, thus increasing the ascorbate content of the salads.

These various different aspects of the degradation of vitamin C have allowed the degradation of ascorbate to be described in more detail, as well as suggesting some novel roles for ascorbate degradation products, especially in relation to plant growth and the production of acyl sugars. The studies on the degradation of ascorbate in salad plants may provide the opportunity for improvement in the washing process of spinach, enabling the production of pre-packaged spinach with an increased vitamin C content.

Materials and methods

2.1 Materials and chemicals

All chemicals used were purchased from Sigma-Aldrich (Poole, UK), Fischer Chemicals (Loughborough, UK) or Megazyme (Bray, Ireland). L-[1-¹⁴C]Ascorbate was purchased from Amersham Pharmacia Biotech UK Ltd. All water used was deionised.

2.2 Plant cell suspension culture

2.2.1 Arabidopsis cell culture media

Arabidopsis thaliana cell culture was grown in Murashige and Skoog (250) basal salt with minimal organics (4.4 g/l Sigma number M-6889) along with *a*-naphthalenetic acid (0.05 mg/l), kinetin (0.05 mg/l) and glucose (20 g/l). The pH was adjusted to 5.8 with 1 M KOH and 180 ml aliquots of media were transferred to 500-ml conical flasks.

2.2.2 Spinach cell culture media

Spinach cell culture was grown in Murashige and Skoog basal salt (4.4 g/l, Sigma number M-5524). Glucose was added to 1% final concentration (10 g/l). The pH was adjusted to 4.4 with 1 M NaOH and 180 ml aliquots of media were transferred to 500-ml conical flasks.

2.2.3 Rose cell culture media

Rose cell (Paul's scarlet rose) suspension culture medium was prepared containing CaCl₂ (74 mg/l), KH₂PO₄ (140 mg/l), KCl (750 mg/l), NaNO₃ (850 mg/l), MgSO₄·7H₂O (250 mg/l), MnSO₄·4H₂O (1 mg/l), H₃BO₃·4H₂O (0.2 mg/l), ZnSO₄·7H₂O (0.5 mg/l), KI (0.1 mg/l), CuSO₄·5H₂O (0.02 mg/l), CoCl₂·6H₂O (0.01 mg/l), Na₂MoO₄·2H₂O (0.02 mg/l), FeCl₃·6H₂O (5.4 mg/l), Na₂EDTA·2H₂O (7.4 mg/l), 2,4-D (1 mg/l), kinetin (0.5 mg/l) and glucose (20 g/l). The pH was adjusted to 6.0 with 1 M NaOH and 50 ml aliquots of media were transferred to 250-ml conical flasks.

2.2.4 Maintenance of cell suspension cultures

Cell suspension cultures were maintained in moderate constant light and a temperature of 25°C. The cultures were shaken constantly (100-115 rpm). Cultures were subcultured every two weeks. For *Arabidopsis* cell suspension cultures, approximately 20 ml of a two-week old

culture was transferred into 200 ml fresh medium. Rose cultures had approximately 15 ml of a two-week old culture transferred into 50 ml fresh medium. Spinach cells were subcultured by removing excess old medium, then dividing the cells into three flasks of 200 ml fresh medium.

One-week old cultures were typically used in experiments, unless stated otherwise.

2.3 Salad leaves growth conditions

2.3.1 Salad leaves grown at Vitacress, Hampshire

Most salad leaves used in experiments were grown commercially on farms in the Hampshire and Wiltshire area for Vitacress Salads Ltd, from June to August of 2013. The salads were processed on an industrial scale at Vitacress Salads premises. Salad leaves used in experiments outside of these dates were either grown at University of Edinburgh or purchased from a local supermarket. The purchased salads originated from Vitacress.

2.3.2 Salad leaves grown in University of Edinburgh facilities

A commercial variety (Toucan) of spinach seeds were provided by Vitacress Salads Ltd. The seeds were grown in soil at controlled temperatures of 21°C (day) and 16°C (night), 16 hour day length, in light levels of 150 $\mu\text{mol m}^{-2} \text{s}^{-1}$ in University of Edinburgh facilities. Leaves were harvested for experiments 4 weeks after sowing.

2.4 High-voltage paper electrophoresis

2.4.1 One dimensional HVPE at pH 2.0 and pH 6.5

Aqueous samples (generally between 5 and 20 μl) were loaded onto Whatman 3MM paper (57 cm in length, with variable width depending on the number of samples) at an origin 12 cm from the bottom of the paper. After the samples had dried onto the paper, the paper was carefully wetted with electrophoresis buffer; pH 2.0 (formic acid/acetic acid/water, 1:35:355, v/v/v) or pH 6.5 (pyridine/acetic acid/ water, 33:1:300 v/v/v). Excess buffer was removed from the paper by blotting with tissue paper. The paper was then placed in a tank (Figure 8), suspended from a trough of electrophoresis buffer (pH 2.0 or pH 6.5). The other end of the paper was submerged in buffer in the bottom of the tank. The rest of the tank was filled with an immiscible coolant (white spirit for pH 2.0 electrophoresis and toluene for pH 6.5 electrophoresis). The tank used for electrophoresis at pH 6.5 had pyridine (~2% final

concentration) added to the toluene coolant, to ensure the pH remained stable during the HVPE run. A voltage (2.5-3.5 kV) was run through the buffers, for 30- 70 minutes, to allow the separation of compounds based on their charge : mass ratio.

Orange G (2 μ l, 0.5% w/v) was added to all samples as an internal marker. Electrophoretic mobilities were calculated relative to orange G (m_{OG}). Neutral compounds move a small distance away from the origin due to electro-endo-osmosis, so mobilities were calculated using a neutral marker (such as glucose) as the zero point.

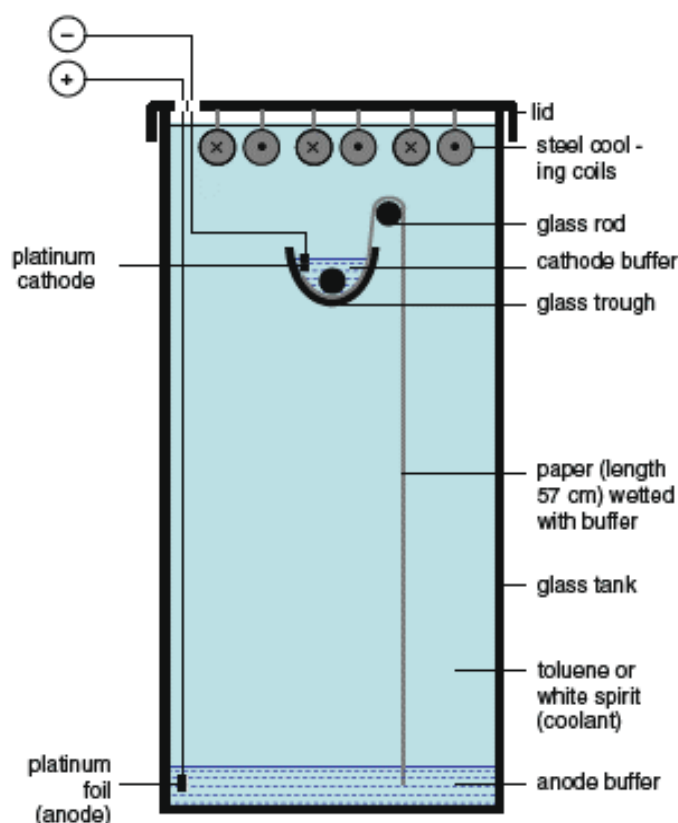


Figure 8: Diagram of HVPE apparatus. The experimental set-up of high-voltage paper electrophoresis. S.C Fry, In The Plant Cell Wall: Methods and Protocols (Z.A Popper, ed.). New York: Springer (5)

Preparative HVPE required the sample for preparation to be loaded onto the origin as a streak, rather than as discrete spots, as with analytical HVPE. The rest of the HVPE procedure is as described previously.

2.4.2 Two dimensional HVPE

A single sample, along with markers, was loaded onto Whatman 3MM paper and subjected to one dimensional paper electrophoresis as described above. After one dimensional HVPE the paper was allowed to dry completely before the lane containing the sample to undergo two dimensional HVPE was carefully cut out. This lane was then sewn onto the origin of a new sheet of Whatman 3 MM paper, so the compounds in the sample lane were lined up along the new origin. This new paper was then subjected to electrophoresis at either pH 2.0 or pH 6.5 as described previously.

2.5 High-pressure liquid chromatography

Aqueous samples (25 µl injection volume) were separated on a Dionex BioLC system with a Phenomenex Rezex ROA column. The samples were eluted in 47 mM H₂SO₄ or 0.1% TFA at a flow rate of 0.5 ml min⁻¹. The products were detected by UV absorbance at 210 nm and 250 nm. The eluate was collected in fractions (every 15 seconds).

Before further analysis, by MS or NMR, the eluate in 47 mM H₂SO₄ required neutralisation. This was done by the addition of Ba(OH)₂. In order to avoid this neutralisation step, some later samples were eluted in 0.1% TFA instead of H₂SO₄. The samples then did not require neutralisation as TFA does not interfere with NMR spectroscopy.

2.6 Thin-layer chromatography

Aqueous samples (generally 2 µl) were loaded onto an origin 1 cm from the base of a 20 cm by 20 cm silica-gel thin-layer chromatography (TLC) plate. After loading, the plate was placed in a glass tank containing 80-100 ml solvent, and the tank sealed with a glass lid. The solvent was allowed to move through the plate by capillary action until the solvent front reached the top of the plate (4-8 hours). The TLC plate was thoroughly dried before staining.

The solvent systems used were:

- i. BuOH: HOAc: H₂O (4:1:1)
- ii. BuOH: HOAc: H₂O (2:1:1)
- iii. BuOH: PrOH: HOAc: H₂O (1:1:1:1)

2.7 Anion-exchange column chromatography

2.7.1 Purification of [¹⁴C]DHA by anion-exchange column chromatography

[¹⁴C]DHA was produced from commercial [¹⁴C]AA, either using ascorbate oxidase (from *Cucurbita* species, 1 U μl^{-1}) or H_2O_2 (2 mol equivalent to [¹⁴C]AA).

A Dowex 1 anion-exchange chromatography column (50 μl bed volume) was set up in a 200- μl pipette tip. The column was washed sequentially in 500 μl of 0.5 M NaOH, 0.5 M formic acid, 2 M sodium formate and 10 mM formate pyridine buffer (pH 5). Some experiments required the column to be washed in H_2O as a final step.

The sample (20-50 μl) was loaded onto the column and the neutral compounds eluted initially in nine loadings of 50 μl of either formate buffer (10 mM, pH 5) or H_2O . The eluate from the column was collected in 50 μl fractions.

The acidic compounds were eluted in six loadings (50 μl each) of increasing concentrations (in 0.05 M increments between 0.1 M and 0.3 M) of formic acid. This was followed by six loadings (50 μl) of 4 M formic acid, then six loadings (50 μl) of 4 M TFA.

All the fractions were stored at -80°C before further analysis.

2.7.2 Purification of DKG-derivatives C and E by anion-exchange column chromatography

A sample of DKG (0.5 ml) was prepared from NaOH-treatment of commercial DHA (section 2.11.1).

A Dowex 1 anion-exchange chromatography column (2-ml bed volume) was set up in a polyprep column. The column was washed sequentially with 4 ml each of 0.5 M NaOH, 0.5 M formic acid, 2 M sodium formate, 10 mM formate pyridine buffer (pH 5) and H_2O (8 ml).

The sample containing DKG and derivatives C and E (0.5 ml) was loaded onto the column and the neutral compounds eluted in nine loadings of 0.5 ml H_2O , collected as 10 0.5 ml fractions. The acidic compounds were eluted in three loadings (1 ml each) of increasing concentrations (in 0.05 M increments between 0.1 M and 0.3 M) of formic acid. This was followed by three loadings (1 ml each) of 4 M formic acid, then 4 M TFA.

All the fractions were dried under vacuum (Savant SPD1010 SpeedVac concentrator) and stored at -80°C before further analysis.

2.8 Detection of non-radiolabelled compounds

2.8.1 Staining of sugars on paper with silver nitrate

Dried paper electrophoretograms were dipped sequentially through three solutions (**i-iii**) with 15 minutes drying in between each step. The papers were dipped through solution **ii** twice. Immediately after dipping through solution **iii**, the paper was placed in cold running water for at least 1 hour, before drying overnight.

- i.** 5 mM AgNO₃ in acetone, minimal H₂O was added to redissolve precipitated AgNO₃.
- ii.** 0.125 mM NaOH in 96% ethanol
- iii.** 10% Na₂S₂O₃ in H₂O

2.8.2 Staining of phosphates on paper with molybdate

Concentrated HCl (3 ml) was added dropwise to rapidly stirring ammonium molybdate solution (17 ml, 11.8% w/v). Perchloric acid (6 ml, 60% v/v) was added dropwise to the solution and stirred until the precipitate redissolved. Acetone (180 ml) was then added to the solution. Paper electrophoretograms were slowly dipped through the molybdate stain solution. The paper was dried and any spots that appeared were marked with a pencil. The paper was then exposed to direct sunlight or UV light (254 nm) for 10 minutes and any new spots that appeared were marked.

2.8.3 Staining of reducing sugars on paper with Wilson's dip (aniline hydrogen-phthalate)

Paper electrophoretograms were dipped slowly through a solution of Wilson's dip (aniline hydrogen-phthalate). The paper was allowed to dry in the fume hood for 5 minutes before heating at 105°C for 15 minutes.

The Wilson's dip solution comprises 0.1 M phthalic acid in 49% acetone, 49% diethyl ether and 2% water. Immediately before using, 0.125ml aniline was added per 25 ml Wilson's dip solution.

2.8.4 Staining of acidic compounds on paper with bromophenol blue

Paper electrophoretograms to be stained with bromophenol blue were first dipped through a solution of methanol : acetone (1:2) several times to remove any traces of acid from the

electrophoresis buffers. The papers were then dried thoroughly in a drying oven overnight before staining.

The paper was dipped slowly through a solution of 0.04% bromophenol blue in 96% ethanol.

2.8.5 Staining of amines on paper in ninhydrin

Amino acids and amines were detected on paper after HVPE using ninhydrin stain. The paper was dipped slowly through a solution of 0.5% ninhydrin in acetone. The paper was allowed to dry for 5 minutes in the fume hood before being heated at 105°C for five minutes.

2.8.6 Staining of sugars on TLC with thymol

Sugars were detected on TLC plates using thymol stain. The thymol stain solution was prepared by adding 0.5 g thymol to 95 ml 96% EtOH. H₂SO₄ (5 ml) was then added drop wise until the thymol had completely dissolved.

The TLC plate was dipped slowly into a tank (containing 500 ml staining solution) and then partially allowed to dry in the fume hood for 5 minutes. Excess staining solution was removed with a paper towel to avoid spots caused by H₂SO₄. The TLC plate was then placed in a drying oven at 105°C for up to 10 minutes, until the spots were clearly visible.

The TLC plate was scanned immediately, as the spots fade over time.

2.8.7 Staining of compounds on TLC with molybdate

The molybdate reagent was prepared by dissolving ammonium molybdate (10% w/v) in 10% v/v H₂SO₄. The staining reagent was then prepared by mixing the 10% ammonium molybdate in H₂SO₄ solution with acetone in a 1:3 (ammonium molybdate: acetone) ratio.

The TLC plate was dipped into this staining solution, and excess solution was removed from the back of the plate with paper tissues, then the plate was allowed to partially air dry before incubating at 105°C for up to 30 minutes, or until there were clearly visible spots on the plate.

2.8.8 Staining of compounds on TLC with ninhydrin

Amino acids and amines were detected on TLC plates by staining in ninhydrin. The plate was dipped in a solution of ninhydrin (0.5%) in acetone. The plate was then heated at 105°C for 15 minutes.

2.9 Detection of radiolabelled compounds

2.9.1 Detection of radiolabelled compounds by autoradiography

Paper electrophoretograms containing [¹⁴C]-labelled compounds were exposed to photography film (Kodak BioMax MR-1 film) in the dark for a period of 5 days to 4 weeks. The films were then developed in an X-ray developer (Konica SRX-101A). Before autoradiography, the papers were marked with radiolabelled (¹⁴C) ink to allow the film to be accurately positioned after development.

2.9.2 Quantification of radiolabelled compounds by scintillation counting

Samples were assayed for radioactivity in a Beckman LS 6500 CE multi-purpose scintillation counter. Aqueous samples were mixed in a 1:10 ratio (sample : scintillant) with Optiphase Hisafe scintillation fluid before assaying for radioactivity. Radiolabelled samples dried on paper were assayed with 2 ml Scintisafe scintillation fluid.

Samples which were suspected to contain ester bonds within the radiolabelled substrate were assayed in homemade scintillant to avoid the hydrolysis of the ester bonds. The scintillant was made up of 2,5 diphenyloxazole (3.3 g/l), and 1,4-bis (5-phenyl-2-oxazolyl) benzene (0.33 g/l) in a solution of toluene and Triton X 100 (2:1).

2.10 Elution of ascorbate derivatives from paper

Derivatives of ascorbate were separated by HVPE. The individual compounds could then be eluted from the paper, providing a preparation of a purified ascorbate degradation product. The compounds were eluted using the syringe barrel method (251).

The compounds to be purified were run by HVPE along with marker compounds. The marker strips were stained in AgNO₃ and then the area corresponding to the compound of interest was marked on the unstained paper. If the compounds to be purified were radiolabelled then the paper was autoradiographed (section 2.9.1) and the position of the compounds marked on the paper using the film as a guide.

The area of the paper electrophoretogram containing the compound of interest was cut out and rolled up as tightly as possible. The rolled up paper was then placed in a 5-ml syringe, which was itself placed in a 15-ml Greiner tube. Water, or in some cases 70% ethanol, (1 ml) was added to the paper in the syringe. The tube, with the syringe, was then centrifuged at 2500 rpm for 5 minutes. Further centrifugation steps after the addition of 0.5 ml water or

ethanol were carried out. After the last 0.5 ml eluate was added, the tube was centrifuged for 15 minutes at 3000 rpm.

After the elution the compounds were dried in a SpeedVac concentrator (Savant SPD1010) and redissolved to an appropriate concentration and stored at -80°C.

2.11 Preparation of diketogulonate

2.11.1 Preparation of diketogulonate from dehydroascorbic acid: method 1

Diketo-L-gulonic acid (DKG) was prepared from commercial DHA by alkali hydrolysis. NaOH (60 mM) was added to a solution of DHA (50 mM). The reaction was stopped after 6 minutes with H₂SO₄ (30 mM). The resulting solution of DKG was stored at -80°C.

2.11.2 Preparation of diketogulonate from dehydroascorbic acid: method 2

A solution of 3 M DHA in DMF (40 µl) was incubated with 200 µl of 0.75 M NaOH for 30 seconds. HOAc (1.5 M, 100 µl) was added to stop the reaction. For use in experiments the DKG was diluted to 50 mM in H₂O. The DKG was stored at -80°C.

2.11.3 Preparation of diketogulonate from ascorbic acid: method 3

A solution of ascorbic acid (0.12 M) was incubated with potassium iodate (0.36 M) for five minutes. After five minutes KOH (1 M) was added dropwise until the solution became colourless. Cold EtOH (8 volumes, -20°C) was added to precipitate the DKG. The precipitated DKG was vacuum filtered, rinsed in 70% EtOH and dried. The DKG was stored at -80°C.

2.12 Mass spectrometry of ascorbate derivatives

Samples were purified for mass spectrometry by preparative HVPE (section 2.4.1) followed by elution from the paper (section 2.10) or by anion-exchange column chromatography (section 2.7). The mass spectrometry analysis was carried out by Dr Logan McKay from the School of Chemistry at the University of Edinburgh.

Negative-ion electrospray ionisation mass spectrometry was carried out on aqueous samples using a Fourier transform ion cyclotron mass spectrometer (Bruker 12 T SolariX).

2.13 Nuclear magnetic resonance spectroscopy of ascorbate derivatives

Samples were purified for NMR spectroscopy analysis by separation by HPLC (section 2.5) or by preparative HVPE (section 2.4.1) followed by elution from the paper (section 2.10). The NMR spectroscopy analysis was carried out by Dr Lorna Murray and Prof Ian Sadler from the School of Chemistry at the University of Edinburgh. Proton NMR and ^{13}C NMR analyses were carried out, on a Bruker Avance NMR spectrometer 500 MHz with DCH cryoprobe optimised for $^{13}\text{C}/^1\text{H}$.

2.14 *In vitro* oxidation of ascorbate derivatives by reactive oxygen species

2.14.1 Conditions used for the ROS reactions

All ROS reactions were carried out in pH 4.8 sodium acetate (0.1 M) buffer. The reactions were carried out over a time course of up to 30 minutes (unless otherwise stated). Singlet oxygen experiments were carried out over 24 hours to allow for the formation of the ROS. The reactions were stopped with the addition of an enzyme (catalase or superoxide dismutase) or EtOH (50% final concentration). The samples were stored at -80°C before further analysis. The samples were analysed by HVPE at pH 6.5 or pH 2.0, and stained in silver nitrate.

Experiments involving [^{14}C]DHA were conducted at lower concentrations, and the paper was subjected to autoradiography after HVPE.

2.14.2 Generation of ROS

- i. Hydrogen peroxide (H_2O_2) was used at equimolar concentrations (unless otherwise stated) to the ascorbate derivative substrate, either DHA or DKG. The reactions were stopped with either the addition of EtOH (50% final concentration) or catalase (from bovine liver, 0.01% final concentration).
- ii. Superoxide ($\text{O}_2^{\cdot-}$) was generated from KO_2 , which is known to produce the superoxide radical in solution. KO_2 was added to the reaction mixture in an equimolar concentration to DHA or DKG, and this was assumed to equate to equate to an equimolar concentration of $\text{O}_2^{\cdot-}$. The reaction was stopped with either the addition of EtOH (50%) or the addition of superoxide dismutase (from bovine erythrocytes, 0.01%).
- iii. Hydroxyl radical ($\cdot\text{OH}$) was generated from the reaction of FeSO_4 and H_2O_2 in the presence of EDTA. These three components were used in equimolar

concentrations to each other. H₂O₂ was the final component to be added to the reaction mixture. The reaction was stopped by the addition of EtOH (50%). This solution of H₂O₂, FeSO₄ and EDTA is referred to as ‘OH-producing mixture’ throughout the report.

- iv. Singlet oxygen (¹O₂) was produced from the photosensitiser dyes eosin, rose Bengal and riboflavin in the presence of light. The samples were incubated with 1 mM or 10 mM photosensitiser dye, under a fluorescent light. Control samples containing the dye but incubated in the dark were also analysed. Riboflavin showed the highest singlet oxygen activity, so most singlet oxygen studies were carried out using riboflavin.

2.15 Alkali treatment of ascorbate derivatives C and E

Compounds C and E, purified by preparative HVPE (section 2.4.1) were treated with alkali to promote lactonisation (formation of compound C). Small aliquots (20 µl) of each compound were incubated in 0.1 M NaOH (final concentration) for up to 16 hours. The reaction was stopped by the addition of excess HOAc (0.2 M). Control samples were incubated in 0.2 M HOAc for up to 16 hours before being neutralised with 0.1 M NaOH.

The samples were analysed by HVPE and detected by silver nitrate staining.

2.16 The fate of radiolabelled ascorbate derivatives to plant cell suspension cultures

2.16.1 The fate of [¹⁴C]AA derivatives in live plant cell suspension cultures

Spinach, rose or *Arabidopsis* cell-suspension cultures (7 days after subculturing, unless otherwise stated) were inoculated with radiolabelled ascorbate derivatives ([¹⁴C]DHA, [¹⁴C]OxT or [¹⁴C]OxA), purified by previously discussed methods in sections 2.7, 2.4.1 and 2.10.

Cells from the cell culture to be used were filtered from the culture medium through four layers of Miracloth. Aliquots of cells (250 mg) were resuspended in 500 µl culture medium in small glass vials. The cell cultures were constantly shaken throughout the experiment to ensure the culture did not become anaerobic. The cultures were also in constant light. The cultures were incubated for at least 1 hour before the addition of the radiolabelled compounds (~ 200 Bq, in 1-5 µl) at time 0.

Samples of culture medium (50 μ l) were taken in triplicate at specified time points and stored at -80°C until further analysis.

Alcohol insoluble residue (AIR), comprising predominantly cell wall components, was prepared from the cell cultures through repeated washing of the cells. Initially the remaining culture medium was removed, and the cells were transferred to a 15-ml Greiner tube. Each washing step involved a 5 ml wash volume, with the samples being incubated on a rotary wheel for at least 20 minutes. After the incubation on the wheel the tubes were centrifuged for 10 minutes at 2500 rpm. After centrifugation the aqueous fraction of the sample was removed, leaving the insoluble pellet to be washed again in the subsequent steps. The cells were washed sequentially in H₂O, 70% EtOH, acidified EtOH (75% EtOH with 5% formic acid), 50 mM EDTA and a repeated 70% EtOH or H₂O step.

After the final wash the AIR was either suspended in a solution (H₂O or EtOH) and mixed with scintillation fluid for quantification by scintillation counting (section 2.9.2), or dried for further analysis.

2.16.2 The fate of [¹⁴C]AA derivatives in frozen/thawed or boiled cell cultures

The effect of boiling or freezing and thawing cell cultures on the metabolism of ascorbate derivatives was tested.

For the boiled cells experiments, 7 day-old cell cultures (spinach, rose or *Arabidopsis*), including the culture medium, were portioned into 40 ml aliquots and boiled at 100°C for 1 hour. The samples were then cooled before treating as described in section 2.16.1.

For experiments involving frozen/thawed cells, 7 day-old cell cultures (spinach, rose or *Arabidopsis*) were portioned into 40 ml aliquots and frozen at -20°C, for at least 16 hours. The samples were thawed before treating as in section 2.16.1. The cells were frozen either in the culture medium, or filtered on Miracloth first and then frozen in minimal additional H₂O.

2.16.3 Alkali hydrolysis of radiolabelled AIR

Radiolabelled AIR, prepared as described in section 2.16.1, was incubated in NaOH (0.1 M, 100 μ l for ~25 mg AIR) for one hour in order to cleave any ester bonds present. After one hour excess HOAc (0.2 M, 100 μ l) was added to stop the reaction.

The entire sample, including the insoluble fraction if possible, was loaded onto Whatman 3 MM paper along with an internal marker of orange G. Markers of [¹⁴C]OxA and non-

radiolabelled Glc were also loaded. The paper was run by HVPE at pH 6.5. After drying, the paper was cut into fractions and each fraction assayed for radioactivity by scintillation counting (section 2.9.2).

2.16.4 Enzyme treatment of radiolabelled AIR

Radiolabelled AIR, prepared as described in section 2.16.1, was incubated with various enzymes that act on the cell wall in order to determine the compounds that have formed an ester bond with [¹⁴C]OxT. The enzymes used were endopolygalacturonase, cellulase (known to also act on xyloglucan), and cellulase (does not act on xyloglucan). All the enzymes were prepared as 0.1% solutions in pyridine: acetic acid: 0.05% chlorobutanol (1:1:98).

Before treating the AIR with the enzymes, the enzymes were analysed for esterase activity. This was done by incubating [¹⁴C]OxT with the enzyme solution for 16 hours, either at room temperature or 37°C. The solution was then run by HVPE at pH 6.5, and the paper exposed to film to create an autoradiogram to determine whether [¹⁴C]OxT was stable in the presence of the enzyme.

2.17 Acyltransferase purification and assay

2.17.1 Eluting cell wall enzymes from plant cell-suspension cultures

Cell wall proteins (including enzymes) were eluted from spinach or *Arabidopsis* cell cultures 7 days after sub-culturing, unless otherwise stated. The spent culture medium of one flask of cell culture (200 ml) was filtered off through 4 layers of Miracloth. The culture medium was then stored at -80°C until required. The remaining cells were rinsed in 500 ml H₂O before being resuspended in 1 M NaCl (100 ml, pH 5 with 5 mM succinate buffer). The resuspended cells were shaken in the salt solution for 1 hour at 4°C. After 1 hour the eluate was separated from the cells by filtering again through 4 layers of Miracloth. The eluate (100 ml) was then placed into dialysis tubing (molecular cut-off 3.5 kDa). Dialysis was carried out against H₂O for 24 hours at 4°C, with multiple changes of H₂O to remove the NaCl from the eluate. After dialysis the enzyme extract was dried by freeze drying (Edwards freeze drier). The freeze dried enzyme extracts were stored at -80°C.

The culture medium removed in the first step was also dialysed and freeze dried, to test the medium for enzyme activity.

2.17.2 Acyltransferase assay with cell cultures

Aliquots of 7 day-old spinach or *Arabidopsis* cell culture (10 µl) were incubated with ~ 200 Bq [¹⁴C]OxT and an acceptor substrate (5% final concentration) such as a sugar or oligosaccharide for a given incubation time (up to 16 hours). Aliquots of cell-free spent culture medium were also incubated with [¹⁴C]OxT and an acceptor substrate.

After the incubation period formic acid (10% final concentration) was added to stop the reaction. The whole sample was loaded onto the origin of Whatman 3 MM paper, along with an internal marker of orange G. The paper was run by HVPE at pH 6.5 (section 2.4.1). The paper was exposed to film for up to 4 weeks to detect any radiolabelled compounds that had formed during the reaction (section 2.9.1). These compounds could then be quantified by scintillation counting (section 2.9.2).

The acceptor substrates used were glucose (Glc), fructose (Fru), mannose (Man), galactose (Gal), xylose (Xyl), arabinose (Ara), maltose (Mal), cellobiose (CB) and sucrose (Suc).

2.17.3 Acyltransferase assay with enzyme extracts

Dialysed and freeze dried cell wall extracts from spinach and *Arabidopsis* were assayed for acyltransferase activity. The reaction mixture contained ~200 Bq of [¹⁴C]OxT, 5% final concentration of an acceptor substrate such as a sugar, and 1% enzyme extract in 10 mM PIPES buffer (piperazine-N, N'-bis(2-ethanesulfonic acid); pH 7). The reaction mixture was incubated for 4 hours (unless otherwise stated) and formic acid (10 % final concentration) was added at the end of the incubation period to stop the reaction.

The entire reaction mixture was loaded onto Whatman 3 MM paper along with an internal marker of orange G, and run by HVPE at pH 6.5 (section 2.4.1). The paper was then exposed to film for up to 4 weeks to detect the radiolabelled compounds, which could be then quantified by scintillation counting (section 2.9).

The acceptor substrates used were glucose (Glc), xyloglucan oligosaccharides (XGOs), raffinose (Raf), cellobiose (CB), glucosamine (GlcN), xyloglucan (XG, from tamarind), xylan (from birch wood), arabinogalactan (AG, from larch wood), arabinan (from sugar beet), homogalacturonan (HG, from orange), pectin (from citrus or apple) and RG I (from soy or potato).

2.17.4 Acyl transferase assay with polysaccharide-impregnated paper

Polysaccharide-impregnated paper was prepared by dipping Whatman 3 MM paper slowly through a 1% solution of polysaccharide: esterified pectin (from citrus fruit), homogalacturonan (from orange), xyloglucan (from tamarind) or xylan (from birch wood). The paper was then allowed to dry before being cut into 1.5 cm by 2 cm rectangles.

These small papers were rolled tightly and placed individually in 0.2-ml PCR tubes. The papers were then wetted with a solution (35 μ l) containing 1% enzyme extract (section 2.17.1) in pH 7 PIPES buffer (10 mM), along with a radiolabelled substrate (OxT, OxA or cOxT). The tubes were sealed tightly and incubated for up to 24 hours. After the incubation period the paper was removed from the tube and placed in 5 ml 70% EtOH or acidified EtOH (75% EtOH with 5% formic acid). The paper in the EtOH was rotated on a mechanical wheel for 30 minutes. The EtOH was then removed and a sample assayed for radioactivity on the scintillation counter (section 2.9.2). The paper was repeatedly washed in EtOH until no more radioactivity was released into the aqueous washings. The paper itself was then assayed for radioactivity by scintillation counting.

Activity of an acyltransferase would result in radiolabelled paper, as the [14 C]OxA group from the starting substrate (of OxT or cOxT) would have been substituted onto the cellulose-polysaccharide matrix of the polysaccharide-impregnated paper, by the formation of an ester bond.

2.18 Determination of ascorbate content of salad leaves using the DCPIP assay

The ascorbic acid content of samples of salad leaves was determined using DCPIP (dichlorophenolindophenol). Salad leaves (1 g) were ground in 5 ml of either metaphosphoric acid (2%), oxalic acid (252) (0.5%) or formic acid (0.5%) using a pestle and mortar. The thoroughly ground samples were then vacuum filtered and the filtrate collected, or the samples were centrifuged at 2500 rpm for 10 minutes and the supernatant collected. Aliquots (1 ml) of the filtrate or supernatant were taken in duplicate. DCPIP (0.1%) was added to each aliquot in 10- μ l shots until a pink colour remained for 10 seconds. The volume of DCPIP added was recorded and compared to a standard curve of ascorbic acid concentrations to calculate the ascorbic acid content of the salad sample.

2.19 Determination of ascorbate content of salad leaves during the washing process

2.19.1 Monitoring the ascorbate content of salad leaves during washing and storage on site at the Vitacress premises

Salad leaves harvested from Vitacress farms were stored on-site at 4°C for up to 10 days, and the ascorbate content of these leaves were analysed by titration with DCPIP (section 2.18) at time intervals. Different variables were tested in relation to loss of ascorbate during storage, including:

(i) The loss of ascorbate during storage of a range of salad species

Salad leaves were collected immediately after the commercial washing process and stored in plastic bags at 4°C for up to 10 days. The salad species used were: rocket (*Eruca sativa*), wasabi rocket, mizuna (*Brassica juncea var. japonica*), watercress (*Nasturtium officinale*), green Batavia (*Lactuca sativa*), iceberg lettuce (*Lactuca sativa*), spinach (*Spinacia oleracea*), red spinach (*Amaranthus dubius*), red chard (*Beta vulgaris, subsp. Vulgaris*), pea shoots (*Pisum sativum*) and fennel (*Foeniculum vulgare*).

(ii) The effect of the washing process on ascorbate loss.

Salad leaves (watercress, spinach and rocket) from the same harvest batch were sampled before and after the commercial washing process.

(iii) The effect of growth stage on ascorbate loss

Salad samples (spinach and watercress) at different growth stages were harvested and the ascorbate content measured throughout storage.

(iv) The effect of vacuum cooling on ascorbate retention in spinach leaves

Spinach leaves from the same harvest batch were taken and one crate was immediately stored at 7°C, whereas another batch was subjected to vacuum cooling (as is the protocol at Vitacress salads) for 1 hour before being stored at 7°C until both crates were transferred to the factory one day later. Vacuum cooling reduces the temperature of the leaves from ambient temperature (20°C) to approximately 5°C, at a pressure of 1 kPa.

2.19.2 Simulating the washing process in the laboratory

The industrial washing process was simulated under laboratory conditions. Spinach leaves grown under controlled conditions (section 2.3.2) were harvested four weeks after sowing. Samples of spinach leaves (1 g, in triplicate) were incubated either in air, in still water or in shaken water (on a small orbital shaker) for 1 hour. After this incubation the leaves were ground in 5 ml 0.5% oxalic acid or 0.5% formic acid, and the sample was vacuum filtered. Samples (1 g in triplicate) were also prepared immediately after harvesting (time 0).

DCPIP (0.1%) was added in 10- μ l shots to aliquots (1 ml, in duplicate) of the filtrate until a pink colour persisted for 10 seconds. The volume of DCPIP added was compared to a standard curve, and the ascorbate content of the sample was calculated (section 2.18).

2.19.3 The effect of chlorine on the retention of ascorbate during washing

The effect of chlorine on the retention of ascorbate in spinach leaves during washing was investigated. Samples of spinach leaves purchased from a local supermarket (1 g in triplicate) were incubated in plastic vials either dry (with no H₂O added), in H₂O or in chlorinated H₂O (100 ppm active chlorine from sodium hypochlorite), all with gentle shaking at 7°C for 1 hour. The ascorbate content was assayed by titration with DCPIP (section 2.18).

2.19.4 Monitoring degradation product formation during the washing process with [¹⁴C]AA

Spinach leaves grown in controlled conditions in the university glass house facilities were harvested 4 weeks after sowing (section 2.3.2). The petiole (cut flat with a razor blade) of a spinach leaf was placed in a round-bottomed tube containing [¹⁴C]AA (8 kBq) diluted to 50 μ l with H₂O. The [¹⁴C]AA was taken up into the leaf by transpiration. After this initial solution has been taken up, three further aliquots (50 μ l) of H₂O were added into the tube, to ensure all the [¹⁴C]AA was taken up. This feeding process was carried out for 1 hour, after which the presence of radioactivity in the leaf was confirmed with a Geiger counter.

One hour after the initial [¹⁴C]AA feeding the leaf was removed from the tube and 1 cm diameter leaf discs were cut out from the leaf, avoiding the main veins. Sets of four equivalent discs were prepared (Figure 9), and each disc within a set was subject to a different treatment. These discs are presumed to be equivalent in terms of the level of

radiolabelled compounds due to their positions. The two halves of the leaf are assumed to be identical. This allows direct comparisons to be made between these four leaf discs.

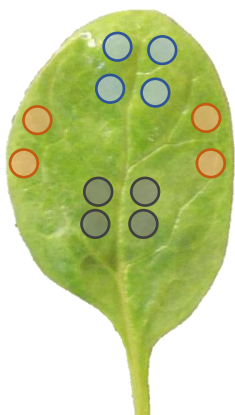


Figure 9: Sampling leaf discs from [^{14}C]AA-fed spinach. After a spinach leaf has been fed [^{14}C]AA leaf disc samples were taken. Discs (1 cm diameter) were punched out of the leaf, and four equivalent discs (shown in different colours, grey, blue and orange) were subjected to four different treatments. The four discs are presumed to contain an equivalent level of radiolabel, due to their position, under the assumption that the two sides of the leaf are identical.

The treatments included ‘time 0’ (the leaf disc extract is taken immediately) and three different washing steps; ‘in air’ (the leaf disc was incubated in an empty vial in humid conditions), ‘in still water’ (the leaf disc was incubated in a vial containing 5 ml H_2O), and ‘in shaken water’ (the leaf disc was incubated in a vial containing 5 ml H_2O and shaken on a mini bench-top shaker at ~200 rpm, Grant Bio PMS-1000). Leaf discs were incubated in the washing steps for 30, 60 or 120 minutes at 7°C . Five replicate sets (of the four treatments) of leaf discs were prepared for each of the three time points. After the appropriate incubation time the leaf disc was removed from the vial and the radiolabelled compounds extracted in 0.5% formic acid (200 μl), by grinding with a mortar and pestle. This extract was stored at -80°C until further analysis.

The extracts were centrifuged at 4000 rpm for 5 minutes, and samples of the aqueous portion were run by HVPE at pH 6.5 and pH 2.0 (section 2.4.1). The presence of [^{14}C]AA and any degradation products formed was detected by autoradiography or scintillation counting (section 2.9).

Results

3.1 Purification and identification of ascorbate degradation products C and E

3.1.1 Introduction to compounds C and E

DHA is known to form DKG under hydrolysing conditions (82). It has also been shown that DKG can be further degraded to form ThrO, xylonic acid and lyxonic acid *in vitro* and in animal tissues via oxidation and decarboxylation (2,253), alternatively DKG can be degraded to form the unidentified compounds C and E, first detected in rose cell-suspension cultures (72). The aims of the work in this chapter were to further identify and characterise the DKG-derivatives, compounds C and E.

3.1.2 Purification of C and E

Compounds C and E have previously been reported to be degradation products of DKG (1,72). The structures of these compounds have been hypothesised as 2-carboxy-xylonolactone and 2-carboxy-xylonate respectively (1), but not fully elucidated. In order to further investigate the nature of these compounds they first required purification.

DKG, the precursor of compounds C and E, was prepared by NaOH treatment of commercial DHA. It was observed that this method of producing DKG also yielded compounds C and E. Commercial DHA (50 mM), when incubated with 0.5 M NaOH, very quickly produced DKG, C and E (Figure 10). Most of the DHA had been hydrolysed to DKG and further degraded to compounds C and E almost immediately, as seen by the decrease in intensity of the silver nitrate-stained spots of DHA and DKG.

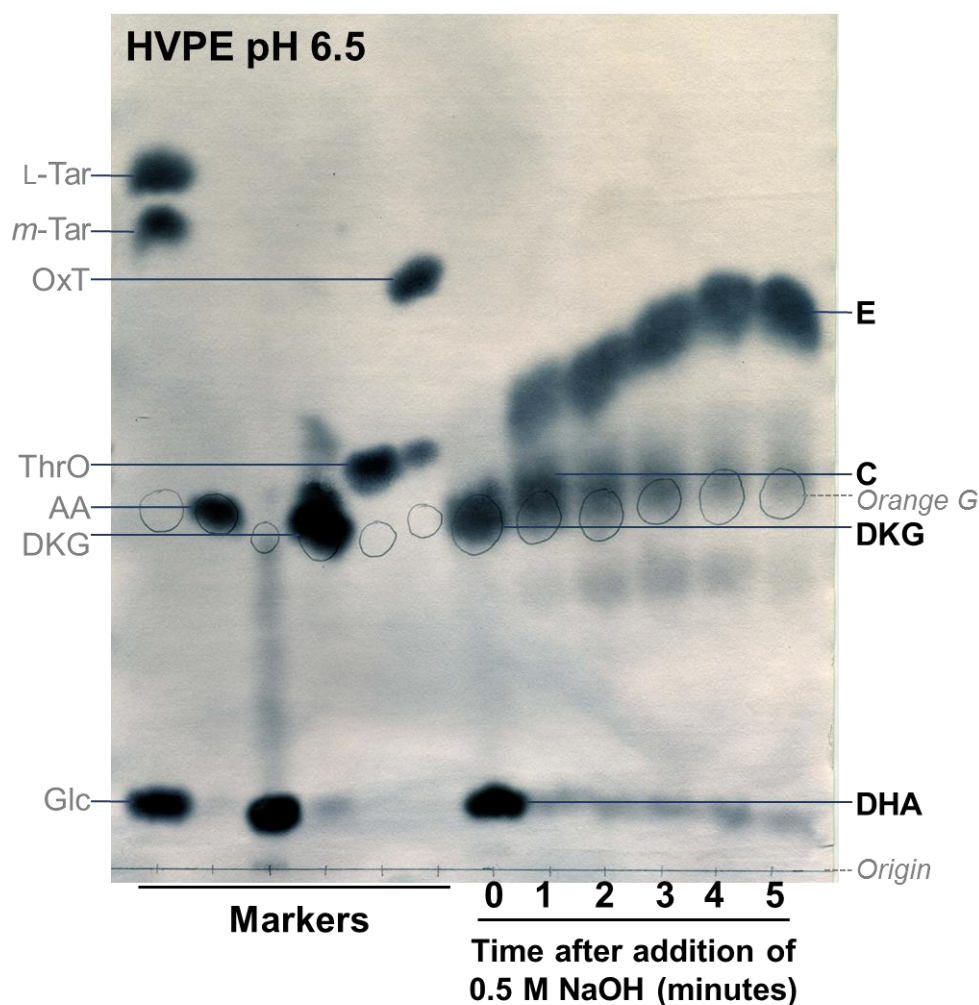


Figure 10: DKG, C and E are formed from NaOH treatment of DHA. 50 mM DHA was incubated with 0.5 M NaOH. Samples (10 μ l) were taken each minute and excess HOAc was added to stop the reaction. The samples were run by HVPE at pH 6.5. The paper was stained in silver nitrate. The 0 minute time point represents DHA which was treated with HOAc prior to the addition of NaOH, so was never in alkaline conditions.

As compounds C and E separate well by HVPE this was the method chosen for purification. An aqueous sample of DHA was hydrolysed with NaOH to form DKG and compound E, and excess HOAc was added to stop the reaction. The sample was subjected to preparative HVPE at pH 2.0. Marker strips from either edge of the paper were stained in silver nitrate to provide a visual guide for the location of the compounds of interest. Compounds C and E, and DKG, were eluted from the unstained portion of the electrophoretogram in H₂O (Figure 11 A), dried and redissolved in H₂O. Small samples of each of the compounds were re-run analytically by HVPE at pH 6.5 to verify their purity and identity (Figure 11 B). The compounds were identified from their mobility relative to orange G (m_{OG}).

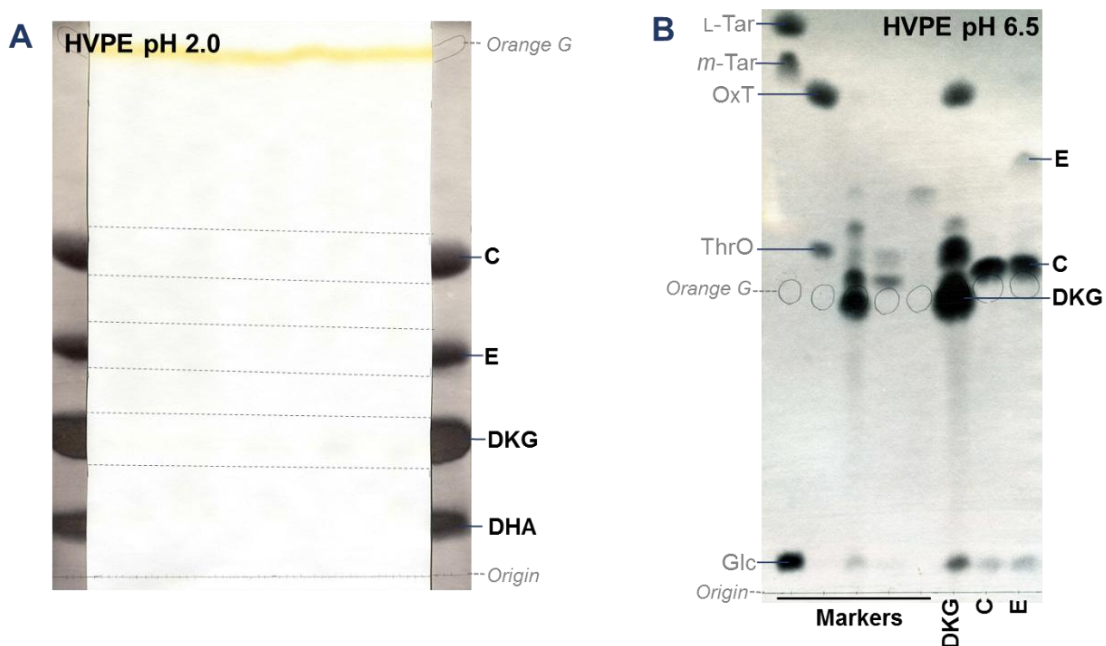


Figure 11: Purification of C and E by HVPE. An aqueous sample of 50 mM DHA (500 μ l) was incubated with 0.1 M NaOH (final concentration) for 7 minutes. The reaction was stopped with the addition of excess HOAc, and the whole sample loaded as a streak, along with orange G as an internal marker. The paper was run by HVPE at pH 2.0 at 2.5 kV for 60 minutes (A). Strips at the edge of the paper were stained in silver nitrate. After elution from the paper by the syringe-barrel method, the compounds were dried, redissolved in H₂O and small samples analysed by HVPE at pH 6.5 (B). The paper was then stained in silver nitrate.

3.1.3 C and E interconvert

Compounds C and E are known to interconvert, as compound C is the lactone of compound E (1). This interconversion can be used to further confirm the identity of these compounds. Alkaline conditions favour the formation of compound E (de-lactonisation), whereas acidic conditions favour re-lactonisation; the formation of compound C. Despite this, compound C was formed upon the NaOH treatment of DHA (Figure 11 A). This is likely to be because excess HOAc was added to the sample after NaOH treatment, resulting in the final solution being slightly acidic, allowing some of compound E to re-lactonise to compound C.

Purified aqueous samples of compound C and compound E were incubated in NaOH or HOAc for 16 hours. The samples were then neutralised, quickly loaded onto paper and analysed by HVPE at pH 6.5 and stained in silver nitrate (Figure 12).

After incubation in acidic conditions, compound C was more prevalent than compound E (Figure 12), whether the starting compound was C or E. Equally, alkaline conditions favoured the formation of compound E, independently of which compound was the starting substrate, C or E. This confirmed the identity of the purified compounds as C and E as defined by Green and Fry (72).

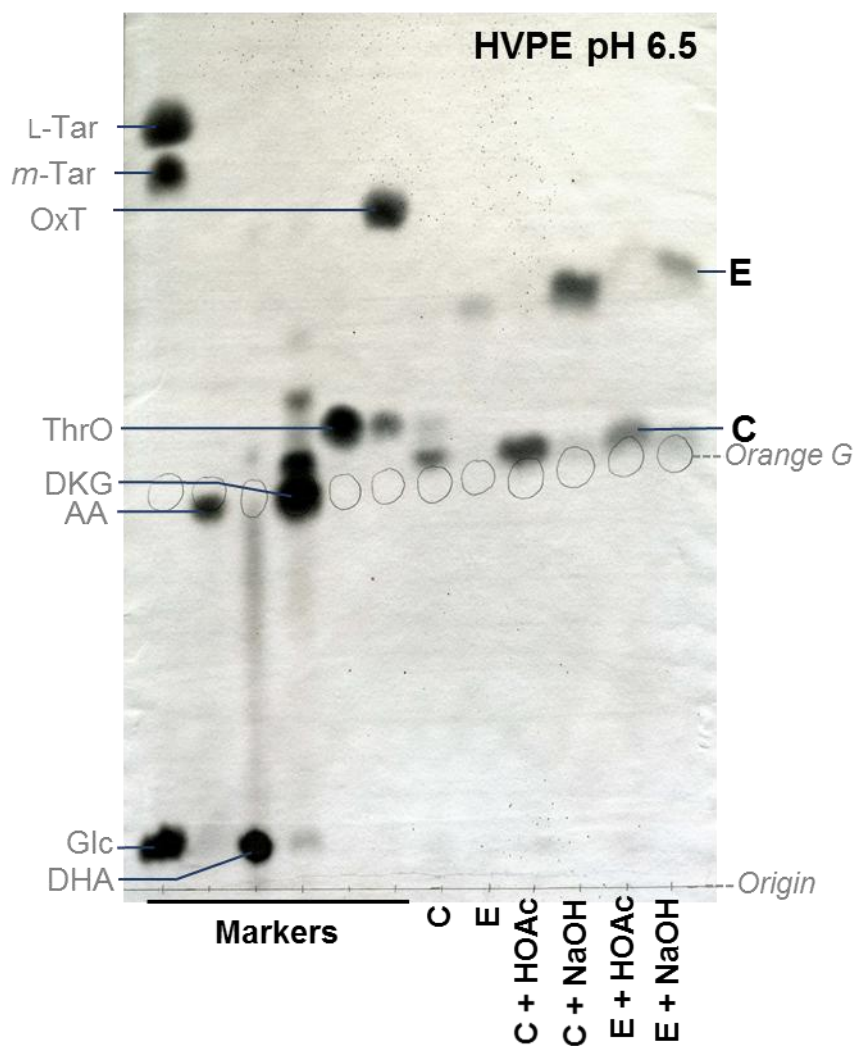


Figure 12: C and E interconvert. Purified aqueous samples of C and E were incubated for 16 hours in the presence of 0.1 M NaOH or 0.2 M HOAc. After incubation the samples were neutralised with either HOAc or NaOH. A small sample (20 μ l) of each was run by HVPE at pH 6.5. After drying the paper was stained in silver nitrate.

3.1.4 Further characterisation of compounds C and E using HVPE

It was observed that samples of compound E (originating from NaOH treatment of DHA and purified by preparative HVPE at pH 2.0) when re-run analytically by HVPE at pH 2.0 contained at least five distinct compounds as stained by silver nitrate (Figure 13). All five compounds were present in the untreated sample of compound E and in the sample treated with acid, which favours the formation of compound C. Only two of the spots were present after alkali treatment of compound E, labelled as E and C* (Figure 13).

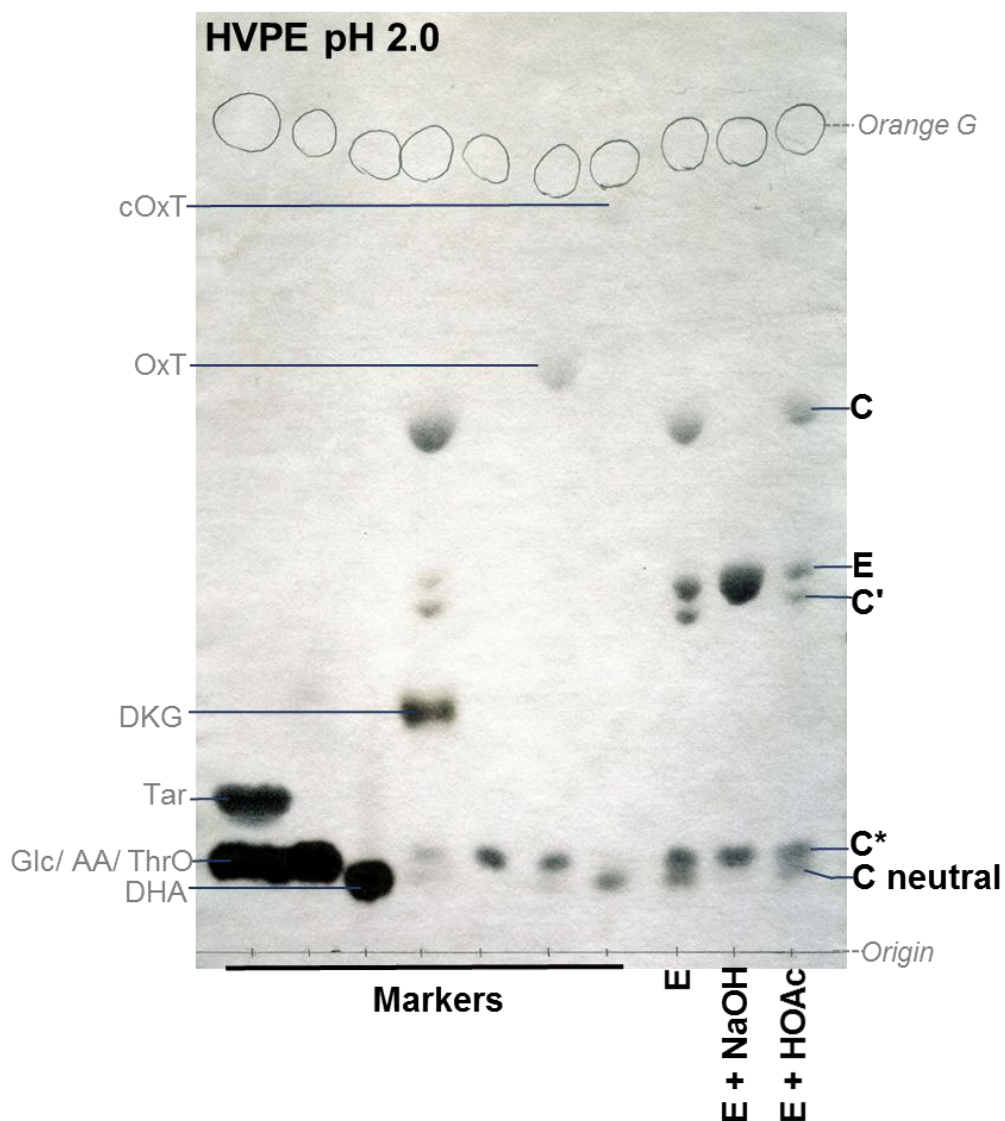


Figure 13: HVPE at pH 2.0 reveals that preparations of compound E contain numerous compounds. A preparation of compound E was incubated with 0.1 M NaOH or 0.2 M HOAc for 16 hours, before being neutralised, loaded onto paper and run by HVPE at pH 2.0. The paper was stained in silver nitrate.

As acidic conditions favour lactonisation, it was hypothesised that the compounds present in 'E + HOAc' sample included compound C, an epimer of compound C and potentially a double lactone of E, which would be neutral and appear in the area marked 'C neutral' (Figure 13). The two epimers of C were named C and C'.

In order to further explore the nature of these numerous compounds that arise during the hydrolysis of DKG, they required purification. This was carried out by preparative HVPE of a preparation of compound E that was known to contain all five of the C and E-related compounds (Figure 14 A). After these compounds were eluted from the preparative electrophoretogram, they were dried and redissolved in H₂O. Small samples of each of the compounds were then run by HVPE to determine their purity (Figure 14 B). All the compounds contained a silver nitrate-stained spot in the neutral position. This neutral product could consist of compounds that originate from the paper itself and had been eluted along with the compounds of interest.

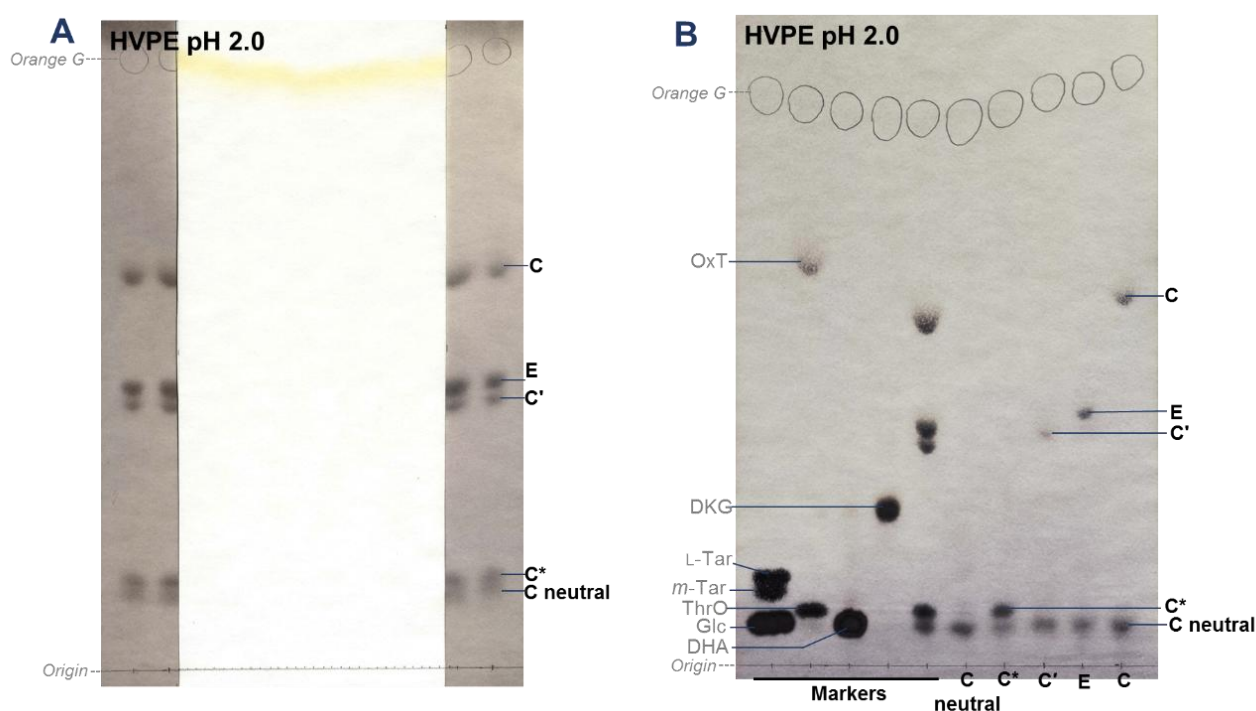


Figure 14: Purification of five C and E-related compounds. A sample of E, known to contain numerous C and E-related compounds was run preparatively by HVPE at pH 2.0. Strips from either edge of the paper were cut off and stained in silver nitrate (A). The areas on the unstained electrophoretogram containing the compounds were cut out and the compounds eluted in H₂O. The eluted compounds were dried then redissolved in a smaller volume of H₂O. Samples (10 µl) of each compound was run by HVPE at pH 2.0, and the paper was stained in silver nitrate (B).

3.1.5 Identification of novel DKG hydrolysis products

In order to determine whether the five C and E-related compounds (named C, C', C*, C neutral and E) interconvert, the samples were subjected to 2D HVPE. Three 10- μ l aliquots of a solution known to contain all the compounds were run by HVPE; two at pH 2.0 and one at pH 6.5, along with markers to be stained in silver nitrate. After running, the lanes were carefully cut out. These strips were sewn onto the origin of a fresh sheet of Whatman 3 MM paper. This paper was run by HVPE at pH 2.0 or pH 6.5 and then stained in silver nitrate (Figure 15).

All five compounds were stable and did not interconvert throughout the duration of the HVPE run and the drying steps (Figure 15 A), as demonstrated by the diagonal line formed by the compounds after HVPE at pH 2.0 followed by HVPE at pH 2.0.

Although all the compounds separated during HVPE at pH 2.0, the compounds did not completely resolve during HVPE at pH 6.5. Compounds C, C' and C* had the same mobility at pH 6.5 (Figure 15 B and C).

Compound C has been proposed to have two epimers (1). The spot corresponding to compound C after HVPE at pH 6.5 comprises three separate spots when run at pH 2.0 (Figure 15 B). It is suggested that two of these spots correspond to the epimers of C (labelled C and C'). In order to determine whether these compounds were epimers of C, all the C and E-related compounds were treated with alkali and acid, which will promote de-lactonisation (formation of E) and re-lactonisation (formation of C) respectively (Figure 16).

Compound C was the most abundant of the five compounds, and clearly converted to compound E upon NaOH treatment (Figure 16). Compound C' also diminished upon NaOH treatment, converting to compound E; however, there was less of this compound so the spots were much fainter. The mobility of compound C* (which has the same mobility as compound C on HVPE at pH 6.5) did not change with alkali treatment, suggesting this compound is not a lactone. This demonstrates that the compounds labelled C and C' are epimers of the C lactone, and compound C* is a different compound.

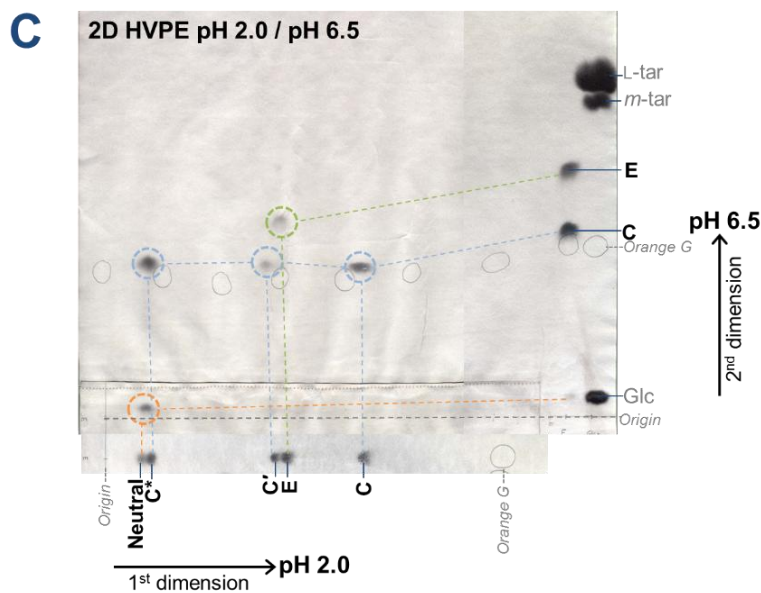
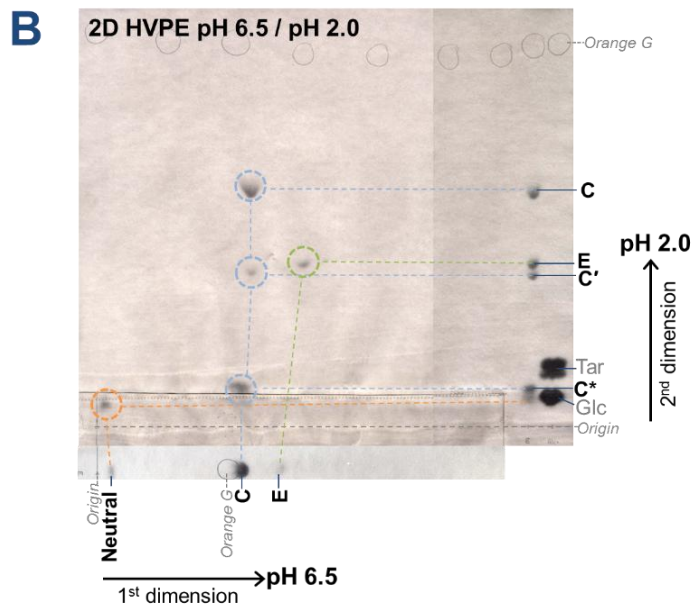
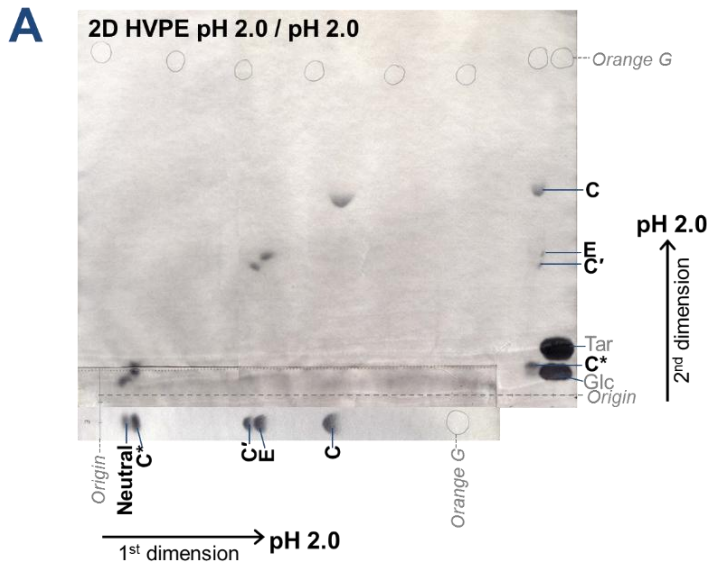


Figure 15: 2D HVPE of C and E-related compounds. Two 10- μ l samples of E (containing the five C and E-related compounds) were run by HVPE at pH 2.0, and one was run at pH 6.5, along with markers. The marker strips were stained in silver nitrate. The strips containing the now separated individual C and E-related compounds were then cut out and sewn onto the origin of a new sheet of Whatman 3 MM paper. These new papers were then run by HVPE at either pH 2.0 or pH 6.5. After the second HVPE run the papers were stained in silver nitrate. Orange G was present in both dimensional runs. For the 2nd dimension, fresh applications of orange G (2 μ l) were loaded along the new origin. The permeations of 2D HVPE include a run at pH 2.0 followed by pH 2.0 (A), a run at pH 2.0 followed by pH 6.5 (B) and a run at pH 6.5 followed by pH 2.0 (C).

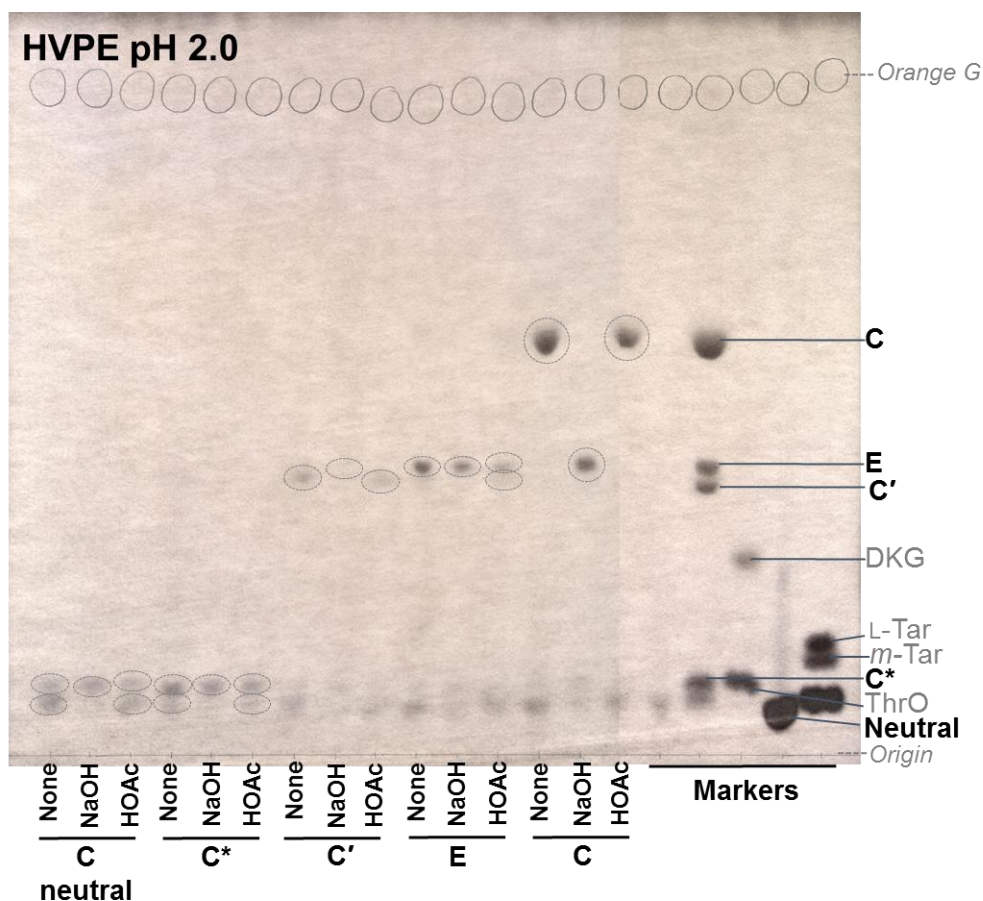


Figure 16: Alkali and acid treatment of individual C and E-related compounds. C and E-related compounds (10 μ l) that had been eluted from an electrophoretogram in H₂O were incubated with 0.1 M NaOH or 0.2 M HOAc or with neither for four hours. After four hours the NaOH samples were neutralised with HOAc and the HOAc samples were neutralised with NaOH, before loading onto paper. The paper was then run by HVPE at pH 2.0 and stained in silver nitrate.

The mobility of C* is similar to that of ThrO (a four-carbon monocarboxylic acid), although the mobility of C* is slightly slower than ThrO after HVPE at pH 6.5; the m_{OG} of ThrO is 1.26 and the m_{OG} of C* is 1.10. This would suggest that the charge : mass ratio of C* is smaller than that of ThrO, so C* is either larger or more charged than ThrO. Xylonic acid is

a five-carbon monocarboxylic acid, which has been reported to derive from ascorbic acid (4). It is hypothesised that the identity of C* could be xylonic acid.

A sample of C* was run alongside markers of xylonic acid, and a further sample of C* was spiked with commercial xylonic acid. After HVPE at pH 6.5, C* and xylonic acid did not resolve from each other (Figure 17). The sample that contained both C* and xylonic acid produced a single spot stained by silver nitrate, showing that C* has the same charge : mass ratio as xylonic acid. This suggests that the identity of C* could be xylonic acid, or a related five-carbon monocarboxylic acid such as lyxonic acid (also known to derive from ascorbic acid (4)) or ribonic acid, which would have the same electrophoretic mobilities at pH 6.5.

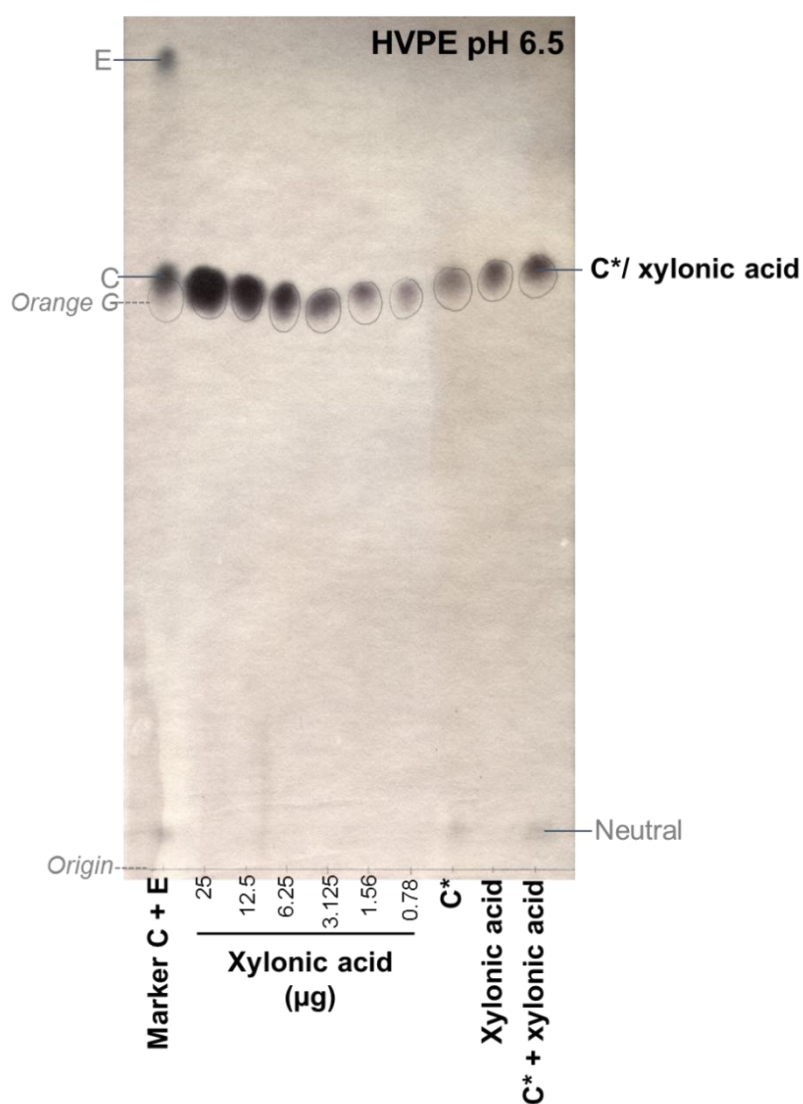


Figure 17: C* co-migrates with xylonic acid by HVPE at pH 6.5. A sample of C* (eluted from a preparative electrophoretogram) was run alongside a dilution series of a marker of commercial (Sigma Aldrich) xylonic acid. A sample of C* and xylonic acid were mixed together and run in one lane. The paper was run by HVPE at pH 6.5 until the orange G internal marker had travelled three quarters of the length of the paper. The paper was then stained in silver nitrate.

The C-neutral spot appeared to diminish upon alkali treatment (Figure 16), possibly forming a faint spot of E. This would support the theory that the neutral spot contains a double lactone of E, as well as contaminating compounds originating from the paper. However, the spot of C* (xylonic acid) in the C-neutral sample seems to have increased upon NaOH treatment. This may hint at the neutral product being a lactone of xylonic acid, xylonolactone. It is possible that the neutral spot contained both xylonolactone and a double lactone of compound E.

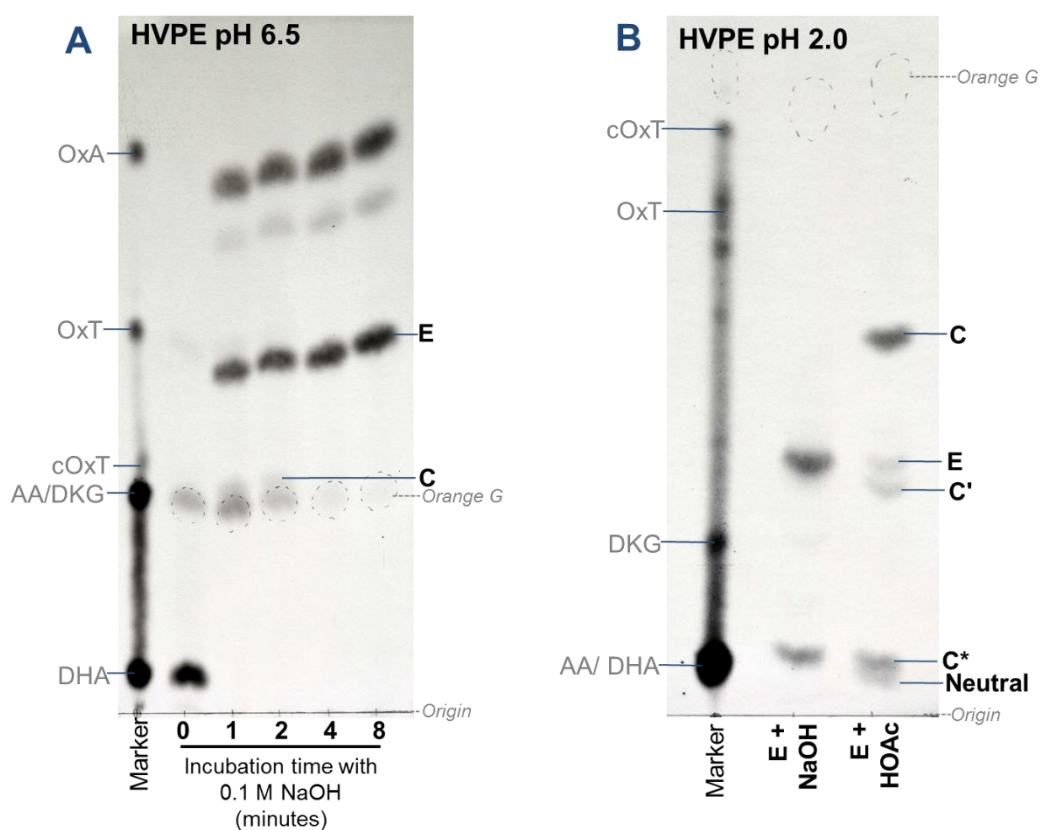


Figure 18: Purification and interconversion of $[^{14}\text{C}]$ E and C. Radiolabelled compound E was obtained through NaOH treatment of $[^{14}\text{C}]$ DHA (A). $[^{14}\text{C}]$ DHA was treated with 0.1 M NaOH for up to 8 minutes; the reaction was stopped by the addition of 0.2 M HOAc at the time points indicated. The samples were run by HVPE at pH 6.5, and then the paper was exposed to film to produce an autoradiogram. The predominant spot of compound E was eluted from the paper in H_2O using the syringe barrel method, then concentrated by vacuum evaporation. The resulting $[^{14}\text{C}]$ E (B) was incubated in 0.1 M NaOH or 0.2 M HOAc for 16 hours. The samples were neutralised and run by HVPE at pH 2.0. The paper was exposed to film to produce an autoradiogram. Internal markers of orange G were run on both electrophoretograms, along with a marker containing various AA degradation products.

Further evidence for the existence of an E double lactone, or xylonolactone, comes from experiments using radiolabelled C and E (Figure 18). [^{14}C]DHA, purified on an anion-exchange chromatography column (as described in sections 2.7.1 and 3.3.4), was treated with NaOH for up to 8 minutes. The [^{14}C]DHA was very quickly hydrolysed to [^{14}C]DKG, which was then further converted to compounds [^{14}C]C and [^{14}C]E, with E being the predominant product (Figure 18 A). These samples of compound E were eluted from the paper, and treated with either NaOH or HOAc (Figure 18 B). A by-product of [^{14}C]OxA was also produced (Figure 18 A), presumably from the oxidation of DKG, which would also yield ThrO, which would not be visible as it does not contain the radiolabelled carbon.

Treatment of [^{14}C]E with HOAc led to the formation of C compounds, including C, C', C* (putatively xylonic acid) and a neutral compound (Figure 18). All the compounds visible on the autoradiogram contain C-1 of the original [^{14}C]AA, as this is the carbon that is radiolabelled. This is especially noteworthy for the neutral spot, as this shows that the neutral compound originated from [^{14}C]E, and cannot be contaminating compounds eluted from the paper itself. The neutral spot is not present in the NaOH sample, suggesting that it was formed by the lactonisation of compound C or of compound C* (xylonic acid). This lends support to the hypothesis that the neutral compound could be a double lactone of compound E or xylonolactone.

3.1.6 The structures of C and E are supported by MS and NMR data

Purified C and E-related compounds were analysed by mass spectrometry (MS) and nuclear magnetic resonance (NMR) spectroscopy, in collaboration with University of Edinburgh School of Chemistry.

NMR studies were carried out on purified samples of compound C, obtained from NaOH hydrolysis of DKG, and separated by preparative HVPE, then eluted from paper in H_2O . Proton NMR (Figure 19) detects hydrogen atoms covalently bound to carbon atoms. The hypothesised structure of compound C contains four such hydrogen atoms. These four C-H bonds were identified on the NMR spectrum, and correspond to the suggested structure (Figure 19 B).

The pattern of the peaks within the spectrum provides information on the neighbouring C-H bonds. For instance the area corresponding to the H bound to C-5 consists of 8 peaks, meaning that C-5 has three neighbouring C-H bonds (one on C-4 and two on C-6). The peaks labelled H-6a and H-6b were distorted, the peaks on the outside of this bundle were smaller

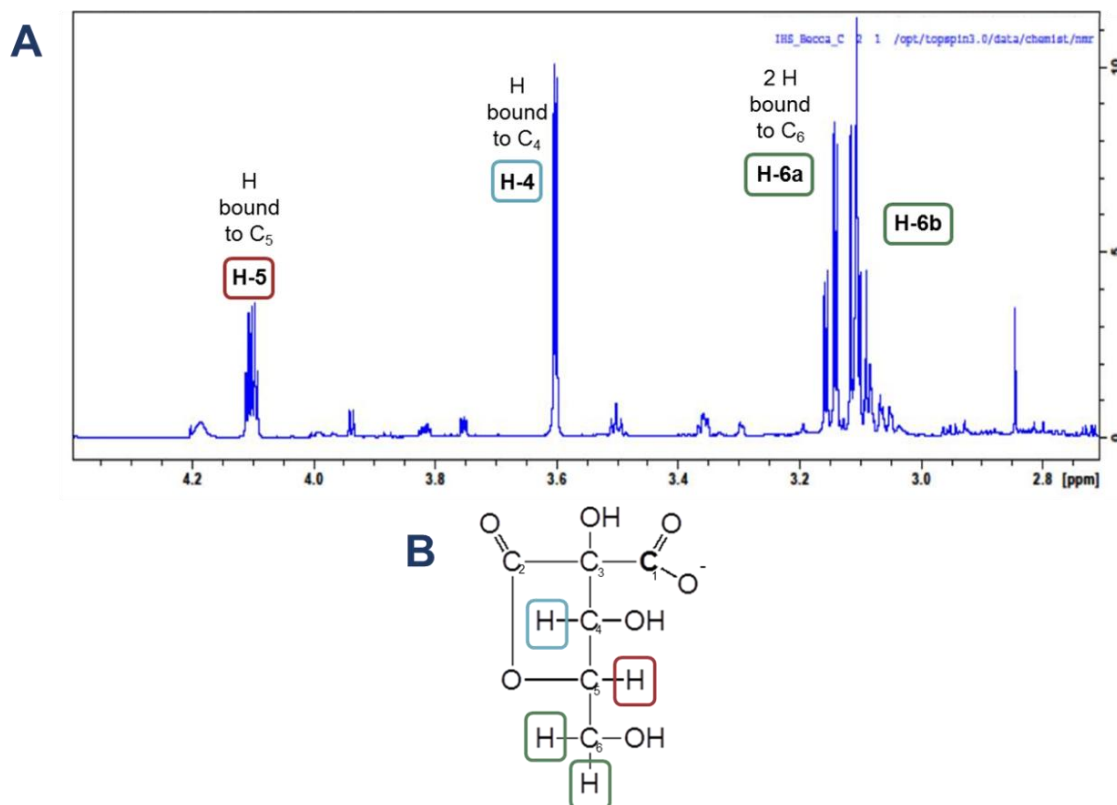


Figure 19: H^+ NMR analysis of compound C. A purified sample of compound C was analysed by H^+ NMR spectroscopy. The expanded carbohydrate region of the spectrum is shown in (A). The peaks corresponding to the C-H bonds present in compound C are labelled. The structure shown in (B) shows the position of the H atoms identified within the compound.

than the peaks towards the centre. This was caused by the proximity of the two C-H bonds, and suggests they could be bound to the same C atom. This also agrees with the suggested structure of C, in which C-6 has two C-H bonds.

^{13}C NMR spectroscopy detects naturally occurring ^{13}C ; approximately 1% of carbon is in the ^{13}C form. Compound C was thought to contain six carbons, all of which can be seen on the ^{13}C NMR spectrum (Figure 20). C-1 and C-2 are in the region known to correspond to acidic moieties. This is in agreement with the structure depicted (Figure 20), showing the

carboxylic acid group at C-1. An epimer of compound C has also been proposed, in which the carboxylic acid group would be on C-2, thus explaining the appearance of a C-2 peak in the acidic region, as it is possible that this preparation is a mixture of C and C'.

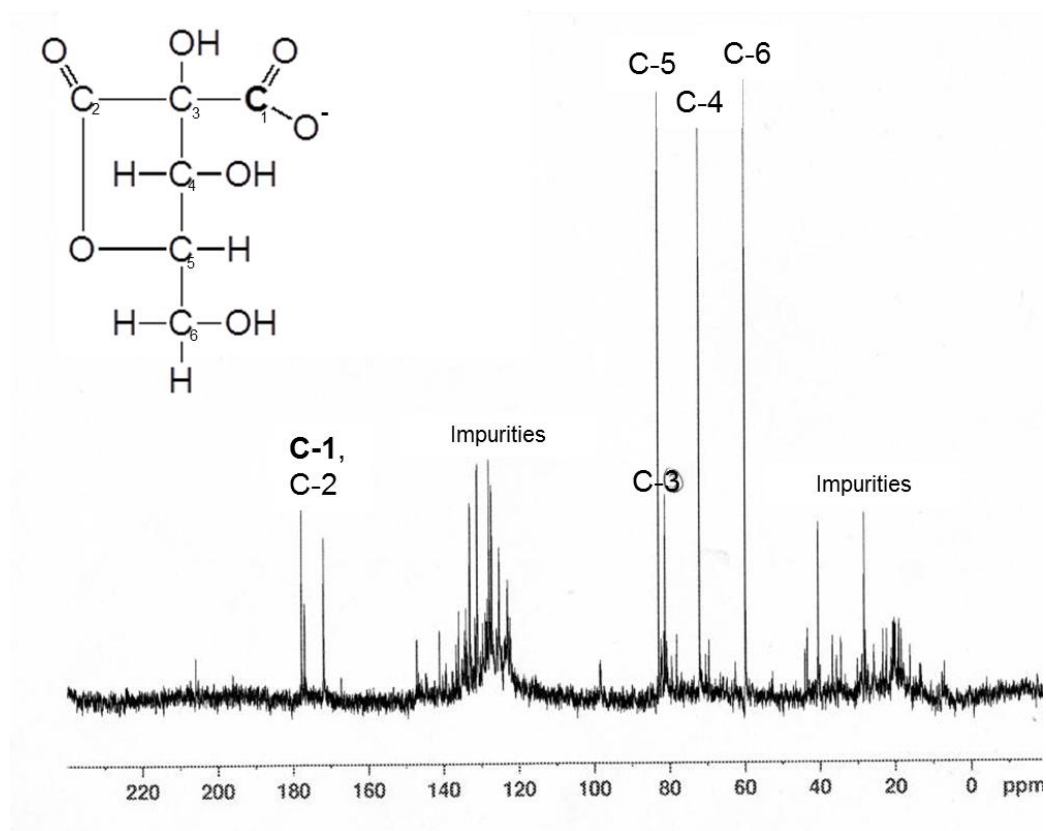


Figure 20: ^{13}C NMR spectroscopy analysis of compound C. A sample of compound C was analysed by ^{13}C NMR spectroscopy. The six carbon atoms within compound C were identified in the spectrum. Impurities, most likely resulting from the paper from which compound C was originally eluted, are also visible.

A sample of compound C, purified by anion-exchange column chromatography to avoid the contamination arising during elution from paper, was subjected to MS analysis. Fraction 30 from the anion-exchange column contained compounds C and C' (Figure 21 A) which are hypothesised to be epimers of each other and so will have the same molecular mass, free from the other compounds. As previous samples of compound C appeared to contain neutral compounds, assumed to originate from the paper from which the compounds were eluted, it was hoped that eluting the compounds from an anion-exchange chromatography column would allow a purer sample to be obtained. However, as seen on the electrophoretogram there is a silver nitrate stained neutral spot in the column fraction containing the two epimers of compound C. It is also possible that this neutral spot is a double lactone of compound E.

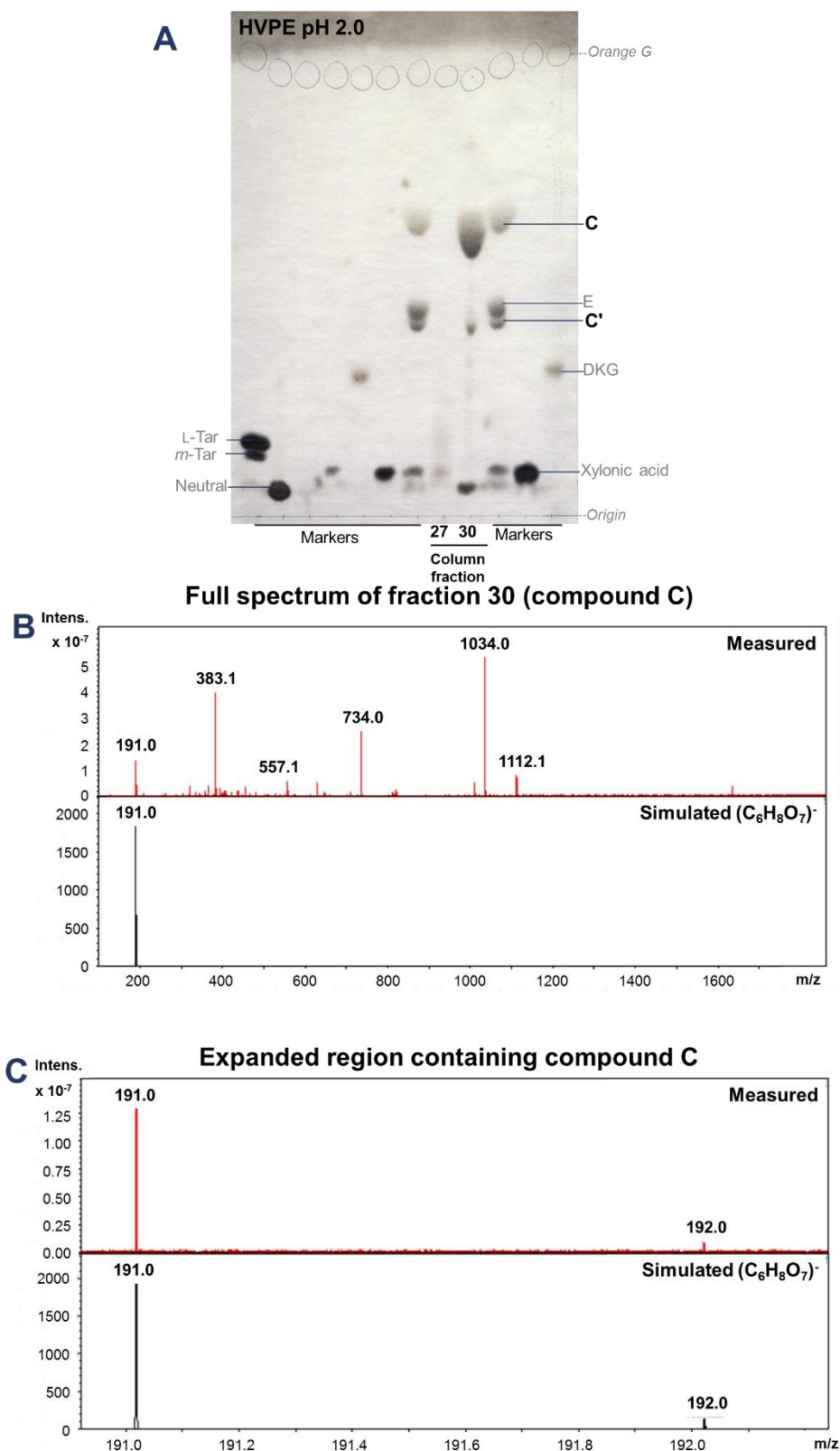


Figure 21: Mass spectrometry analysis of compound C purified by anion-exchange column chromatography. C and E compounds were separated by anion-exchange column chromatography. The compounds were eluted in increasing concentrations of formic acid, and samples from the fractions containing the putative xylonic acid and compound C (fractions 27 and 30 respectively) were run by HVPE at pH 2.0, then the paper stained in silver nitrate (A). Several marker compounds were also run, as well as an internal marker of orange G. A further sample of fraction 30 was analysed by mass spectrometry. The full spectrum (B) is shown, along with the expanded region containing the hypothesised compound C (C). The actual measured spectra are shown above the simulated spectra for a compound with the formula $(C_6H_8O_7)^-$.

The spot of compound C on the electrophoretogram was stained fairly heavily, suggesting that this sample of C was fairly concentrated (Figure 21 A). For this reason, this sample from the anion-exchange chromatography column was used for negative ion electrospray MS analysis. The spectrum for this sample showed a peak of m/z of 191, (Figure 21 B and C) which corresponds to the hypothesised structure of $C_6H_7O_7^-$ (Figure 20), supporting that compound C is a structure of this molecular mass.

That there was just one peak in the region of 191 on the spectrum (Figure 21 B and C) also supports the theory that C and C' are epimers and so are of the same molecular mass. The peaks with larger m/z values were assumed to be contaminants (Figure 21 B). As the electrophoretogram shows both C and C' were present in the sample, if they were not epimers then it would have been expected that two distinct peaks would be formed.

Samples of the other C and E-related compounds, purified from preparative HVPE, were also analysed by MS (Figure 22). As these samples were eluted from paper the samples were not particularly pure because they also contained material that originated from the paper itself. Compound C was the most abundant compound, with the others being present in much lower concentrations. However the MS analysis yielded more support for the identity of these compounds.

Both compounds C and C' contained peaks of 191 (as seen in Figure 22 B and C), as in the more concentrated samples discussed previously (Figure 21). This peak at 191 was absent in the C* sample (data not shown), further confirming that compounds C and C' are the epimers of each other, and C* is a separate compound completely.

The compound C* sample contained a peak at 165 (Figure 22 D), corresponding to the mass of xylonic acid, further supporting the hypothesis that the identity of C* is a C_5 monocarboxylic acid, potentially xylonic or lyxonic acid.

Compound E, the de-lactonised form of compound C, showed a peak at 209 on the mass spectrum (Figure 22 A), which matches the proposed structure, with the formula $(C_6H_9O_7)^-$.

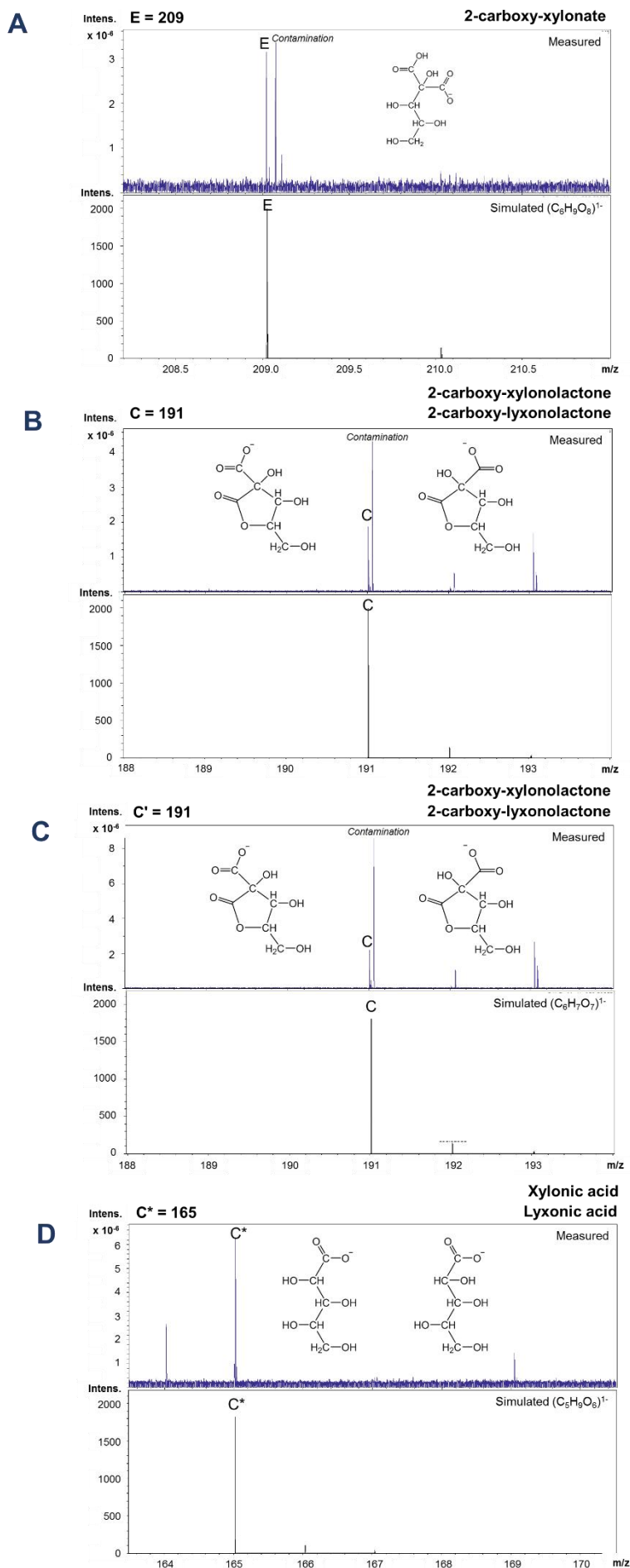


Figure 22: MS analysis of compounds E, C, C' and C*. Samples of compounds E, C', C'' and C* were prepared by preparative HVPE followed by elution in H₂O using the syringe barrel method. The individual samples were analysed using mass spectrometry. The actual measured spectra are shown above the simulated spectra for a compound with the formula (C₆H₉O₈)⁻ for compound E (A), (C₆H₇O₇)⁻ for compounds C' and C'' (B and C), and (C₅H₉O₆)⁻ for compound C* (D). The corresponding names and chemical structures are shown for each compound's proposed identity.

Taken together, the data support the hypothesis that there are two epimers of compound C, shown to have an m/z of 191. These epimers can be separated by HVPE at pH 2.0, but not HVPE at pH 6.5. The identities of the epimers of compound C are likely to be 2-carboxy-xylonolactone and 2-carboxy-lyxonolactone, as suggested previously (1). The structural characterisation of compound C using NMR also agrees with the proposed structures of 2-carboxy-xylonolactone and 2-carboxy-lyxonolactone.

Compound E is the de-lactonised form of C, 2-carboxy-xylonate. This de-lactonisation has been demonstrated during the alkali treatment of the samples, which is known to favour de-lactonisation. The structural identity of this compound is supported by the MS data, showing a peak at 209, which would be expected for this structure. Unlike compound C, compound E is unable to have epimers, as the functional carbon is symmetrical, with identical COOH groups on either side. Compound E is likely to have two negative charges, which would result in a compound with an m/z value of 104. This value is below the measured values during the MS analysis, so was unable to be detected.

Compound C* was shown to have the same electrophoretic mobility as xylonic acid after HVPE at pH 6.5 and pH 2.0. The MS data also support the identity of this compound as a C₅ aldonic acid, most likely to be xylonic or lyxonic acid, as these compounds have been previously reported as ascorbate degradation products (4).

The neutral spot present in samples of C, was assumed to contain, at least in part, contaminating material that originated from the paper the compounds were eluted from, rather than from the C and E-related compounds themselves. However, it is also possible that a neutral double lactone of compound E and/or xylonolactone was also present in the neutral sample. When the neutral sample was treated with NaOH there appeared to be a decrease in the intensity of the neutral spot, suggesting that the alkali had de-lactonised the compound, so it was no longer neutral. This is further supported by the presence of a radiolabelled neutral compound in an acid treated preparation of [¹⁴C]E after HVPE at pH 2.0.

This work has confirmed the identity of previously unidentified degradation products of DKG, as well as providing new information about the degradation pathway of DHA. The structures of these novel compounds are shown in Figure 23, along with the xylonolactone and the hypothetical structure of the neutral double lactone of compound E.

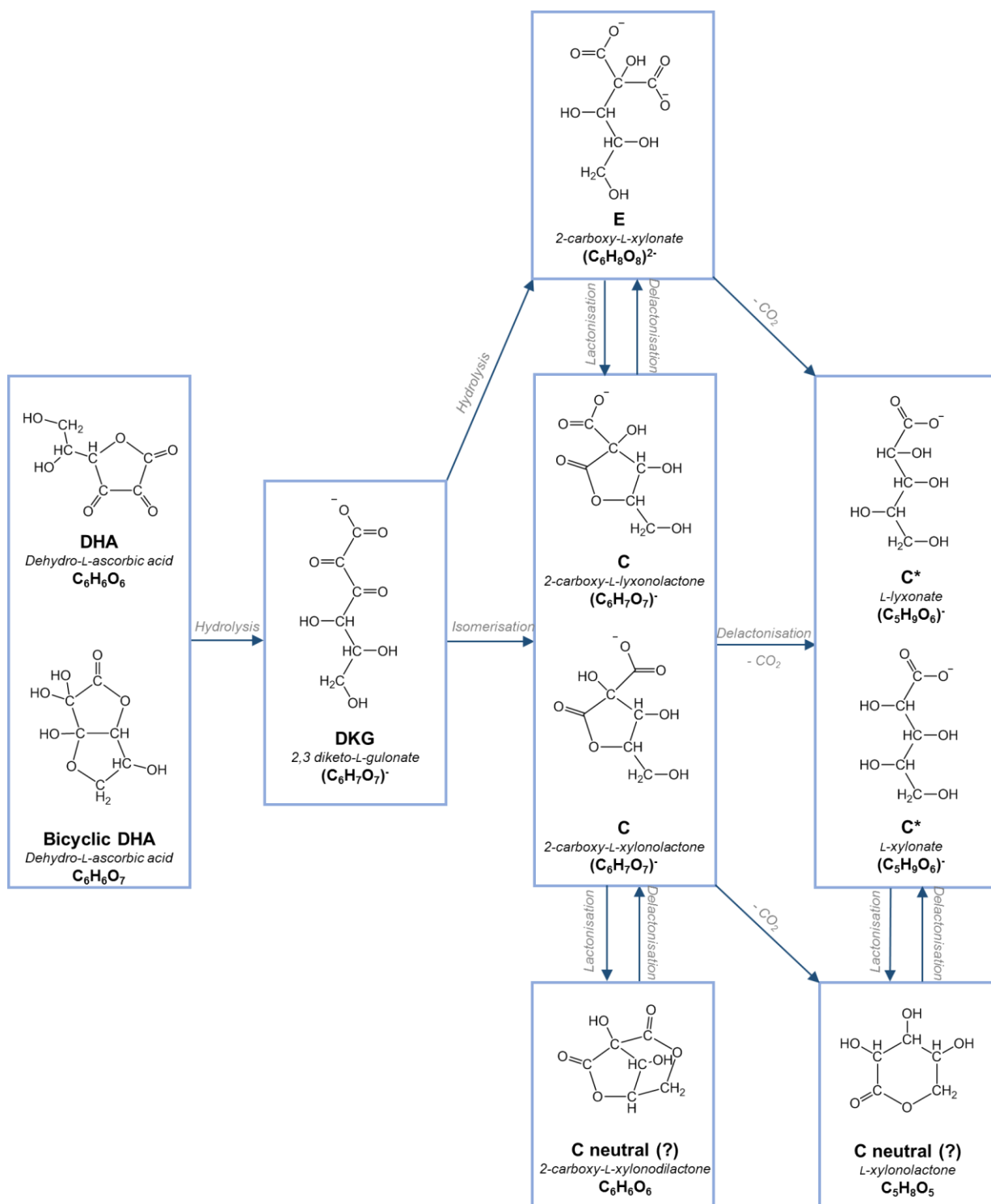


Figure 23: The hydrolysis pathway of DHA. The names, structures and formulas of each compound in the hydrolysis pathway are shown. The pathway begins with the hydrolysis of DHA to DKG. DKG can then be undergo isomerisation into compounds C (including both epimers, C and C') and E, which interconvert. The hypothetical C neutral compounds of 2-carboxy-L-xylonodilactone and xylonolactone are shown. Compound C* (identified as xylonate or lyxonate), formed by the decarboxylation of compound E or delactonisation and decarboxylation of compound C, is also shown.

3.2 Purification of an ascorbate-derived peroxidase-inhibitor

3.2.1 Introduction to an ascorbate-derived peroxidase-inhibitor

Previous work (A. Kärkönen and S.C. Fry, unpublished) identified a product derived non-enzymically from aged DKG which acted to inhibit peroxidase activity (84). The unknown DKG-degradation product was separated by HPLC and detected by UV absorbance at 250 nm. The peroxidase inhibitory activity of this compound was determined by a peroxidase activity assay, using horseradish peroxidase type II and a substrate of either *o*-dianisidine or ABTS, 2,2'-azino-bis(3-ethylbenzthiazoline-6-sulfonic acid) with H₂O₂. (A. Kärkönen and S.C. Fry, unpublished). It was found that the HPLC fraction containing the majority of the 250 nm-absorbing unknown compound showed the highest inhibitory effect on peroxidase. This was measured by the extent to which a time lag was induced before the oxidation of the peroxidase substrates, upon treatment of the peroxidase assay solution with the fractions from the HPLC column (A Kärkönen and S.C Fry, unpublished).

This work aimed to further purify and characterise this unknown ascorbate degradation product which acted to inhibit peroxidase activity.

3.2.2 Purification of peroxidase inhibitor using HPLC

Samples of DKG were prepared from a solution of commercial DHA treated with NaOH. The preparations of DKG, in sodium acetate buffer, pH ~4, were aged on ice for up to 24 hours. Samples of these DKG preparations were separated by HPLC, and the products detected by UV absorbance at 250 nm and 210 nm. DKG itself is known to show absorbance at 210 nm, with no absorbance shown at higher wavelengths (254).

The peroxidase inhibitor (known as P_xI) showed a peak of absorbance at 11 minutes at 250 nm, eluting slightly behind the peak of DKG at 210 nm (Figure 24).

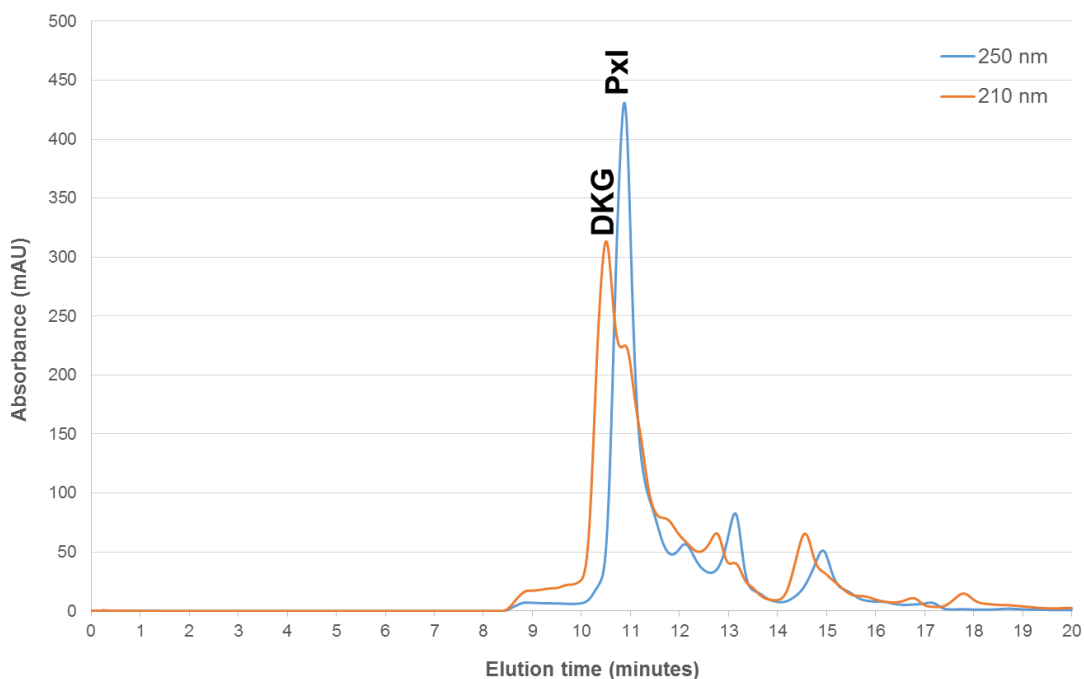


Figure 24: HPLC profile of DKG aged for 24 hours on ice. A solution of DKG (50 mM, prepared from commercial DHA treated with NaOH) was aged on ice for 24 hours. A small sample (25 μ l) was injected onto a Rezex HPLC column and eluted in 47 mM H₂SO₄. The separated compounds were detected by UV absorbance at 250 nm and 210 nm. The peaks of DKG and the peroxidase inhibitor (PxI) are labelled.

The eluted fractions containing PxI (10.5 minutes to 12 minutes) were collected and pooled. This pooled sample was re-run on the HPLC column to check for the presence of PxI (Figure 25 A). A peak of PxI was present, as seen by the absorbance at 250 nm. The preparation also contained some DKG, as seen by the absorbance at 210 nm. The peak labelled ‘blank’ was an artefact from the column, as this peak was present even when a sample containing only H₂O was run on the column

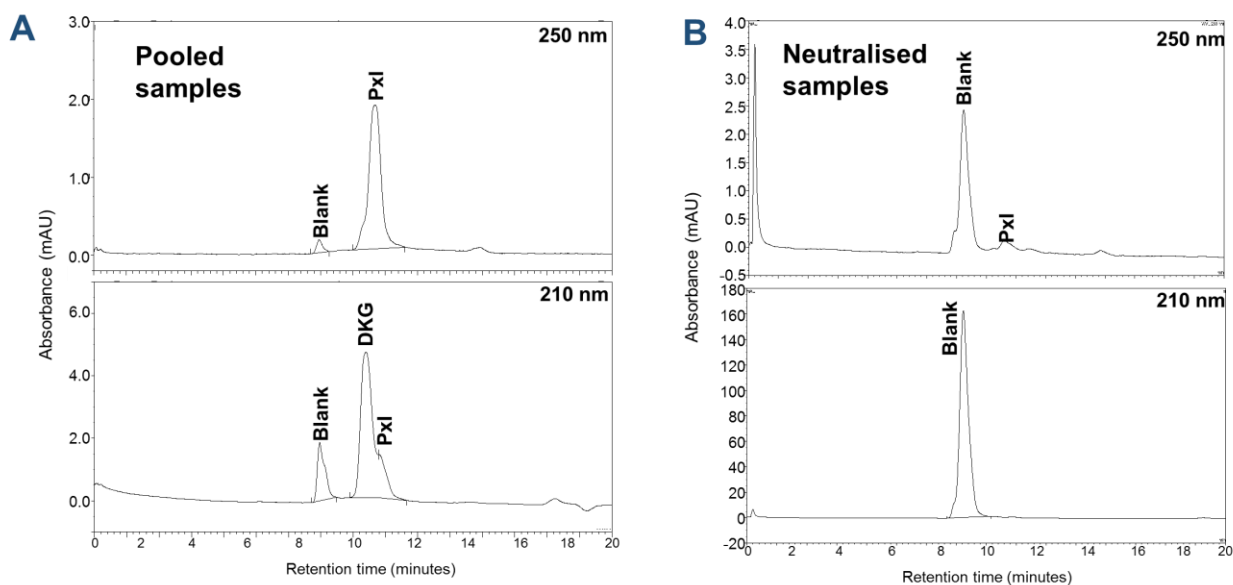


Figure 25: HPLC profile of pooled and neutralised fractions containing Pxl. Fractions collected from HPLC column containing Pxl were pooled and a small sample (25 μ l) was re-run on HPLC (A). The products were detected by absorbance at 250 nm and 210 nm. As the sample was in 47 mM H_2SO_4 it required neutralisation before further characterisation. This was achieved by the addition of BaCO_3 . A small sample (25 μ l, equivalent to the sample in A) of the neutralised Pxl preparation was re-run on HPLC (B), and the products detected by absorbance at 250 nm and 210 nm.

As the products were eluted in 47 mM H_2SO_4 , they required neutralisation before further characterisation. The sample was neutralised with $\text{Ba}(\text{OH})_2$. After the re-running of the neutralised sample on HPLC, the peak of the peroxidase inhibitor had diminished (Figure 25 B). This suggests that the neutralisation step has caused the degradation of the peroxidase inhibitor compound. The absorbance at 210 nm shows that DKG has also diminished upon neutralisation.

The Pxl preparation was eluted from the HPLC column in 0.1% TFA instead of H_2SO_4 (Figure 26 A) to avoid the neutralisation step. TFA has the advantage that it is volatile, and so samples in TFA can be analysed by MS or NMR without the prior need to neutralise them.

Preparations of DKG aged on ice were eluted from an HPLC column in 0.1% TFA (Figure 26A) and the profile looked equivalent to that obtained when the compounds were eluted in H_2SO_4 (Figure 24), with DKG eluting before Pxl. Fractions were collected between 9

minutes and 12.5 minutes and small samples of each were re-injected onto the column (Figure 26 C); and the area of the Pxl peak in each fraction was calculated (Figure 26 B). The fractions containing the greatest amount of Pxl were fractions between 10.5 and 11.25 minutes. These fractions were pooled for further analysis.

The recovery of Pxl was approximately 25%, as calculated from the total Pxl area in the original profile (Figure 26 A) and the total peak area in the re-run fractions (Figure 26 B). It is presumed that this loss of Pxl was due to degradation of the compound.

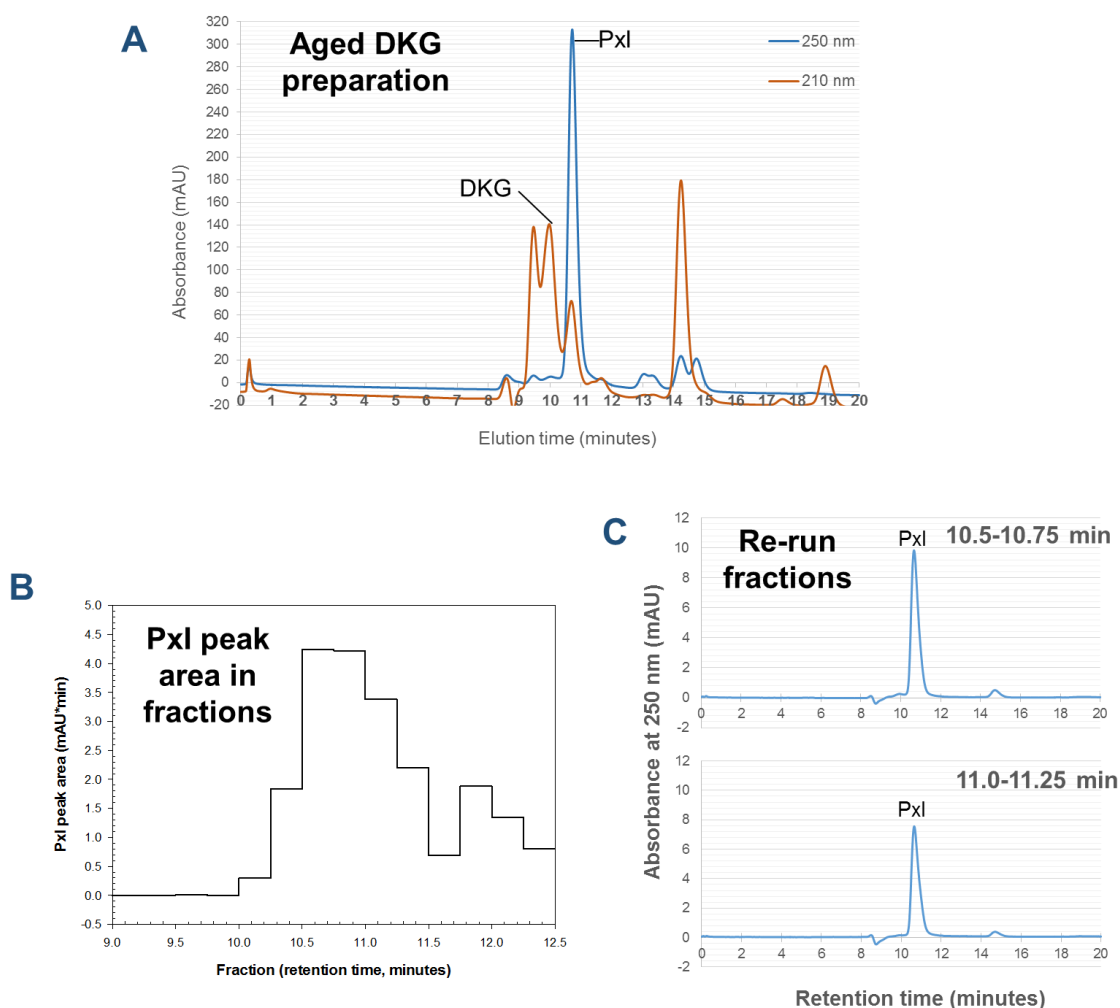


Figure 26: Pxl eluted from HPLC column in TFA. Samples of DKG aged on ice for 24 hours were eluted from a Rezex HPLC column in 0.1% TFA. The products were detected by UV absorbance at 250 nm and 210 nm (A). Fractions were collected from the column between 9 and 12.5 minutes, every 15 seconds. Small samples (25 μ l) from each fraction were re-run on HPLC and the area of the Pxl peak in each fraction, as measured by UV absorbance at 250 nm, was recorded (B). Representative profiles of re-run fractions (10.5-10.75 minutes and 11.0-11.25 minutes), as measured by UV absorbance at 250 nm are shown (C).

3.2.3 The characterisation of the peroxidase inhibitor using HVPE was inconclusive

Fractions containing Pxl eluted from the HPLC column in 0.1% TFA were pooled and dried under vacuum. Small samples of this pooled Pxl preparation were run on HVPE in pH 2.0 and pH 6.5 (Figure 27) and stained in silver nitrate.

The preparations of Pxl contained DKG, which was expected as DKG elutes from the column very close to Pxl. The solution also contained a compound that co-migrates with compound C (discussed in section 3.1). Compound C is known to form from DKG in aqueous conditions (1), so had possibly accumulated after being eluted from the column.

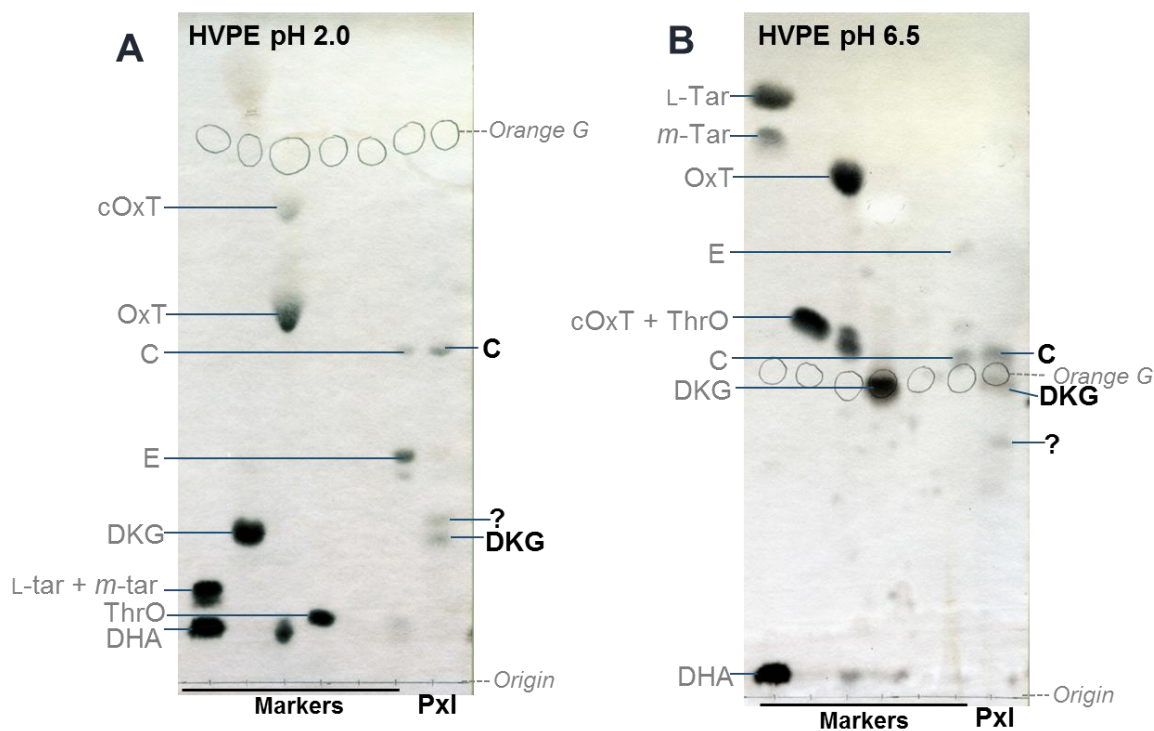


Figure 27: Analysis of peroxidase inhibitor by HVPE. Pxl was prepared from ageing a solution of DKG, running on an HPLC column and collecting the fractions. Fractions eluted from an HPLC column containing Pxl (eluted in 0.1% TFA) were pooled and dried. Small samples (20 μ l) of this preparation were run by HVPE at pH 2.0 (A) and pH 6.5 (B). The papers were stained in silver nitrate.

Interestingly there were unknown compounds present after HVPE at pH 2.0 (Figure 27 A) and pH 6.5 (Figure 27 B). A compound (m_{OG} of 0.22) migrating very close to DKG (m_{OG} of 0.18) at pH 2.0 was observed, as well as a compound with m_{OG} of 0.80 at pH 6.5. These compounds could potentially be PxI. Compound C was also present in the PxI sample, with m_{OG} of 0.55 at pH 2.0 and 1.06 at pH 6.5.

3.2.4 The peroxidase inhibitor is not compound C or E

The peroxidase inhibitor is a degradation product of DKG, and known degradation products of DKG include the previously unidentified compounds C and E (1,72) (discussed further in section 3.1). It was suggested that the identity of the peroxidase inhibitor could be compound C. Compound C was favoured over compound E as the potential identity of PxI because the compound was eluted in acid and acidic conditions are known to favour the formation of lactones (e.g. compound C), rather than delactonisation (e.g. compound E).

HVPE analysis of the PxI preparation showed a compound assumed to be compound C based on its mobility (m_{OG}) in pH 6.5 and pH 2.0 (Figure 27). However, this compound could be contaminating, rather than the active compound.

In order to eliminate compound C from the possible identity of PxI, a sample containing compounds C and E (eluted from paper after preparative HVPE) was injected onto an HPLC column and eluted in TFA. A sample of PxI was run immediately after these samples so the profiles could be compared. Both compounds C and E showed greater absorbance at 210 nm (Figure 28 D); however, PxI showed greater absorbance at 250 nm (Figure 28 A). This suggests that the identity of PxI is not compound C or compound E. The major peaks of C and E also eluted earlier than the peak of PxI (Figure 28), further confirming that PxI is not compound C or E.

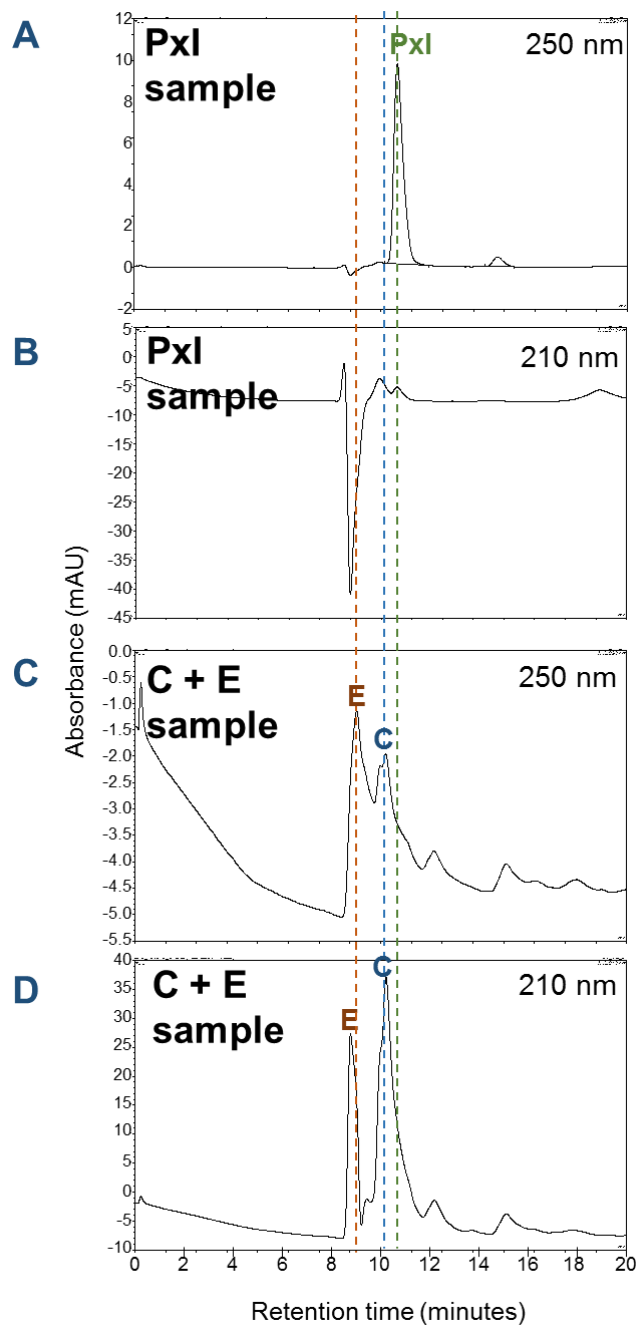


Figure 28: Pxl is not compound C or compound E. A sample of Pxl, purified by HPLC eluted in 0.1% TFA, was re-run by HPLC. The products were detected by UV absorbance at 250 nm (A), and 210 nm (B). A sample containing compounds C and E (prepared by alkali treatment of DHA and subsequent elution from preparative HVPE) was also injected onto the HPLC column and eluted in 0.1% TFA. The compounds were detected by absorbance at 250 nm (C) and 210 nm (D). The position of Pxl is marked with a green dotted line and the positions of compounds C and E are marked with blue and orange lines respectively.

3.2.5 Analysis of purified peroxidase inhibitor by NMR

To obtain enough material for MS or NMR analysis, repeated samples of aged DKG were injected onto the column and the relevant fractions collected and pooled. The concentration of original DKG was increased from 50 mM to 200 mM to scale up the production of Pxl (Figure 29).

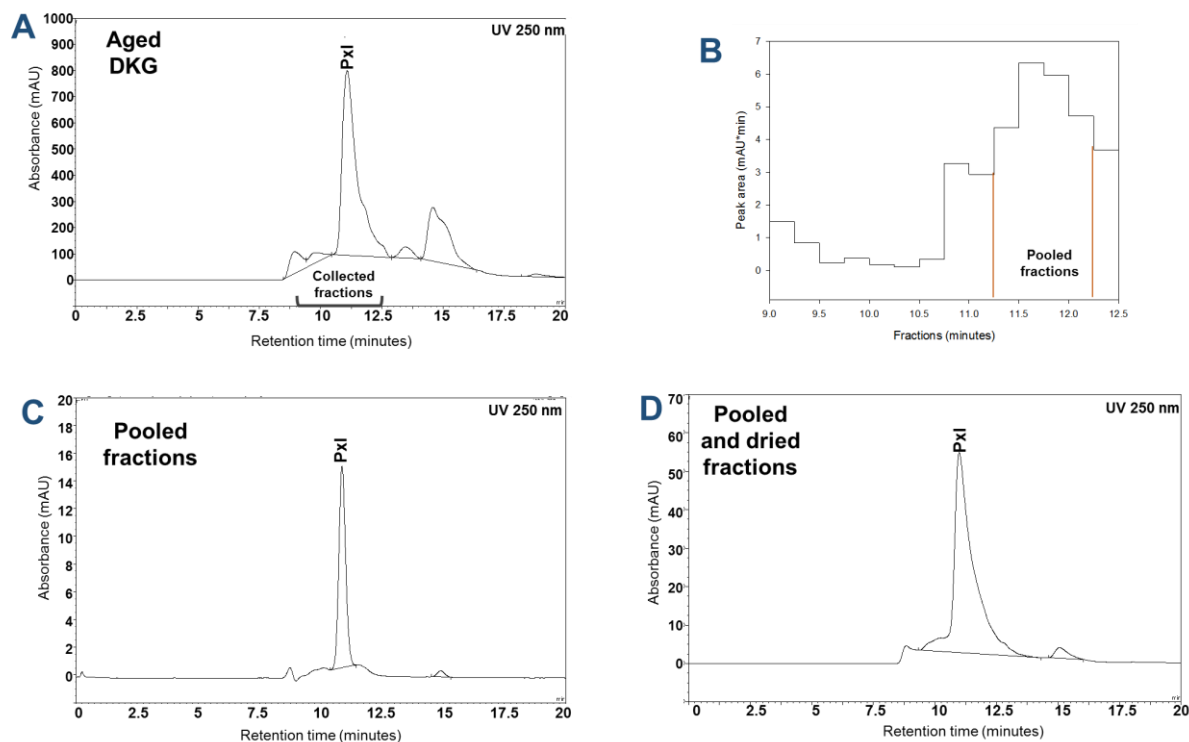


Figure 29: Purification of Pxl from 200 mM DKG for NMR. DKG (200 mM) was aged on ice for 4 hours before being injected onto an HPLC Rezex column in 25 μ l aliquots. The products were eluted in 0.1% TFA and were detected by UV absorbance at 250 nm (A). Fractions (15 seconds each) were collected between 9 and 12.5 minutes elution time (B). The fractions indicated in B, showing the Pxl peak area, were pooled and a small aliquot was re-run on HPLC (C). The remainder of the pooled sample was dried under vacuum and re-dissolved in a small volume of D₂O. An aliquot was re-run by HPLC (D).

Fractions containing Pxl were collected from an HPLC Rezex column (Figure 29 A and B). These fractions were then pooled (Figure 29 C) and dried (Figure 29 D). The peak of Pxl was still present after drying and re-dissolving in D₂O (Figure 29 D), in preparation for NMR analysis. After drying (Figure 29 D) the sample of Pxl was redissolved in a smaller volume of D₂O and so is more concentrated than the pooled samples (Figure 29 C). UV absorbance at 210 nm could not be analysed, as TFA shows strong absorbance at 210 nm. This means that any DKG, or other compound absorbing at 210 nm, such as compound C,

cannot be detected, so it is not known whether the sample contains other compounds. It is very likely that DKG was also present in the sample, as the peak of DKG overlaps with that of PxI. This potentially means that the sample also contains other DKG derivatives, such as C and E-related compounds (discussed in section 3.1), which would further complicate attempts to identify PxI.

A small peak at 15 minutes (Figure 29 C and D) can be seen in the pooled and dried samples of PxI. This compound arises spontaneously in preparations of PxI and can be seen in Figure 26 C and Figure 28 A also. All the fractions collected from the column throughout the 20 minute retention time and immediately re-run also contained this peak at 15 minutes.

This preparation of PxI was analysed by ^1H NMR, however the resulting spectrum (Figure 30 A) contained numerous peaks. An expansion of the carbohydrate region (Figure 30 B) also contained too many peaks to decipher.

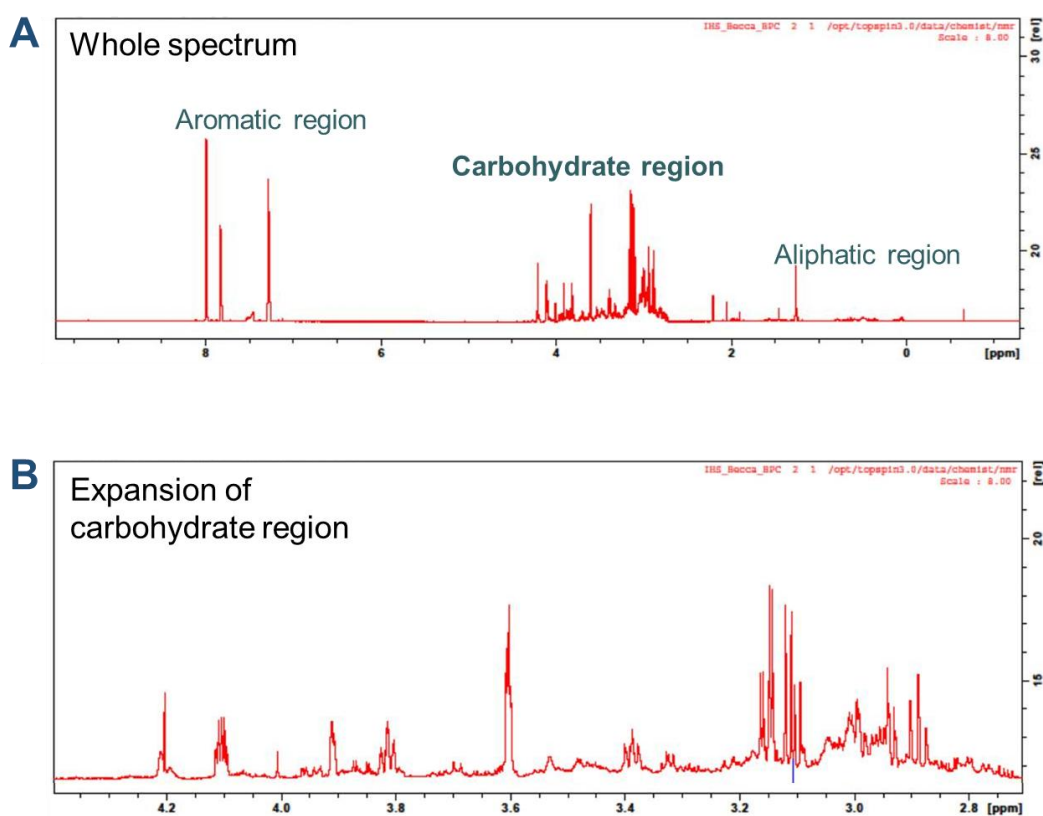


Figure 30: ^1H NMR analysis of PxI. A sample of PxI (originating from aged 200 mM DKG) that has been eluted from an HPLC Rezex column and dried, before being redissolved in D_2O was analysed by ^1H NMR spectroscopy. The whole spectrum is shown in (A) and the expansion of the carbohydrate region is shown in (B).

Unfortunately it seems to be the case that P_xI is an unstable compound and breaks down to produce numerous compounds spontaneously. This means that it was not possible to identify the compound responsible for the inhibition of peroxidase, as first described by A. Kärkönen and S.C Fry.

3.3 The *in-vitro* reaction of DHA and DKG with reactive oxygen species

3.3.1 Introduction to the reaction of DHA and DKG with reactive oxygen species

One of the major roles of ascorbate within the plant is as an antioxidant (74). Ascorbate acts to quench harmful reactive oxygen species that may otherwise damage cell membranes or DNA. Although it is well documented that ascorbate and DHA can reduce the level of reactive oxygen species (50), the fate of DHA itself after these reactions is not well known. These experiments aim to identify the products arising from DHA and DKG during the reaction of these compounds with various reactive oxygen species.

3.3.2 The *in-vitro* reaction of DHA with different reactive oxygen species

Commercial DHA (stored at 3 M in DMF) was diluted to 50 mM final concentration in sodium acetate buffer (pH 4.8). Equimolar ROS were added to this solution, and samples were run by HVPE at pH 6.5 and pH 2.0. The products formed were detected by staining in silver nitrate.

3.3.2.i. *DHA + hydrogen peroxide*

Hydrogen peroxide is a by-product of many metabolic processes within the cell (255). It is the most long-lived ROS and in fact other ROS breakdown to form H₂O₂.

DHA (50 mM) was incubated with 50 mM H₂O₂ in pH 4.8 buffer for up to 30 minutes. At each time point catalase was added to the solution to stop the reaction. The samples were then run by HVPE at pH 6.5 and pH 2.0 before being stained in silver nitrate.

The major product formed during the reaction of equimolar DHA and H₂O₂ was OxT (Figure 31). HVPE at pH 2.0 allowed the minor products of cOxT and ThrO to be distinguished, as these compounds have the same mobility at pH 6.5, and the minor product formed from this reaction of DHA with H₂O₂ was identified as cOxT (Figure 31 B). However it is evident from the samples run by HVPE at pH 2.0 that some ThrO is also produced, as a compound moving slightly further than the neutral DHA is present (Figure 31 B).

OxT and cOxT were formed within 5 minutes after the addition of H₂O₂, (Figure 31 A and B). After 15 minutes the starting material (DHA) had predominantly been broken down into OxT and cOxT, so that very little DHA remained in the sample (Figure 31 A). A spot remained in the neutral zone, close to the origin, in the electrophoretogram run at pH 2.0 (Figure 31 B); however, as most of the DHA had gone by 15 minutes, this compound was

likely to be ThrO. ThrO has a relatively low mobility at pH 2.0, moving only slightly faster than neutral compounds. ThrO and cOxT had the same electrophoretic mobility at pH 6.5, and so the ThrO present in the samples run at pH 6.5 may have been masked by cOxT.

These results agree with previous published data (2) that the oxidation of DHA is a branched pathway, with cOxT, OxT and ThrO (necessarily with OxA) being formed simultaneously.

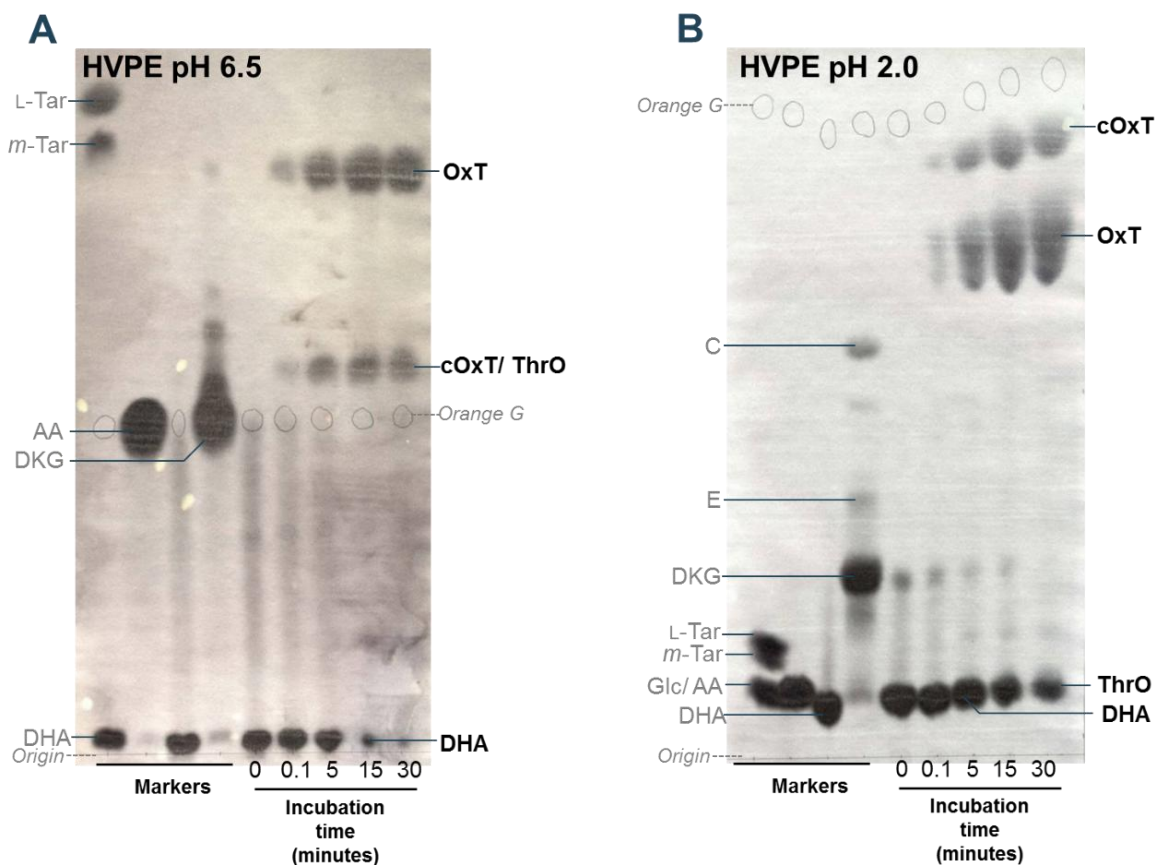


Figure 31: Reaction of DHA with H₂O₂: DHA (50 mM) was incubated with H₂O₂ (50 mM) in 0.2 M sodium acetate buffer (pH 4.8) for up to 30 minutes, with samples (20 μ l) taken at various time points and stopped with catalase (0.01% final concentration). The samples (10 μ l) were loaded onto Whatman 3 MM paper and run by HVPE at pH 6.5 (A) or pH 2.0 (B). The papers were then stained in silver nitrate to detect the products. The 0 time point represents DHA without the addition of H₂O₂.

3.3.2.ii. DHA + superoxide

The superoxide radical ($O_2^{\cdot-}$) was supplied as KO_2 . The reaction with DHA was achieved by incubating a 50 mM solution of DHA, buffered at pH 4.8, with 50 mM KO_2 . In solution KO_2 dissociates, producing $O_2^{\cdot-}$. The superoxide reaction was stopped with superoxide dismutase (SOD) at each time point.

As with the reaction of DHA with H_2O_2 , the major product of the reaction of DHA with $O_2^{\cdot-}$ was OxT. HVPE at pH 2.0 allows the separation of different isomers of OxT, as seen by the presence of two distinct spots in the OxT region of the electrophoretogram run at pH 2.0 (Figure 32 B). OxT is thought to be a mixture of three isomers (4-OxT, 3-OxT and 2-OxT) of which 4-OxT and 3-OxT are expected to be the more stable (72).

ThrO and cOxT were also produced during the reaction with $O_2^{\cdot-}$. The production of cOxT

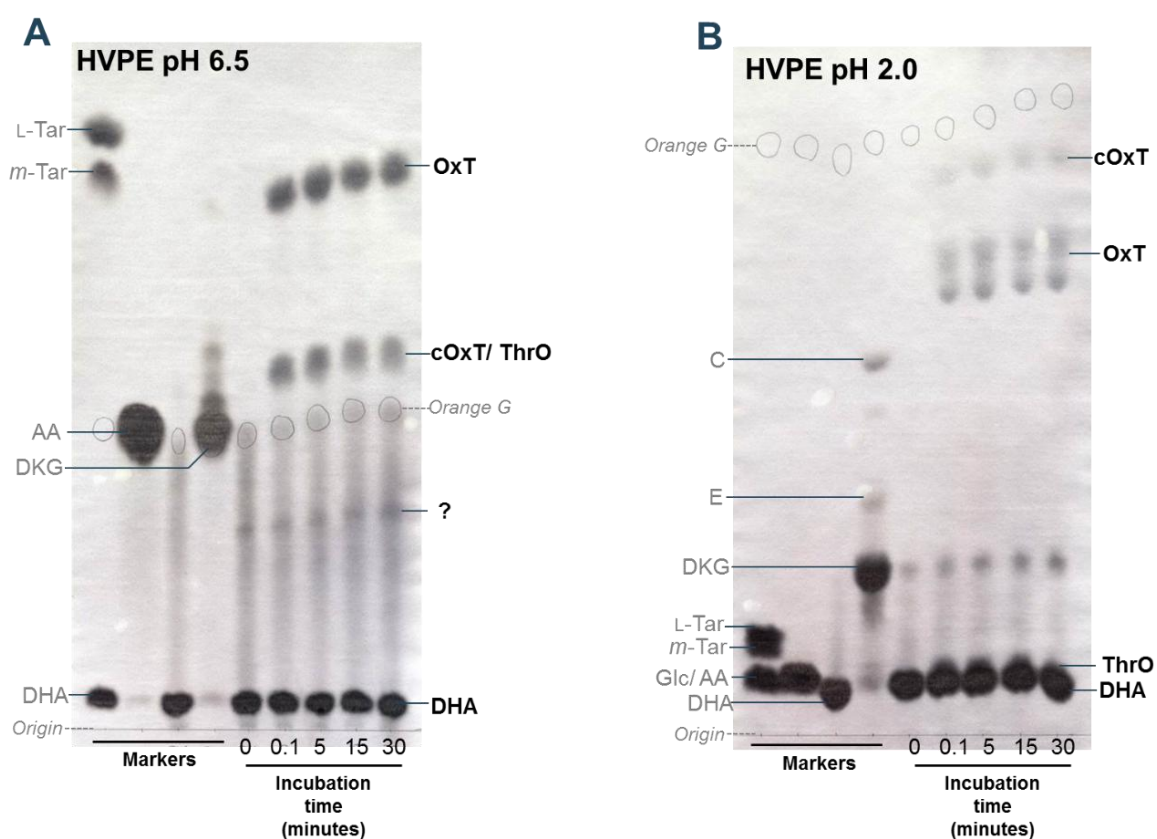


Figure 32: Reaction of DHA with superoxide radical: DHA (50 mM) was incubated with KO_2 (50 mM) in 0.2 M sodium acetate buffer (pH 4.8) for up to 30 minutes, with samples (20 μ l) taken at various time points and the reaction stopped by the addition of 0.01% SOD. The samples (10 μ l) were loaded onto Whatman 3 MM paper and run by HVPE at pH 6.5 (A) or pH 2.0 (B). The papers were then stained in silver nitrate to detect the products. The 0 time point represents DHA without the addition of KO_2 .

was much reduced compared to the reaction of DHA with H_2O_2 , (as determined by HVPE at pH 2.0; Figure 31 B compared to Figure 32 B) whilst the production of ThrO was increased in the $\text{O}_2^{\cdot-}$ reaction compared with H_2O_2 . The production of ThrO from DHA requires the carbon backbone of DHA to be cleaved between carbons 2 and 3, with carbons 3-6 forming ThrO and carbons 1-2 forming OxA. Therefore the presence of ThrO suggests that OxA is also present, but OxA is not able to be stained with silver nitrate so does not appear on these electrophoretograms.

The reaction of $\text{O}_2^{\cdot-}$ with DHA was not as complete as the reaction of H_2O_2 , as there is still most of the neutral DHA remaining after 30 minutes (Figure 32). The remaining DHA has the opportunity to hydrolyse to DKG during the 30 minute incubation time, resulting in the increasing spot of DKG especially apparent on the electrophoretogram run at pH 2.0 (Figure 32 B). The reaction with $\text{O}_2^{\cdot-}$ must be very rapid as the half-life of this ROS is very short (microseconds (110)) and the reaction can only continue as long as any $\text{O}_2^{\cdot-}$ remains. The reaction occurred instantly (by 0.1 minute) and then did not continue, suggesting all the $\text{O}_2^{\cdot-}$ was used up almost instantaneously.

3.3.2.iii. *DHA + hydroxyl radical*

The hydroxyl radical ($\cdot\text{OH}$) was produced by incubating FeSO_4 , EDTA and H_2O_2 in equimolar quantities. The reaction of DHA (50 mM) with various concentrations of this mixture was investigated. These increasing concentrations of FeSO_4 , EDTA and H_2O_2 indicate increasing amounts of $\cdot\text{OH}$, but the exact concentrations of the short-lived $\cdot\text{OH}$ within the solutions was not known.

Analysis of the products formed from the reaction with $\cdot\text{OH}$ by HVPE at pH 6.5 (Figure 33) showed that OxT was the dominant product, similar to the reaction with H_2O_2 . Unexpectedly there does not appear to be a marked difference in the products formed with 50 mM, 12.5 mM and 1 mM of the $\cdot\text{OH}$ -producing mixture.

As well as OxT, a compound, or compounds, co-migrating with cOxT and/or ThrO was also produced. HVPE at pH 6.5 with 50 mM of the $\cdot\text{OH}$ -producing solution potentially contains two spots in the cOxT/ThrO region, as the spot corresponding to cOxT/ ThrO seems distorted, as if it may be two separate compounds which overlap. This could indicate that both these compounds were present. This is not the case with the 1 mM $\cdot\text{OH}$ -producing solution, in which it seems that only one compound was present. HVPE at pH 2.0 resolved

these compounds (Figure 34), and the use of [^{14}C]DHA as a substrate (discussed in section 3.3.5) will indicate whether [^{14}C]cOxT has been formed. Any ThrO formed during this reaction will not be visible as ThrO does not contain the radiolabelled C-1 of [^{14}C]AA.

HVPE at pH 2.0 of the reactions containing 50 mM and 25 mM of the $\cdot\text{OH}$ -producing solutions (Figure 34 A) shows a suspicious lack of products formed, apart from a potential spot of ThrO overlapping with the neutral DHA. However analysis of the same samples by HVPE at pH 6.5 (Figure 33) shows a relatively heavily-stained spot of OxT. It is possible that the fairly high concentrations of FeSO_4 and EDTA present in these samples could be interfering during the

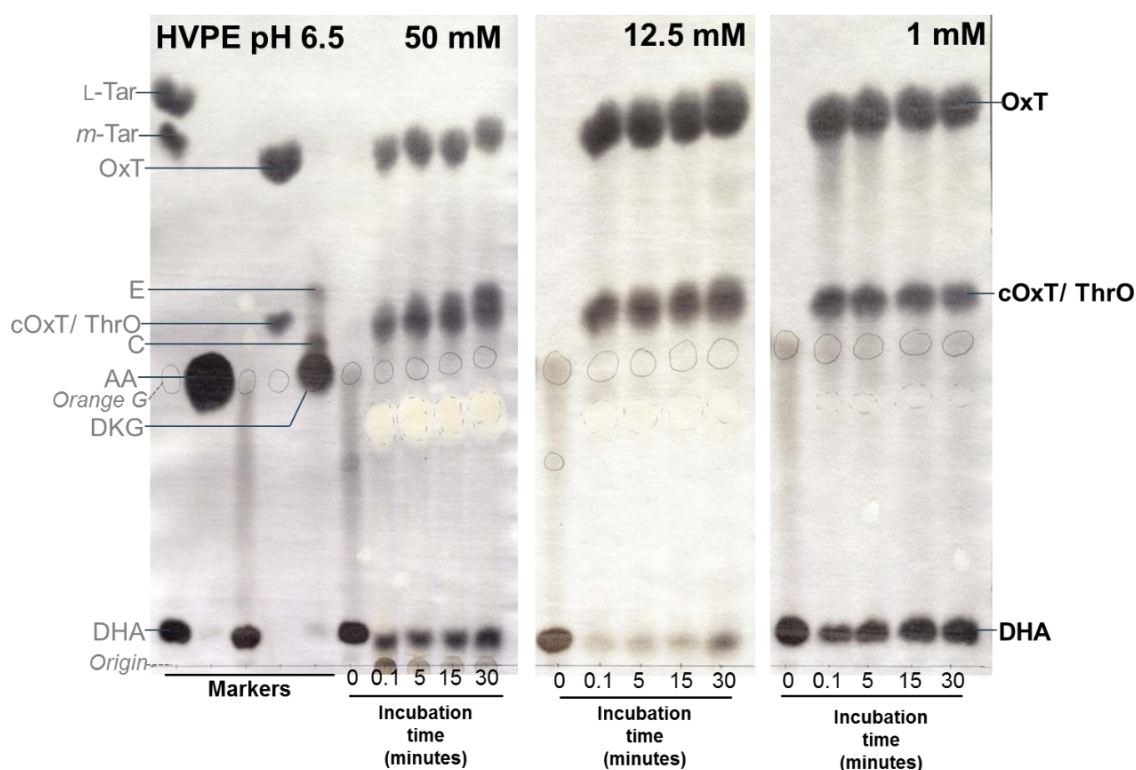


Figure 33: Reaction of DHA with the hydroxyl radical analysed by HVPE at pH 6.5. DHA (50 mM) was incubated with EDTA, FeSO_4 and H_2O_2 (50, 12.5 or 1 mM each) in 0.2 M sodium acetate buffer (pH 4.8) to produce $\cdot\text{OH}$ radical. The reaction mixtures were incubated for up to 30 minutes, with samples taken at various time points and the reaction stopped by the addition of EtOH (50% final concentration). The samples (10 μl) were loaded onto paper and run by HVPE at pH 6.5. The papers were then stained in silver nitrate to detect the products.

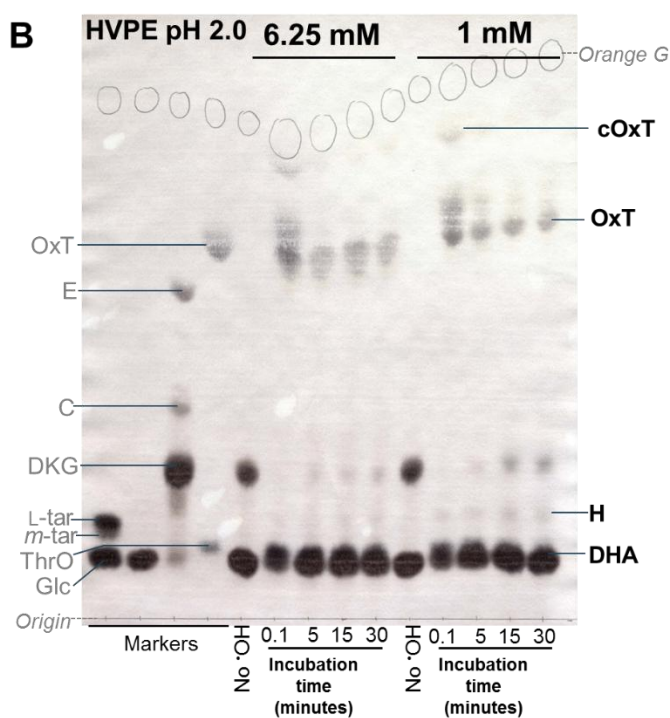
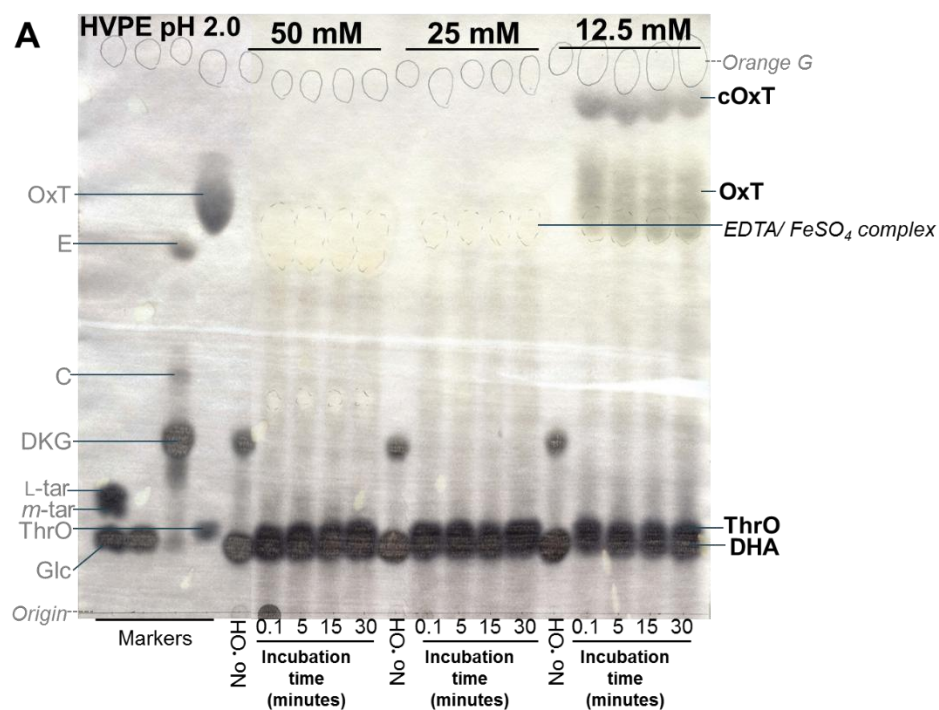


Figure 34: Reaction of DHA with the hydroxyl radical analysed by HVPE at pH 2.0. DHA (50 mM) was incubated with EDTA, FeSO₄ and H₂O₂, 50, 25 or 12.5 mM (A) and 6.25 or 1 mM (B) each in 0.2 M sodium acetate buffer (pH 4.8) to produce ·OH. The reaction mixtures were incubated for up to 30 minutes, with samples taken at various time points. The reactions were stopped by the addition of EtOH (50% final concentration). The samples labelled 'No ·OH' samples represent DHA incubated in buffer without FeSO₄, H₂O₂ and EDTA for 30 minutes. The samples were loaded onto paper and run by HVPE at pH 2.0. The papers were then stained in silver nitrate.

running of the compounds at pH 2.0, especially as EDTA does not function as a chelating agent at such a low pH. A yellow spot (Figure 34 A) can be seen just below the position of OxT, which is assumed to be due to a complex of FeSO₄ and EDTA.

The samples containing 12.5 mM of [•]OH-producing mixture show clear spots of cOxT, OxT and ThrO, as well as some neutral compounds, presumably unreacted DHA (Figure 34 A). The intensity of the cOxT spot is comparable to that formed with H₂O₂ (Figure 31 B), and more intense than that formed with O₂^{•-} (Figure 32 B).

In the samples containing lower amounts of [•]OH, 6.25 mM and 1 mM of the [•]OH-producing mixtures (Figure 34 B), cOxT was formed immediately, but then diminished over time. The isomer of OxT (discussed more in section 3.3.5) formed initially also seems to change to a different, potentially more stable, OxT-isomer over time.

A further compound, labelled H (Figure 34 B), was also formed with 1 mM [•]OH. Compound H is thought to be an intermediate compound in the oxidation of DKG to ThrO (2). It is possible that the low amount of [•]OH allowed some hydrolysis of DHA, producing DKG, to occur, as seen in the 15 and 30 minute samples with 1 mM of the [•]OH-producing mixture (Figure 34 B). This DKG could then have been oxidised, forming compound H, as well as ThrO.

DHA incubated in buffer without [•]OH ('No [•]OH' samples in Figure 34) for 30 minutes showed more DKG than those samples containing FeSO₄, H₂O₂ and EDTA. This suggests that the presence of these compounds prevented the hydrolysis of DHA to DKG.

3.3.2.iv. *DHA + singlet oxygen*

Singlet oxygen ($^1\text{O}_2$) is the excited state of molecular oxygen (triplet oxygen, O_2^{2*}). Singlet oxygen is more oxidising than triplet oxygen because it has two unpaired electrons in the outer orbital, thus making it more reactive. Within the plant, singlet oxygen has been reported to be the major ROS responsible for damage within leaves (125). Singlet oxygen can be produced from photosensitiser dyes, including riboflavin and rose Bengal, in the presence of light (256).

For the experiments discussed here riboflavin was used to produce singlet oxygen. The mechanism of producing this ROS required that the timescale of these experiments was longer, 24 hours compared to 30 minutes in previously discussed experiments, to allow the formation of singlet oxygen to occur. Singlet oxygen is only produced in the presence of light, so the samples incubated with riboflavin in the dark serve as a control in which no ROS is generated. This longer incubation time allowed DHA to hydrolyse to DKG during the experiment, (Figure 35). This leads to the possibility that the compounds produced from singlet oxygen could be derived from either DHA or DKG.

As with H_2O_2 , $^{\bullet}\text{OH}$ and $\text{O}_2^{\bullet-}$, OxT was the predominant oxidation product, (Figure 35). However there was no evidence for the production of cOxT. Instead a slower-moving compound (labelled ?) was produced (Figure 35 A). This compound has a similar m_{OG} to compound C at pH 6.5, but HVPE at pH 2.0 suggested that this compound was not compound C, as there was no spot visible in the appropriate region on the electrophoretogram (Figure 35 B). However there was a spot of similar intensity as the spot labelled '?' (Figure 35 A) running slower than DKG at pH 2.0 (Figure 35 B). The mobility of this compound corresponds to a hypothesised 5-carbon intermediate of DKG oxidation to ThrO, named compound H (1). Interestingly there is no evidence of the formation of ThrO from this reaction.

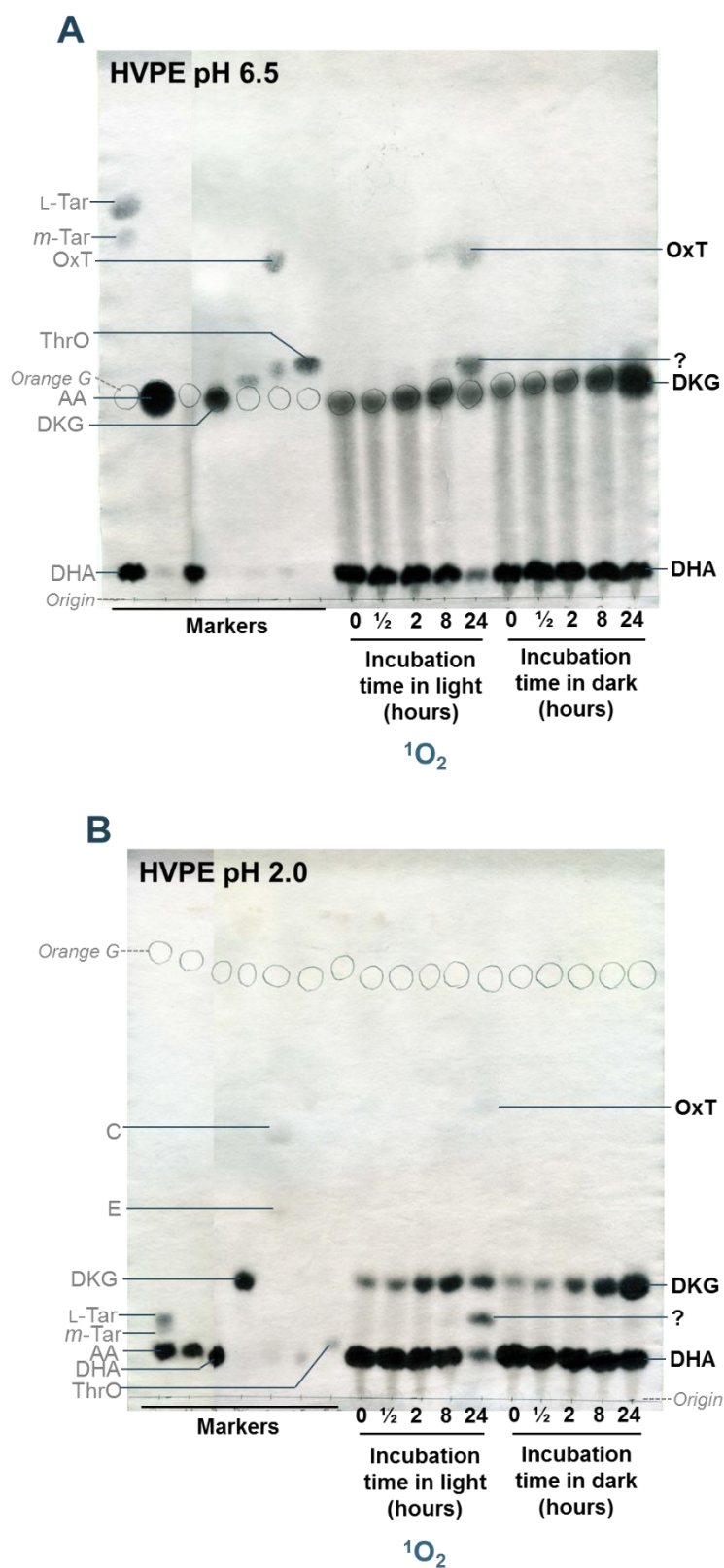


Figure 35: Reaction of DHA with singlet oxygen. DHA (50 mM) in 0.1 M acetate buffer (pH 4.5) was incubated with riboflavin (1 mM) in either light or dark conditions for up to 24 hours. Samples were taken at time points and stored at -80°C . Aliquots of each sample (20 μl) were loaded onto two separate Whatman 3 MM papers, along with the internal marker orange G (marked with pencil circles) and various markers. One paper (**A**) was run by HVPE at pH 6.5 and the other paper (**B**) was run by HVPE at pH 2.0. Both papers were stained in silver nitrate after drying.

It is possible that the compound marked with a “?” could have originated from riboflavin itself rather than from DHA or DKG. To test this, control samples containing only riboflavin were incubated in the light, to allow the formation of singlet oxygen, for up to 24 hours. The samples were then analysed by HVPE followed by silver nitrate staining (Figure 36).

Riboflavin is a yellow compound and can be seen as a small streak just above the origin on electrophoretograms run at both pH 6.5 and pH 2.0 (Figure 36 A and B). A silver nitrate stainable compound is visible in the neutral position in samples incubated for 24 hours, presumably a product generated through the oxidation of riboflavin itself. There are no compounds visible in the regions that would contain compound “?” at both pH 6.5 and pH 2.0. This suggests that the unknown compound (possibly compound H) does in fact originate from an ascorbate derivative, and not riboflavin.

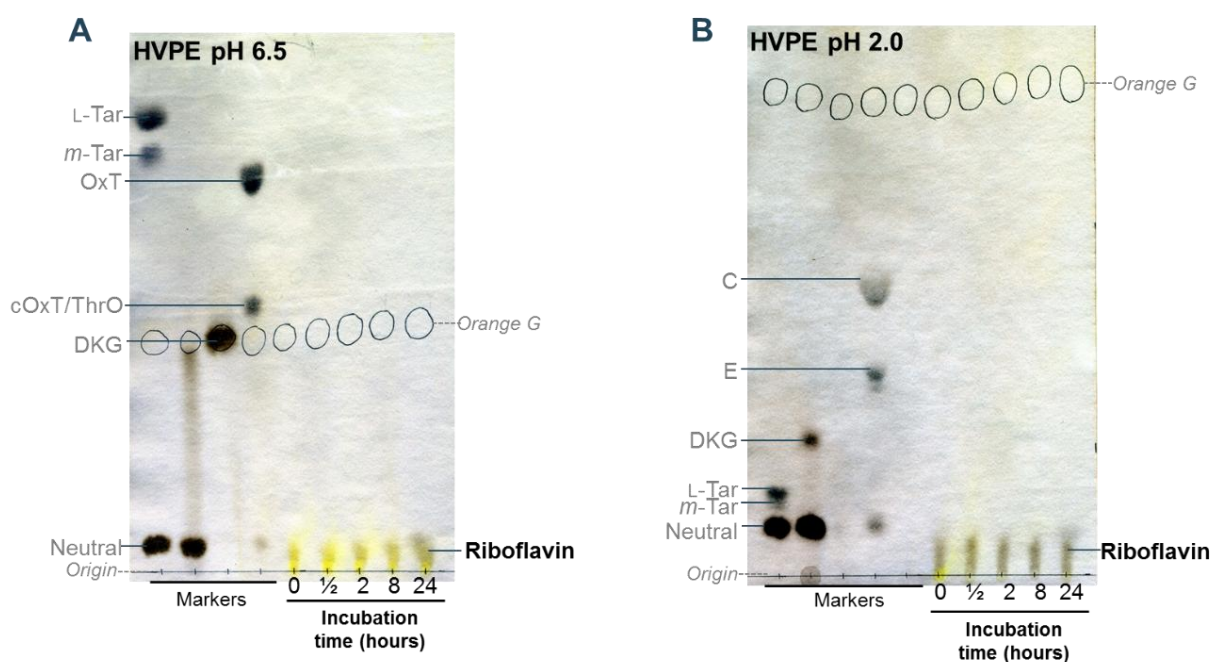


Figure 36: Compounds formed during the degradation of riboflavin by singlet oxygen. Aliquots of riboflavin (1 mM in 0.1 M pH 4.5 acetate buffer) were incubated for up to 24 hours in continuous light. Samples were taken at time points and stored at -80°C before loading 20 µl aliquots on paper and running by HVPE at pH 6.5 (A) or pH 2.0 (B). The papers were stained in silver nitrate, and the position of the internal marker orange G is marked with pencil circles.

3.3.3 The *in-vitro* reaction of DKG with different reactive oxygen species

DHA is fairly unstable in aqueous solutions and readily hydrolyses to DKG (82). DKG is present in the apoplast (72) and so has the potential to participate in reactions with apoplastic ROS.

3.3.3.i. *The reaction of DKG with H₂O₂*

DKG was prepared from the reaction of ascorbate with potassium iodate (82) (section 2.11.3). The resulting DKG was precipitated in EtOH and dried under vacuum. A sample of this purified DKG (60 mM) was incubated with 60 mM H₂O₂ in pH 4.8 buffer for up to 8 hours (Figure 37) and the products were run by HVPE at pH 6.5 and pH 2.0.

As previously reported (1) the major product formed was ThrO, via an unknown intermediate, labelled as H. This intermediate is clearly seen on the electrophoretogram run at pH 2.0 (Figure 37 B). Compound H co-migrates with ThrO at pH 6.5 (2) (Figure 37 A). Compound H has previously been suggested to be a C-5 compound, speculatively a form of 2-ketoxylonate (2). A small amount of OxT can also be seen after 60 minutes.

The duration of the reaction, which was not complete until 120 minutes, was surprising,

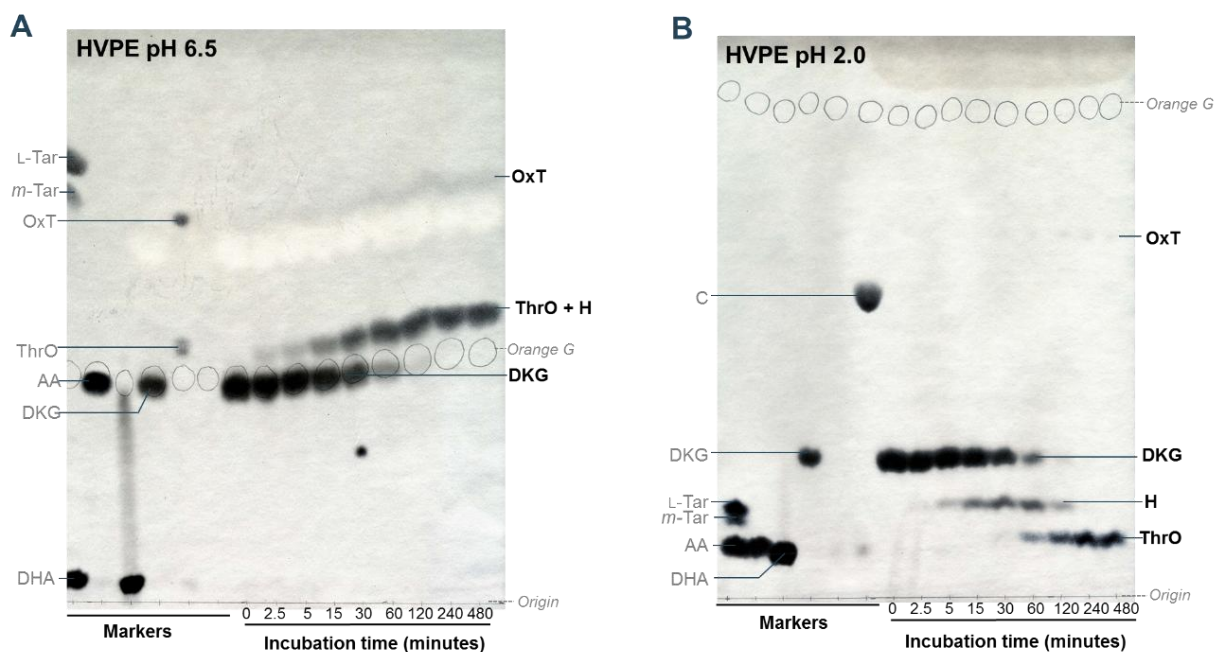


Figure 37: Reaction of DKG with H₂O₂. Purified DKG (60 mM in pH 4.8 sodium acetate buffer), prepared from ascorbate treated with KI, was incubated with H₂O₂ (60 mM) for up to 8 hours. Samples were taken at time-points and the reaction stopped with 0.1% catalase. The samples were then stored at -80°C. Aliquots (20 µl) were loaded onto two separate Whatman 3 mm papers and one paper was run by HVPE at pH 6.5 (A) and the other by HVPE at pH 2.0 (B). The papers were stained in silver nitrate. The position of the internal marker orange G is marked with pencil circles.

especially considering the reaction of DHA with H_2O_2 occurred almost immediately. It is suggested that there was something present in the DKG preparation acting to stabilise, and so reduce the degradation of, the DKG. There is a white spot on the electrophoretogram run at pH 6.5 close to the position of OxT present in all the samples containing DKG. This spot is likely to be an iodate ion, which was presumably precipitated along with DKG during its preparation. It could be that the presence of this compound is slowing down the breakdown of DKG. DKG has been reported to produce compounds C and E (discussed in chapter 3.1) in solution (1,72), so it is suspicious that they are not produced during the 8-hour incubation of this experiment, lending further support for the presence of a compound acting to stabilise DKG.

This experiment was repeated with DKG produced from the alkali treatment of DHA to avoid the potential interference of a stabilising iodate compound (section 3.3.3.iii).

3.3.3.ii. *The reaction of DKG with superoxide*

The products of the reaction of potassium iodate-generated DKG with superoxide were very similar to those produced with H_2O_2 . However, the pattern of the formation with $\text{O}_2^{\cdot-}$ was different. The initial reaction seems to have occurred more quickly with $\text{O}_2^{\cdot-}$ than with H_2O_2 , as an intense spot of compound H formed almost immediately with $\text{O}_2^{\cdot-}$ (Figure 38 B), whereas an equivalently intense spot of compound H was only formed after 15 minutes with H_2O_2 .

The pH 6.5 run shows some DKG remaining up to 60 minutes (Figure 38 A), but the pH 2.0 run does not (Figure 38 B). This was unexpected as the samples were identical. It could be possible that the samples loaded onto paper for HVPE at pH 2.0 were incubated on the paper before running for longer than the samples loaded for HVPE at pH 6.5. This may have allowed the degradation of DKG to continue for longer whilst the samples were on the paper. The control DKG samples run at pH 2.0 also show small amount of compound H, whereas no degradation products of the control samples were visible after HVPE at pH 6.5.

Other than compound H, the most predominant product formed was ThrO, with a small amount of OxT also being produced (Figure 38). The white spot present on the electrophoretogram run at pH 6.5 (Figure 38 A) is thought to be an iodate compound present in the preparation of DKG.

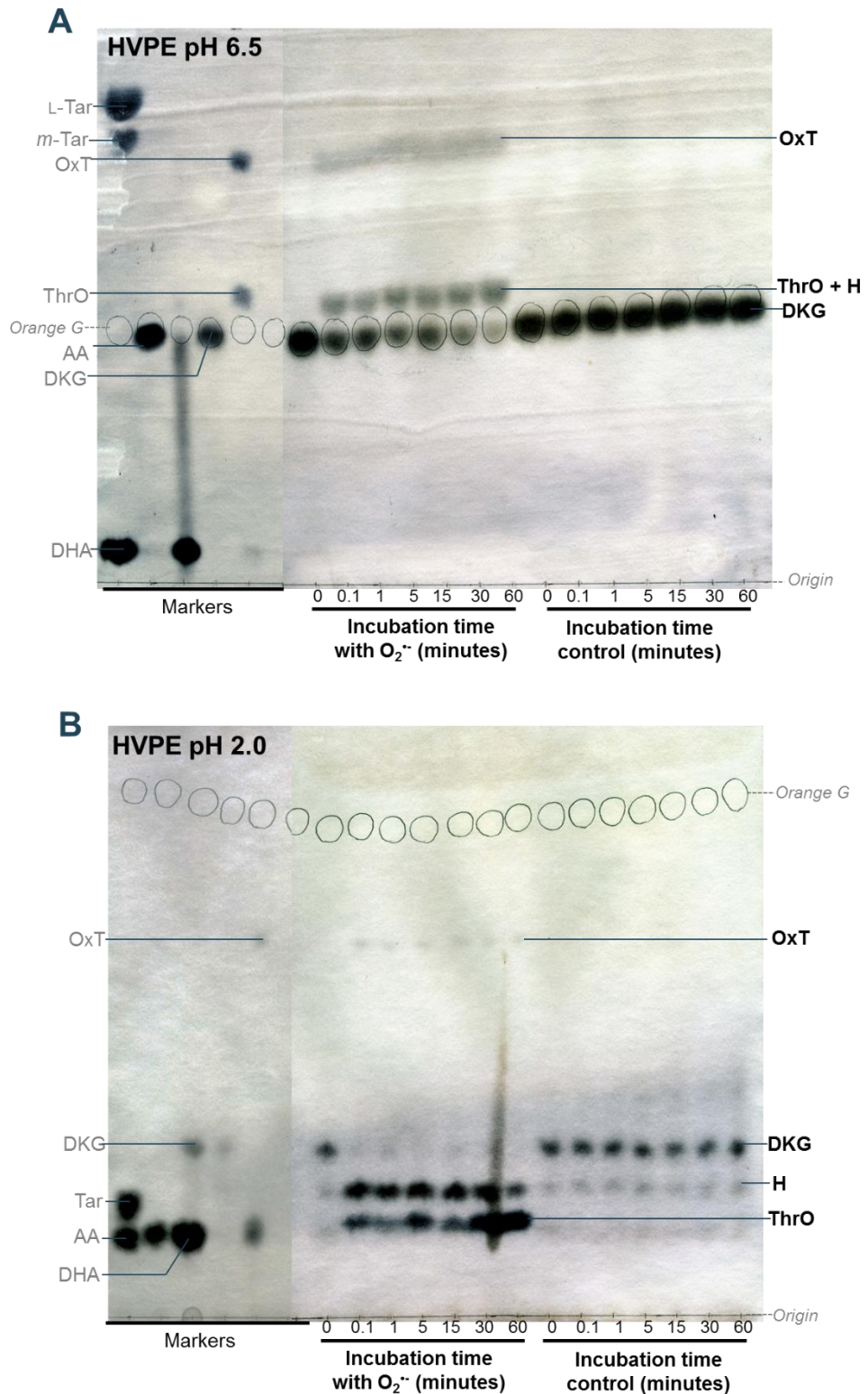


Figure 38: Reaction of DKG with superoxide. Purified DKG (50 mM in 0.1 M, pH 4.8 sodium acetate buffer), prepared from potassium iodate treated ascorbate, was incubated with KO_2 (50 mM) for up to 60 minutes. Samples were taken at time-points and the reaction stopped with 0.1% superoxide dismutase. The samples were then stored at -80°C . Aliquots (20 μl) were loaded onto two separate Whatman 3 MM papers and one paper was run by HVPE at pH 6.5 (A) and the other by HVPE at pH 2.0 (B). The papers were stained in silver nitrate. The position of the internal marker orange G is marked with pencil circles.

3.3.3.iii. The reaction of DKG with H_2O_2 and $O_2^{\cdot-}$ free from iodate

As this iodate compound was believed to be stabilising DKG, the reactions of DKG with H_2O_2 and $O_2^{\cdot-}$ were repeated with DKG produced from alkali treatment of DHA, which will result in a preparation of DKG free from any contaminating iodate compounds.

This preparation of DKG contained contaminating compounds C and E (which are discussed further in section 3.1; Figure 39). These compounds were present in the control mixture containing no ROS, and remained stable in the presence of both H_2O_2 and $O_2^{\cdot-}$. This suggests that these compounds (C and E) are not formed by an oxidation reaction, and are not oxidised themselves.

Differences are apparent in the products formed by the reaction of H_2O_2 and $O_2^{\cdot-}$ (Figure 39). Compound H was formed with $O_2^{\cdot-}$ but not with H_2O_2 . However, the amount of compound H formed in this reaction was much less than in the previous experiment (Figure 38). The appearance of compound H with H_2O_2 in the previous experiment (Figure 37) could be

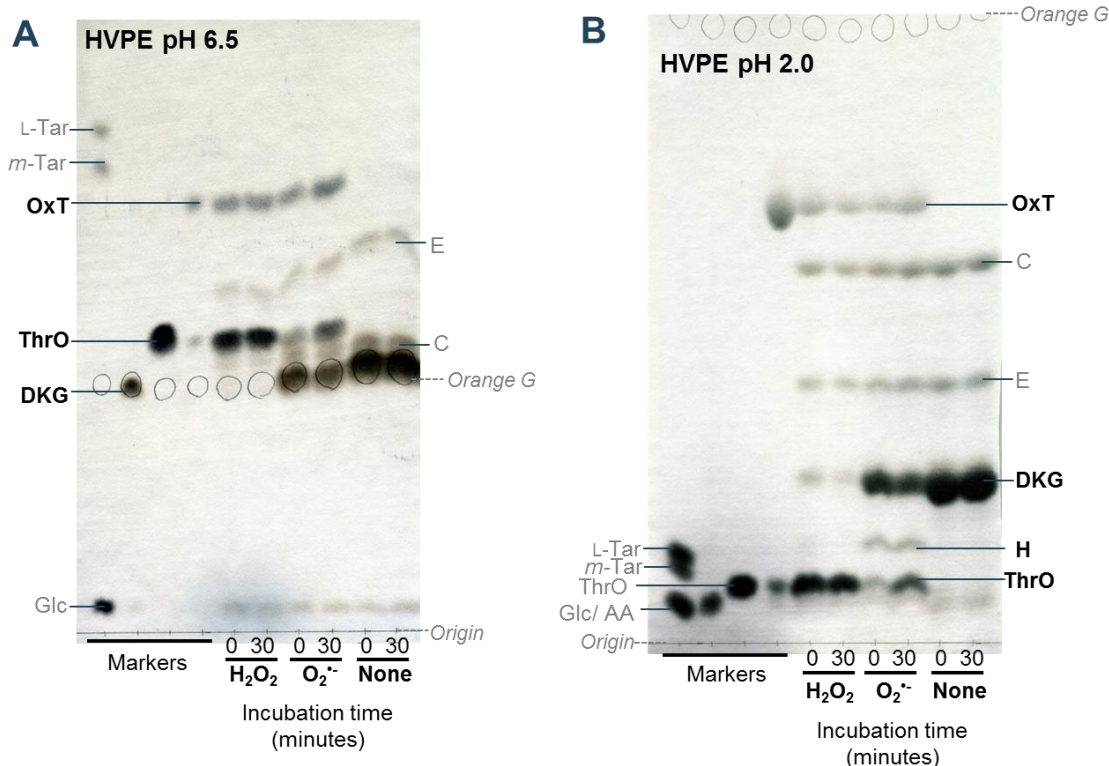


Figure 39: Reaction of DKG with H_2O_2 and $O_2^{\cdot-}$. DKG (50 mM in 0.1 M acetate buffer) produced via alkali treatment of DHA, was incubated with H_2O_2 or KO_2 (both 50 mM) for up to 30 minutes. The reaction was stopped with either catalase (for H_2O_2) or superoxide dismutase (for KO_2), both at 0.01% final concentration. Aliquots of each of the samples were run by HVPE at pH 6.5 (A) or pH 2.0 (B), and the papers were stained in silver nitrate. The position of the internal marker orange G was marked with pencil circles.

explained by the presence of the stabilising contaminant. This compound could have protected DKG from H_2O_2 , causing the oxidation to ThrO to progress more slowly, so the formation of the intermediate compound H was visible. Without the stabilising presence of the iodate compound the oxidation of DKG to ThrO was able to occur much more quickly, so the formation of compound H was not seen, as it was immediately degraded to ThrO. Equally, the iodate compound could have acted to stabilise compound H, preventing the further degradation of compound H to ThrO, resulting in the greater quantities of compound H that were observed in the presence of the iodate compound.

The reaction of DKG with $\text{O}_2^{\cdot-}$ appears to progress more slowly, or less completely, than with H_2O_2 , as seen by the presence of compound H (Figure 39 B). Compound H was thought to be a transient intermediate product (1), rather than an end product, so this suggests the reaction has not gone to completion. The reaction with $\text{O}_2^{\cdot-}$ has correspondingly produced less ThrO than with H_2O_2 . The level of OxT appears consistent between the two ROS. More OxT seemed to be produced without the iodate compound (Figure 39 compared to Figure 37 and Figure 38) further supporting the stabilising action of a contaminating iodate compound.

3.3.3.iv. *The reaction of DKG with the hydroxyl radical*

The reaction of the hydroxyl radical with DKG was studied using 1 mM and 50 mM FeSO_4 , EDTA and H_2O_2 ($\cdot\text{OH}$ -producing mixture). HVPE at pH 2.0 revealed that ThrO and OxT were produced with the 1 mM $\cdot\text{OH}$ -producing mixture (Figure 40). Compounds C and E (degradation products of DKG; discussed further in section 3.2) were also produced during the reaction.

The reaction of DKG with the 50 mM $\cdot\text{OH}$ -producing mixture yielded ThrO as the major product. There was less OxT produced with the 50 mM $\cdot\text{OH}$ -producing mixture compared to the 1 mM $\cdot\text{OH}$ -producing mixture. There was also a decrease in the amount of compound H formed with the 50 mM $\cdot\text{OH}$ -producing mixture. This suggests that the reaction with the 50 mM $\cdot\text{OH}$ -producing mixture was more complete than with 1 mM $\cdot\text{OH}$ -producing mixture, as compound H is assumed to be an intermediate compound between DKG and ThrO. The yield of ThrO appears much lower than the starting material of DKG, this may be due to the presence of EDTA and SO_4^{2-} which may have interfered with the detection of compounds by silver nitrate. OxT can be hydrolysed to form OxA and ThrO, which could explain the increased amount of ThrO as well as the decreased amount of OxT in the samples containing 50 mM $\cdot\text{OH}$ -producing mixture.

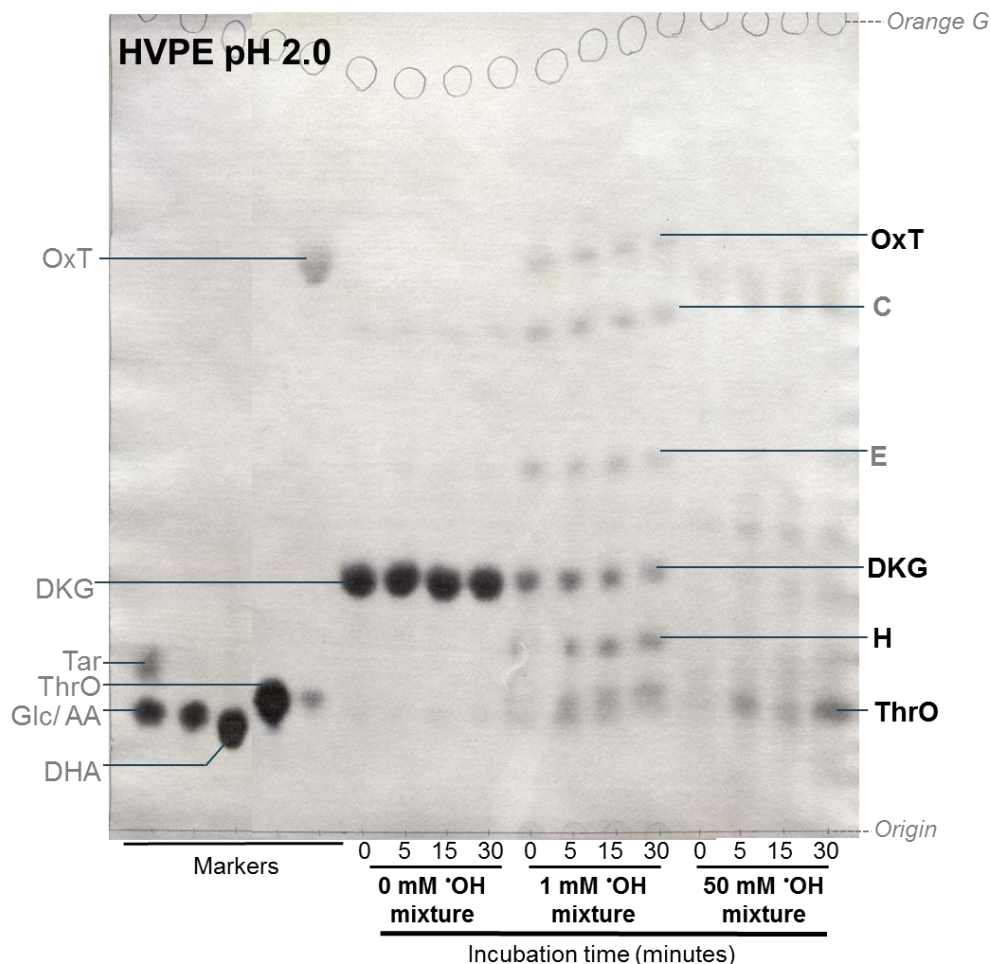


Figure 40: Reaction of DKG with hydroxyl radical. Purified DKG (50 mM in pH 4.8 sodium acetate buffer), prepared from potassium iodate treatment of ascorbate, was incubated with EDTA, FeSO₄ and H₂O₂ in equimolar concentrations (\cdot OH mixture, 0 mM, 1 mM or 50 mM) for up to 30 minutes. Samples were taken at time-points and the reaction stopped with EtOH (50% final concentration). The time 0 sample represents DKG with FeSO₄, EDTA and H₂O₂ and the immediate addition of EtOH. The samples were then stored at -80°C. Aliquots (20 μ l) were loaded onto paper and run by HVPE at pH 2.0. The paper was stained in silver nitrate. The position of the internal marker orange G is marked with pencil circles.

3.3.3.v. The reaction of DKG with singlet oxygen

Riboflavin (vitamin B₂) was used to produce singlet oxygen in the presence of light in the experiments discussed here. The DKG used in these experiments was prepared by the alkali treatment of DHA, for the reasons discussed previously.

DKG was incubated with riboflavin for up to 24 hours in the presence of light to produce singlet oxygen. Controls of DKG with riboflavin in the dark, and DKG incubated without riboflavin in the presence of light were also analysed (Figure 41).

ThrO was the major product of the reaction of DKG with $^1\text{O}_2$, with OxT being produced in smaller quantities. There was a contaminating neutral spot in all the samples, but this spot seemed to be more intense in the 24 hours sample with $^1\text{O}_2$, this is likely to be attributable to oxidation of riboflavin itself as seen in Figure 36. This preparation of DKG contained contaminating compounds including compounds C and E (discussed further in chapter 3.1).

The majority of the DKG had gone after 24 hours incubation in the presence of $^1\text{O}_2$ (Figure 41). This is surprising, as the concentration of riboflavin used was much lower than the concentration of DKG, however the production of $^1\text{O}_2$ from riboflavin may be more dependent on the O_2 present in the solution, rather than the concentration of riboflavin itself (257).

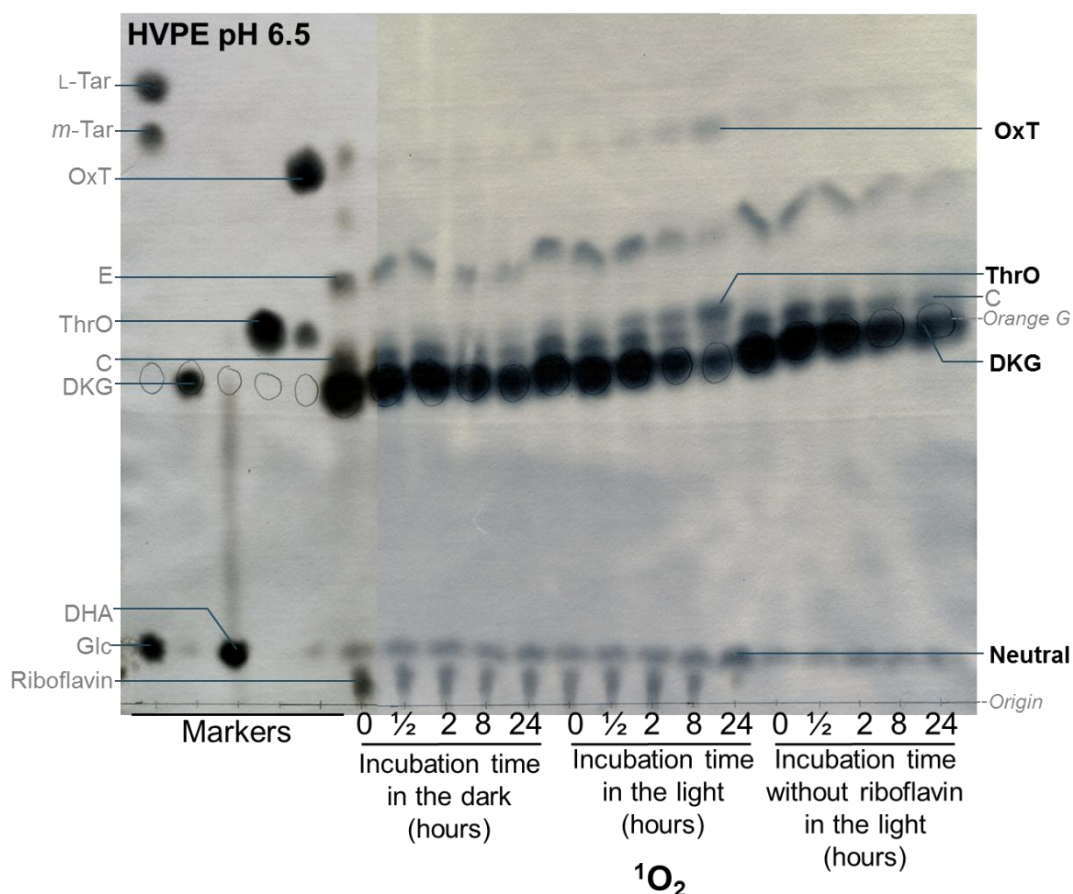


Figure 41: Reaction of DKG with singlet oxygen. DKG (50 mM in 0.1 M pH 4.8 sodium acetate buffer), prepared by alkali treatment of DHA, was incubated with riboflavin (1 mM) in the presence or absence of light for up to 24 hours. A control of DKG incubated in the light without riboflavin was also included. The samples incubated with riboflavin in the light represent the samples exposed to singlet oxygen ($^1\text{O}_2$). Samples were taken at time points and stored at -80°C . Aliquots ($20\ \mu\text{l}$) were loaded onto Whatman 3 MM paper, along with a series of markers and an internal marker of orange G (marked on the paper in pencil circles). The samples were run by HVPE at pH 6.5, then stained in silver nitrate.

3.3.4 Purification of [¹⁴C]DHA

In order to further study the reactions of ROS with DHA, radiolabelled DHA was used. The use of [¹⁴C]DHA allows the formation of OxA to be observed, compared to silver nitrate staining which does not stain OxA. Autoradiography is also much more sensitive than silver nitrate staining, allowing the reactions to be observed at lower concentrations, which are more biologically realistic. The use of [¹⁴C]DHA allows the quantification of the reaction products, by the use of scintillation counting.

[¹⁴C]DHA was purified from commercial [¹⁴C]AA. The [¹⁴C]AA was treated with ascorbate oxidase (AO), which catalyses the oxidation of AA to DHA (154). The sample of enzyme-treated AA was then loaded onto an anion-exchange chromatography column. The radiolabelled products in the sample were separated on the basis of charge, with the neutral DHA being eluted first (Figure 42), followed by the more negatively charged compounds in subsequent eluents.

The peak present in the formate buffer fractions (Figure 42 A) represents DHA, as seen on the autoradiogram (Figure 42 B) and accounts for the majority of the radioactivity. This demonstrates a successful method for the production and purification of [¹⁴C]DHA for use in further ROS experiments.

Further compounds were also eluted from the chromatography column, including what presumably is DKG (Figure 42 B, 0.25 M formic acid fraction) and OxT and OxA (Figure 42 B, 4 M TFA fraction).

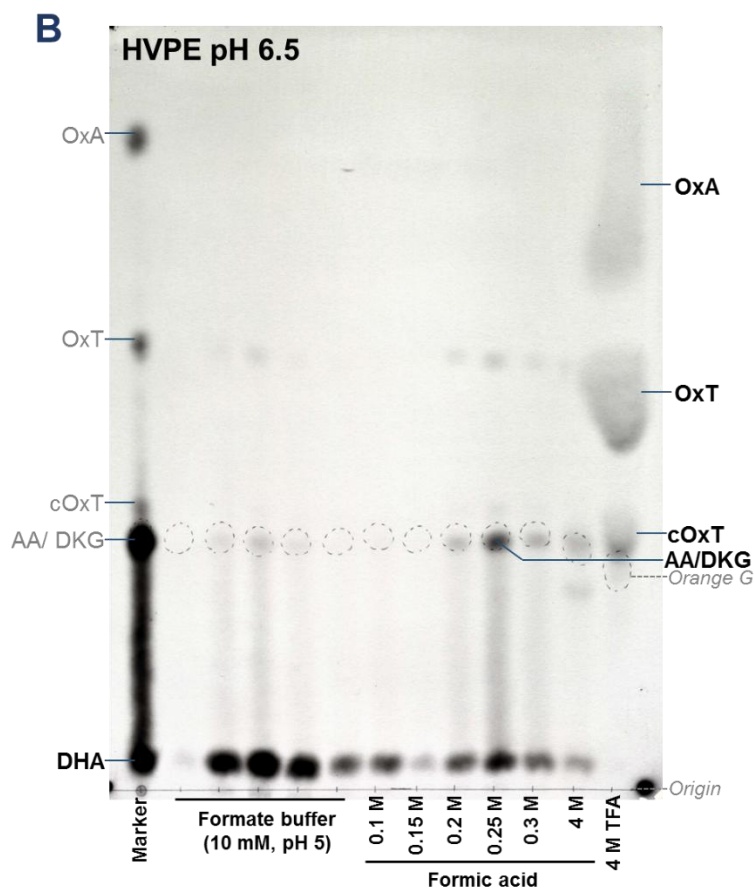
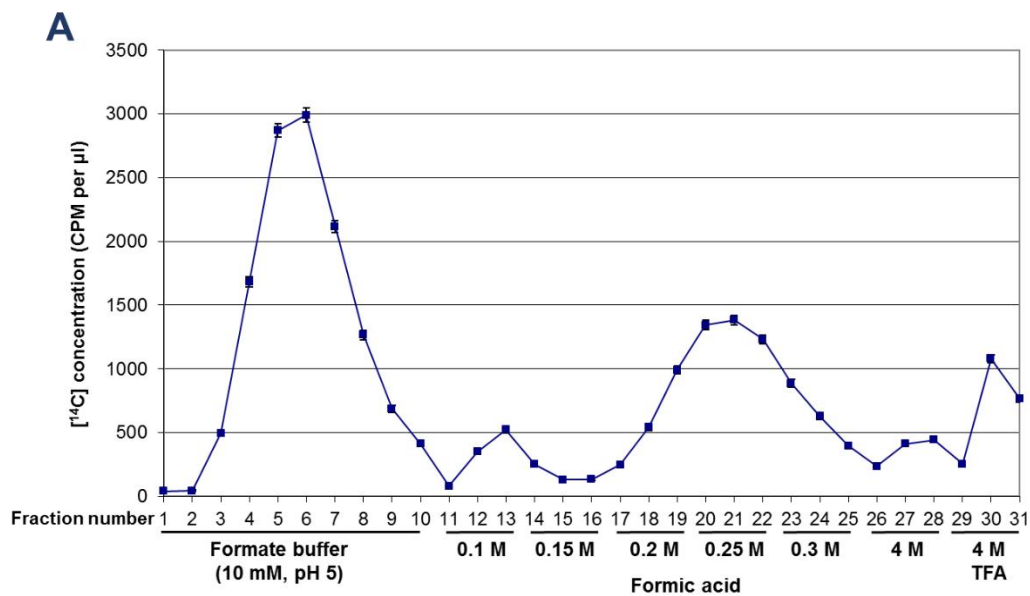


Figure 42: Purification of [¹⁴C]DHA by anion-exchange column chromatography. Commercial [¹⁴C]AA (50 µl, ~1 mM) was treated with AO (10 µl, 1 U µl⁻¹), then loaded onto an anion-exchange chromatography column (Dowex 1, 200 µl bed volume). The radiolabelled compounds were eluted in successive applications of sodium formate buffer (10 mM, pH 5), 0.1 to 0.3 M formic acid in 0.05 M increments, 4 M formic acid and 4 M TFA. Fractions (50 µl) of each eluate were collected, and aliquots (10 µl) from the fractions were dried onto squares of Whatman 3 MM paper and assayed for radioactivity by scintillation counting (**A**). Further aliquots (10 µl) of various fractions were loaded onto Whatman 3 MM paper and run by HVPE at pH 6.5. The paper was exposed to film for 1 week (**B**). The position of the internal marker orange G was marked with dotted circles.

3.3.5 The reaction of radiolabelled DHA with reactive oxygen species

3.3.5.i The reaction of [^{14}C]DHA with H_2O_2 and $\text{O}_2^{\cdot-}$

[^{14}C]DHA (approximately 0.3 mM) purified from anion-exchange column chromatography was treated with H_2O_2 or $\text{O}_2^{\cdot-}$ for up to 30 minutes. The products of these reactions were analysed by HVPE at pH 6.5 (Figure 43 A) and pH 2.0 (Figure 43 B). The autoradiograms show differences between the products formed with the two ROS. As with non-radiolabelled DHA, a greater proportion of cOxT was formed with H_2O_2 than with $\text{O}_2^{\cdot-}$. The use of radiolabelled DHA allows OxA to be visualised, whereas silver nitrate does not stain OxA. It can be seen that more OxA was formed with $\text{O}_2^{\cdot-}$ compared to H_2O_2 (Figure 43 A). The OxA is not visible after HVPE at pH 2.0. This could be due to a lack of chelating agent, resulting in OxA forming a streak (as in the marker lane in Figure 42 B) because it had bound to impurities such as calcium in the paper. OxA would run just above orange G at pH 2.0, with

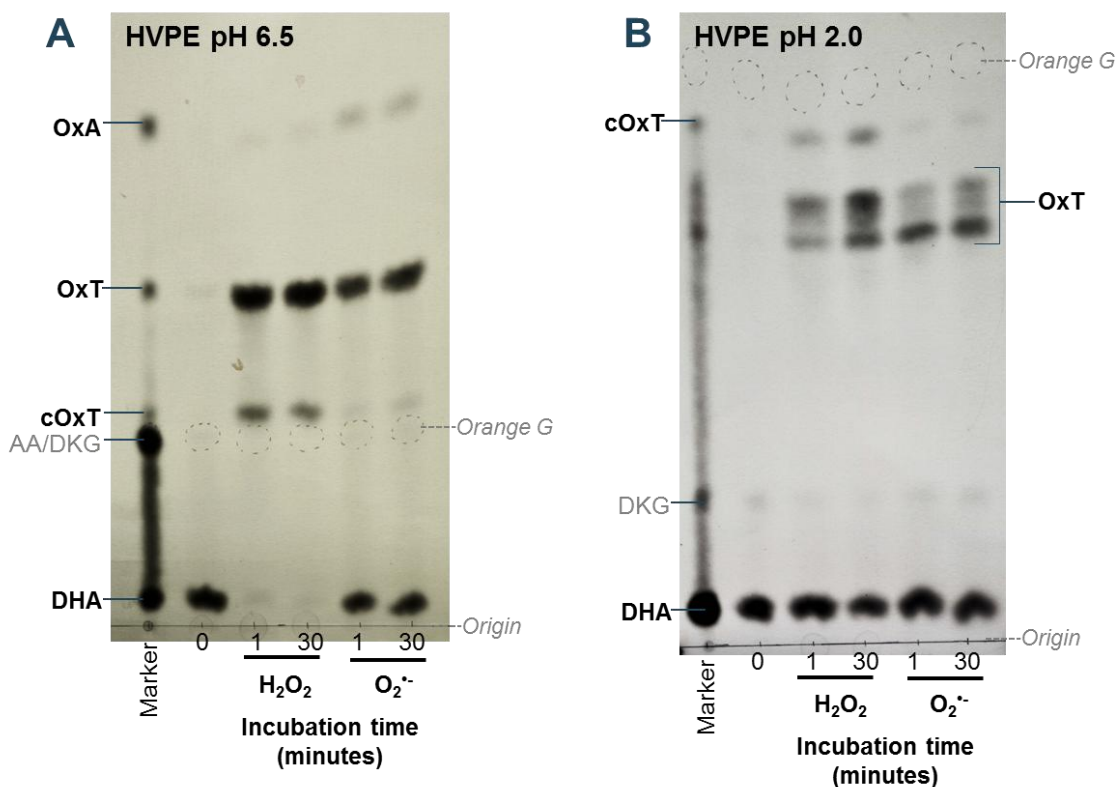


Figure 43: Reaction of [^{14}C]DHA with H_2O_2 and $\text{O}_2^{\cdot-}$. [^{14}C]DHA (approximately 0.3 mM), purified on an anion exchange chromatography column, was incubated with 2.5 mM H_2O_2 or KO_2 for up to 30 minutes. The reactions were stopped with catalase or superoxide dismutase (0.01% final concentration) respectively. Samples of each reaction were run by HVPE at pH 6.5 (A) or pH 2.0 (B), and the papers were exposed to film for 1 week. The position of the internal marker orange G is marked with dotted pencil circles.

a m_{OG} of 1.05.

HVPE at pH 2.0 resolves the three isomers of OxT (2) (Figure 43 B). Interestingly the abundance of the individual isomers varied between $O_2^{\cdot-}$ and H_2O_2 . The reaction with H_2O_2 produced more of the fastest-moving isomer whereas $O_2^{\cdot-}$ produced more of the slowest-moving isomer (Figure 43 B). It has been suggested that 3-OxT and 4-OxT would be more stable than 2-OxT (2), owing to the proximity of the two COOH groups in the 2-OxT isomer (Figure 44). It had been previously reported that H_2O_2 produced more 4-O-OxT than 3-O-OxT (2) so the faster-moving spot could be assumed to be 4-O-OxT. The slower-moving compound, formed predominantly with $O_2^{\cdot-}$, would then be assumed to be 3-O-OxT.

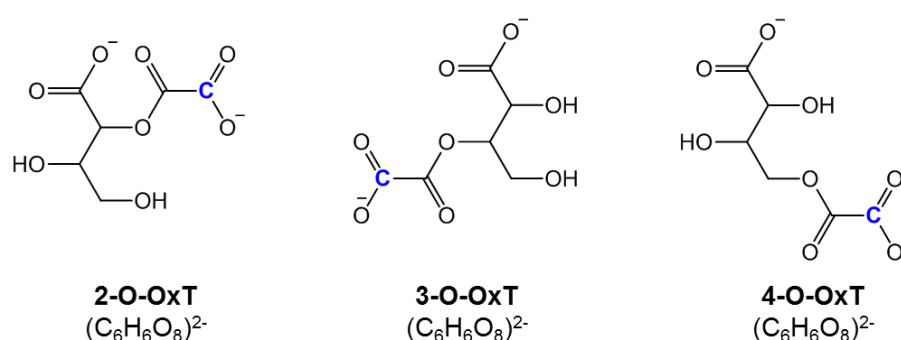


Figure 44: Structures of OxT isomers. The structures of the three isomers (2-O-OxT, 3-O-OxT and 4-O-OxT) are shown, along with the chemical formula. C-1 of the original [^{14}C]AA is indicated with a blue C.

A further advantage of using radiolabelled substrates is that it allowed the quantification of the initial substrate and products formed. The individual products from the samples of [^{14}C]DHA treated with H_2O_2 and $O_2^{\cdot-}$, run by HVPE at pH 6.5 (Figure 43 A) and at pH 2.0 (Figure 43 B), were quantified by scintillation counting (Figure 45). This allows the relative proportions of products formed to be ascertained.

After the reaction of [^{14}C]DHA with H_2O_2 (Figure 45 A) the ratio of OxT : cOxT was approximately 6:1, with very little OxA formed, compared to a ratio of approximately 6:1:1 (OxT : cOxT : OxA) as has been previously reported (2). The reaction of DHA with $O_2^{\cdot-}$ yielded OxT, cOxT and OxA in a ratio of approximately 6:1:1, which is more similar to the reported ratio, with equal amounts of cOxT and OxA (Figure 45 B).

HVPE at pH 2.0 allowed the separation of different isomers of OxT. The reaction of DHA with H_2O_2 produced more of OxT isomer b (the fastest migrating isomer; Figure 43 B) with the ratio of isomer b : isomer a being approximately 1.75:1 (Figure 45 C). Conversely, the reaction of [^{14}C]DHA with $\text{O}_2^{\cdot-}$ yielded more of OxT isomer a, with a ratio of isomer b : isomer a of approximately 1:2 (Figure 45 D).

There was a difference between the apparent amount of [^{14}C]DHA remaining after the reaction with H_2O_2 when analysed by HVPE at either pH 6.5 or pH 2.0, with more remaining in the samples run at pH 2.0 (figures 43 and 45). The reason for this is unclear, but potentially the acidity of the pH 2.0 buffer promoted the formation of a neutral product which was then assumed to be DHA, but any other neutral product would not be distinguishable. Alternatively, the pH 6.5 buffer could have acted to promote the further degradation of DHA while the sample was wetted with buffer before the HVPE run, meaning no DHA remained at the origin.

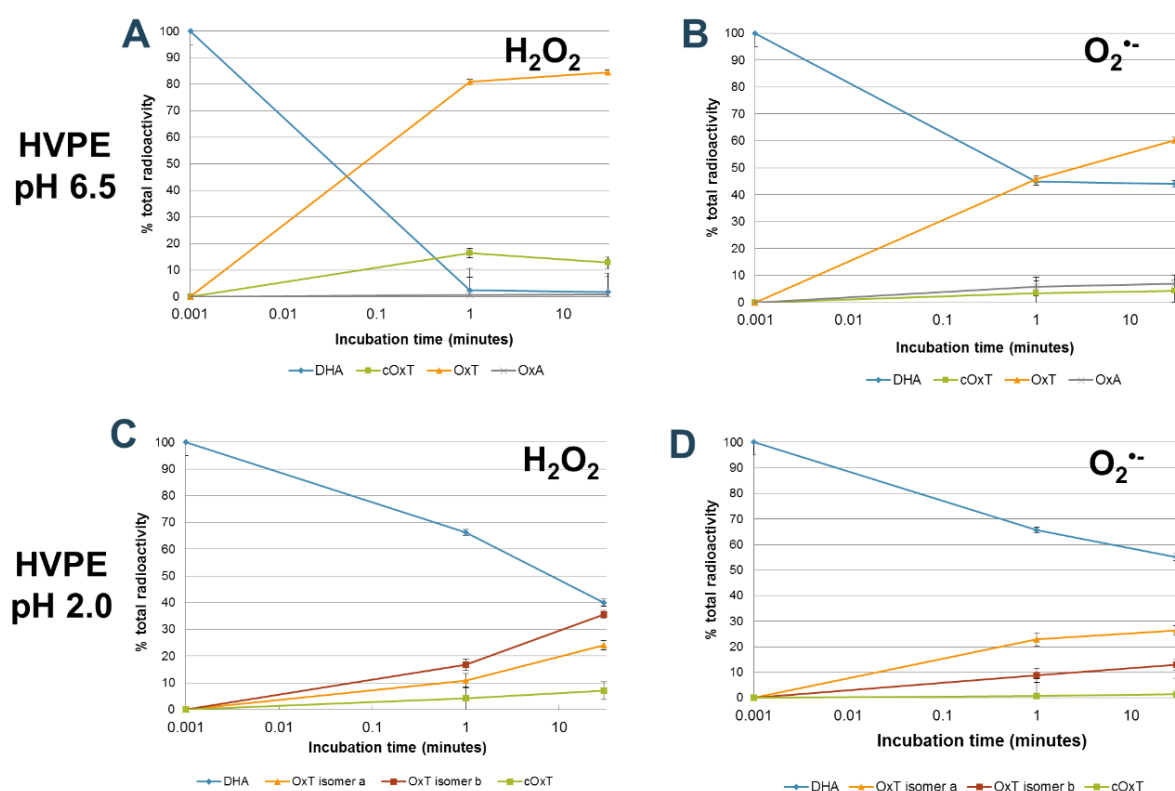


Figure 45: Quantification of products formed from the reaction of [^{14}C]DHA with H_2O_2 and $\text{O}_2^{\cdot-}$. [^{14}C]DHA (approximately 0.3 mM) was treated with H_2O_2 (A and C) or KO_2 (B and D) for up to 30 minutes, and the reaction mixture was then run by HVPE at pH 6.5 (Figure 43 A) or at pH 2.0 (Figure 43 B). After autoradiography the radiolabelled compounds were carefully cut out from the paper and assayed for radioactivity by scintillation counting. The radioactivity is reported as a percentage of the total radioactivity (the sum of all the radiolabelled compounds in each sample).

3.3.5.ii. The reaction of [^{14}C]DHA with the hydroxyl radical

[^{14}C]DHA, approximately 0.3 mM, purified from anion-exchange column chromatography, was treated with various concentrations of an $\cdot\text{OH}$ -producing solution and the products were analysed by autoradiography following HVPE at pH 6.5 (Figure 46). The predominant product with all the concentrations was OxA. This product would not have been visible in the experiments using non-radiolabelled DHA. However ThrO, which would be formed along with OxA, was visible with silver nitrate staining (Figure 33 and Figure 34).

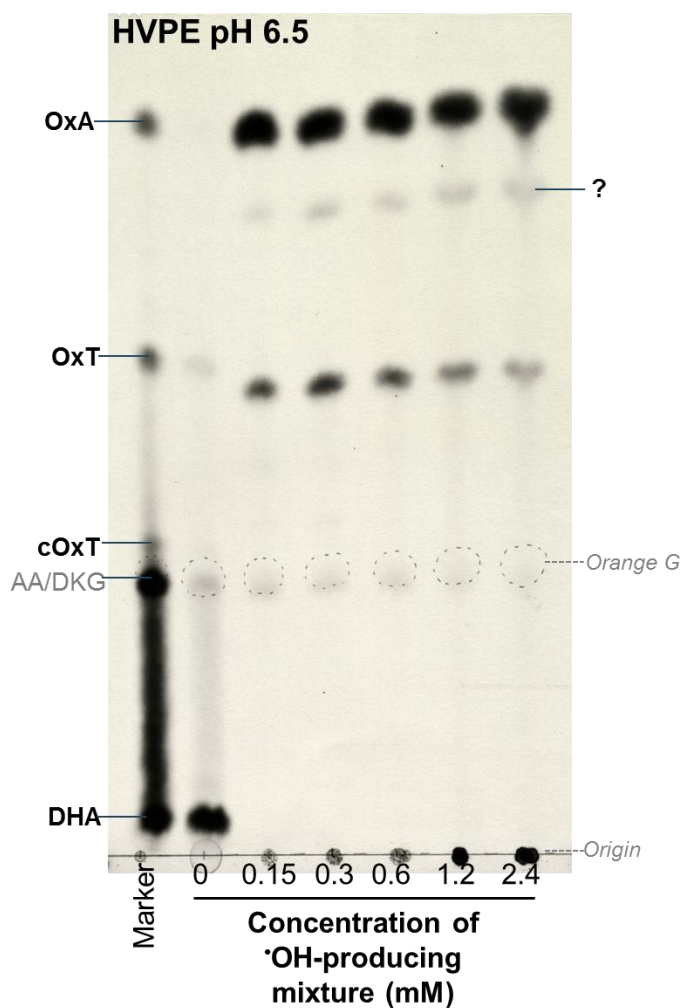


Figure 46: The reaction of [^{14}C]DHA with various concentrations of hydroxyl radical. [^{14}C]DHA, purified from anion exchange column chromatography, was incubated with increasing amounts of $\cdot\text{OH}$ (generated from equimolar FeSO_4 , EDTA and H_2O_2) for 5 minutes. The reaction was stopped by the addition of EtOH (50% final concentration). Small samples of each reaction were loaded onto paper and run by HVPE at pH 6.5. The paper was exposed to film for 1 week. The position of the internal marker orange G is marked in dotted pencil circles.

Interestingly a greater proportion of OxT was formed in the reactions containing lower amounts of $\cdot\text{OH}$. It is possible that the higher amounts of $\cdot\text{OH}$ have led to the further degradation of OxT, forming the [^{14}C]OxA seen in Figure 46, and non-radiolabelled ThrO (not visible in Figure 46). High pH values could result in the hydrolysis of OxT to OxA and ThrO; however, the pH of the $\cdot\text{OH}$ -producing solution was checked and found to be in the range of pH 4-5, so the increase in [^{14}C]OxA is not likely to be because of an increase in the pH of the solution.

Low levels of an unidentified compound, migrating just below OxA (labelled with '?', Figure 46), have also been formed. The fast migration of this compound suggests that it has a strong negative charge, along with a small mass.

With increasing $\cdot\text{OH}$ amounts more radioactivity becomes trapped at the origin (Figure 46). It is likely that this radioactivity has become a part of an insoluble compound, such as an oxalate salt, which could have occurred due to the high levels of OxA present in these samples.

3.3.6 Summary of the oxidation of DHA and DKG by various ROS

The overall oxidation pathway is shown in Figure 47. This pathway shows that cOxT originates from DHA and not DKG (Figure 47), whereas OxT was produced from both starting compounds. Equally, compound H was produced only from DKG and not from DHA.

As well as differences between the products formed from DHA and DKG, there were also differences in the products formed by different ROS. For example, OxT was the major product formed from DHA with H_2O_2 and $\text{O}_2^{\cdot-}$, whereas the major product formed from $\cdot\text{OH}$ was ThrO, along with OxA (Figure 48). Although OxT was the major product of the reaction of DHA with both H_2O_2 and $\text{O}_2^{\cdot-}$, the isomer of OxT differed with the two ROS, as demonstrated in Figure 43 B, with more of the 4-O-OxT isomer being produced with H_2O_2 and the 3-O-OxT isomer being produced more with $\text{O}_2^{\cdot-}$ (Figure 48).

The formation pattern of the minor products also varied with ROS. The first (referring to the most abundant of the minor products, rather than to the sequence in which the products were formed) minor product of the reaction between DHA and H_2O_2 was cOxT, whereas the first minor product with $\text{O}_2^{\cdot-}$ was ThrO, along with OxA (Figure 48). $^1\text{O}_2$ was notable for being

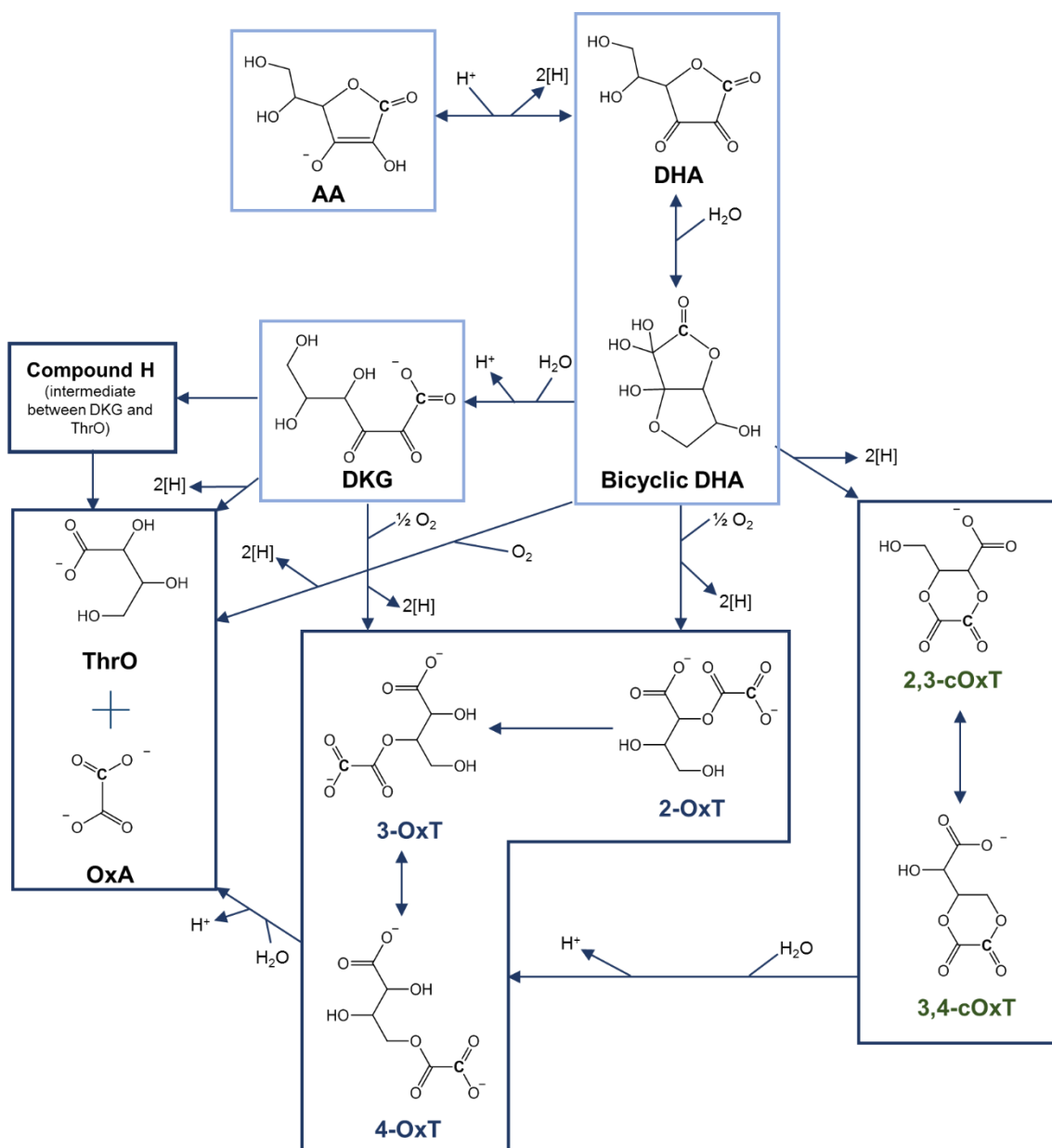


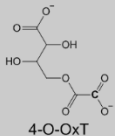
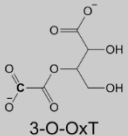
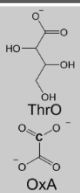
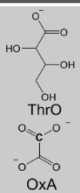
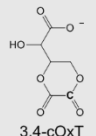
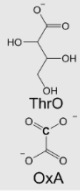
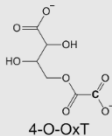
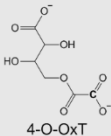
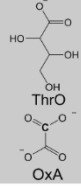
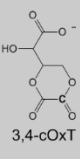
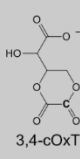
Figure 47: Oxidation pathways of ascorbate. The degradation of ascorbic acid is shown, including the hydrolysis step between DHA and DKG. The structures of products formed from both DHA and DKG by various ROS are shown. Oxidation steps are shown with 2[H]. The reactions involving compound H are unknown, so the arrow is unlabelled.

the only ROS that did not produce any cOxT or ThrO from DHA. However, the reaction did produce an unknown compound in addition to OxT, cautiously identified as compound H. Compound H has previously been reported to be an intermediate product between DKG and ThrO. It is possible that in the case of 1O_2 the unknown compound originated from DKG rather than directly from DHA, as the incubation time was 24 hours, and some of the starting DHA had been hydrolysed to DKG over the course of the experiment, thus it is possible that the unknown compound produced from the reaction with 1O_2 was compound H.

The products formed from DKG did not vary with different ROS. The only difference was that compound H was not observed in the reaction with $^1\text{O}_2$, whereas it was with the other ROS tested (Figure 48). The major product of the reaction of DKG with each of the ROS was OxT, with ThrO and OxA being produced in smaller quantities. In the case of DKG the formation of OxA was assumed, as only ThrO was observed with silver nitrate stain. However the formation of ThrO necessitates that OxA is also formed, as it involves splitting the DKG molecule between carbons 2 and 3, with C1 and C2 forming OxA and C3-6 forming ThrO.

This work has produced more in-depth detail of the oxidation pathways of ascorbate. It has been demonstrated that different ROS produce different oxidation products during the reaction with DHA. Equally, DHA and DKG produce different oxidation products. Interestingly, the production of compounds C and E was not observed during these experiments, providing further evidence that these compounds are not oxidation products.

Potentially, the different products formed *in vivo* from different ROS, or a lack of ROS (in the case of compound C and E formation), could act as signatures for the specific oxidative stress that a plant has been subjected to.

A	DHA	H_2O_2	$\text{O}_2^{\cdot-}$	$\cdot\text{OH}$	$^1\text{O}_2$
Major product	 4-O-OxT	 3-O-OxT	 OxA	 OxA	? (compound H?)
1 st minor product	 3,4-cOxT	 OxA	 4-O-OxT	 4-O-OxT	
2 nd minor product	 OxA	 3,4-cOxT	 3,4-cOxT		

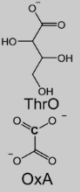
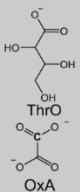
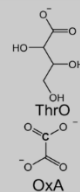
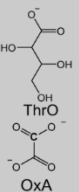
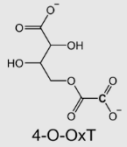
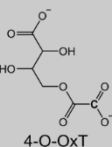
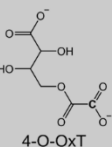
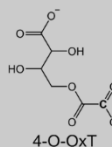
B	DKG	H_2O_2	$\text{O}_2^{\cdot-}$	$\cdot\text{OH}$	$^1\text{O}_2$
Major product	 OxA	 OxA	 OxA	 OxA	
1 st minor product	? (compound H?)	? (compound H?)	? (compound H?)	? (compound H?)	 4-O-OxT
2 nd minor product	 4-O-OxT	 4-O-OxT	 4-O-OxT		

Figure 48: Summary of products formed from DKG and DHA by different ROS. The oxidation products from the reaction of DHA (**A**) or DKG (**B**) with ROS (H_2O_2 , O_2 , OH and $^1\text{O}_2$) are shown. OxT is shown in the 4-O isomer, and cOxT is shown in the 3-4 isomer, as these are assumed to be most stable and so the most probable forms of the compounds. The predominant (major product), second most predominant (1st minor product) and the third most predominant (2nd minor product) products of each reaction are shown. The labels of first and second minor products merely reflect the abundance of the products, and provide no implications of the sequence of formation. ThrO and OxA are shown in the same box, as the formation of one requires that the other is also formed.

3.4 The fate of radiolabelled ascorbate degradation products in plant cell suspension cultures

3.4.1 Introduction to ascorbate and plant cell suspension cultures

The oxidation products OxT and cOxT, formed from the oxidation of DHA (discussed in section 3.3), contain 'activated' oxalyl groups, which could potentially form an oxalyl ester bond with components of the cell wall by transacylation. This could provide a novel mechanism for cell wall cross-linking via the formation of an oxalyl bridge (Figure 49). The presence of two oxalyl ester linkages in cOxT means that this compound is more likely to be the substrate to form the hypothetical cross-linking oxalyl bridge than OxT, containing only oxalyl ester linkage.

This hypothesis was tested by investigating the fate of radiolabelled OxT in spinach, *Arabidopsis* and rose cells. The use of radiolabelled substrates fed to cell cultures allowed the monitoring of the fate of these compounds *in vivo*. Specifically, the incorporation of radioactivity into the cell wall was monitored, as this would provide evidence for the formation of oxalyl esters with cell wall components.

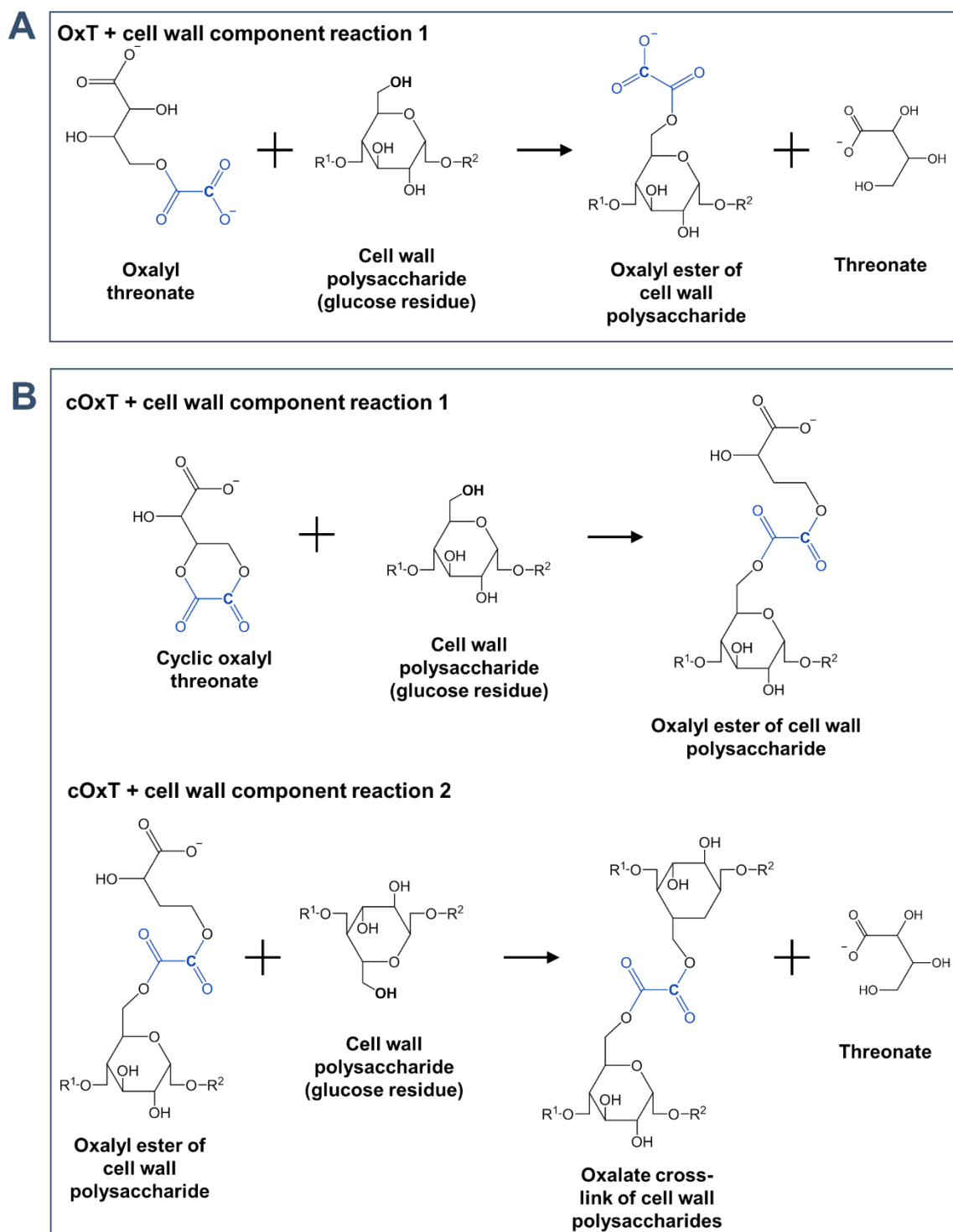


Figure 49: Schematic of potential oxalate cross-link formation in the cell wall. The hypothetical formation of oxalyl esters with an acceptor (in this case a glucose residue from a polysaccharide) from OxT (**A**) and cOxT (**B**) is shown. The activated oxalyl groups are shown in blue, with the ^{14}C (from C-1 of the original $[^{14}\text{C}]\text{AA}$ used to purify these compounds) shown with a bold **C**. The OH group most readily available for ester formation on the glucose residue is also shown in bold.

3.4.2 Fate of [¹⁴C]DHA in spinach, rose and *Arabidopsis* cell cultures

[¹⁴C]DHA was purified by anion-exchange column chromatography (as described in section 3.3.4). Aliquots of this [¹⁴C]DHA were fed to cell suspension cultures of spinach, *Arabidopsis* and rose.

The majority of the radiolabel had gone from the medium of rose and spinach cell cultures within 3 hours (Figure 50). This radioactivity was then mostly released when the cells were washed with EtOH, which causes the cell membranes to be disrupted, thus releasing intracellular EtOH-soluble, low-molecular weight compounds. The presence of a large proportion of the radioactivity in the EtOH wash suggests that the [¹⁴C]DHA, or a derivative of [¹⁴C]DHA, had entered the protoplasts. Further washes with acidified EtOH, aiming to thoroughly wash out all alcohol-soluble compounds, released only small additional amounts of radioactivity. There was very little radioactivity remaining in the alcohol-insoluble residue (AIR). This AIR represents high-molecular weight compounds, predominantly comprising cell wall components. Thus any radioactivity present in the AIR could indicate a

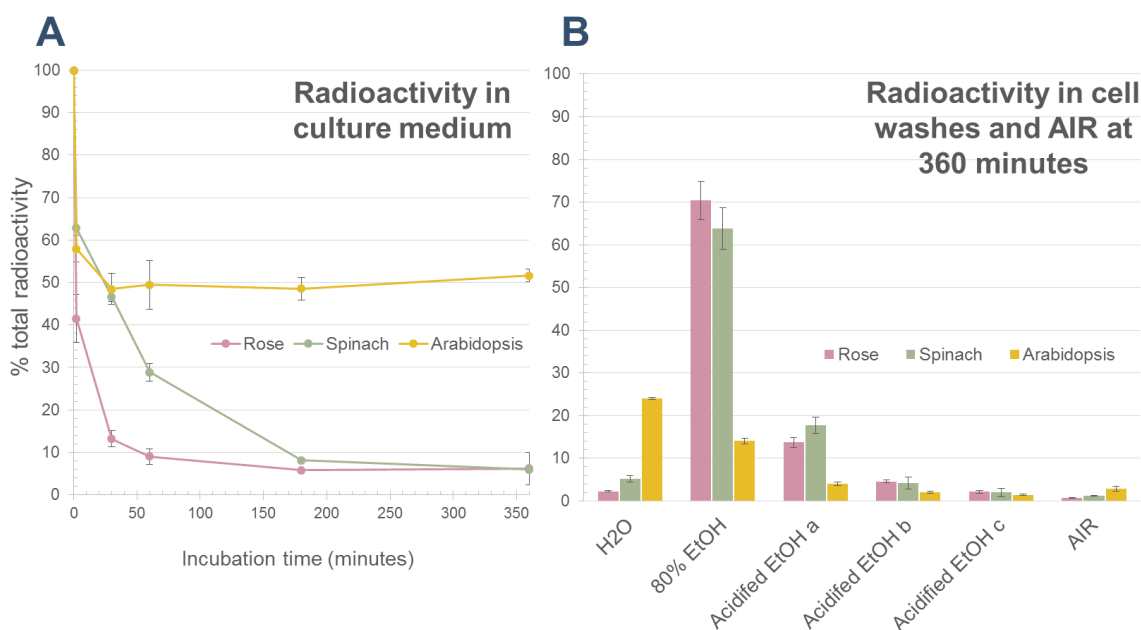


Figure 50: [¹⁴C]DHA enters the cells of *Arabidopsis*, rose and spinach cell cultures. Mini-cultures of rose, spinach and *Arabidopsis* cells (250 mg cells in 500 μ l medium, 1 week after subculturing) were inoculated with [¹⁴C]DHA (purified on an anion-exchange chromatography column; approximately 0.5 μ M final concentration). Samples of medium (50 μ l) were taken at intervals up to 6 hours, and assayed for radioactivity by scintillation counting. The radioactivity remaining in the culture medium at each time point is plotted (A). After 6 hours the medium was removed from the cells and the cells were washed sequentially in H₂O, EtOH and three times in acidified EtOH. The resulting material left after the washes (AIR) comprises predominantly cell wall material. The radioactivity present in each of the washes and in the AIR was assayed by scintillation counting (B). The bars labelled 'H₂O' represent the radioactivity present in the medium and the first wash in H₂O combined. Each point is an average of three replicate cultures \pm SE.

radiolabelled compound that had formed a covalent bond with cell wall material.

Conversely, approximately half of the radioactivity fed to *Arabidopsis* cells remained in the culture medium for the 6-hour incubation time (Figure 50 A). There was a very rapid immediate decrease in the radioactivity in the culture medium (Figure 50 A). It is not clear what causes this, as the loss is too fast, within two minutes of inoculation, to be attributable to active uptake by the cells.

A small proportion of the radioactivity incubated with *Arabidopsis* cells remained insoluble throughout the washing process, resulting in radiolabelled AIR. This potentially represents radioactivity that has become bound to cell wall material via an ester bond. Alternatively, this insoluble radioactivity could be in the form of calcium oxalate (177) (CaOxA), which is insoluble in EtOH and H₂O.

The majority of [¹⁴C]DHA incubated in spinach and rose cell-suspension cultures entered the cells themselves, as demonstrated by the release of radioactivity after washing the cells in EtOH. However, more radioactivity remained in the culture medium of *Arabidopsis* cell culture. Some of this radioactivity incubated with *Arabidopsis* cells remained insoluble after multiple EtOH and acidified EtOH washes, suggesting that it may be covalently bound to cell wall material, potentially via an oxalyl ester bond.

There are numerous possible fates of DHA within the plant cell, including conversion back to AA via the action of DHAR (67), which occurs rapidly after DHA has been transported into the cell (33). As well as this, DHA can be hydrolysed to DKG, which can be further degraded to C and E (discussed in section 3.1), or DHA can be oxidised to OxT, cOxT and OxA (2,72). To gain more precise information about the potential cross-linking of cell walls, a starting substrate of OxT was used instead of DHA.

3.4.3 Fate of [¹⁴C]OxT in spinach and *Arabidopsis* cell cultures

[¹⁴C]OxT was incubated in plant cell-suspension cultures to further study the potential oxalyl ester formation within the plant cell wall.

[¹⁴C]OxT was prepared by preparative HVPE of [¹⁴C]AA treated with H₂O₂. The bands of [¹⁴C]cOxT, OxT and OxA, as well as DHA were cut out of the paper and the compounds eluted in H₂O. The compounds were then dried and re-dissolved in H₂O.

Radiolabelled OxT was used rather than cOxT because the original reaction of AA with H₂O₂ produced more OxT than cOxT (in a 6:1 ratio, OxT: cOxT, as previously reported (2)), so there was more OxT available. The OxT preparation was also more pure than the cOxT preparation. It proved very difficult to produce a pure sample of cOxT, as some straight-chain OxT was always produced. It seems that cOxT was not stable during the elution or drying step of purification.

It was not known whether spinach and *Arabidopsis* cell cultures contained an oxalyl esterase (72) in the apoplast (represented by the culture medium). This enzyme would potentially degrade [¹⁴C]OxT into [¹⁴C]OxA and non-radiolabelled ThrO. Samples of [¹⁴C]OxT-fed

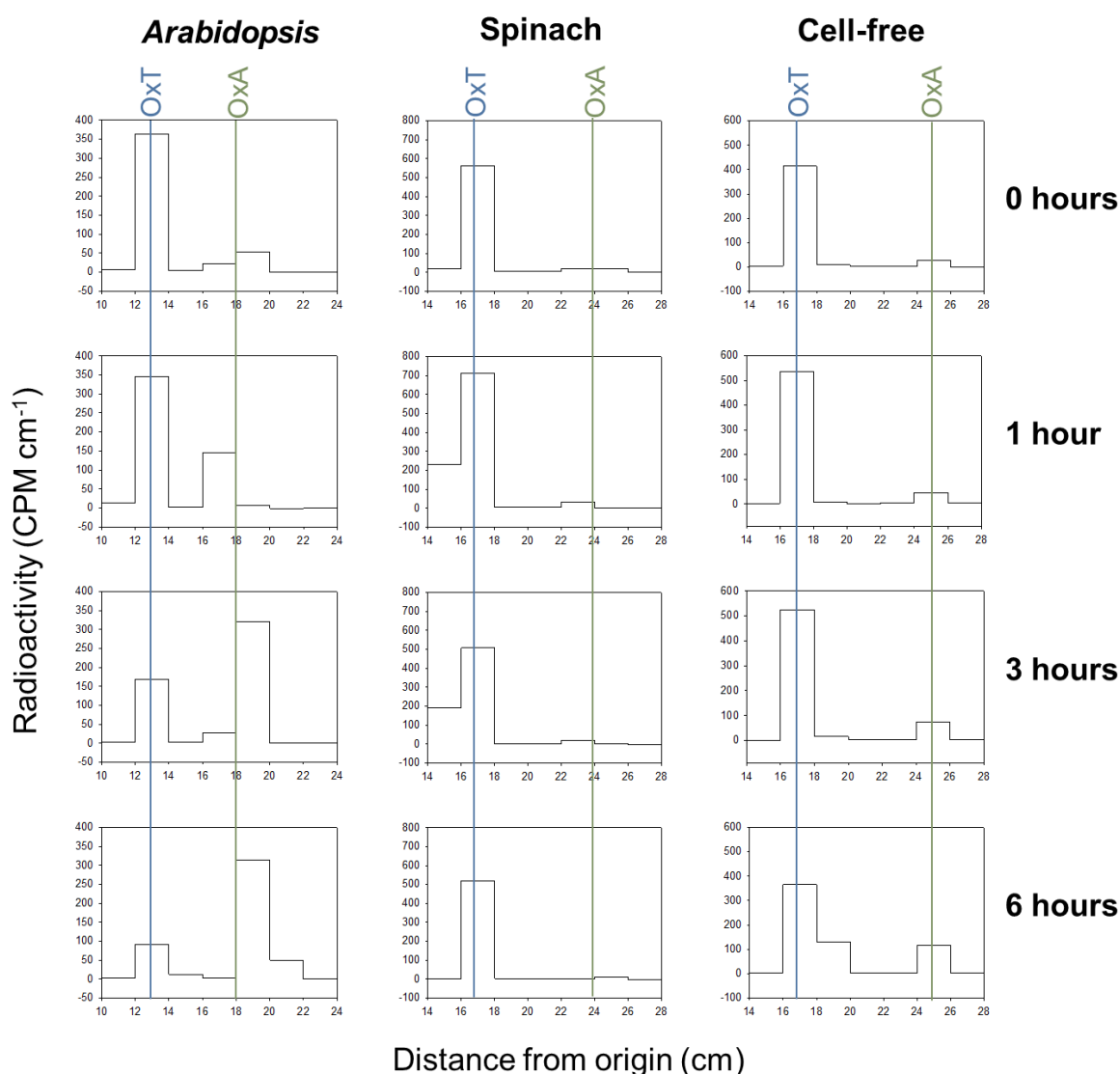


Figure 51: Fate of [¹⁴C]OxT in *Arabidopsis* and spinach cell culture. Samples of culture medium (50 μ l) collected from spinach or *Arabidopsis* cell cultures (250 mg cells with 500 μ l medium) or pH 4.5 buffer (cell free) incubated with [¹⁴C]OxT (approximately 5 μ M) for up 6 hours were run by HVPE at pH 6.5. After drying, the areas of the papers known to contain OxT and OxA (as deduced by the position of the internal marker orange G) were cut into 2-cm strips, which were assayed for radioactivity by scintillation counting. The exact positions of OxT and OxA were determined by the use of these compounds as markers alongside the samples on the paper.

Arabidopsis cell culture, spinach cell culture and cell free buffer from various time-points were run analytically by HVPE at pH 6.5 to determine whether an oxalyl esterase was present in *Arabidopsis* or spinach culture medium.

After 1 hour in *Arabidopsis* cell culture the [^{14}C]OxT had begun to be hydrolysed to [^{14}C]OxA (Figure 51), showing that *Arabidopsis* cell cultures contain an extra-cellular oxalyl esterase. Conversely, spinach cell culture does not contain an extracellular oxalyl esterase, or spinach culture medium contains a compound that acts to prevent OxT hydrolysis. This can be seen as [^{14}C]OxT appears stable, and does not produce [^{14}C]OxA during the incubation time of this experiment (Figure 51). The [^{14}C]OxT was fairly stable in the cell-free buffer control, though a small amount of [^{14}C]OxA was produced over time.

For the purpose of investigating the formation of oxalyl cross-links with cell wall components the stability of OxT in the culture medium was important so spinach cell cultures were used in further experiments.

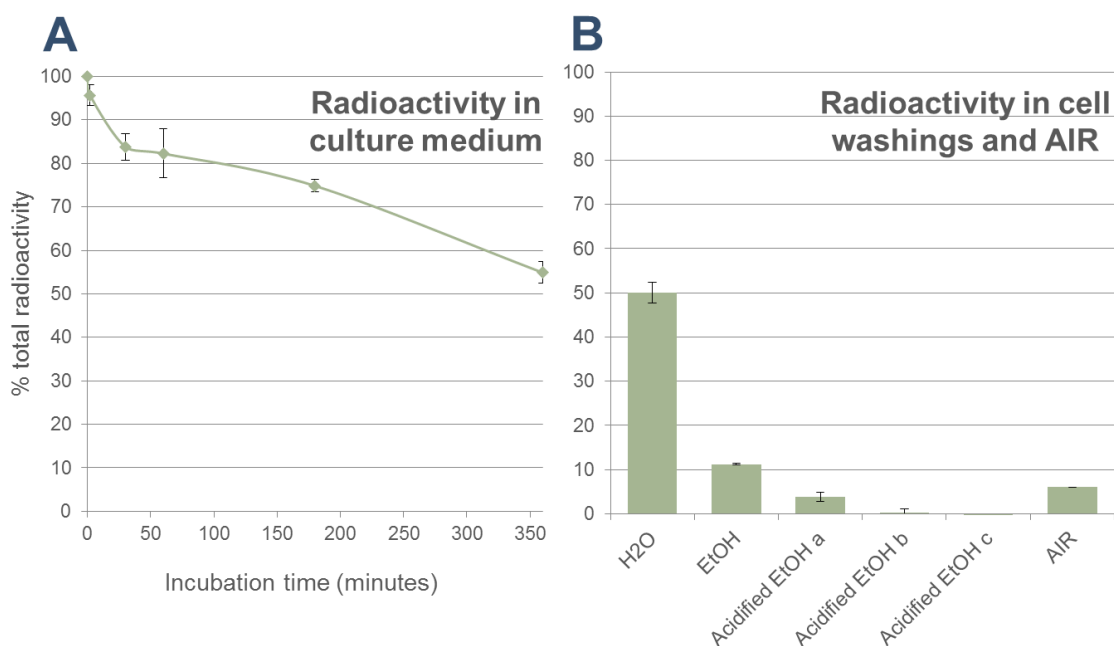


Figure 52: Radioactivity accumulates in AIR of spinach cell cultures incubated with [^{14}C]OxT Mini-cultures of spinach cells (250 mg cells in 500 μl medium, 1 week after subculturing) were fed [^{14}C]OxT (approximately 5 μM final concentration; previously purified by preparative HVPE). Samples of medium (50 μl) were taken at intervals up to 6 hours, and assayed for radioactivity by scintillation counting. The radioactivity remaining in the culture medium at each time point is plotted (A). After 6 hours the medium was removed from the cells and the cells were washed sequentially in H₂O, EtOH and acidified EtOH. The resulting material left after the washes (AIR) comprises predominantly cell wall material. The radioactivity present in each of the washes and in the AIR was assayed by scintillation counting (B). The bar labelled 'H₂O' represents the radioactivity present in the medium and the first wash in H₂O combined. Each point is an average of three replicate cultures \pm SE.

Spinach cell cultures were incubated with aliquots of [^{14}C]OxT (approximately 5 μM final concentration). The loss of radioactivity from the medium, either by uptake into the cells or adsorption to the cell walls, throughout the incubation period was monitored. A greater amount of radioactivity remained in the culture medium after inoculation with [^{14}C]OxT compared to the radioactivity remaining in the medium after inoculation with [^{14}C]DHA (Figure 50 and Figure 52). Equally, the radioactivity released in the EtOH wash (representing low molecular weight intracellular compounds) is much lower after inoculation with [^{14}C]OxT compared to [^{14}C]DHA, demonstrating that [^{14}C]OxT is not taken up into the cells as readily as [^{14}C]DHA. This suggests that there is not a membrane carrier for OxT in spinach cells, as there is for DHA (258).

3.4.4 Radiolabeled oxalate is released from radiolabelled AIR produced from spinach cells incubated with [^{14}C]OxT

A proportion of radioactivity, from [^{14}C]OxT, incubated in spinach cell cultures remained firmly bonded to cell wall material (AIR) after repeated washing in EtOH and acidified EtOH (Figure 52).

If this radioactivity was bound to the AIR by an oxalyl ester bond then treatment of the AIR with NaOH would break the ester bond, causing the release of free radiolabelled OxA. This free [^{14}C]OxA would be detectable by scintillation counting, after the sample has been run by HVPE.

The radiolabelled AIR produced from incubating spinach cell cultures with [^{14}C]OxT was treated with NaOH and the resulting soluble material was analysed by HVPE at pH 6.5. The sample contained [^{14}C]OxA (Figure 53), which indicates that the radioactivity was bound to the cell wall via an oxalyl ester bond. Some radioactivity remained at the origin of the paper; suggesting that this radioactivity was in the form of insoluble material. This could be CaOxA, which is insoluble in both EtOH and NaOH. CaOxA could have formed if there was any free OxA and calcium present in the sample.

The incorporation of radioactivity into the cell wall of spinach cell-suspension cultures was monitored over time. Replicate mini cell cultures of spinach were incubated with [^{14}C]OxT and AIR was prepared from the cultures at various time points up to 6 hours. The radioactivity bound to the AIR increased over time (Figure 54), as would be expected if this incorporation of radioactivity was due to an enzyme.

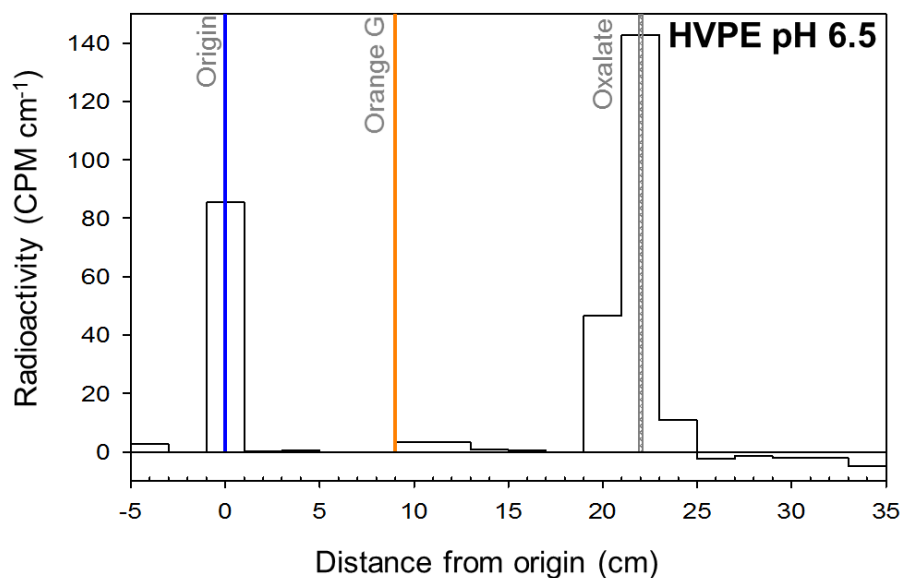


Figure 53: NaOH hydrolysis of radiolabelled spinach AIR releases free oxalate. Radiolabelled AIR, produced from spinach cells incubated with [¹⁴C]OxT for 6 hours then washed sequentially in H₂O, EtOH and acidified EtOH, was incubated with 0.1 M NaOH for 1 hour. After 1 hour, a slight excess of HOAc was added, and the whole sample run by HVPE at pH 6.5. After the paper had dried, it was cut into 2-cm strips. The strips were assayed for radioactivity by scintillation counting. The positions of the origin, the internal marker orange G and a marker of [¹⁴C]OxA are shown.

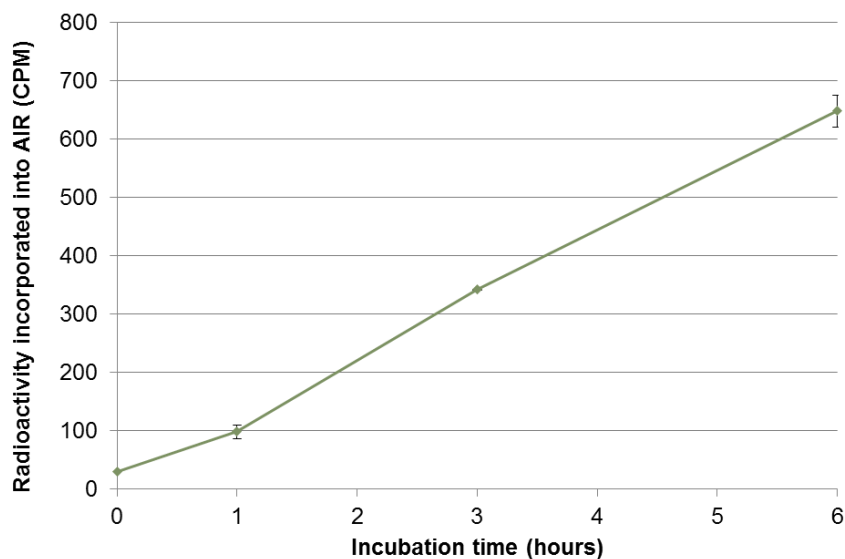


Figure 54: Incorporation of radioactivity from [¹⁴C]OxT into the AIR of spinach cells over time. Replicate spinach cell cultures (250 mg cell in 500 μl medium) were fed [¹⁴C]OxT. At time points (0, 1, 3 and 6 hours) the medium of the cell cultures was removed and the cells washed in H₂O, EtOH and acidified EtOH to produce AIR. The radioactivity present in the AIR of each of the cultures was assayed by scintillation counting. Each point is an average of 3 individual cultures ±SE.

3.4.5 The incorporation of radioactivity into the cell wall material of spinach cells requires an enzyme

It was hypothesised that the incorporation of radioactivity into the cell wall material is reliant on an enzyme. Boiled, frozen/thawed and untreated cells were incubated with [¹⁴C]OxT. Any enzymes present in the cell culture would have been denatured by boiling, so the boiled cell samples represent enzyme-free cultures. Freezing the cells would permeate the cell membranes, so any intracellular material, including enzymes, would then be in contact with the apoplastic material in the culture medium, including [¹⁴C]OxT. The disruption of the cell membranes could lead to enzymes not normally present in the apoplast acting on OxT and potentially cell wall components.

The boiled cells showed very little incorporation of radioactivity into the AIR (Figure 55 B), suggesting that the incorporation of radioactivity into the AIR was dependent on an enzyme. Much of the radioactivity remained in the culture medium of the boiled cells after 6 hours (Figure 55 A).

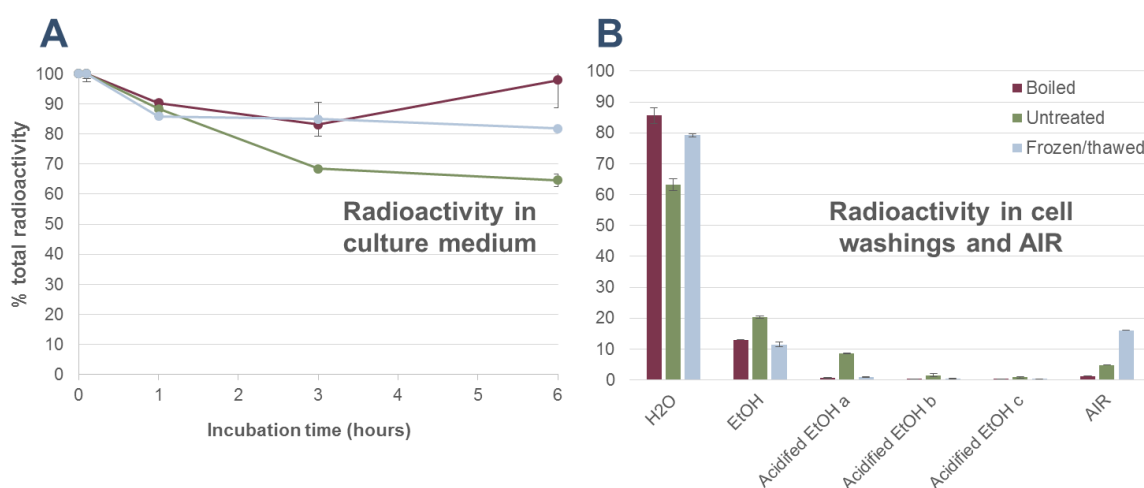


Figure 55: Boiled, frozen/thawed and untreated spinach cells incubated with [¹⁴C]OxT. Spinach cells (1 week after subculturing) were either boiled in the culture medium for 30 minutes then allowed to cool (**boiled**), frozen at -20°C overnight and allowed to thaw (**frozen/thawed**) or not treated (**untreated**), then incubated with [¹⁴C]OxT (approximately 5 μM final concentration). The radioactivity present in the medium was assayed at intervals (**A**) and after 6 hours the cells were washed sequentially in H₂O, EtOH and acidified EtOH to produce AIR. The radioactivity present in the washes and the AIR was assayed by scintillation counting (**B**). The H₂O samples represent the radioactivity remaining in the culture medium and in the first H₂O wash combined. Each point represents the average of 3 individual cell cultures ±SE.

The untreated (neither frozen/thawed nor boiled) cell cultures showed the greatest loss of radioactivity from the culture medium (Figure 55 A), and this was mainly released in the H₂O, EtOH and acidified EtOH washes (Figure 55 B), suggesting that some [¹⁴C]OxT had been taken up into, or become bound to, the cells. A small amount of radioactivity was also incorporated into the AIR, potentially via an oxalyl ester.

The frozen/thawed cells showed the greatest incorporation into the AIR, which could suggest that an enzyme responsible for this incorporation was originally intraprotoplasmic, but freezing and thawing the cells had permeabilised the membranes, allowing intracellular solutes to enter the apoplastic space.

HVPE analysis was carried out to determine whether OxT was stable in the medium (representing the apoplast) of frozen/thawed spinach cell culture. This analysis (Figure 56) revealed that while OxT was stable in the untreated cell culture, as described previously in Figure 51, OxT in frozen/thawed cell culture was not stable. The radioactivity in the medium of frozen/thawed cell culture showed that the OxT was degraded, presumably by an oxalyl esterase, to OxA (Figure 56). This suggests that spinach cells contain an intraprotoplasmic oxalyl esterase, which became exposed to the apoplast after the disruption of the cell membranes by freezing and thawing.

As the radioactivity present in the frozen/thawed sample was in the form of [¹⁴C]OxA, this suggests that the radioactivity in the AIR (Figure 55 B) could have been insoluble CaOxA, rather than radioactivity incorporated via an oxalyl ester bond. OxA cannot form an oxalyl ester with cell wall material as oxalyl esters cannot be formed *de novo* from OxA

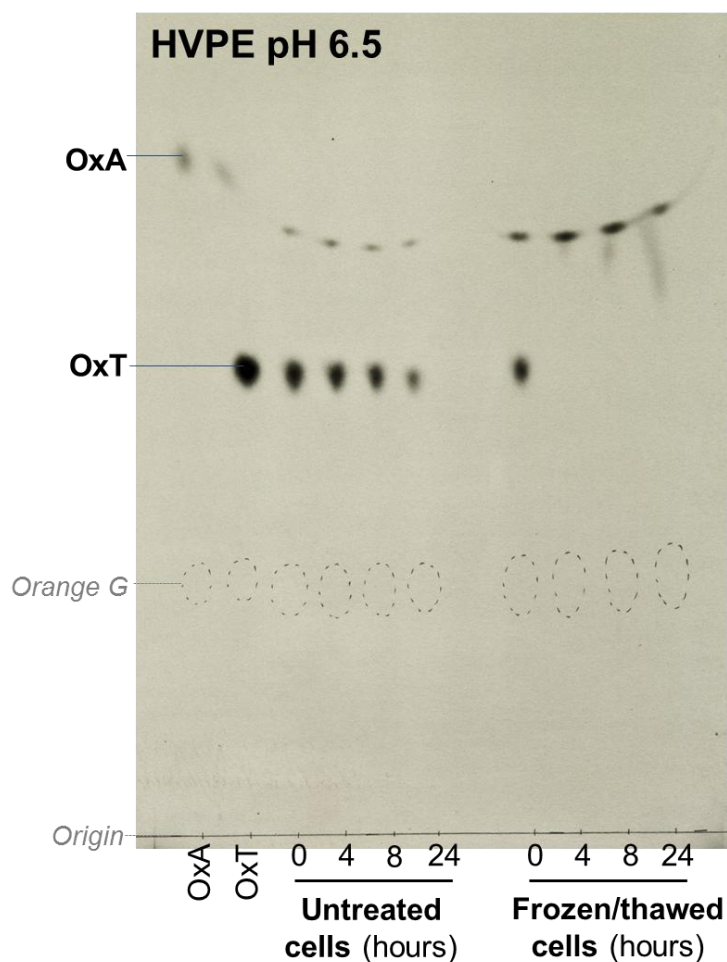


Figure 56: The fate of $[^{14}\text{C}]\text{OxT}$ in untreated and frozen/thawed spinach cell cultures. Spinach cell culture (200 ml, 7-day old) was frozen overnight at -20°C and then thawed. This frozen/thawed culture, along with an untreated 7-day old spinach cell culture was inoculated with $[^{14}\text{C}]\text{OxT}$ for up to 24 hours. Samples of culture medium ($50\ \mu\text{l}$) were collected at time intervals from both the spinach cell cultures. The samples were run by HVPE at pH 6.5, and the paper was exposed to film for 3 weeks.

To eliminate the possibility of AIR containing CaOxA , a washing step in EDTA was included. CaOxA is soluble in Na-EDTA so any radiolabelled CaOxA present would release soluble $\text{Na}[^{14}\text{C}]\text{OxA}$ in this step. Frozen/thawed spinach cells and untreated spinach cells were incubated with $[^{14}\text{C}]\text{OxT}$ and then washed in various solvents, including EtOH, acidified EtOH and Na-EDTA (Figure 57).

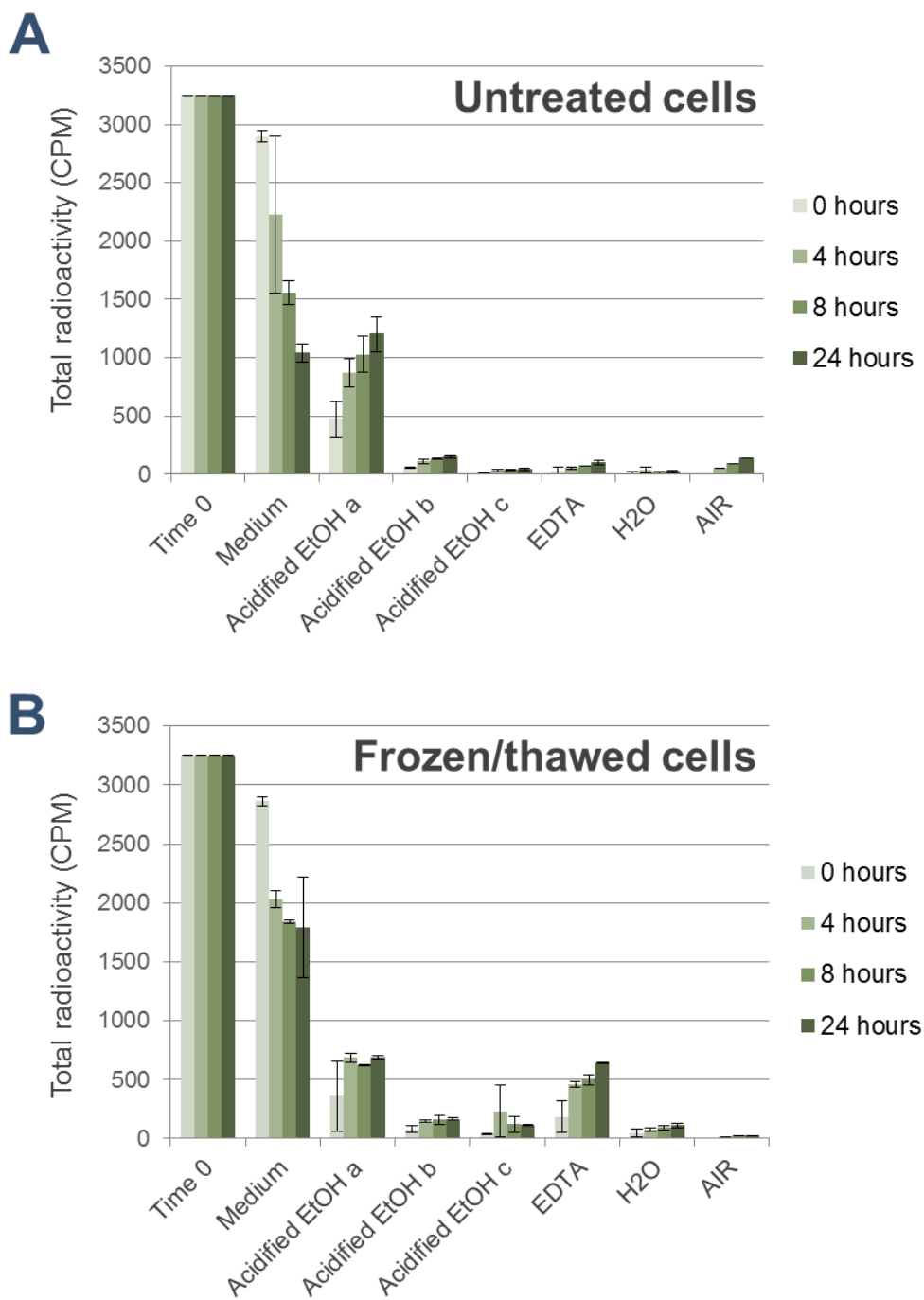


Figure 57: AIR produced from spinach cells incubated with $[^{14}\text{C}]\text{OxT}$ after washing in EtOH and EDTA. Replicate spinach cell cultures (250 mg cell in 500 μl medium) either untreated (A) or frozen/thawed (B), were incubated with $[^{14}\text{C}]\text{OxT}$ (approximately 5 μM final concentration). At time points (0, 4, 8 and 24 hours) the medium of the cell cultures was removed and the cells were washed in EtOH, acidified EtOH, Na_2EDTA (pH 6) and H_2O to produce AIR. The radioactivity present in the washes and the AIR of each of the cultures was assayed by scintillation counting. Each point is an average of 3 individual cultures $\pm\text{SE}$.

Radioactivity was incorporated into the AIR of the untreated cells over time, but not the frozen/thawed cells (Figure 57). The EDTA wash of the frozen/thawed cells released some radioactivity, presumably from CaOxA. This was more likely to form in the frozen/thawed cells as the [¹⁴C]OxT was quickly degraded to [¹⁴C]OxA, which in turn could have reacted with trace amounts of calcium present in the culture medium to form CaOxA. In the untreated cells, the oxalyl esterase remains intracellular, away from the [¹⁴C]OxT in the culture medium (apoplast), meaning that very little [¹⁴C]OxA was produced, so very little radiolabelled CaOxA was produced.

The radioactivity present in the AIR of untreated (i.e. not frozen/thawed) spinach cells was likely to be in the form of an ester-bonded oxalyl groups, providing evidence for oxalate side-chain formation on cell wall components.

3.4.6 Treatment of the radiolabeled spinach AIR with cell wall degrading enzymes

Radiolabelled AIR (from spinach cells incubated with [¹⁴C]OxT) was incubated with various cell wall enzymes to investigate which component of the cell wall material the oxalyl ester had bound to. If the radioactivity was bound to a specific moiety that is cleaved by a specific enzyme, this would provide a clue as to the acceptor substrate for the oxalyl ester link. To test whether the enzymes contained oxalyl esterase activity, they were incubated with [¹⁴C]OxT before testing the radiolabelled AIR samples. The enzymes tested included Driselase, EPG (endo-polygalacturonase), cellulase and cellulase that also digests xyloglucan (Cellulase + XG).

Driselase is a commercially available mixture of cell wall enzymes that comes from fungi (Basidiomycetes sp.). This enzyme mixture would have proved very useful in determining the nature of the acceptor substrate of the oxalyl cross-link, but unfortunately Driselase contains oxalyl esterase activity. This was demonstrated by the production of [¹⁴C]OxA from [¹⁴C]OxT after treatment with Driselase (Figure 58). The negative control containing denatured Driselase shows a small amount of [¹⁴C]OxA along with [¹⁴C]OxT, this could be because the sample of OxT used in this experiment was not freshly prepared and so had degraded slightly upon storage, producing OxA (Figure 58). If the radiolabelled AIR was treated with Driselase then free [¹⁴C]OxA would be produced, and no meaningful information would be gained

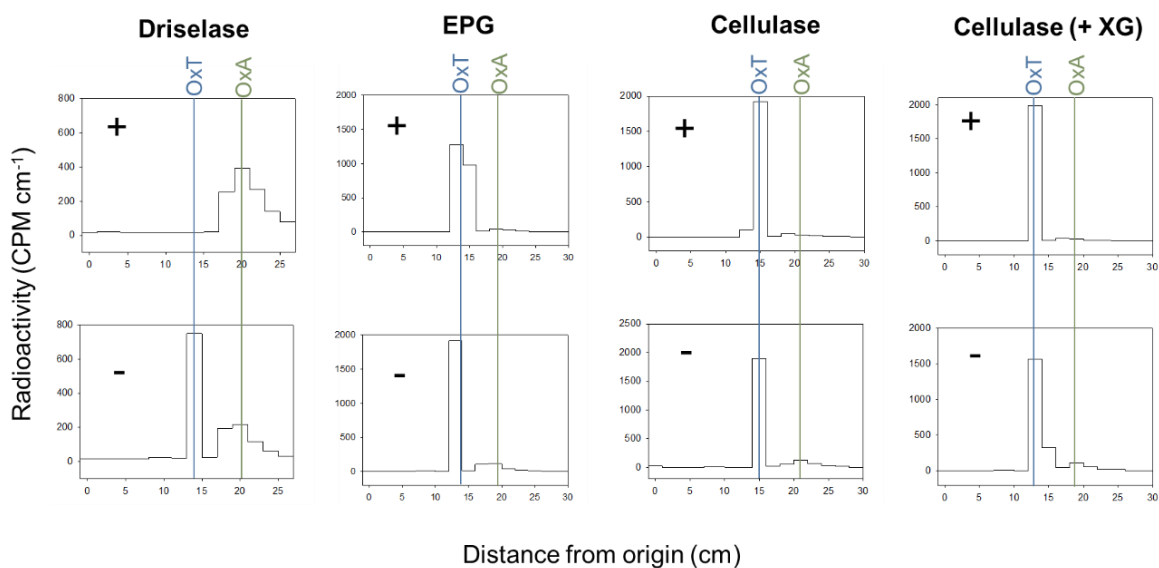


Figure 58: Oxalyl esterase activity of commercial cell wall-cleaving enzymes. [^{14}C]OxT (purified by preparative HVPE) was incubated with various enzymes including Driselase (1% final concentration), EPG (endo-polygalacturonase), cellulase and cellulase that also acts on xyloglucan (all at 0.1 U / μl in P:A:W, 1:1:98 buffer) for 16 hours. The samples were then run by HVPE at pH 6.5, and the paper cut into 2-cm strips and assayed for radioactivity by scintillation counting. The positions of OxT and OxA were determined with radiolabelled markers of each. Samples containing the enzyme are shown with + and samples with a denatured enzyme (samples were incubated with 10% formic acid to denature the enzyme) are shown with -.

Three of the enzymes tested (EPG, cellulase and cellulase that also digests xyloglucan) showed no oxalyl esterase activity, as seen by the lack of [^{14}C]OxA produced from [^{14}C]OxT during the incubation (Figure 58).

Radiolabelled AIR, produced from spinach cell culture that had been incubated with [^{14}C]OxT, was treated with these three cell wall degrading enzymes (Figure 59). Although radioactivity was released during the incubation of the AIR with each of the enzymes, it was also released in the enzyme-free control, which contained only buffer. This was unexpected, as the radioactivity had previously been insoluble in repeated washing with H_2O , EtOH, and EDTA, but was now soluble in pH 4.5 buffer. This means that the radioactivity released in the presence of the enzymes may not be due to the enzymes themselves, but released non-enzymically in the buffer solution.

It is possible, in fact likely, that the formation of an oxalyl ester bond, from acyltransferase activity between [^{14}C]OxT and cell wall components, is reversible. This leads to the

possibility that during the drying of the AIR, or subsequent storage before treatment with enzymes, the bond incorporating the radioactivity into the cell wall material may have broken, leading to [¹⁴C]OxA being released. This experiment was repeated, and the AIR treated with enzymes as soon as possible after drying, to reduce the possibility that [¹⁴C]OxA would be released during storage. However, the results (data not shown) were the same as in Figure 59, with even the enzyme-free control releasing radioactivity into the supernatant.

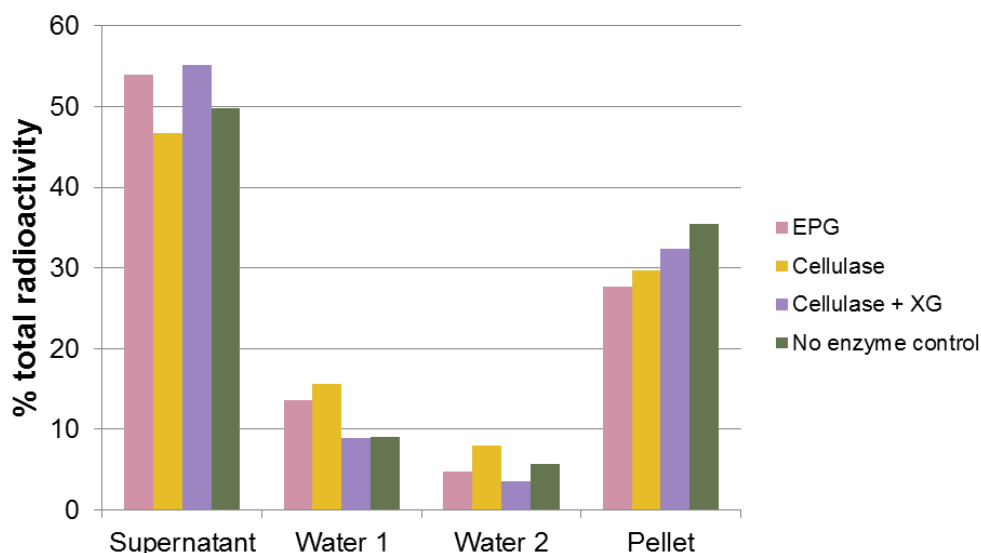


Figure 59: The treatment of radiolabelled spinach AIR with cell wall-degrading enzymes. Radiolabelled spinach AIR (obtained by incubating spinach cells with [¹⁴C]OxT then washing in H₂O, EtOH and acidified EtOH) was incubated with various enzymes (endo-polygalacturonase, cellulase and cellulase that digests xyloglucan; all at 0.01U/ μl). A no enzyme control incubated in the enzyme buffer (pyridine/HOAc/water, 1:1:98) was also included. The samples were incubated (1 mg AIR in 1 ml enzyme solution) for 16 hours. The supernatant was then removed, and the remaining material washed in water twice. Samples of the supernatant, the water washes and the remaining pellet were assayed for radioactivity by scintillation counting.

As this experimental set-up was unsuccessful in determining the acceptor substrates to which [¹⁴C]oxalyl groups had become bound to, a different approach was taken, which will be discussed in detail in section 3.5.

This work has shown that *Arabidopsis* cell cultures contain an oxalyl esterase in the apoplast, whereas spinach cell cultures do not, so [¹⁴C]OxT was stable in spinach cell cultures. The feeding of [¹⁴C]OxT to spinach cell-suspension cultures led to the incorporation of some of this radioactivity into the cell wall. This radioactivity was released as free [¹⁴C]OxA upon alkali treatment, suggesting that the radioactivity was bound by an ester bond. This oxalyl ester bond formation suggests a potential role for ascorbate derivatives in cell wall modifications, by the formation of oxalate side-chains within the cell wall.

Although the substrate used in this work (OxT) has only one oxalyl linkage, so is only able to form side-chains, this work hints at the possibility of oxalyl groups originating from ascorbate-derivatives forming cross-links within the cell wall. If cOxT (which contains two oxalyl ester linkages) were used as the starting substrate then a cross-link between cell wall polysaccharides would be theoretically possible.

This hypothesis was tested further, and will be discussed in the following section.

3.5 A novel enzyme catalysing a reaction between ascorbate derivatives and cell wall components

3.5.1 Introduction to the reaction of ascorbate derivatives with cell wall components

As has been previously discussed (section 3.4), some radioactivity became bound to the cell wall material of spinach cell cultures when incubated with [¹⁴C]OxT. The experiments discussed in this chapter will elaborate on and provide further characterisation of this reaction. Previous attempts, using cell wall-degrading enzymes, to discover the nature of the acceptor substrate *in vivo* were unfortunately unsuccessful (section 3.4), so a different approach was used. Various potential acceptor substrates were added to very small volumes of cell culture or cell culture extracts along with a radiolabelled donor substrate, and the products formed were monitored by HVPE. The expected reactions (depicted in section 3.4, Figure 49) involve the transfer of the oxalyl group from OxT or cOxT to an acceptor substrate, such as a sugar residue from a polysaccharide.

3.5.2 Plant cell cultures incubated with radiolabeled OxT and non-radiolabeled sugars produce novel oxalyl sugars

A selection of potential acceptor substrates (in this case sugars) were added in abundance to very small volumes of spinach cell cultures, along with [¹⁴C]OxT. The whole sample was then run by HVPE at pH 6.5, and the radioactive products were detected by autoradiography.

Spinach cell cultures were incubated with [¹⁴C]OxT and a range of sugars, including hexoses, pentoses and disaccharides (Figure 60). Radiolabelled compounds with a lower charge : mass ratio and so running slower than OxT were detected with each of the acceptor substrates. Oxalyl sugars would be predicted to have lower electrophoretic mobility compared to OxT because they would have only one negative charge (from the oxalyl group) compared to two negative charges on OxT, and a greater number of carbons, for instance 8 in an oxalyl hexose compared to 6 in OxT (259). The radiolabelled compounds correspond to these predicted mobilities of oxalyl sugars, providing evidence that the radiolabelled oxalyl group from OxT has been transferred onto the acceptor sugar. As would be expected, the smallest sugars, xylose and arabinose, formed oxalyl sugars with a greater mobility (m_{OG} of

0.94), and disaccharides, being the largest substrates tested, formed oxalyl sugars with the least mobility (m_{OG} of 0.66).

The hexoses produced the greatest yields of oxalyl sugars (m_{OG} of 0.88); this could be due to the more readily accessible OH group on C-6. All the sugars tested were used at a concentration of 5% (Figure 60), so the molar concentration of disaccharides was half that of the hexoses, which would explain the relatively low yield of oxalyl disaccharides despite the accessibility of the OH groups on the two C-6s in maltose for example.

The marker lane containing OxT represents the time 0 sample. It can be seen that the level of OxA increased in all the samples incubated for 16 hours (Figure 60), suggesting that there was an enzyme responsible for the hydrolysis of OxT to OxA present in the spinach cell cultures.

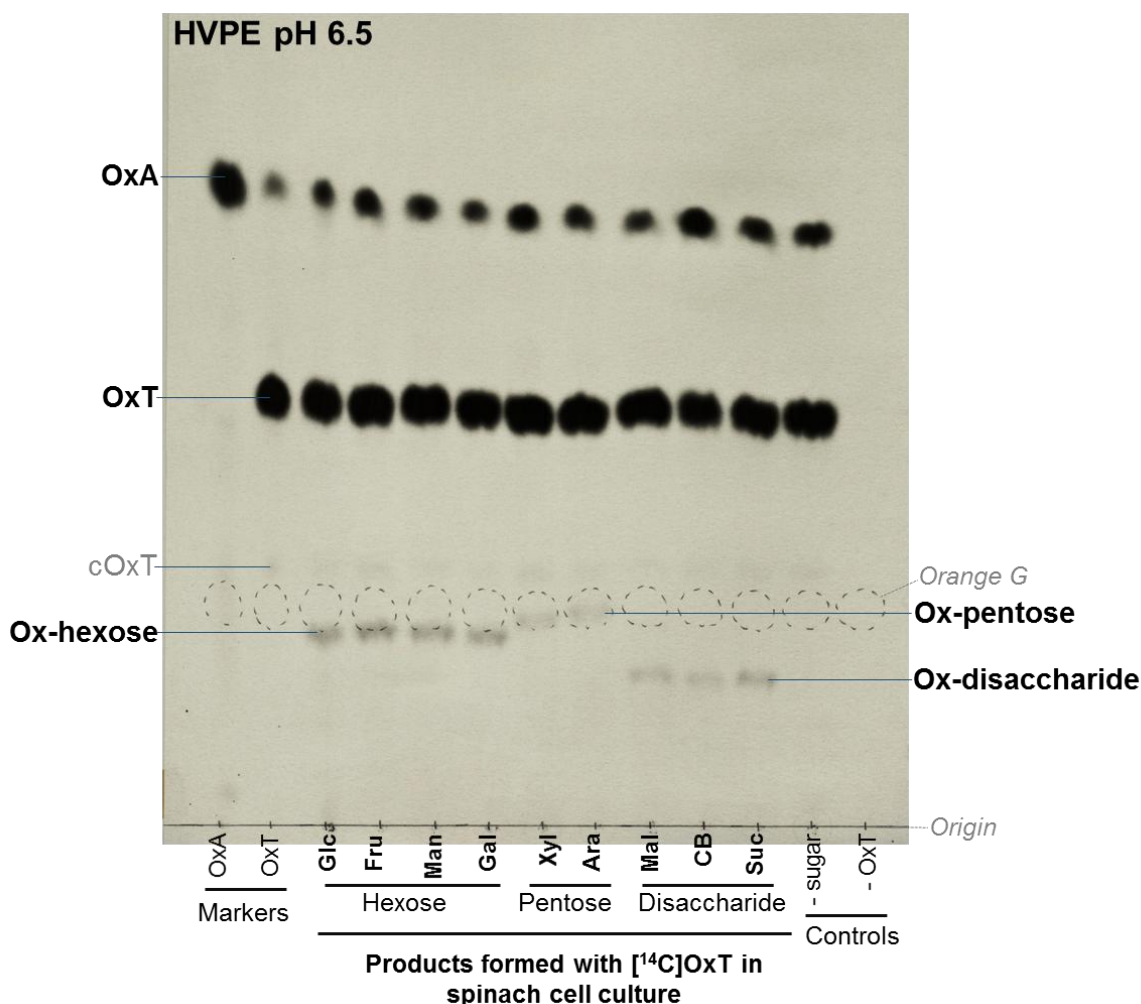


Figure 60: Formation of oxalyl sugars in spinach cell cultures with [¹⁴C]OxT and sugars. Small aliquots (20 μ l) of spinach cell culture, including cells, were incubated with [¹⁴C]OxT (purified by preparative HVPE and eluted from the paper, approximately 50 μ M) and 5% final concentration of various sugars for 16 hours. The sugars used were Glc (glucose), Fru (fructose), Man (mannose), Gal (galactose), Xyl (xylose), Ara (arabinose), Mal (maltose), CB (cellobiose) and Suc (sucrose). The whole sample of each was then run by HVPE at pH 6.5. The resulting paper was exposed to film for 3 weeks.

To determine whether the formation of these oxalyl sugars was reliant on an enzyme bound to the cell wall or a free extracellular enzyme present in the culture medium, the experiment was repeated with spent spinach culture medium, free of cells, instead of intact cell culture.

The production of oxalyl sugars was markedly less when cell-free spinach culture medium was used (Figure 61). OxA was not produced during the incubation period either, with the levels of OxA present in the time 0 sample the same as the samples that had been incubated for 16 hours. This suggests that the enzyme responsible for the hydrolysis and transfer of the oxalyl group (an acyltransferase) of OxT to a sugar acceptor substrate is dependent on cells

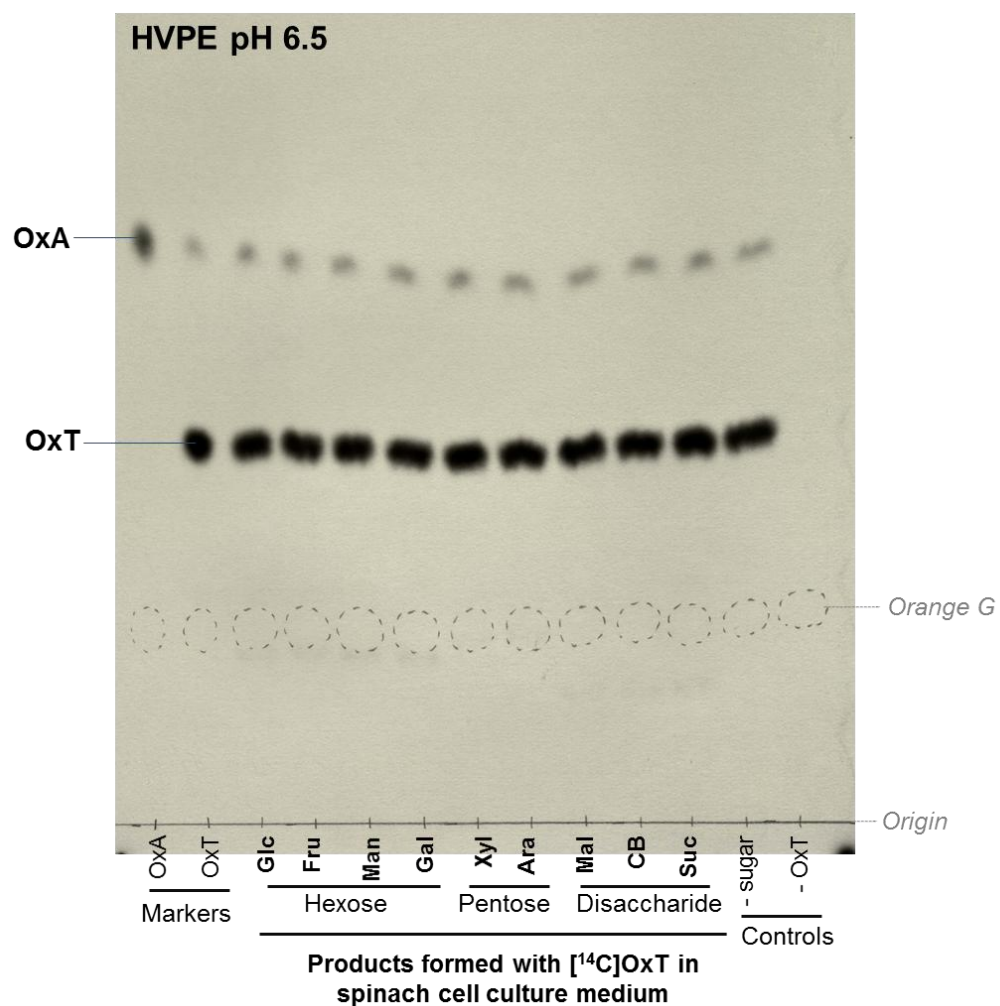


Figure 61: Oxalyl sugars are not formed in the absence of cells. Small aliquots (20 μ l) of spinach cell culture medium, excluding cells, were incubated with [¹⁴C]OxT (purified by preparative HVPE and eluted from the paper, approximately 50 μ M) and 5% final concentration of various sugars for 16 hours. The sugars used were Glc (glucose), Fru (fructose), Man (mannose), Gal (galactose), Xyl (xylose), Ara (arabinose), Mal (maltose), CB (cellobiose) and Suc (sucrose). The whole sample of each was then run by HVPE at pH 6.5. The resulting paper was exposed to film for 3 weeks.

being present.

The acyltransferase activity was also detected with *Arabidopsis* cells in addition to the previously discussed spinach cells. Cells of different ages, up to two weeks after sub-culturing, were incubated with [¹⁴C]OxT and either glucose or sucrose (Figure 62). The proportion of oxalyl glucose (OxG) formed increased with the age of the cell cultures, more clearly with spinach cells (Figure 62 A and C), though this may be because there are a greater number of cells present in the older cell cultures compared to the newly sub-cultured cell cultures.

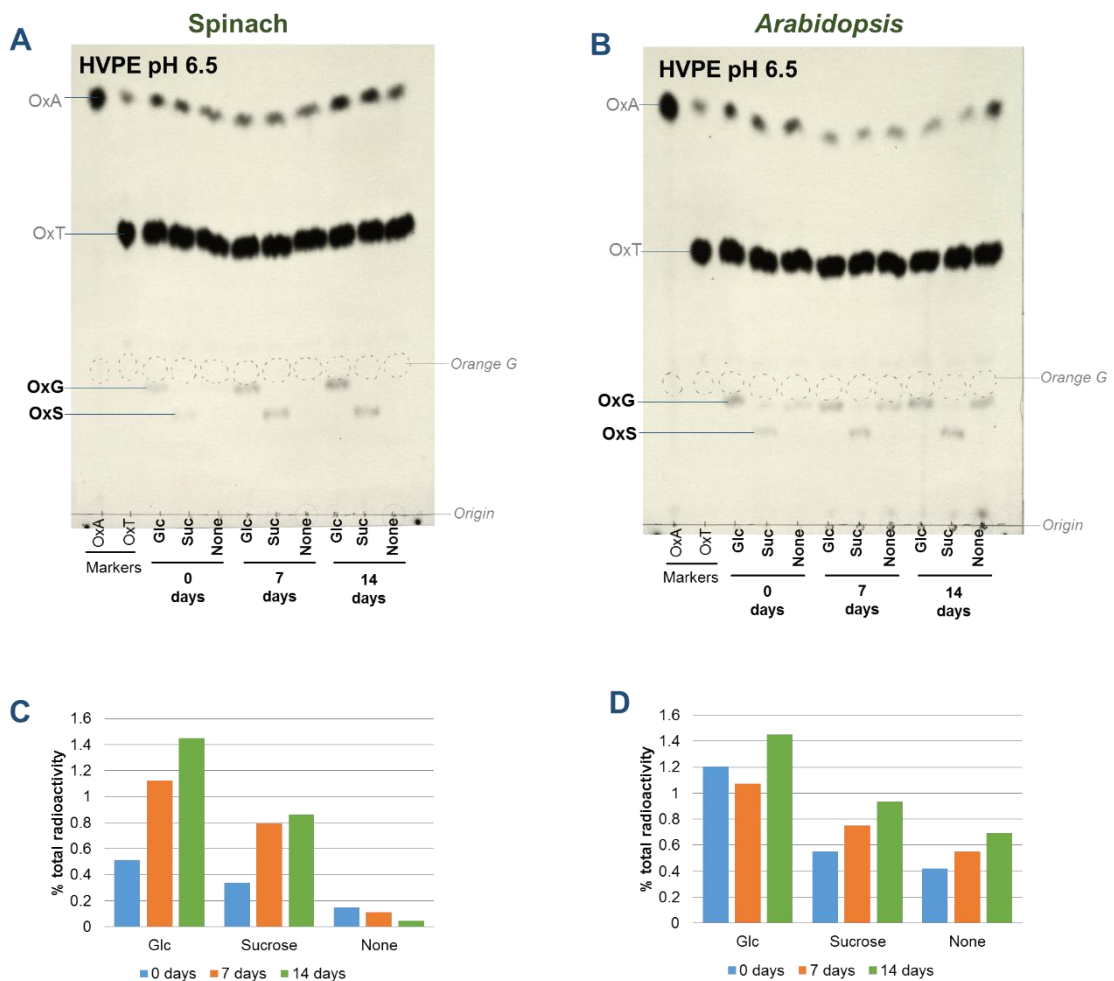


Figure 62: Oxalyl sugars were formed in the presence of Arabidopsis and spinach cells of increasing ages. Small aliquots of spinach (A and C) and *Arabidopsis* (B and D) cell cultures, including cells, of different ages, either 0, 7 or 14 days after subculturing, were incubated with [¹⁴C]OxT (approximately 50 μM) and glucose or sucrose (5% final concentration) or no sugar for 16 hours. The whole samples were run by HVPE at pH 6.5 and the papers exposed to film for 3 weeks (spinach cells are shown in A and *Arabidopsis* cells are shown in B). The OxG (oxalyl glucose) or OxS (oxalyl sucrose) produced was quantified by scintillation counting. The quantification of products from spinach cells are shown in C and from *Arabidopsis* in D. For the samples containing no sugar (labelled 'none'), the areas corresponding to OxG and OxS were both cut out and assayed for radioactivity, and the sum of these two areas was included in the bar charts in C and D.

The *Arabidopsis* cell cultures incubated with [^{14}C]OxT but no additional sugar also formed radiolabelled OxG (samples labelled ‘none’, Figure 62 A). *Arabidopsis* cell culture medium contains 2% glucose as the carbon source, whereas spinach culture medium contains only 1% glucose. This means that the *Arabidopsis* cells had more glucose available, even in the cell cultures that had not had glucose deliberately added, resulting in the formation of radiolabelled OxG. Small amounts of radiolabelled OxG can also be seen in the samples containing [^{14}C]OxT and sucrose for the same reason, and because the cell cultures may partially hydrolyse sucrose to produce glucose and fructose, which then participate in the oxalyl transfer reaction themselves.

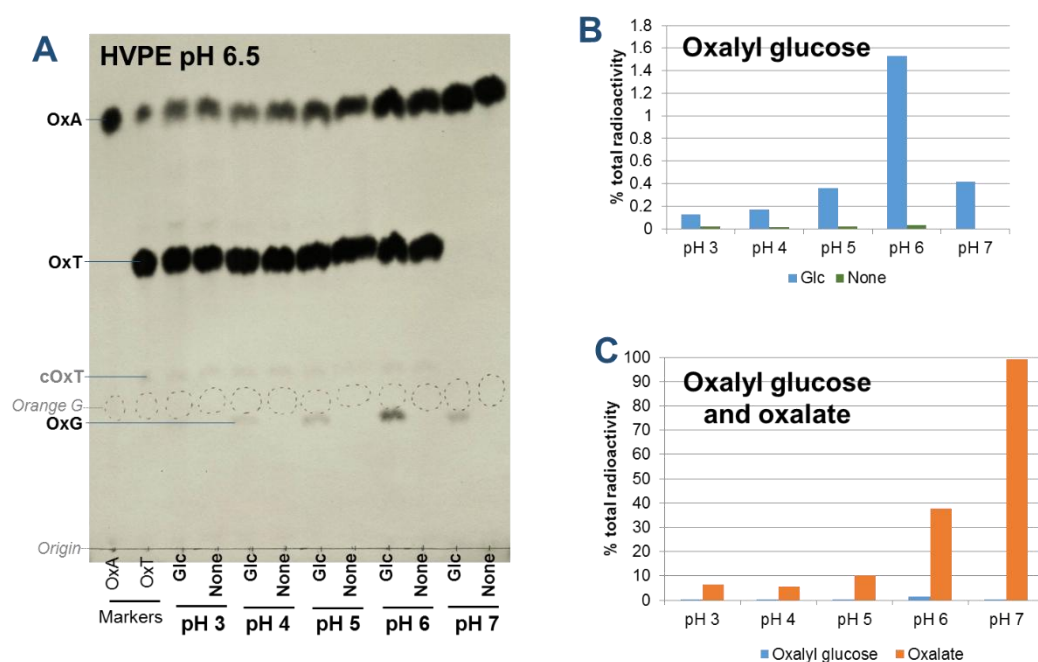


Figure 63: Oxalyl glucose production is greater in higher pH buffers. Spinach cells (1 week after subculturing) were removed from culture medium and incubated in buffers of various pH values along with [^{14}C]OxT (approximately 50 μM) and glucose (**glc**; 5% final concentration), or no glucose (**None**). The buffers used were; for pH 3 and pH 4 tartaric acid, for pH 5 and pH 6 phthalic acid and for pH 7 PIPES, all 10 mM) After 16 hours incubation the samples were run by HVPE at pH 6.5 and the paper exposed to film for 3 weeks (**A**). The bands of [^{14}C]OxG and [^{14}C]OxA were cut out of the paper and quantified by scintillation counting. **B** shows the production of OxG with and without glucose present in the sample, and **C** shows the relative production of OxG and OxA in the samples which contained glucose.

Spinach cells were incubated in buffers of varying pH (3-7) to determine the optimum pH for acyltransferase activity. Buffers known to be tolerated by cell cultures were used. An increase in pH resulted in greater acyltransferase activity. The autoradiogram (Figure 63 A) shows that the cells incubated at pH 7 completely hydrolysed [^{14}C]OxT to [^{14}C]OxA. The

transfer of the oxalyl group onto the substrate (in this case glucose) was presumed to be reversible, and the new oxalyl–sugar bond formed during the incubation could be a target for further hydrolysis, producing free OxA. It is likely that this was the case in the pH 7 sample,

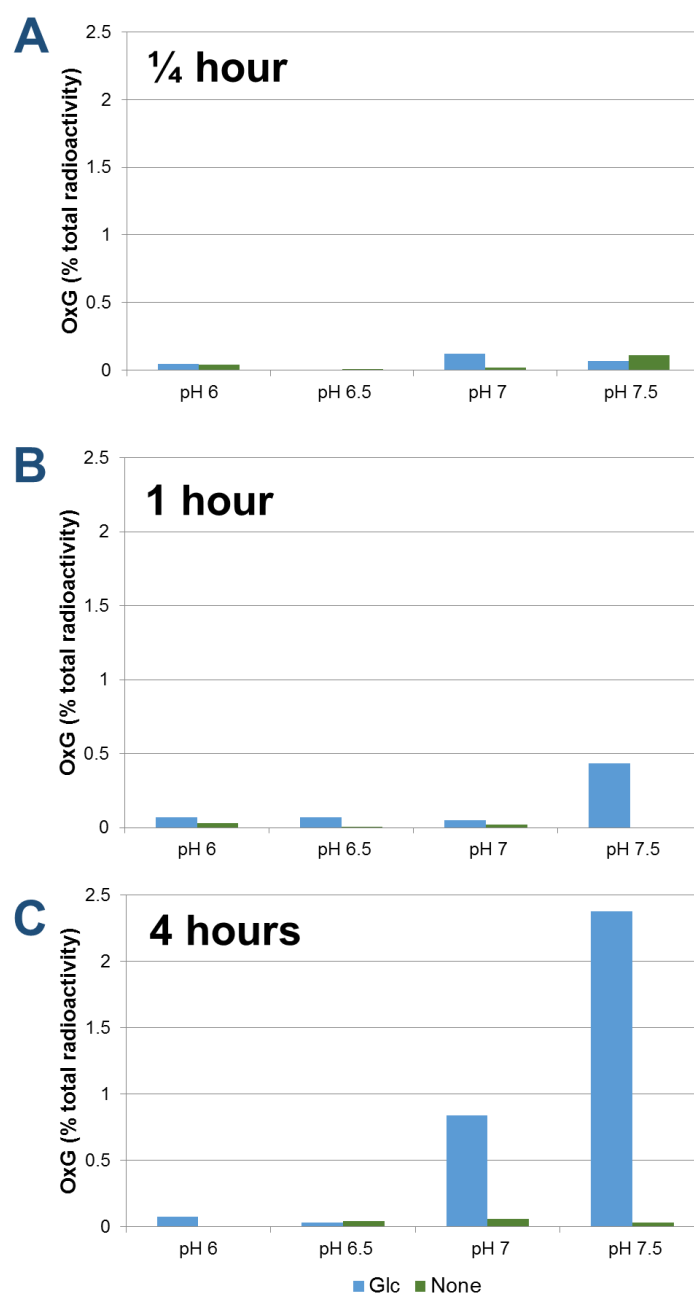


Figure 64: OxG formation over time at different pH values. Spinach cells (1 week after subculturing) were removed from culture medium and incubated in buffers of various pH values along with [¹⁴C]OxT with (blue) or without (green) glucose (5% final concentration). The buffers for pH 6 and pH 6.5 were 10 mM phthalic acid, and the buffers for pH 7 and pH 7.5 were 10 mM PIPES. Samples were incubated for either 1/4 hours (A), 1 hour (B), or 4 hours (C). The reaction was stopped with 10% formic acid at the specified time points, before running the products by HVPE at pH 6.5. The paper was cut into strips and the radioactivity quantified by scintillation counting. The area corresponding to OxG was identified and plotted for samples both with and without glucose.

and owing to the long incubation time (16 hours), very little oxalyl glucose can be seen (Figure 63 B and C). However, it is interesting that some OxG but no OxT remains in the pH 7 sample. This suggests that OxG must be a poorer substrate than OxT for hydrolysis,

A time-course of OxG production was set up to investigate whether OxG was produced more quickly in buffers with a higher pH (Figure 64). OxG was formed more quickly at pH 7 and pH 7.5, within 1 hour at pH 7.5 (Figure 64 B), than at pH 6 and pH 6.5.

3.5.3 The putative acyltransferase can be eluted from the cell walls of plant cell cultures

The nature of this novel putative acyltransferase activity was investigated and steps were taken towards the purification of the enzyme responsible.

As the activity was found to be reliant on cells being present rather than on spent medium, which would include secreted free apoplastic enzymes, it was hypothesised that the enzyme may be bound to the cell wall. Ionically wall-bound compounds from cell cultures of spinach and *Arabidopsis* were extracted with concentrated salt solution (1 M NaCl). This concentration of NaCl is expected to release any compound ionically, but not covalently, bound to the cell wall. As the membranes of the cells were not disrupted, no intraprotoplasmic compounds would be released.

After dialysis, to remove the salt, the cell wall eluate was freeze-dried and then used at a standard concentration (1%) in further acyltransferase assays. As a control, spent culture medium, filtered from the cells before eluting ionically cell wall-bound compounds, was also dialysed, freeze-dried and tested for acyltransferase activity.

The enzyme mixture eluted from *Arabidopsis* (Figure 65 A) was much more active than that from spinach cells (Figure 65 B). The *Arabidopsis* enzyme extract produced OxG within 15 minutes, whereas OxG was only visible after 4 hours with the spinach enzyme extract. OxA was also produced in large quantities from both enzyme extracts. It is not known whether the same enzyme is responsible for the transfer of the oxalyl group from OxT to OxG, and the release of free OxA from either OxG or OxT.

The [¹⁴C]OxT in the presence of *Arabidopsis* extract was completely gone after 4 hours. The OxG also disappeared after 4 hours, suggesting the presence of an enzyme that acted to release free OxA from OxG. This provides evidence for the reversible nature of the ester

bond formation. Free OxA was also produced in the absence of glucose, from the hydrolysis of OxT.

The initial extracts (Figure 65) were taken from 1-week old cell cultures, but it is possible that the activity of the acyltransferase enzyme varies through development (preliminary experiments investigating this are described in Figure 62). Extracts of ionically-bound cell wall enzymes were taken at 4-day intervals from immediately after sub-culturing up to 16 days. As cell cultures were ordinarily sub-cultured every 14 days, the 16-day samples represent the oldest cell cultures used.

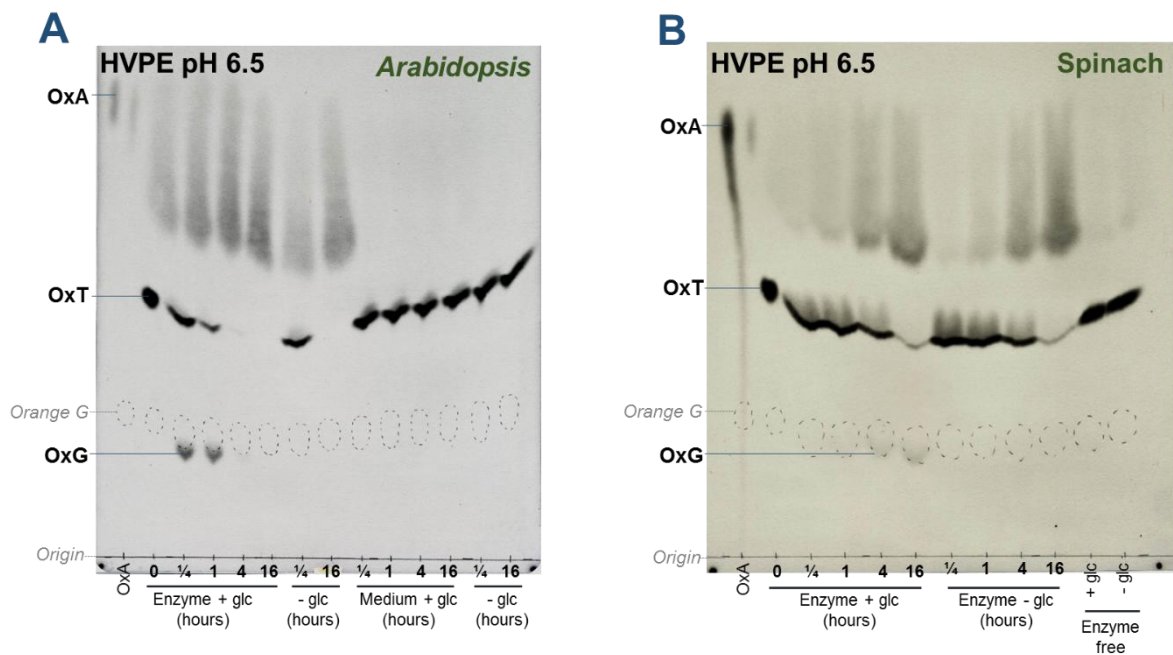


Figure 65: Acyltransferase activity was present in *Arabidopsis* and spinach cell wall extracts. Cell wall extracts from Spinach and *Arabidopsis* cell cultures (1 week after subculturing) were obtained by removing the cells from the culture medium, rinsing in H₂O then re-suspending in 1 M NaCl (pH 5 with 5 mM succinate buffer) and shaking for 1 hour. The eluate was then separated from the cells, and dialysed to remove the NaCl (culture medium was also dialysed to serve as a control). The dialysed eluate and medium were then freeze dried. The resulting material was redissolved in 10 mM pH 7 PIPES buffer (1% final concentration) and incubated with [¹⁴C]OxT (approximately 50 μM final concentration) and glucose (5% final concentration). Samples were incubated between 0 and 16 hours, including controls containing no glucose. The reaction was stopped with 10% formic acid. The samples were run by HVPE at pH 6.5 and the papers exposed to film for 3 weeks. The *Arabidopsis* cell wall extract is shown in **A** and the spinach cell wall extract is shown in **B**.

The overall yield of OxG was higher from *Arabidopsis* cell wall extracts than from spinach cell wall extracts (Figure 66), which is consistent with previous experiments. The yield of OxG did not vary with the age of cell culture in spinach cells, and did not vary in *Arabidopsis* cells after 4 days old.

Interestingly, the *Arabidopsis* eluate extracted immediately after sub-culturing contained almost no acyltransferase activity at all (Figure 66 A), despite the cells being equivalent to the 16 day-old culture (as this is the approximate age at which the cells were sub-cultured, by transferring a small volume of old cells into fresh culture medium). This result was repeated in a replicate experiment. A few proteins are known to react to stress by firmly binding to the cell wall (260), rendering them inextractable by the usual methods. It is possible that plunging the *Arabidopsis* cells suddenly into fresh medium could have elicited a stress response, and the acyltransferase became inextractable immediately after sub-culturing. This would not necessarily mean the acyltransferase activity was absent from these cells, merely not extractable with 1 M NaCl. The spinach cell wall extracts showed a similar trend (Figure 66 B), though not as pronounced as the extracts from *Arabidopsis*.

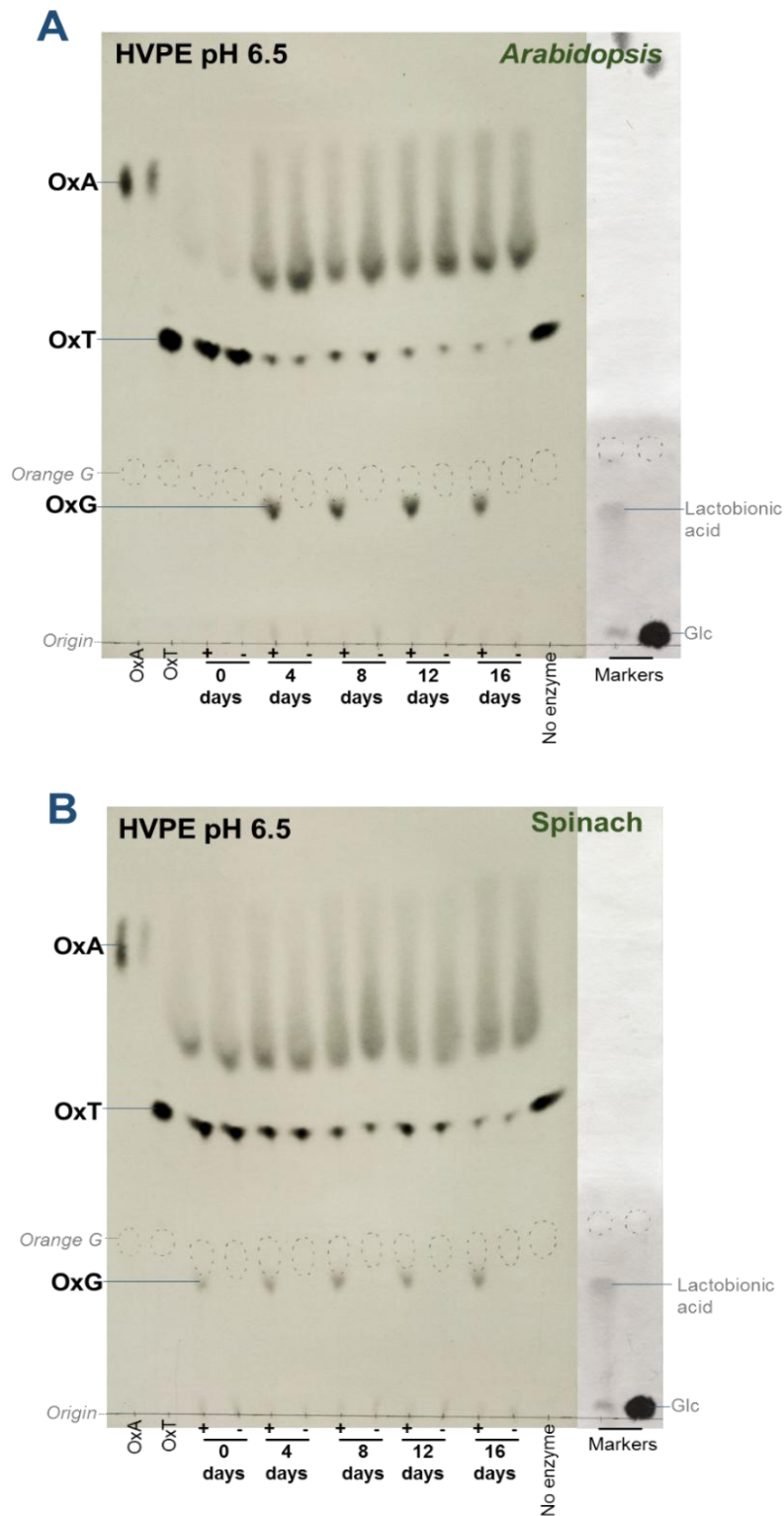


Figure 66: Acyltransferase time course *Arabidopsis* and spinach. Cell wall extracts from spinach and *Arabidopsis* cell cultures (0, 4, 8, 12 and 16 days after subculturing) were obtained by removing the cells from the culture medium, rinsing in H₂O then re-suspending in 1 M NaCl (pH 5 with 5 mM succinate buffer) and shaking for 1 hour. The eluate was then separated from the cells, and dialysed to remove the NaCl. The dialysed eluate was then freeze dried. The resulting material was redissolved in 10 mM pH 7 PIPES buffer (1% final concentration) and incubated with [¹⁴C]OxT and with (+) or without (-) glucose (5% final concentration) for 4 hours. The reaction was stopped with 10% formic acid. The samples were run by HVPE at pH 6.5 and the papers exposed to film for 3 weeks. Non-radiolabelled markers run alongside the samples were stained in silver nitrate. The *Arabidopsis* cell wall extracts are shown in **A** and the spinach cell wall extracts are shown in **B**.

3.5.4 The reaction of [¹⁴C]OxT with various acceptor substrates catalysed by an acyltransferase

The effect of increasing glucose concentrations on OxG formation with spinach acyltransferase extract was tested (Figure 67). The formation of OxG increased with glucose, until 25%, above which the formation of OxG plateaued (Figure 67 B). This concentration of glucose may be considered unnaturally high, but within the cell wall matrix the concentration of glucose residues within polysaccharides could easily reach this concentration.

Although the formation of OxG increases with glucose concentration, the formation of OxA begins to decrease with the highest glucose concentrations (Figure 67 C). It could be that very high concentrations of glucose (above 10%) act as an inhibitor of hydrolysis but not of transesterification.

The experiments discussed so far have only involved acceptor substrates disaccharide-sized or smaller. As the hypothesis being tested involves the formation of oxalate cross links

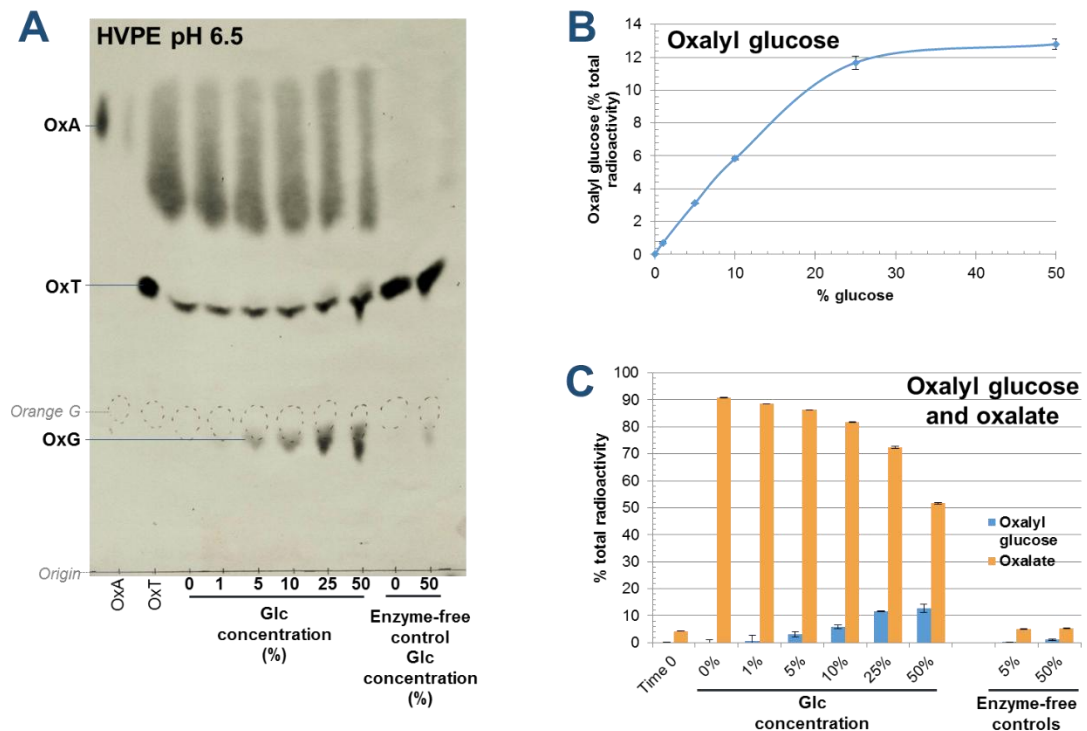


Figure 67: Oxalyl glucose production increases with glucose concentration. Enzyme extract (from *Arabidopsis*) was incubated with [¹⁴C]OxT and increasing concentrations of glucose (0-50%) in a pH 7 buffer for 4 hours. Enzyme free controls containing 0% and 50% glucose were also incubated. The samples were run by HVPE at pH 6.5 and the paper was exposed to film for 3 weeks (A). The bands of OxG and OxA were carefully cut out of the paper and quantified by scintillation counting. The increasing OxG production with increasing glc concentration is shown in B, and the relative production of OxA and OxG is shown in C.

between cell wall components it was necessary to test larger acceptor substrates. The method of detecting acyltransferase activity discussed so far requires the substrates used to be soluble at relatively high concentrations. For this reason, a selection of soluble substrates was used (Figure 68), including a mixture of xyloglucan oligosaccharides (XGOs), raffinose (Raf, a trisaccharide consisting of galactose, glucose and fructose), cellobiose (CB; a disaccharide comprising β 1,4 linked glucose residues) and glucosamine (GlcN).

The reaction of OxT with XGOs in the presence of an acyl transferase did not yield any oxalyl ester compounds (Figure 68). If oxalyl-XGO compounds had been formed they would have had a mobility lower than that of OxG, as they would have a larger mass and one negative charge. The compounds would run in the area between the origin and orange G on the electrophoretogram, but this area appears empty, suggesting no such compounds had been formed (Figure 68). This area of the electrophoretogram was also assayed for radioactivity by scintillation counting, with only background levels detected.

The reaction of OxT with Raf and CB in the presence of an acyltransferase produced two compounds corresponding to an oxalyl-hexose and an oxalyl-disaccharide. As raffinose is a trisaccharide, the production of these compounds suggests that there was an enzyme present in the cell wall extract that breaks down raffinose to a monosaccharide and a disaccharide. Equally, cellobiose is a disaccharide of β -linked glucose, but has produced a compound corresponding to an oxalyl-hexose (OxG), suggesting that cellobiose has been broken down at least partly, by an enzyme present in the extract, to free glucose.

Interestingly, a neutral compound has been formed during the reaction of OxT with GlcN in the presence of an acyltransferase (Figure 68). GlcN itself is a positively charged compound, owing to the presence of an amine group on C-2. As the compound resulting from the acyltransferase activity was neutral, this suggests that the amine group is still present, so it is likely that the oxalyl group was positioned on C-6, which would be the OH group most readily available for esterification. The alternative would have been for the oxalyl group to be positioned directly on the N of the amine group, resulting in a compound with an overall negative charge, thus detected as a mobile compound after HVPE.

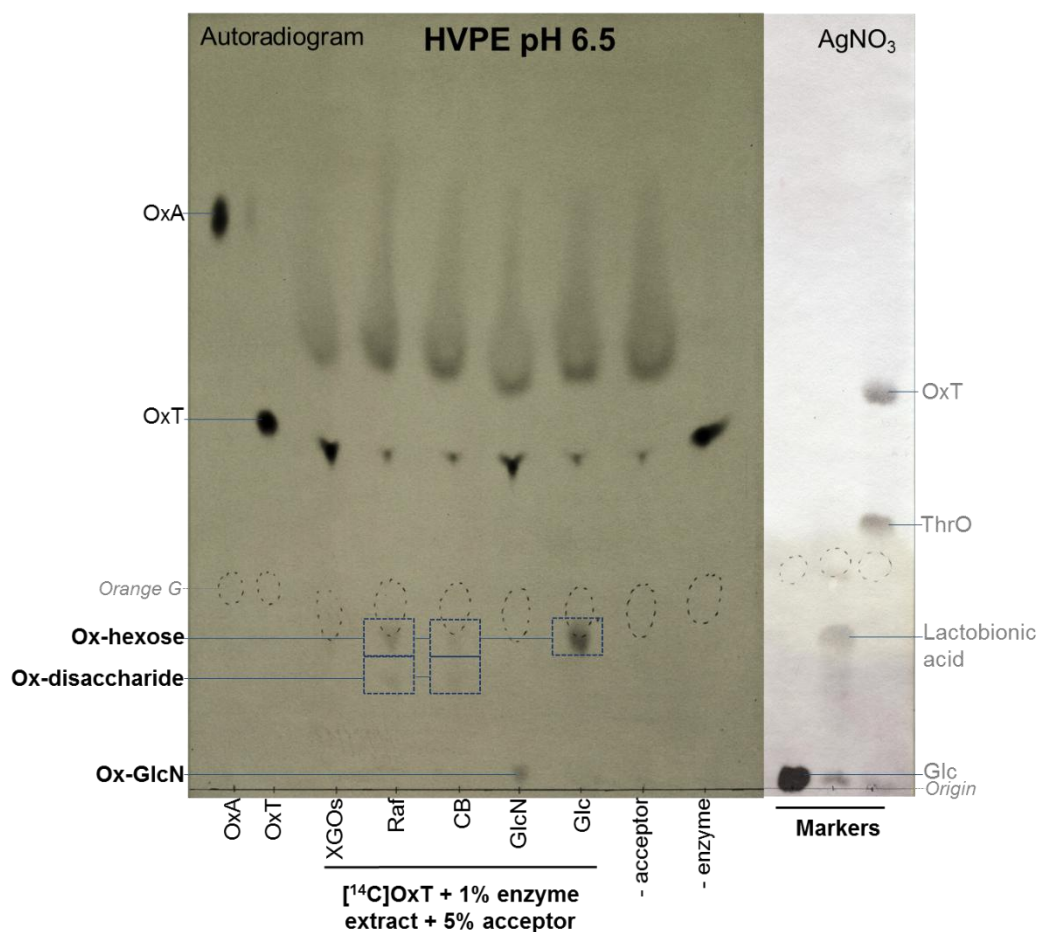


Figure 68: The reaction of acyltransferase activity with $[^{14}\text{C}]\text{OxT}$ and oligosaccharides. Enzyme extract (from *Arabidopsis*) was incubated with $[^{14}\text{C}]\text{OxT}$ (approximately 50 μM) and 5% acceptor substrate for 4 hours at pH 7 (10 mM PIPES buffer). The acceptor substrates included XGOs (xyloglucan oligosaccharides), Raf (raffinose), CB (cellobiose), GlcN (glucosamine) and Glc (glucose). Controls lacking either an acceptor substrate or the enzyme extract were also included. The samples were run by HVPE at pH 6.5, along with non-radiolabelled markers. The radiolabelled portion of the paper was exposed to film for 3 weeks and the non-radiolabelled markers were stained in silver nitrate.

Acylation can occur using OH groups or NH_2 groups. Amine groups are present in the cell wall, often in the form of structural proteins, e.g. extensin (261). It would be possible that the acceptor for the novel acyltransferase activity could be an amine group, forming an oxalyl amide. GlcN has been proven to act as an acceptor for acyltransferase (Figure 68), but the formation of an oxalyl amide bond was not observed. In order to test whether amines can act as acceptor substrates for acyl transfer, $[^{14}\text{C}]\text{OxT}$ was incubated in the presence of the *Arabidopsis* cell wall extract along with an acceptor substrate such as an amino acid (lysine or histidine) or a polyamine (spermine, spermidine, putrescine, poly-lysine and poly-histidine) (Figure 69). Spermine, spermidine and putrescine are found in the plant cell (262),

and poly-lysine and poly-histidine are a useful models for some basic proteins involved in cell growth, e.g. extensins (263).

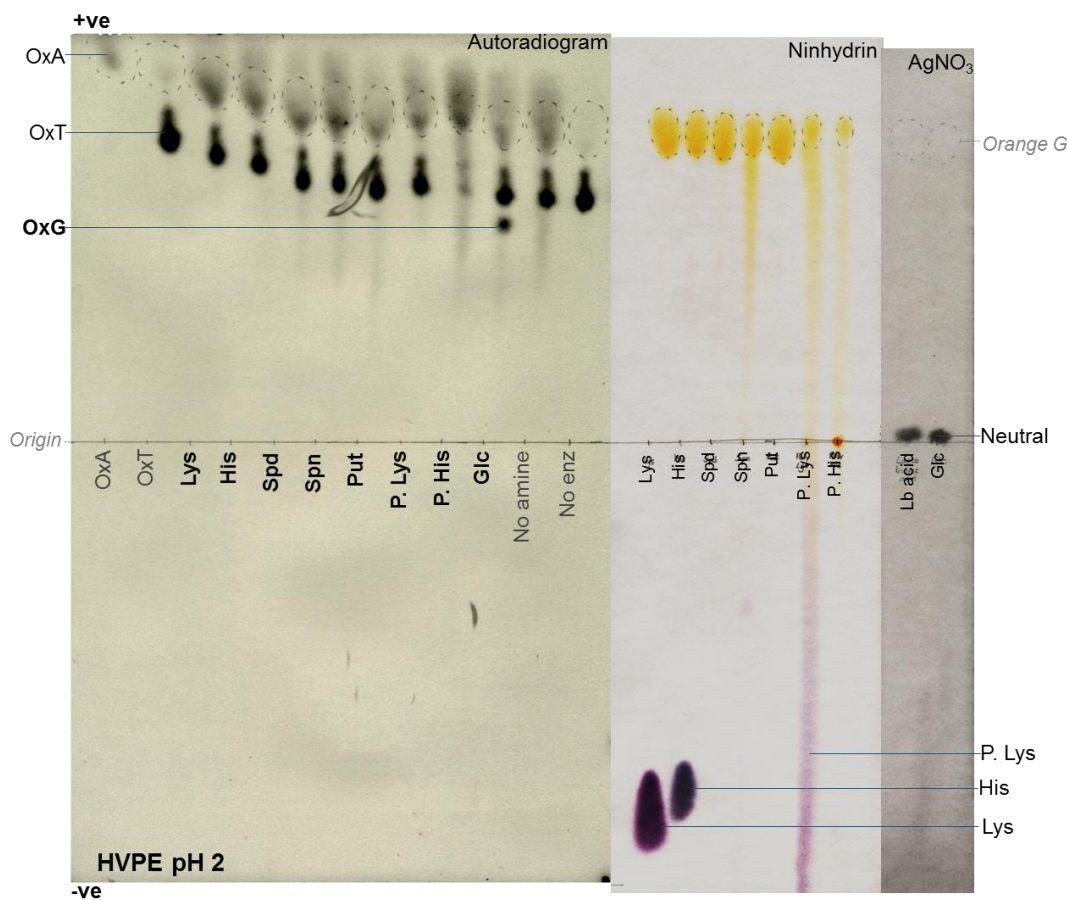


Figure 69: The reaction of [¹⁴C]OxT and polyamines catalysed by acyltransferase. Enzyme extract (from *Arabidopsis*; used at 1% final concentration) was incubated with [¹⁴C]OxT and 1% acceptor substrate for 4 hours at pH 7. The acceptor substrates included Lys (lysine), His (histidine), Spd (spermidine), Spn (spermine), Put (putrescine), P. Lys (poly-lysine), P. His (poly-histidine) and Glc (glucose). Controls lacking either an acceptor substrate or the enzyme extract were also included. The samples were run by HVPE at pH 2.0, along with non-radiolabelled markers. The markers containing amines were stained in ninhydrin and markers of glucose and lactobionic acid (Lb acid) were stained in silver nitrate. The radiolabelled portion of the paper was exposed to film for 3 weeks.

The reaction products from these amine samples were analysed by HVPE at pH 2.0 instead of pH 6.5 as amines and amino acids are likely to be fully ionised at pH 2.0, allowing improved separation of the compounds (259). The samples were loaded in the middle of the

paper to allow for the positively charged amines to migrate towards the cathode, and the negatively charged substrates (radiolabelled OxT, OxA and OxG) to migrate towards the anode. The hypothetical oxalyl amide compounds (produced via acyltransferase action) would be either neutral or positively charged, though less so than the original amine substrate, so would be expected to either be present close to the origin or have migrated towards the cathode.

The autoradiogram showed no radiolabelled compounds present in the amine samples (in bold), other than the starting material of [^{14}C]OxT and the hydrolysis product [^{14}C]OxA (Figure 69). This suggests that the acyltransferase does not act upon amines. The positive control of [^{14}C]OxT with glucose showed a clear spot of OxG, demonstrating that the enzyme extract was active.

The samples containing poly-histidine showed a much greater production of OxA than the other samples, with a corresponding depletion of OxT (Figure 69). This would seem to suggest that the presence of poly-histidine was somehow increasing the rate of hydrolysis of OxT.

Another likely substrate to test for potential oxalyl ester formation, and in turn oxalate cross-links, within cell walls would be cell wall polysaccharides themselves. The experimental design of the experiments discussed so far requires a relatively concentrated solution of the acceptor substrate, and it proved difficult to produce solutions of polysaccharides of a sufficiently high concentration. Nonetheless, 1% (the highest concentration manageable) solutions of various polysaccharides, including hemicelluloses and pectins, were obtained and subsequently used in the experiment.

If an oxalyl ester bond formed with a polysaccharide then a radiolabelled spot at the origin would be expected. Many polysaccharides bind to paper, so would not move from the origin during HVPE. No such radiolabelled product was visible after the incubation of polysaccharides with [^{14}C]OxT in the presence of an acyltransferase (Figure 70), suggesting that polysaccharides are not the preferred acceptor substrate for this enzyme, although at only 1% this is lower than the concentration of Glc (5%) routinely used. The OxG production with 1% Glc was fairly low (Figure 67), so it is possible that the acceptor substrate concentration used was too low to detect any oxalyl-products formed.

Interestingly the pectins, and to a lesser extent RG-I from soy, seemed to inhibit the production of OxA (Figure 70). Pectins are acidic polysaccharides and it is possible that this acidity may be inhibiting the hydrolysis of OxT to OxA, although this is unlikely as the

solutions were buffered at pH 7. Conversely, RG-I from potato appeared to have promoted the hydrolysis of OxT, as all the OxT had been converted to OxA (Figure 70).

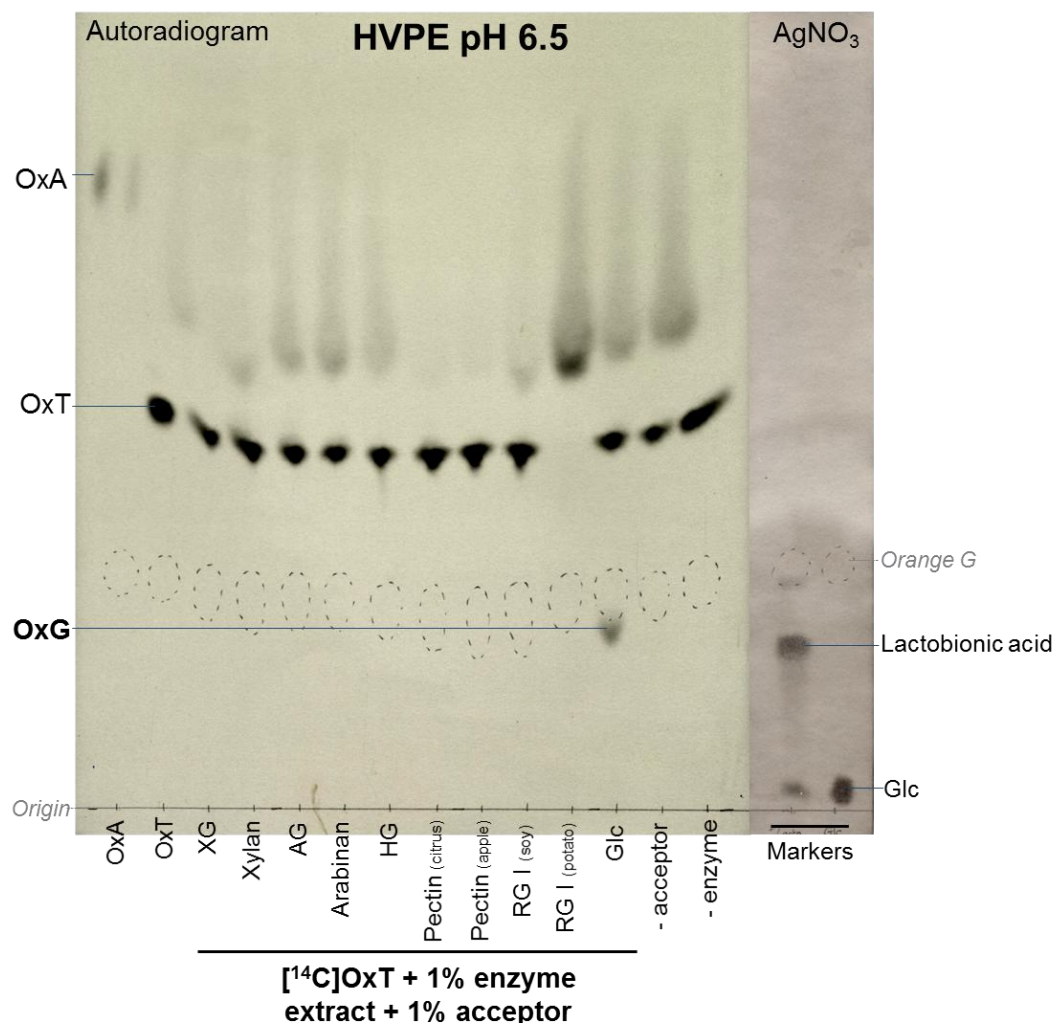


Figure 70: [¹⁴C]OxT reaction with acyltransferase and polysaccharides. Enzyme extract (from *Arabidopsis*) was incubated with [¹⁴C]OxT and 1% acceptor substrate for 4 hours at pH 7. The acceptor substrates included XG (xyloglucan), xylan, AG (arabinogalacturonan), arabinan, HG (homogalacturonan) pectin (from citrus or apple), RG-I (rhamnogalacturonan I) from soy or potato and Glc (glucose). Controls lacking either an acceptor substrate or the enzyme extract were also included. The samples were run by HVPE at pH 6.5, along with non-radiolabelled markers. The radiolabelled portion of the paper was exposed to film for 3 weeks and the non-radiolabelled markers were stained in silver nitrate.

A limitation of this method is that some polysaccharides at this concentration (1% w/v) had a gel-like consistency, which may have prevented the enzyme from acting at full capacity, so limited any possible oxalyl ester products being formed. This may mean that *in vivo* this enzyme may indeed act upon cell wall polysaccharides, but we were unable to detect this using this method. Also, a 1% concentration of polysaccharides is not very realistic, as the

concentration of polysaccharide within a cell wall would be much higher. This demonstrates a need for an alternative method for testing the ability of polysaccharides to act as acceptor substrates for the acyltransferase catalysed reaction.

Whatman 3 MM paper (almost pure cellulose) was dipped slowly through 1% solutions of various polysaccharides, then allowed to dry, forming polysaccharide–cellulose complexes which contained a high concentration of polysaccharides and serve as useful models for cell wall components. The polysaccharide-impregnated papers were cut into uniform sections.

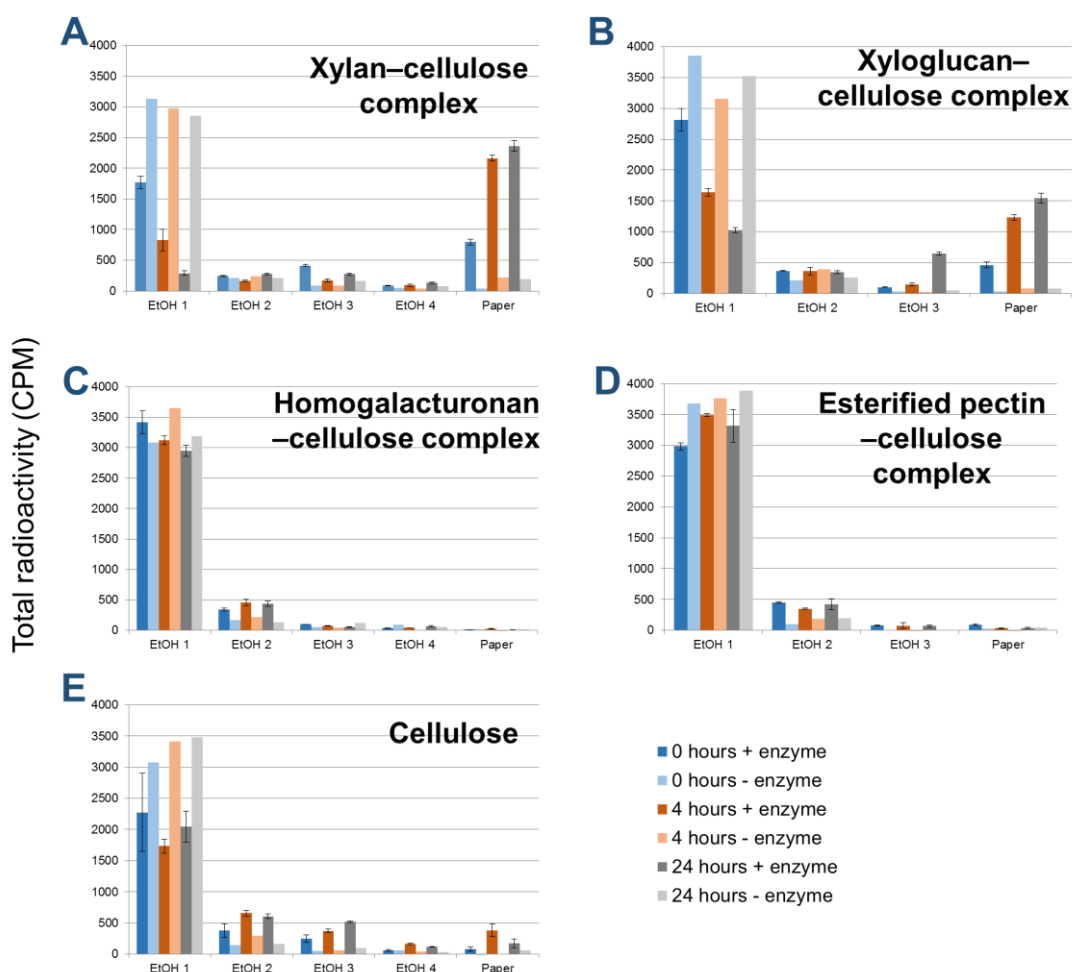


Figure 71: The formation of oxalyl esters with polysaccharide–cellulose complexes and $[^{14}\text{C}]\text{OxT}$ catalysed by an acyltransferase. Polysaccharide-cellulose complexes (polysaccharide-impregnated paper) were incubated with *Arabidopsis* enzyme extract and $[^{14}\text{C}]\text{OxT}$ in pH 7 PIPES buffer, for 0 hours, 4 hours or 24 hours. Controls with no enzyme extract were also analysed. The polysaccharide-cellulose complexes were prepared by dipping Whatman 3 MM paper through 1% solutions of various polysaccharides: xylan (A), xyloglucan (B), homogalacturonan (C), esterified pectin (D), or untreated paper (cellulose, E). After the specified incubation times the papers were washed repeatedly in EtOH (70%) and then the radioactivity present in the washes and the radioactivity that remained bound to the paper throughout the washing was assayed by scintillation counting. Each sample containing enzyme was in triplicate, and the no-enzyme controls were single samples.

These papers were incubated with the enzyme extract containing the acyltransferase and [^{14}C]OxT in pH 7 buffer. After the incubation period the papers were washed repeatedly in EtOH. If the acyltransferase had transferred the oxalyl group from [^{14}C]OxT to the polysaccharide–cellulose complex, then the radioactivity would become covalently bound to the paper, and would not be removed in EtOH washes. Any free [^{14}C]OxT, or [^{14}C]OxA that had formed during the reaction, would be soluble in EtOH, and so removed during the washing of the papers in EtOH. Therefore, if radioactivity was detected on the paper after repeated washings, this would provide evidence for the formation of an oxalyl ester between [^{14}C]OxT and the polysaccharide–cellulose complex, and therefore acyltransferase activity.

The hemicellulose–cellulose complexes, with xylan (Figure 71 A) and xyloglucan (Figure 71 B) showed significant incorporation of radioactivity into the paper, which increased over time up to 24 hours. The controls containing no enzyme extract showed very little radioactivity remaining in the paper after repeated washings. This would seem to suggest that esters had formed between the hemicellulose and the oxalyl group from OxT.

Conversely, the pectic–cellulose complexes, with homogalacturonan (Figure 71 C) or methyl-esterified pectin (Figure 71 D) showed no incorporation of radioactivity into the paper. This would suggest that the pectic polysaccharides do not act as acceptor substrates for this acyltransferase.

The untreated paper (cellulose only; Figure 71 E) showed slight incorporation of radioactivity into the paper, peaking after 4 hours incubation. The loss of radioactivity from into the paper between 4 and 24 hours could be because an enzyme was acting to hydrolyse the ester bond formed between cellulose and the oxalyl group from OxT, which would release free [^{14}C]OxA. This would be soluble in EtOH ([^{14}C]OxA was purified by preparative HVPE and successfully eluted from the paper in EtOH during the current study) and so removed during the washing of the paper.

The hydrolase responsible for the release of free OxA from oxalyl esters (including OxT and OxG) would also be present in the hemicellulose–cellulose samples (Figure 71 A and B), as the enzyme extract was identical. However, these samples do not show a loss of radioactivity in the paper between 4 and 24 hours. This could be because the acyltransferase has a higher affinity for hemi-celluloses than cellulose, so oxalyl ester formation was favoured over hydrolysis, meaning less OxA was released, and more oxalyl esters were formed.

An important control was missing from this experiment, so the experiment was repeated using [^{14}C]OxA as a donor, which theoretically cannot form oxalyl esters so serves as a

negative control, as no radioactivity should become bound to the polysaccharide–cellulose complexes. The xylan–cellulose complex previously showed the greatest incorporation of radioactivity into the paper (Figure 71), so this was the complex used in further experiments, along with a cellulose-only sample.

The samples incubated with [¹⁴C]OxT and the xylan–cellulose complex, in the presence of the enzyme extract, again showed some incorporation of radioactivity into the paper (Figure 72 A), whereas the enzyme-free controls showed no incorporation of radioactivity. The cellulose-only samples incubated with [¹⁴C]OxT also showed no incorporation of radioactivity into the paper (Figure 72 C). The overall incorporation of radioactivity into paper when incubated with [¹⁴C]OxT was lower than in the previous experiment; this was

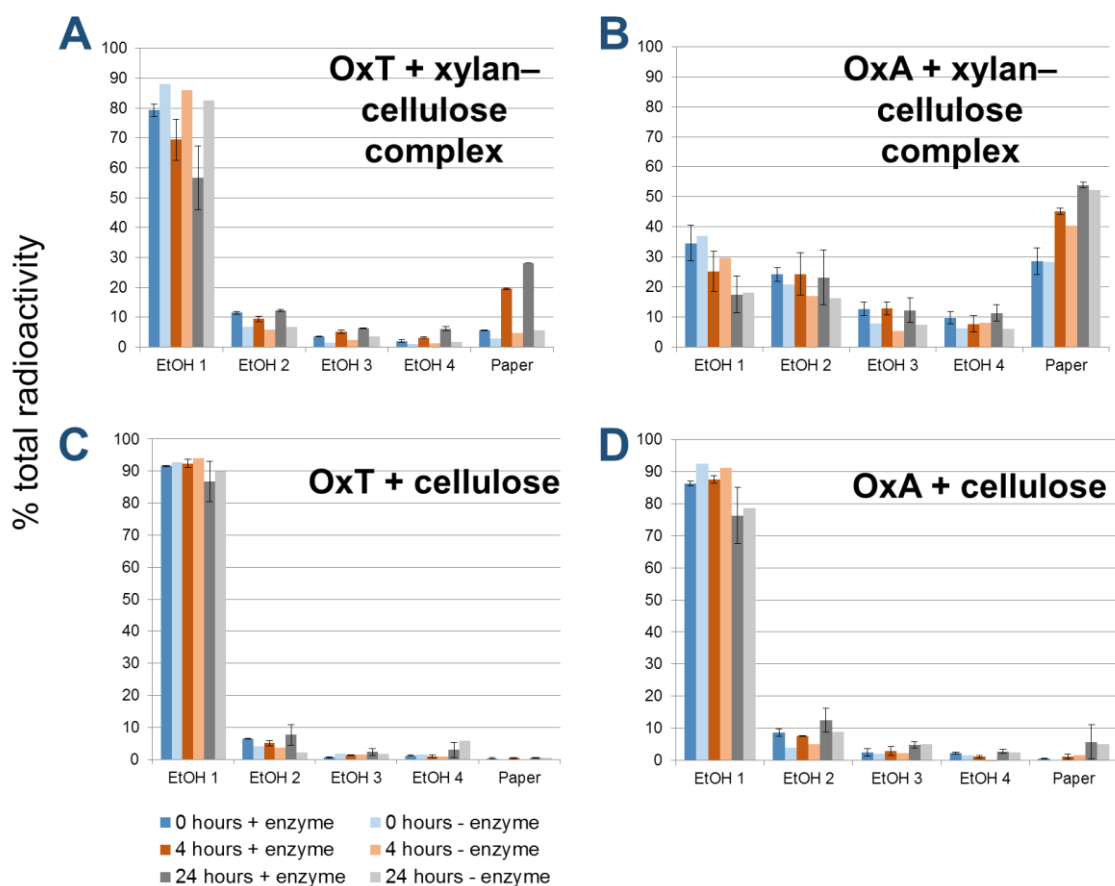


Figure 72: [¹⁴C]OxA becomes trapped in the cellulose-polysaccharide complex. Samples of a xylan–cellulose complex (xylan-impregnated paper, **A** and **B**) and untreated paper (cellulose, **C** and **D**) were incubated with *Arabidopsis* enzyme extract and [¹⁴C]OxT (**A** and **C**) or [¹⁴C]OxA (**B** and **D**) in pH 7 PIPES buffer, for 0 hours, 4 hours or 24 hours. Controls with no enzyme extract were also analysed. After the specified incubation times the papers were washed repeatedly in EtOH and then the radioactivity present in the washes and the radioactivity that remained bound to the paper throughout the washing was assayed by scintillation counting.

presumably because the activity of the enzyme had diminished slightly over time while being stored frozen.

The samples that had been incubated with [^{14}C]OxA and the xylan-cellulose complex, acting as the negative control, (Figure 72 B) showed even greater incorporation of radioactivity into the paper, with or without the enzyme extract present. This cannot be due to oxalyl ester formation, as OxA is unable to form ester bonds under the condition used; this suggests that the OxA is merely becoming trapped within the paper complex, and not becoming covalently bound. This has not occurred in the cellulose-only samples (Figure 72 D), so the xylan-cellulose complex may contain something that is acting to sequester the [^{14}C]OxA, rendering it unable to be removed during EtOH washing. One candidate for this phenomenon could be calcium, possibly present at trace levels in the xylan solution. OxA readily binds to calcium to form insoluble calcium oxalate (177), which would be likely to remain bound to the paper throughout the washing process.

This leads to the likelihood that the previously observed binding of radioactivity to hemicellulose-paper complexes after being incubated with [^{14}C]OxT (Figure 71) could be due to trapped [^{14}C]OxA, rather than the formation of an oxalyl ester. An enzyme present in the cell wall extract, possibly the acyltransferase itself, acts to hydrolyse oxalyl ester bonds, forming free OxA, as seen in the previous experiments in this section; this means that [^{14}C]OxA could be produced from [^{14}C]OxT during the incubation with the enzyme extracts.

It was hypothesised that prolonged washing of the papers, to fully ensure all the free OxA and OxT was removed, would improve the method. Therefore, in a repeat experiment (using xyloglucan-cellulose, homogalacturonan-cellulose and cellulose-only samples incubated with either [^{14}C]OxT or [^{14}C]OxA with and without the enzyme extract) the papers were washed in EtOH for a longer period. Replicate samples were assayed for radioactivity at intervals after washing in EtOH until no radioactivity remained on the paper of the negative controls (those incubated with [^{14}C]OxA but without the enzyme extract). After it was determined that no radioactivity remained bound to the control papers, all the other samples, having been washed for the equivalent time, were assayed for radioactivity.

After 24 hours' incubation with both [^{14}C]OxT and [^{14}C]OxA all the polysaccharide complexes showed negligible incorporation of radioactivity into the paper (Figure 73). As incubation with [^{14}C]OxT did not lead to radiolabelled paper substrate, it was concluded that the acyltransferase does not act upon polysaccharide acceptors.

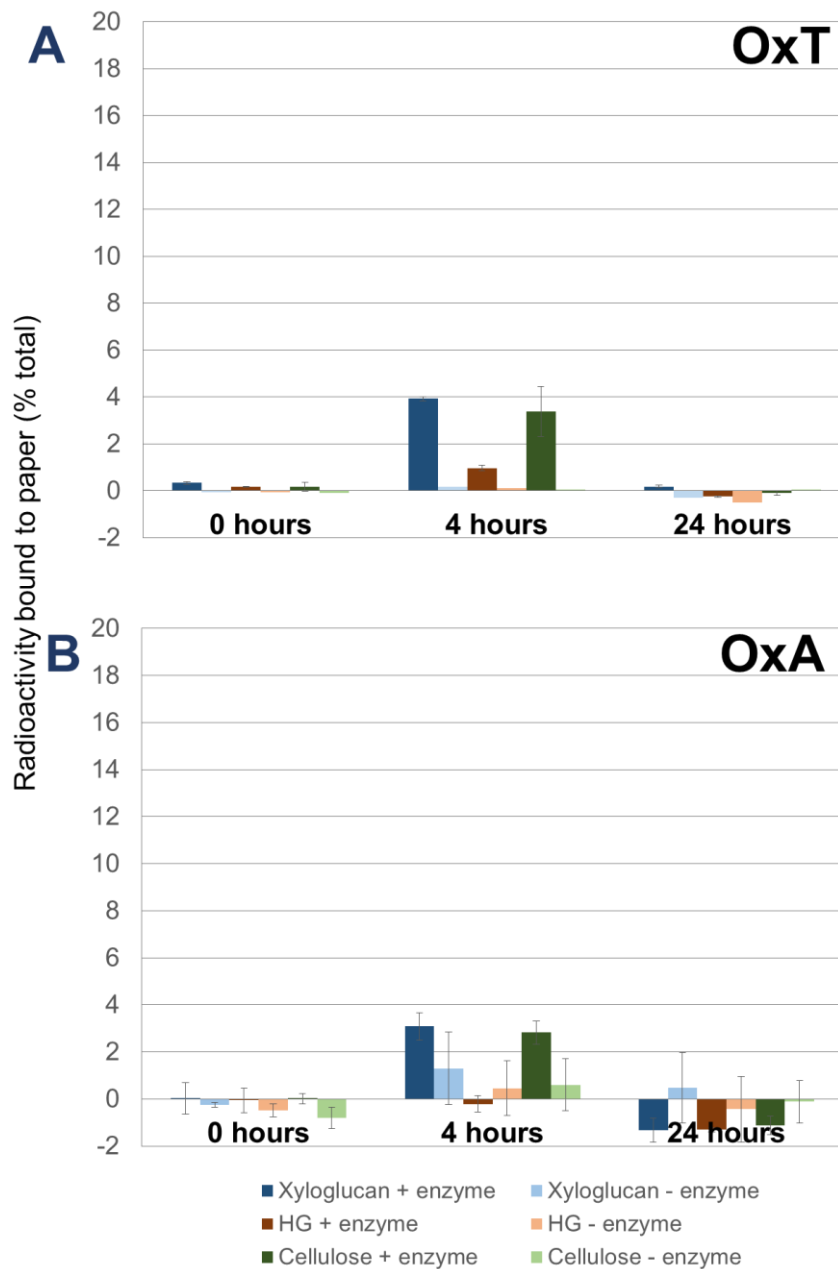


Figure 73: Radioactivity bound to paper incubated with acyltransferase and [^{14}C]OxT or [^{14}C]OxA after prolonged washing. Samples of a xyloglucan–cellulose complex, HG–cellulose complex and untreated paper (cellulose were incubated with *Arabidopsis* enzyme extract and [^{14}C]OxT (A) or [^{14}C]OxA (B) in pH 7 PIPES buffer, for 0 hours, 4 hours or 24 hours. Controls with no enzyme extract were also analysed. After the specified incubation times the papers were washed repeatedly in EtOH until no radioactivity remained on control papers incubated with [^{14}C]OxA and no enzyme extract (as determined by scintillation counting paper washed at intervals throughout washing). The radioactivity that remained bound to the paper throughout the washing was assayed by scintillation counting, after the control papers showed only background levels of radioactivity.

After 24 hours' incubation with both [^{14}C]OxT and [^{14}C]OxA all the polysaccharide complexes showed negligible incorporation of radioactivity into the paper (Figure 73). As incubation with [^{14}C]OxT did not lead to radiolabelled paper substrate, it was concluded that the acyltransferase does not act upon polysaccharide acceptors.

The 4-hour samples incubated with the xyloglucan–cellulose complex or cellulose only showed slight incorporation of radioactivity into the paper, but this occurred in samples incubated with both OxT and OxA (Figure 73 A and B), so would not be indicative of oxalyl ester formation. The levels observed were also much lower than the levels previously observed (in Figure 71 and Figure 72). An alternative explanation for the apparently negligible acyltransferase activity observed in Figure 73 could be that the enzyme had denatured during storage between the experiments described in Figure 71 and Figure 73, thus losing its activity.

In conclusion, these experiments do not provide any conclusive evidence to support the hypothesis that oxalyl esters were formed from the reaction of OxT with cell wall components via the action of an acyltransferase. However, the formation of OxG (as described earlier in this section) as well as the incorporation of radioactivity into cell wall preparations of spinach cells incubated with [^{14}C]OxT (section 3.4.3) suggests that this avenue warrants further investigation.

3.5.5 The activity of acyltransferase with different donor substrates

As discussed previously (section 3.4.1), OxT would be able to form only one oxalyl ester bond, whereas cOxT, having two available oxalyl ester linkages, has the potential to form two oxalyl esters, creating an oxalate bridge (Figure 49). OxA, on the other hand, would not be able to form an oxalyl ester at all, as it does not contain an 'activated' carboxy group.

A cell wall extract from *Arabidopsis*, shown to contain acyltransferase activity (Figure 65), was incubated with glucose and [^{14}C]OxT, [^{14}C]cOxT or [^{14}C]OxA. [^{14}C]OxA was included as a negative control, as this compound would not be able to form an oxalyl ester. [^{14}C]OxG was formed from both [^{14}C]cOxT and [^{14}C]OxT, but, as was expected, not from [^{14}C]OxA (Figure 74).

The preparation of cOxT also contained some OxT. This was due to the instability of cOxT, which spontaneously breaks down to form OxT during the purification process (involving the elution of the compound from paper). As the sample of cOxT also contains OxT, it would be possible that the OxG had formed from OxT rather than cOxT. This is in fact the

likely scenario as the reaction of cOxT with glucose would yield a product with a greater mass than OxG, as it would still contain the ThrO moiety. This product (pictured in section 3.4.1, Figure 49) would be negatively charged, but larger than OxG, so run below OxG during HVPE at pH 6.5. There was no spots visible beneath OxG in the cOxT sample, suggesting that this product was not formed. Equally, if an oxalate cross-link had formed between two glucose molecules, as would be theoretically possible if cOxT were the donor substrate, then a neutral radiolabelled compound would be formed. This would be positioned just above the origin after HVPE at pH 6.5, but this area was free of radioactivity, suggesting that this reaction had not occurred.

The [^{14}C]cOxT had diminished in the samples containing cOxT and the enzyme extract

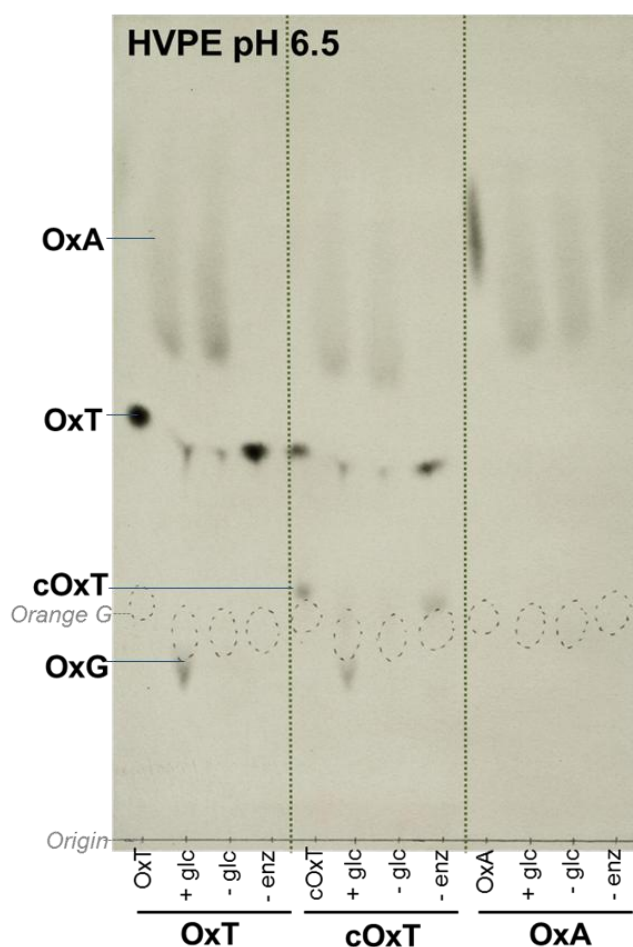


Figure 74: OxG is formed from cOxT and OxT but not OxA. Cell wall enzyme extract from *Arabidopsis* was incubated with [^{14}C]OxT, [^{14}C]cOxT or [^{14}C]OxA (all of which had previously been eluted from a preparative electrophoretogram and used at a concentration of $\sim 5 \mu\text{M}$) and 5% glucose in pH 7 buffer. Controls containing wither no glucose or no enzyme extract were also incubated. The sample were incubated for 4 hours, and then run by HVPE at pH 6.5. The samples labelled OxT, cOxT and OxA represent time 0 samples. The resulting electrophoretogram was exposed to film for 3 weeks.

(Figure 74), as had the OxT present in those samples. The end products of these reactions were OxA and OxG. There is the possibility that the enzyme extract contained hydrolases that converted cOxT to OxT, and subsequently to OxA. This means that it is possible that the cOxT was converted to OxT, then the acyltransferase acted on OxT and glucose to produce OxG. OxT and OxG could both undergo hydrolysis to form OxA, and non-radiolabelled ThrO or Glc.

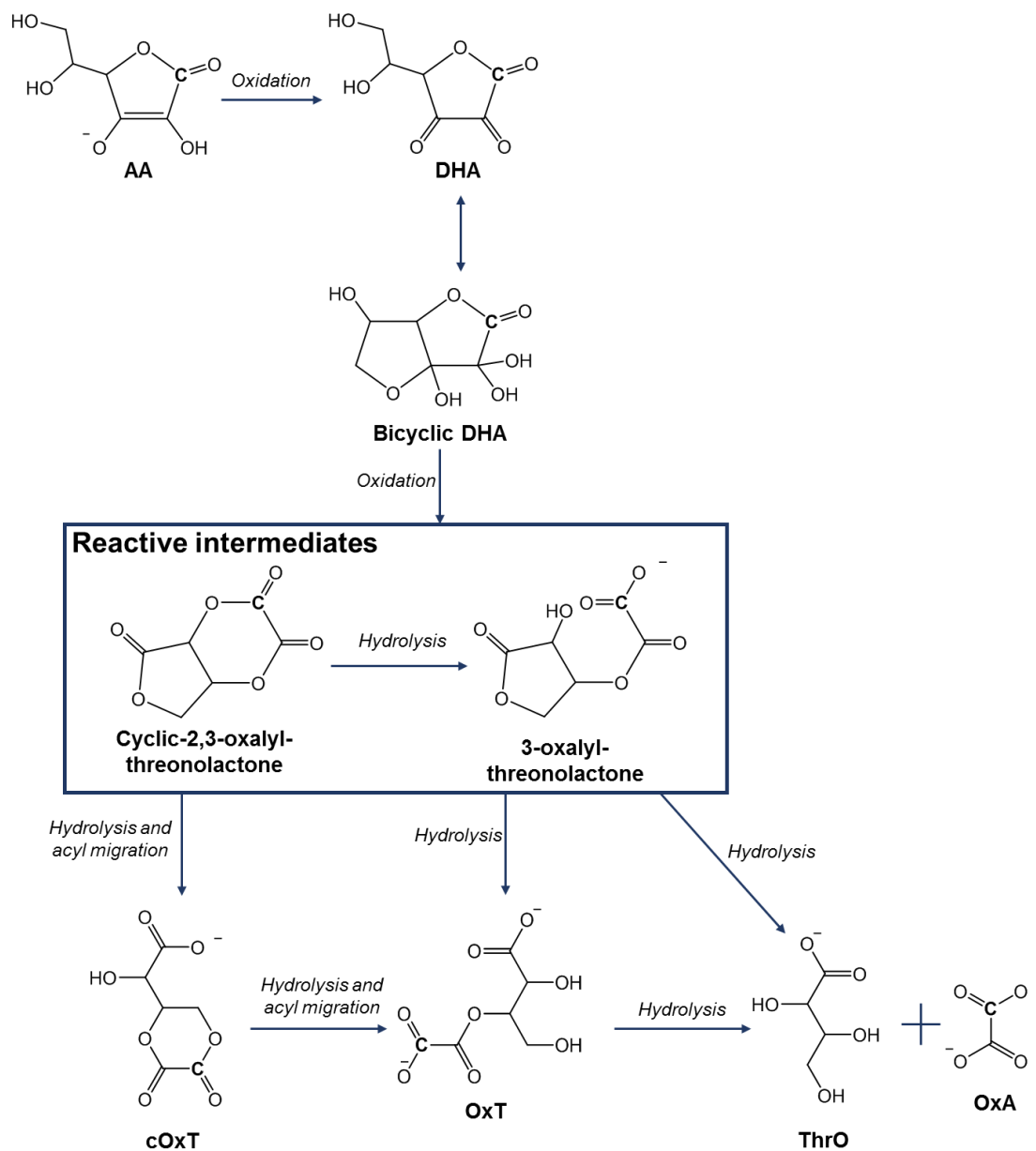


Figure 75: Formation of reactive intermediates during the oxidation of AA. The oxidation of AA via highly reactive intermediates (cyclic 2,3-oxalyl-threonoactone and 3-oxalyl-threonoactone) is shown. The radiolabelled carbon (C-1 of [^{14}C]AA) is shown with a bold **C**. For a more detailed ascorbate oxidation pathway, including other isomers of cOxT and OxT, see section 1.5.1, **Figure 4**.

As well as cOxT and OxT, further high-energy intermediate compounds have been hypothesised to form during the oxidation of AA (Figure 75) (2). These short-lived compounds (hypothesised to be cyclic-2, 3-oxalyl threonolactone and 3-oxalyl-threonalactone; Figure 75) would not be able to be purified, owing to their unstable nature, but it would be very likely that they would occur *in vivo*. It was hypothesised that these compounds may have the potential to act as oxalyl donors for acyltransferase activity. To determine whether this was the case, [¹⁴C]AA was incubated with glucose, a cell wall extract from *Arabidopsis*, and varying concentrations of H₂O₂ in order to generate the hypothesised high-energy intermediate oxidation products *in situ* (Figure 76). Non-radiolabelled AA was also added to the reaction mixture with the aim of stabilising the low concentration of [¹⁴C]AA. The non-radiolabelled AA would act to protect the [¹⁴C]AA from degradation, by virtue of the non-radiolabelled AA being far in excess of [¹⁴C]AA, so it would be more likely for the non-radiolabeled AA to degrade than the [¹⁴C]AA.

The samples that were incubated with [¹⁴C]AA, glucose and the enzyme extract produced a small amount of OxG, regardless of whether H₂O₂ was present (Figure 76). The increasing H₂O₂ concentrations did not correspond to an increase in AA oxidation products. In fact the controls containing [¹⁴C]AA and the enzyme extract, with and without H₂O₂ (but without glucose) showed very low levels of total oxidation products. The control samples without the enzyme extract present showed greater amounts of oxidation products formed than the samples containing the enzyme extract. This suggests that there was something present in the enzyme extract that was preventing the H₂O₂ from oxidising AA. It is possible that a peroxidase or catalase was eluted from the cell wall (264) of the *Arabidopsis* cell culture, which was acting to detoxify H₂O₂ before the AA could react with it. It is also possible that the 5 mM AA present in the samples swamped the hypothetical enzyme, preventing oxalyl sugars compounds being produced.

During the 4-hour incubation, most of the AA was oxidised to DHA. This DHA was then partially further oxidised to OxT and OxA (Figure 76), but very little cOxT, which may have been expected according to the reaction of DHA and H₂O₂ described in section 3.3.2. The OxG that was formed was likely to have originated from OxT. There was also a radiolabelled product running between AA and OxT (labelled X, Figure 76) present in the samples that contained both enzyme extract and glucose, but not in the controls. This compound could be another glucose ester of an AA derivative. The mobility of this compound suggests that it would have a greater charge : mass ratio than OxG, so perhaps

two negative charges, rather than the one negative charge of OxG, or the compound would have a much smaller mass than OxG, and one negative charge.

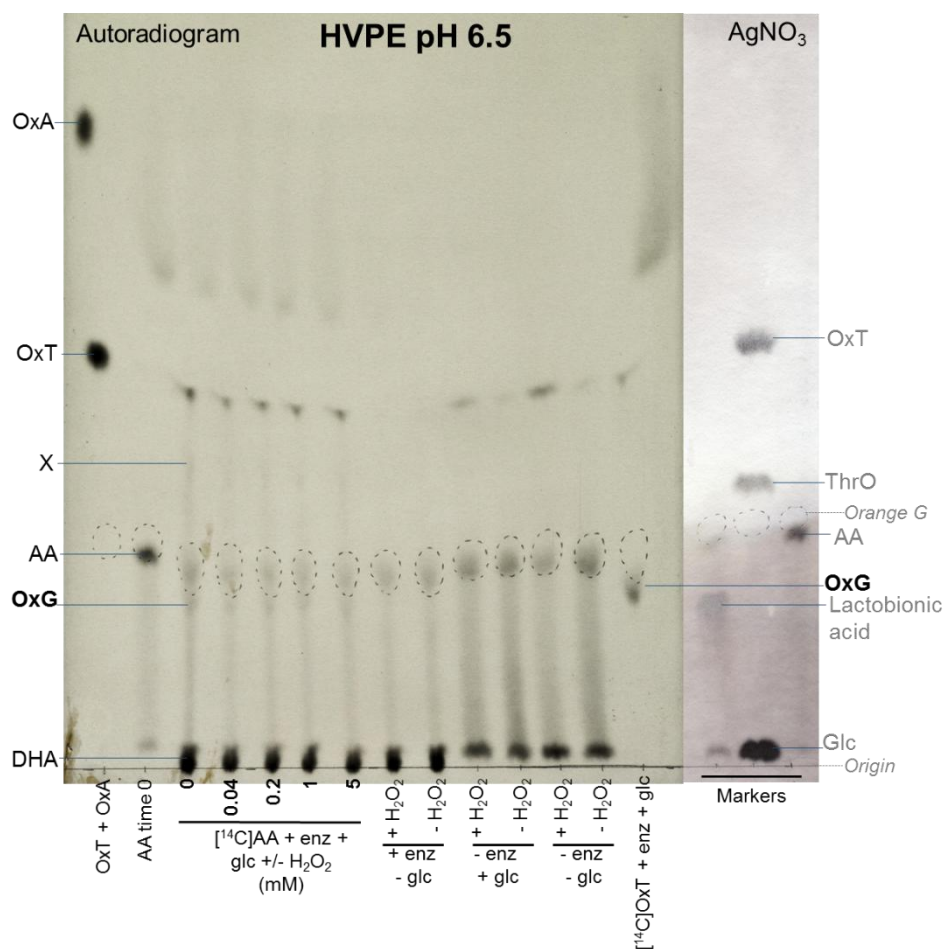


Figure 76: The reaction of $[^{14}\text{C}]\text{AA}$ with acyltransferase extract and glucose and H_2O_2 . $[^{14}\text{C}]\text{AA}$ (approximately $20\ \mu\text{M}$) was incubated with *Arabidopsis* enzyme extract (1% final concentration), glucose (5%) and increasing concentrations of H_2O_2 (up to 5 mM). Non-radiolabelled AA (5 mM) was also added to the samples to stabilise the $[^{14}\text{C}]\text{AA}$. The samples were incubated in pH 7 buffer (10 mM PIPES) for 4 hours, before running by HVPE at pH 6.5. Controls lacking combinations of enzyme extract (enz), glucose and H_2O_2 were also analysed. The controls contained either 0 mM ($-\text{H}_2\text{O}_2$) or 5 mM H_2O_2 ($+\text{H}_2\text{O}_2$). A positive control of $[^{14}\text{C}]\text{OxT}$ with enzyme extract and glucose was included. Non-radiolabelled markers (subsequently stained in silver nitrate) were run alongside the radiolabelled samples. The radiolabelled portion of the paper was exposed to film for 3 weeks.

The neutral spot was assumed to contain DHA, as this is a likely product of the reaction of AA and H_2O_2 (265); however, it was not possible to distinguish DHA from any other neutral compound using this technique. This means that if the acyltransferase had produced a neutral

compound, such as the theoretical compound containing an oxalyl cross-link and two glucose residues, this would not be visible using this detection system.

The most predominant product formed during the reaction of oxidised AA with acyltransferase was OxG. The repeated formation of OxG in these experiments suggests that this compound is a relatively stable end-product, and is perhaps being formed for a biological role unrelated to cell wall cross-linking.

3.5.6 Investigating the fate of oxalyl glucose *in vivo*.

[¹⁴C]OxG was purified to further investigate the possibility that OxG could serve a role *in vivo*. This was achieved by incubating [¹⁴C]OxT with excess glucose and the acyltransferase extract. The sample was run preparatively by HVPE at pH 6.5 and then the band of [¹⁴C]OxG was eluted in water (Figure 77).

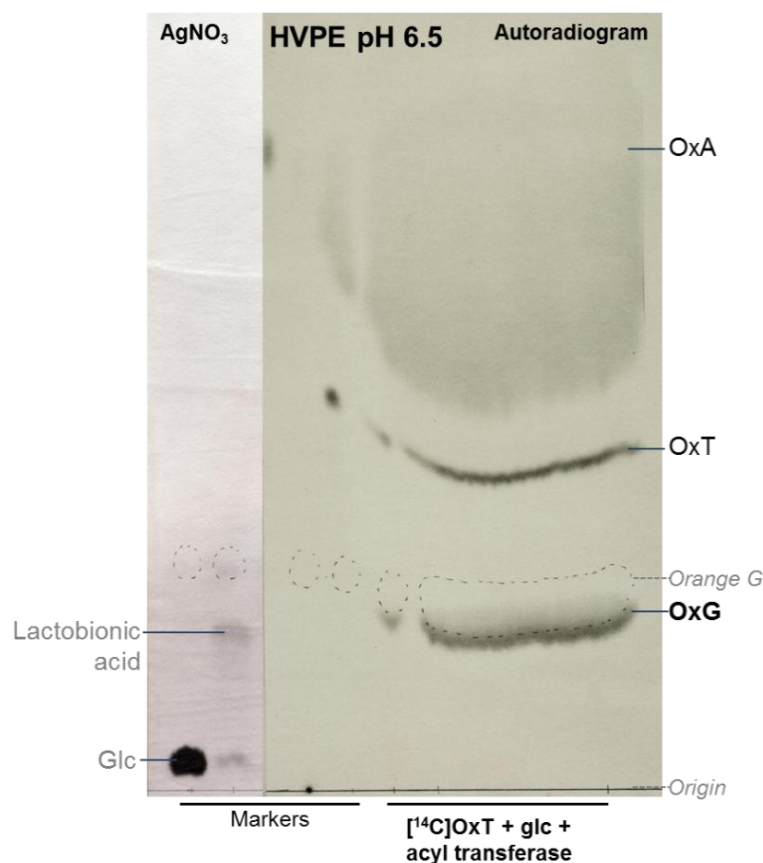


Figure 77: Purification of OxG. Enzyme extract (1%, from *Arabidopsis*) was incubated with glucose (5%) and [¹⁴C]OxT (50 μ M) in pH 7 (10 mM PIPES) buffer for 4 hours. The sample was run preparatively by HVPE at pH 6.5, along with non-radiolabelled markers of glucose and lactobionic acid. The non-radiolabelled markers were stained in silver nitrate and the radiolabelled portion of the paper was exposed to film for 3 weeks.

The fate of [^{14}C]OxG in cell culture was investigated. Spinach cell cultures were incubated with either [^{14}C]OxT, [^{14}C]OxA or [^{14}C]OxG for up to 24 hours. The culture medium from each of the cultures was sampled at various time-points and run by HVPE at pH 6.5 to investigate the stability of each of the compounds (Figure 78). As had been previously observed (in section 3.4.3), OxT remained fairly stable in culture medium for 6 hours. However, OxT was gone from the culture medium after 24 hours. Very little OxA was present in the 24-hour sample incubated with OxT, suggesting that the OxT had not simply been hydrolysed to [^{14}C]OxA and non-radiolabelled ThrO. It is possible that the OxT had been taken up into the cells via membrane transporters by 24 hours, or the radioactivity from

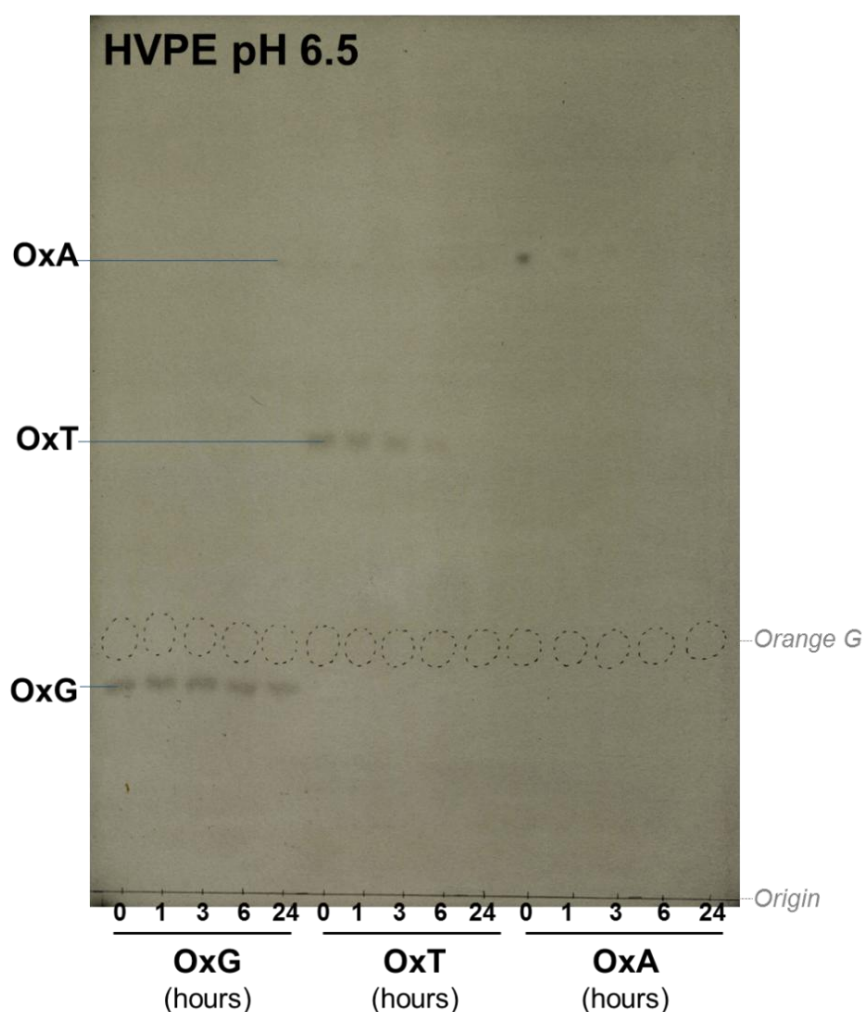


Figure 78: [^{14}C]OxG is stable in spinach cell culture. Spinach cell mini-cultures (250 mg cells with 500 μl medium) were incubated with [^{14}C]OxG, [^{14}C]OxT or [^{14}C]OxA ($\sim 0.5 \mu\text{M}$), all of which were eluted from paper after preparative HVPE. Samples (50 μl) or culture medium were taken at time-points up to 24 hours after feeding. The samples were run by HVPE at pH 6.5, and the paper was exposed to film for 4 weeks.

the OxT had been incorporated into the cell wall, and so removed from the medium.

The OxA incubated in the cell cultures appeared to have mostly gone from the culture medium after 1 hour (Figure 78). It is possible that the OxA had bound to calcium, present in the medium at trace levels, and thus become insoluble and so removed from the medium. Equally, the OxA could have been transported inside the cells, either in the form of free OxA, or in a complex with calcium.

OxG, on the other hand, appeared to be stable for the whole of the 24 hour incubation period (Figure 78). The intensity of the band of OxG did not diminish significantly over time, though a very small amount of OxA can be seen in the 24 hour sample, suggesting partial hydrolysis, though this is unlikely to be due to an enzyme, as the amount of product is so low.

After the 0, 6 and 24 hour time-points, the cells were washed repeatedly in acidified EtOH to create AIR comprising predominantly cell wall material (Figure 79). The cells were also washed in EDTA, with the aim of releasing any [^{14}C]OxA that may have been in the form of insoluble CaOxA.

The cells that had been incubated with [^{14}C]OxA showed a significant proportion of the radioactivity in the AIR (Figure 79); however, this cannot be due to the formation of oxalyl esters, as OxA cannot form an ester bond, so it may be that the EDTA wash was not sufficient to release all the OxA from CaOxA. A large proportion of the radioactivity (around 60%) was present in the EtOH wash of the 6-hour samples. This suggests that the radioactivity had been taken up into the cells, then released when the membranes were permeated with EtOH.

The cells that had been incubated with [^{14}C]OxT also showed some incorporation into the AIR (Figure 79), but owing to the incorporation of [^{14}C]OxA into the AIR, this cannot be taken as evidence of oxalyl ester formation.

The cells that had been incubated with [^{14}C]OxG show almost no radioactivity in the AIR (Figure 79), which would have been expected because OxG remained stable in the culture medium for the 24-hour duration (Figure 78).

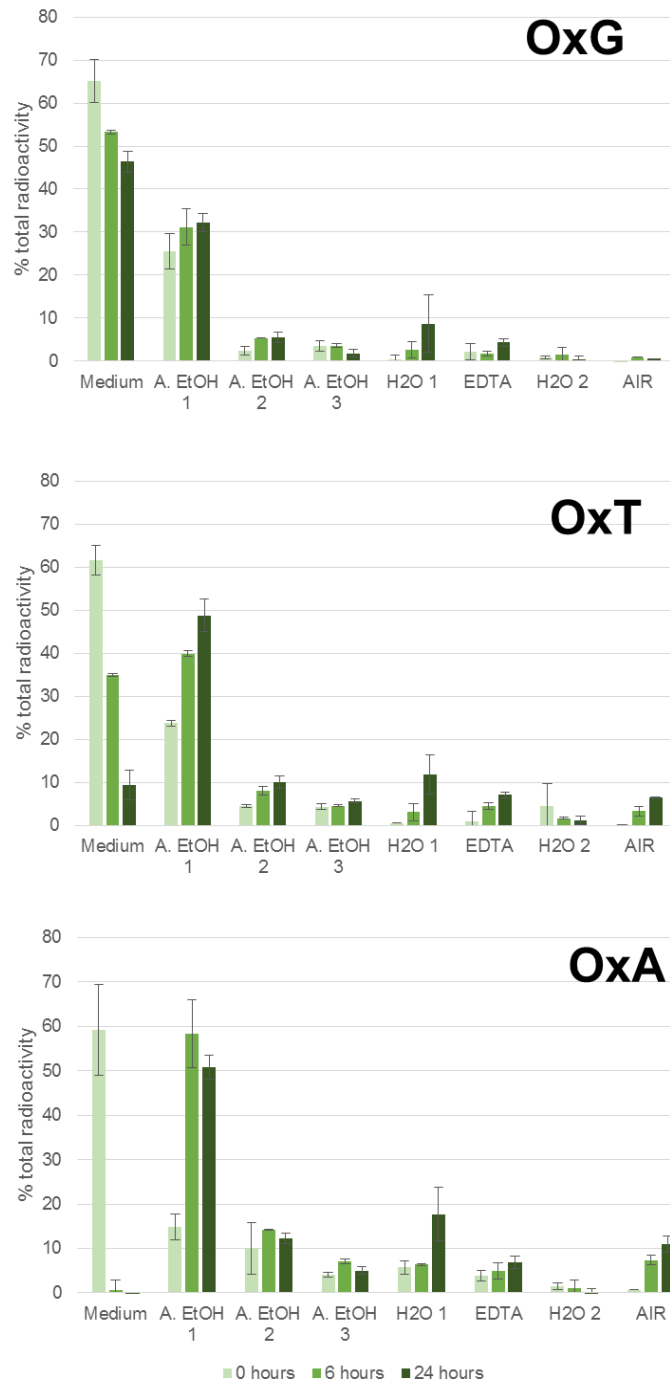


Figure 79: Washing of cells fed $[^{14}\text{C}]\text{OxG}$, $[^{14}\text{C}]\text{OxT}$ or $[^{14}\text{C}]\text{OxA}$. Spinach cell cultures (1 week after subculturing, 250 mg with 500 μl culture medium) were fed with $[^{14}\text{C}]\text{OxG}$, $[^{14}\text{C}]\text{OxT}$ or $[^{14}\text{C}]\text{OxA}$ ($\sim 0.5 \mu\text{M}$). Replicate cultures were set up, and after either 0, 6 or 24 hours incubation the culture medium was removed from the cells. The cells were then washed sequentially in acidified EtOH 3 times, followed by H_2O , EDTA and a second wash in H_2O . The resulting AIR was assumed to comprise mainly cell wall components. The radioactivity present in the washes and AIR was quantified by scintillation counting.

In conclusion, there is evidence for the formation of novel compounds, oxalyl sugars, formed from the reaction of OxT, an ascorbate derivative, and a variety of sugars, including hexoses, pentoses and disaccharides, among others. This reaction is catalysed by a novel acyltransferase activity, and the enzyme responsible for this activity can be eluted from the cell walls of plant cell-suspension cultures by NaCl treatment, suggesting it was ionically bound to the cell wall.

There is no conclusive evidence to suggest that this novel acyltransferase activity could be involved in forming oxalate cross-links in the cell wall, as polysaccharides did not seem to serve as suitable acceptor substrates; however this merits further investigation.

3.6 Ascorbate degradation in harvested salad leaves

3.6.1 Introduction to ascorbate in salad leaves

Salad leaves are an important source of dietary vitamin C (244), and pre-packed salads are becoming more popular because of their convenience, with up to 50% of people preferring pre-packed salads to preparing them themselves (266-268). Vitacress is a leading company in the area of pre-packaged salads in the UK. The factory is based in Hampshire, UK, and they have numerous farms in the south of England, as well as suppliers in Portugal (www.vitacress.com).

The aim of this work was to determine the level of ascorbate during the washing and postharvest storage of packaged salad leaves. The accumulation of ascorbate degradation products was also analysed. Much of this work took place on site in the Vitacress premises, and the salad leaves were sourced from the farms belonging to Vitacress.

3.6.2 Ascorbate content of a selection of salad leaves during cold storage

There is a great variety in ascorbate levels between different salad species and these species also vary in their ability to retain this level of ascorbate during post-harvest storage (269,270). The ability of various salad leaves, grown by Vitacress, to retain their ascorbate levels was investigated. Salad leaves were stored at 4°C after the standard commercial washing and packaging process. At time intervals, from 0 days' storage to 10 days' storage, samples of leaves were assayed for ascorbate content by the DCPIP titration method.

All the salads showed a loss of ascorbate over the 10-day storage period at 4°C, although the difference in ascorbate content of rocket and mizuna (a type of rocket) was not significant suggesting these species showed the greatest retention of ascorbate (Figure 80). This 10-day storage period is slightly longer than the recommended storage time (the 'best before end' date is generally 5-7 days after packaging, rather than 10 days), but this time period is often used to study the effects of post-harvest storage time.

The lettuces (Asteraceae) showed the lowest levels of ascorbate, as suggested in the literature (236). Conversely, fennel (Apiaceae) and pea shoots (Fabaceae) showed the highest levels of ascorbate, after both 0 and 10 days of storage. Watercress showed high levels of ascorbate initially but also showed a large decrease over the storage time tested (Figure 80).

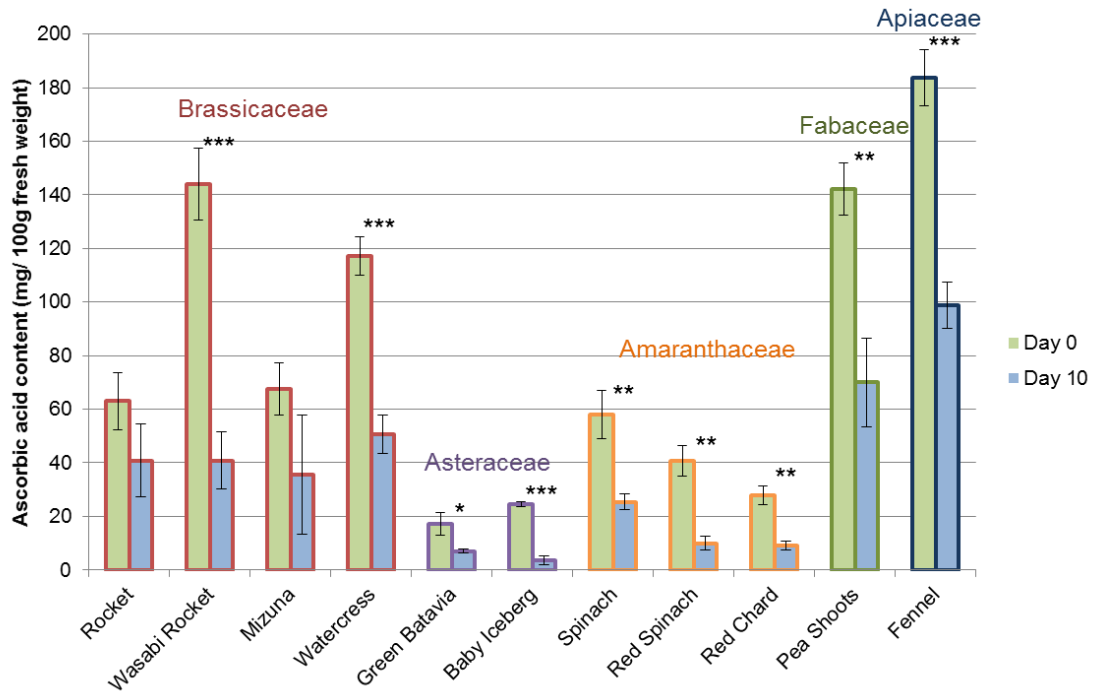


Figure 80: The ascorbic acid content of salad leaves during storage at 4°C. Salad samples were processed at Vitacress Salads then immediately assayed (in the case of the 0 days storage samples) or stored at 4°C. Samples of the leaves were assayed using the DCPIP titration method at stages throughout the storage time. The results from day 0 and day 10 of storage are summarised here. Significant differences (Student's t-test, * p<0.05, ** p<0.01, *** p<0.001, n=6) between the ascorbic acid levels at day 0 and day 10 are indicated. Each bar is an average of 6 separate measurements ± SE.

3.6.3 Effect of washing on ascorbate content of salad leaves

The salad washing process at Vitacress involves a counter-current conveyer belt system with leaves loaded at one end and spring water entering the other end. The leaves are submerged in the water, and undergo turbulence to remove particles of soil and grit. The leaves are then spun surface-dry, before being packaged in plastic packaging and distributed to supermarkets. This washing process could potentially be causing a loss of ascorbate before the salad leaves reach the supermarket shelves.

Samples of spinach, watercress and rocket leaves were taken before and after washing to test this hypothesis. The before and after samples were taken from the same harvest batch.

There was a significant difference (Student's t-test, $p < 0.05$; Figure 81) between the ascorbate content of spinach before and after washing, but no difference with watercress or rocket. This loss of ascorbate could be due to mechanical damage of the leaves, as spinach leaves are more susceptible to damage such as bruising, resulting in leaves being torn or becoming discoloured, than rocket and watercress leaves.

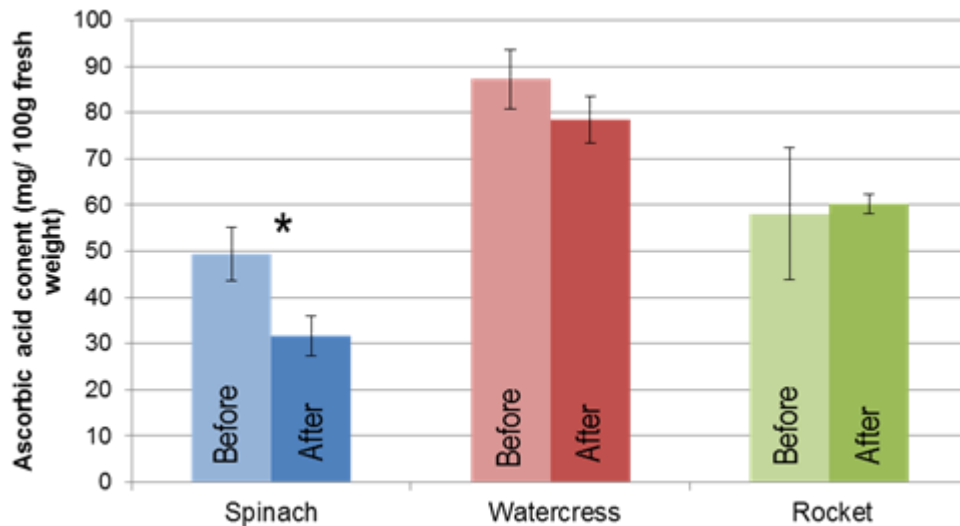


Figure 81: The ascorbic acid content of salad leaves before and after the washing process. Salad leaf (spinach, watercress and rocket) samples (1 g each) assayed for ascorbate by the DCPIP titration method before and after the washing process at Vitacress. The before and after samples originated from the same batch. The difference between the ascorbate content before and after washing was analysed by the Student's t-test ($p < 0.05$, $n = 6$). Each bar represents an average of 6 separate measurements \pm SE.

These same samples of washed and unwashed leaves were then stored under identical conditions in open plastic bags at 4°C for up to 10 days in the dark. The ascorbate content of the leaves was measured at various intervals (Figure 82).

The unwashed spinach leaves showed consistently higher ascorbate levels than the washed spinach (Figure 82 A) throughout the time course, though ascorbate levels decreased significantly in both samples during the 10-day storage time. The difference between unwashed and washed samples of watercress and rocket (Figure 82 B and C) was less distinct. After 10 days of storage washed watercress leaves showed marginally lower levels of ascorbate than unwashed leaves.

It is also interesting to note that the ascorbate levels in spinach begin to decline immediately, whereas in watercress and rocket, both of which have a greater amount of ascorbate to start

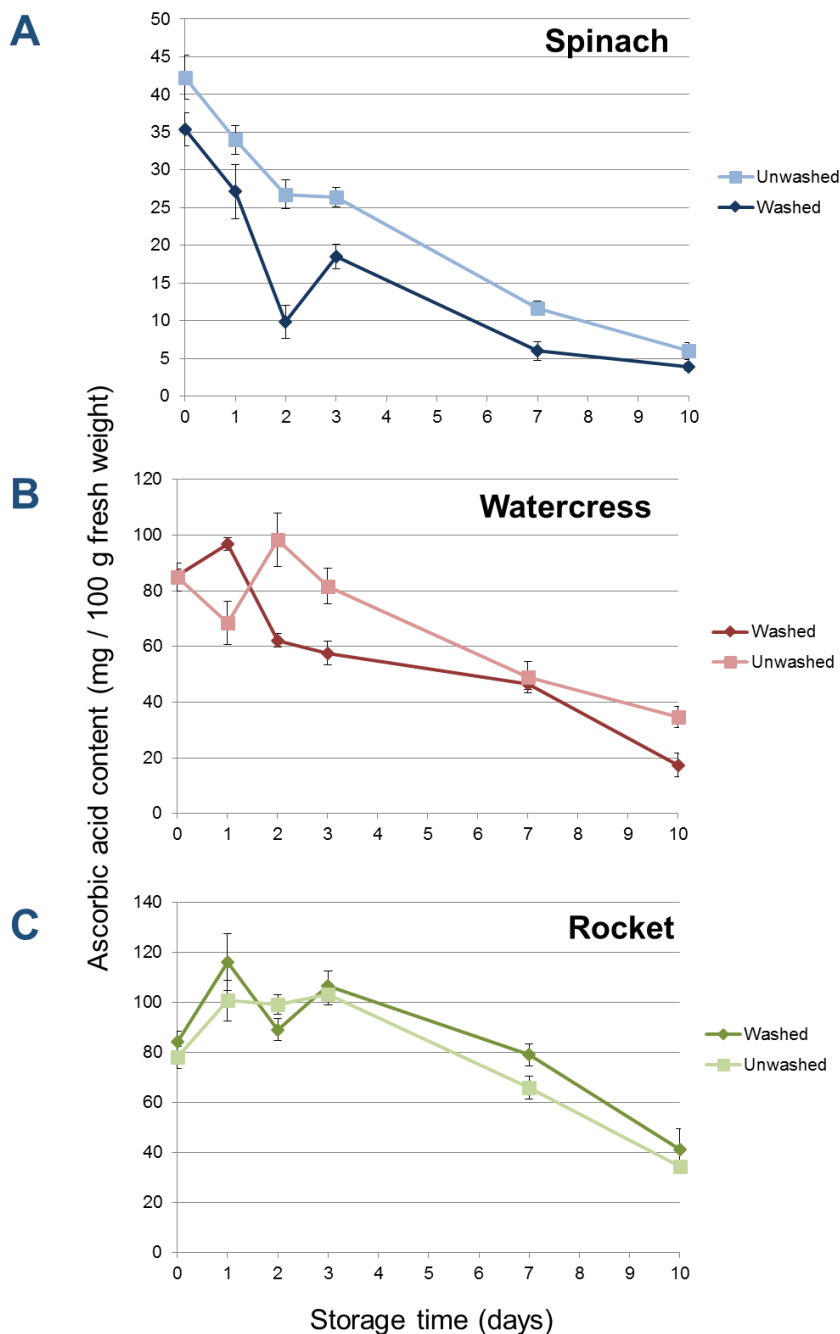


Figure 82: Ascorbic acid content of washed and unwashed salad leaves during storage. Samples of spinach, watercress and rocket leaves were taken from the same batch before and after the washing process. The leaves were then stored in plastic bags at 4°C in the dark for up to 10 days. Samples were taken at time points and the ascorbate content measured using the DCPIP titration method. The error bars represent the standard error of three individual samples.

with, the level of ascorbate remained fairly stable for the first 3 days (Figure 82).

As standard procedure at Vitacress, spinach leaves are vacuum-cooled (to approximately 5°C at 1 kPa) for 1 hour immediately after harvesting. This process cools the leaves quickly, by evaporating water and thus removing heat from the leaves under vacuum. This is done with the aim of increasing shelf life and to improve the quality of the product (237). Vacuum cooling has been reported to improve the sensory quality of spinach (239). Two crates of spinach harvested from the same farm at the same time were taken to investigate the effect of vacuum-cooling on spinach leaves. One crate was vacuum cooled, as standard. The other crate was stored immediately in the fridge, bypassing the vacuum-cooling step (as in Figure 83 A). Both crates were then stored in the fridge for two days before being collected and the leaves assayed for ascorbate content (Figure 83 B).

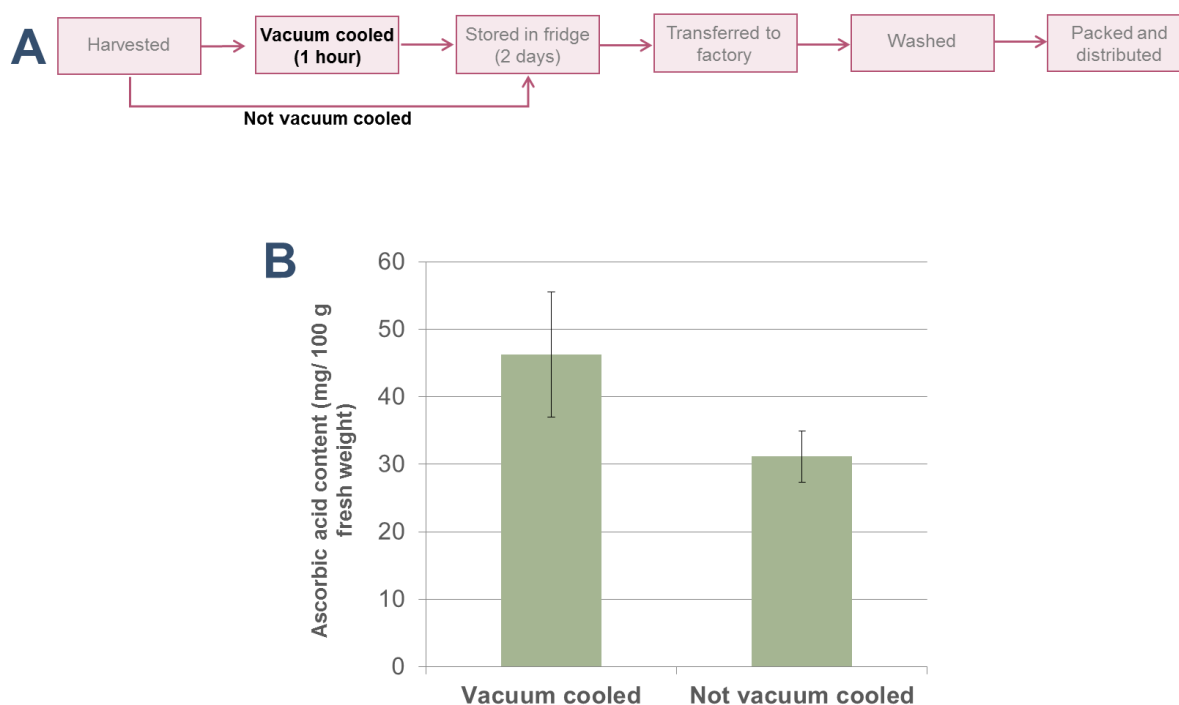


Figure 83: Effect of vacuum cooling on ascorbic acid content of spinach leaves. Spinach leaves were harvested, then a proportion were vacuum cooled, whereas an equivalent proportion were transferred straight to storage in the fridge in the dark for two days. Both samples were then processed as normal (A) and the ascorbate content of both samples was measured using the DCPIP titration method (B). The error bars represent the standard error of 3 individual samples, each the average of duplicate measurements. The difference in ascorbate content between vacuum cooled and not vacuum cooled was not significant (Student's t-test, $p > 0.05$, $n = 3$).

The vacuum cooled leaves showed slightly higher levels of ascorbate, but the difference was not statistically significant (Student's t-test, $p > 0.05$; Figure 83 B). If a greater number of samples were assayed then it is possible that the result would be significant, as the beneficial effects of vacuum cooling on ascorbate content in iceberg lettuce have been previously reported (238), and so the effect in spinach leaves may well warrant further investigation.

The washing process was mimicked in the lab with the aim of investigating the loss of ascorbate in spinach leaves during washing in more detail.

Spinach leaves, either grown in University of Edinburgh facilities or purchased from Sainsbury's supermarket (supplied by Vitacress), were incubated in different washing conditions of varying severity. The leaves were incubated either with no added H₂O (in air), submerged in H₂O (in still water) or submerged in water and shaken on a benchtop shaker to create turbulence (in shaken water), then the ascorbate levels of the leaves were assayed. The ascorbate levels at time 0 (immediately after harvesting or at the onset of the experiment) were also assayed.

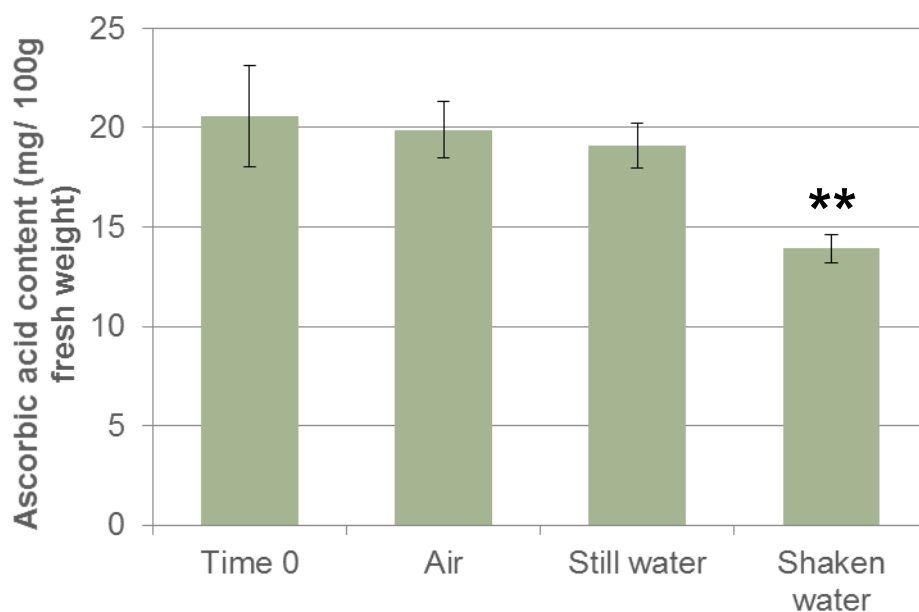


Figure 84: Ascorbic acid content of spinach leaves throughout washing. Spinach leaves (grown in University of Edinburgh glasshouses) were harvested, and incubated for 1 hour either in air, submerged in 20 ml H₂O (still water), or submerged in 20 ml H₂O and shaken (shaken water). Ascorbate was extracted from the samples in 0.5% formic acid and the ascorbate level was determined by the DCPIP titration method. Time 0 samples were assayed immediately after harvesting. The difference between time 0 and shaken samples was significant (Student's t-test, ** $p < 0.01$, $n = 3$).

The ascorbate content of leaves that had been submerged and shaken was significantly lower than the ascorbate level at time 0 (Student's t-test, $p < 0.01$, $n = 3$, Figure 84). The level of ascorbate in the sample incubated in air was equivalent to the time 0, showing that ascorbate is not lost during the hour incubation time. Equally, the sample incubated in still water also showed no significant difference in the ascorbate content, suggesting that the shaking was causing the loss of ascorbate.

Samples of these extracts (from Figure 84) were run by HVPE with the aim of determining the compounds that had been formed upon the degradation of ascorbate (Figure 85).

Unfortunately the HVPE was inconclusive. This was due to the fact that the extract contained numerous compounds which were able to be stained with silver nitrate, not only compounds originating from ascorbate. Although the silver nitrate stain is very sensitive (for example ThrO is visible down to $0.5 \mu\text{g}$ (data not shown) and arabinose is detectable to $0.1 \mu\text{g}$ (271)), in order to have enough ascorbate present to be visible with the stain, a relatively large sample ($100 \mu\text{l}$) was required. This led to the overloading of the sample, which can be seen by the distortion of the internal marker orange G (Figure 85). HVPE at pH 2.0 shows a particularly severe distortion of orange G. This is likely to be due to the presence of OxA in the samples, which is known to accumulate in spinach (272). OxA has an electrophoretic mobility (m_{OG}) of 1.03, overlapping with orange G, so overloading of OxA would result in the distortion of orange G.

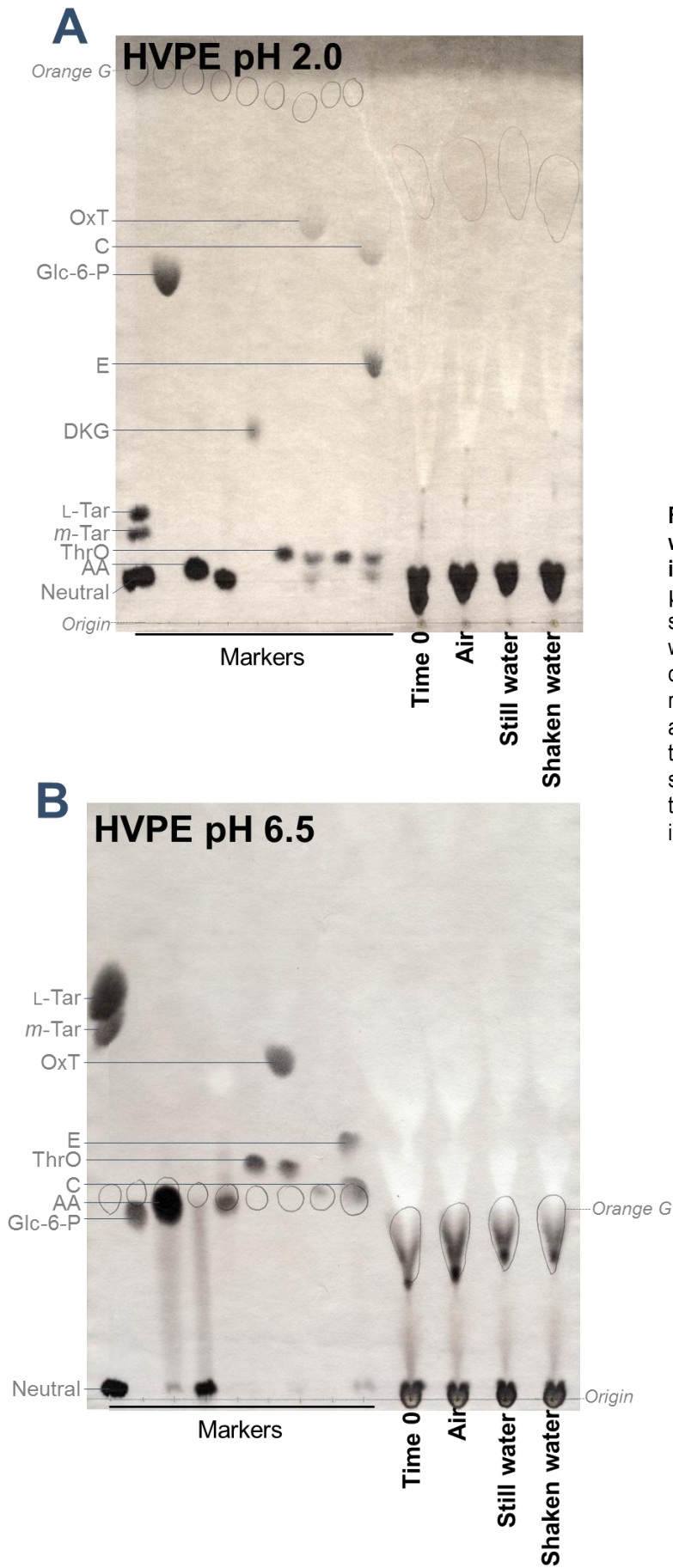


Figure 85: HVPE analysis of washed spinach was inconclusive. Extracts (100 μ l, in 0.5% formic acid) from spinach leaves after various washing treatments, as described in figure 5, were run by HVPE at pH 2.0 (A) and at pH 6.5 (B). After HVPE the papers were stained in silver nitrate. The position of the internal marker orange G is marked with pencil circles.

[¹⁴C]AA was used to monitor the degradation products formed directly from ascorbate. Any radiolabelled compounds detected would necessarily originate from ascorbate. The detection of ¹⁴C compounds is also more sensitive than detection by silver nitrate, so the samples would not require overloading. However, a downside to this method is that it was not known whether the ascorbate monitored was intracellular or apoplastic, which may mean that the [¹⁴C]AA measured may not necessarily be representative of the majority of the endogenous ascorbate.

The experimental set-up of washing radiolabelled spinach leaves required the use of leaf discs, rather than whole leaves. To ensure that spinach leaf discs were equivalent to whole spinach leaves in terms of ascorbate content, the experiment described in Figure 84 was repeated with leaf discs.

Leaf discs were incubated either in air, in still water or in shaken water for 1 hour or 2 hours (Figure 86). The ascorbate content of the discs at time 0 was also assayed. After an incubation of 2 hours the shaken samples showed a considerable loss of ascorbate. The difference within 1 hour was not significant but may be indicative of a trend. The samples submerged in still H₂O also showed a loss of ascorbate over the time course. This may be

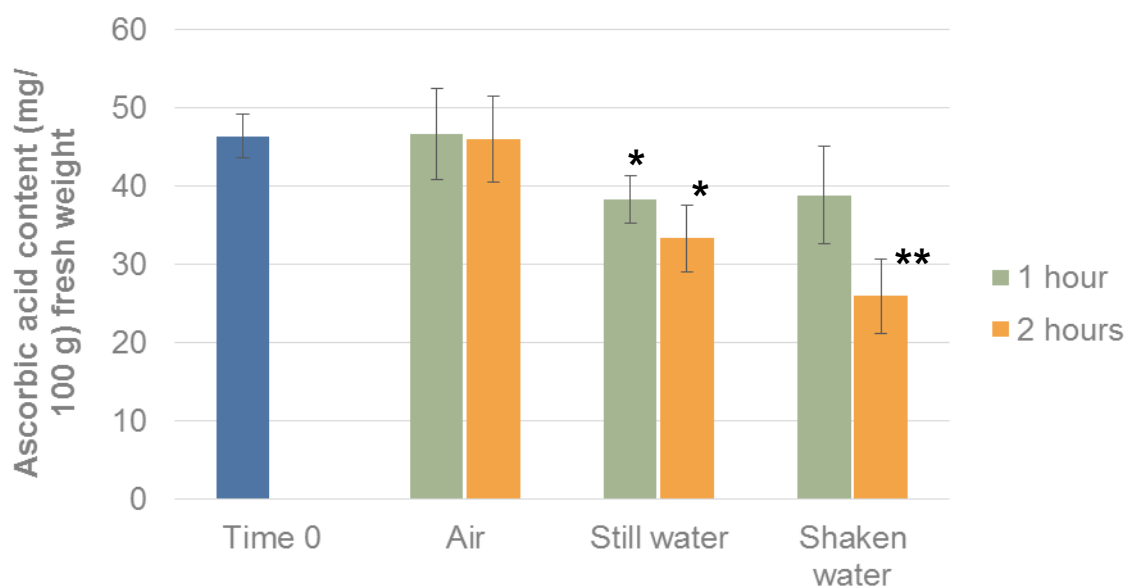


Figure 86: Ascorbic acid content during washing of spinach leaf discs. Leaf discs (1 cm in diameter) were cut out of spinach leaves purchased from a local supermarket. Samples of leaf discs (250 mg) were incubated in sterilin pots (60-ml volume) at 7°C in the dark either in **air**, submerged in 5 ml H₂O (**still water**) or submerged in 5 ml H₂O and shaken on a small orbital shaker, (**shaken water**) for 1 hour or 2 hours. A sample of leaf discs was taken immediately after cutting out (**time 0**). Extracts of the leaf discs were taken in 0.5% formic acid, and assayed for ascorbate content by the DCPIP titration method. Each bar represents the average of three individual samples ±SE. Samples that were significantly different (Student's t-test, * p<0.05, ** p<0.01, n=3) to the time 0 sample are shown.

because the edge of the leaf disc is effectively a wound, and some ascorbate may have leaked out of the sample via this cut and into the water, or the ascorbate may have been consumed in antioxidant processes in the wound healing process.

The overall pattern of ascorbate content during the washing of spinach leaf discs showed a similar pattern to whole spinach leaves (Figure 84 and Figure 86). With this confirmed, the radiolabelling experiment could go ahead.

Commercial [^{14}C]AA was fed through the petiole of a freshly harvested spinach leaf. After the initial solution containing [^{14}C]AA had been taken up into the leaf via transpiration, additional H_2O was added to the tube, ensuring the continued transport of the ascorbate into the leaf. This was continued until the presence of radioactivity in the lamina was confirmed using a Geiger counter. Leaf discs were then cut out, avoiding main veins, in groups of four equivalent discs (as described in section 2.19.4). These leaf discs were then individually incubated either in air, in still water or in shaken water, before the ascorbate and its metabolites were extracted in formic acid. Aliquots of these extracts were run by HVPE at pH 6.5. The use of four equivalent discs (time 0, and the three incubation treatments) meant that although these four discs were directly comparable, comparisons between the different sets of discs would be more difficult to make. This was due to the fact that the [^{14}C]AA was likely to be unevenly distributed across the lamina, and potentially the ascorbate had been degraded to varying degrees in different areas of the leaf.

The samples incubated for 2 hours (Figure 87) show the clearest loss of [^{14}C]AA (Figure 87 A; quantified in Figure 87 B). The major product of this degradation of ascorbate was OxA, which increased with the severity of the washing. OxT was also present in all the samples, but did not increase with either time or washing.

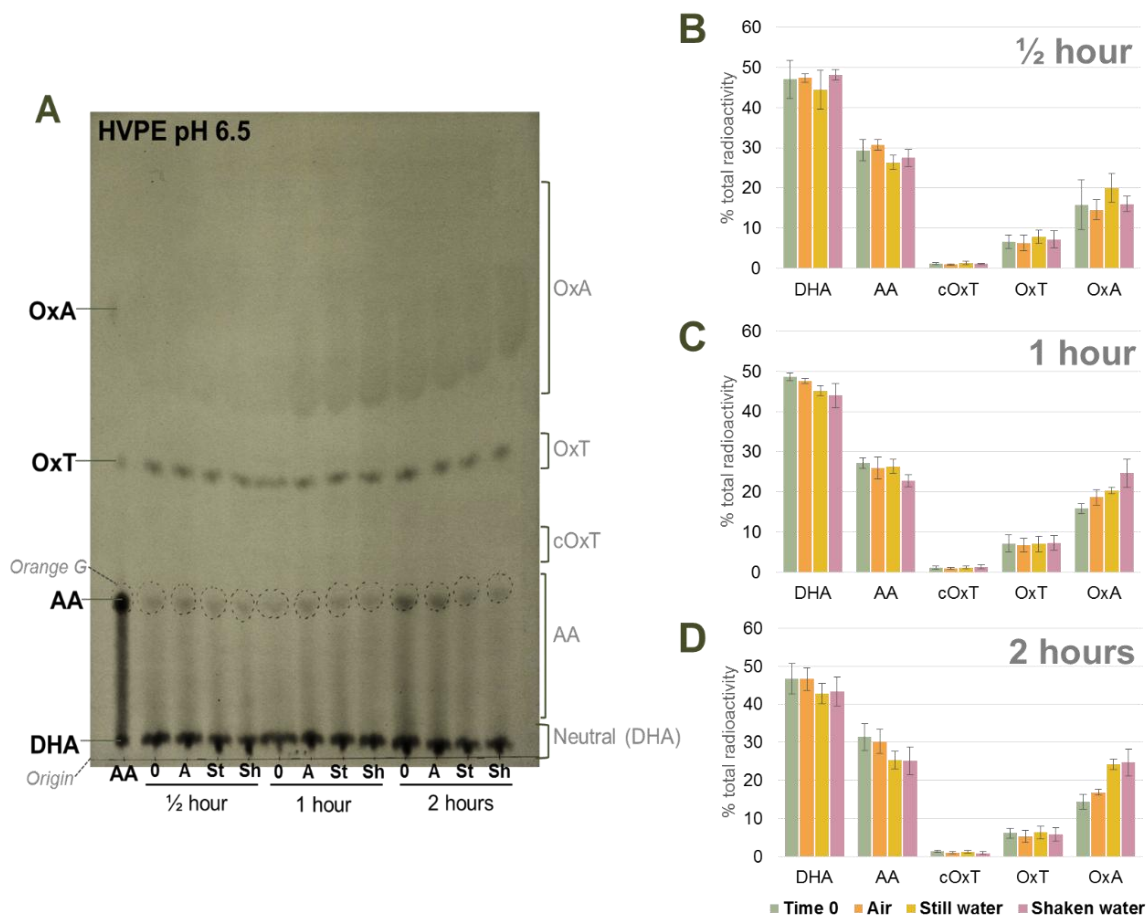


Figure 87: The degradation of $[^{14}\text{C}]\text{AA}$ fed to spinach leaves throughout washing. Spinach leaves (three individual leaves) were fed $[^{14}\text{C}]\text{AA}$ (approximatel 0.5 mM in 50 μl) through the petiole. Leaf discs were cut out and treated for 0.5, 1 or 2 hours at 7°C in the dark in plastic vials of 20-ml volume. The treatments were in air (A), in still water (St) and in shaken water (Sh). Time 0 is represented with 0. Extracts were taken of the leaf discs in 0.5% formic acid (200 μl per 1-cm leaf disc), and samples (50 μl) were run by HVPE at pH 6.5. The paper was exposed to film for 3 weeks (A). The radioactivity present in each sample was quantified by scintillation counting. Quantification of AA includes the streak (as shown in A), as the streak comprises AA that has oxidised to DHA during the run. The radioactivity present in the spots after incubation for 0.5 hours, 1 hour and 2 hours are shown (B, C and D respectively). The bars in B, C and D each represent the mean of 3 individual leaf disc measurements \pm SE.

The washing procedure employed by Vitacress differs from standard commercial salad washing. Vitacress wash the salads in spring-water only, whereas other companies wash the salads in chlorinated water, as an anti-microbial wash. As chlorine is an oxidising agent it is

plausible that washing salad leaves in the presence of chlorine could lead to a loss of ascorbate, via ascorbate oxidation.

Spinach leaves (grown and packaged by Vitacress) were washed in deionised H₂O or water containing 100 ppm active chlorine. The standard level of active chlorine used in industry is generally 20-150 ppm.

Leaves incubated in still water, either chlorinated or non-chlorinated, did not differ in their ascorbate levels (Figure 88 A). Spinach leaves shaken in chlorinated water showed a slightly greater loss of ascorbate than those shaken in non-chlorinated water (Figure 88 B). The difference between time 0 and the leaves incubated in shaken non-chlorinated water was not

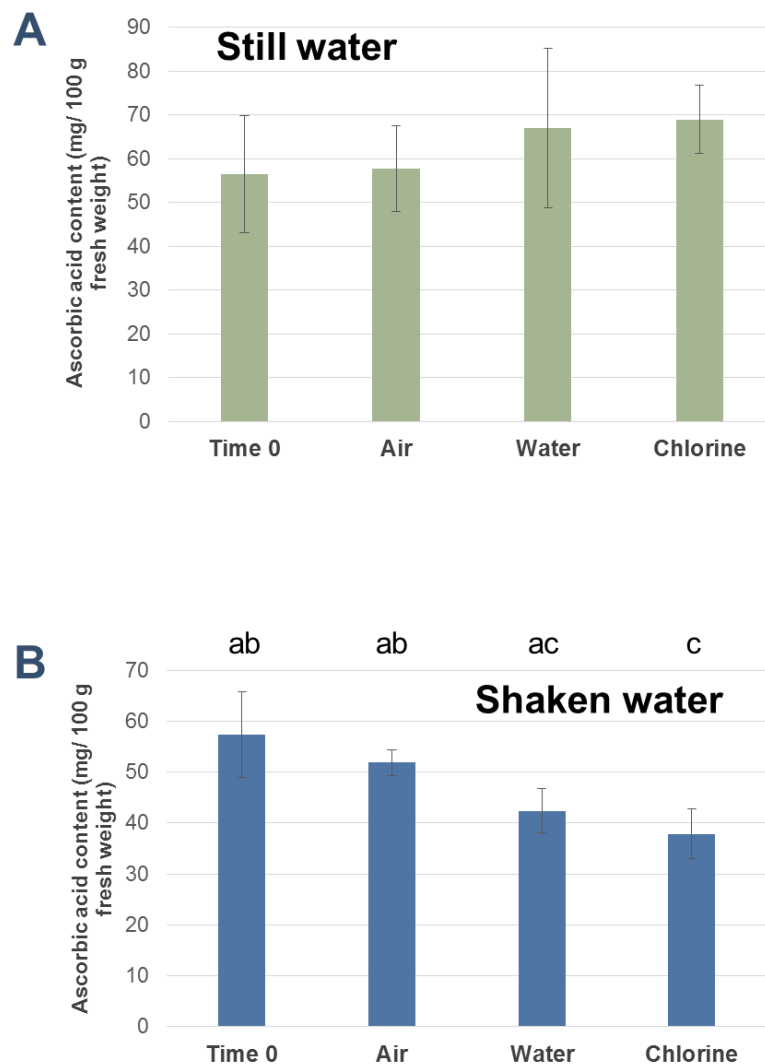


Figure 88: The effect of chlorine on the ascorbic acid content of spinach leaves. Spinach leaves (1 g per sample, purchased from a local supermarket) were incubated for 1 hour either in **air**, submerged in 20 ml H₂O (**water**), or submerged in 20 ml chlorinated H₂O (100 ppm active **chlorine**). The samples incubated in water and chlorine were incubated either still (**A**) or shaken (**B**) on a mini orbital shaker for the duration of the incubation. Ascorbate was extracted from the samples (1 g leaves in 5 ml 0.5% formic acid) and the ascorbate level was determined by DCPIP titration method. **Time 0** samples were assayed at the start of the experiment. Each bar represents the mean of three individual samples \pm SE. Different letters above the bars in **B** represent statistically significant differences (Student's t-test, $p < 0.05$, $n = 3$). There was no significant difference between any of the samples in **A** (Student's t-test, $p > 0.05$, $n = 3$).

statistically significant in this experiment, but the difference between time 0 and the leaves shaken in chlorinated water was significant (Student's t-test, $p < 0.05$; Figure 88 B). The difference between leaves incubated in shaken non-chlorinated water versus shaken chlorinated water was not significant. This suggests that there is no difference in ascorbate levels in spinach washed in chlorinated or non-chlorinated water.

3.6.4 Ascorbate retention in different ages of salad leaves

Various different cultivars of spinach are used by Vitacress, and the harvest time of these cultivars differs. Two late-stage and two early-stage cultivars (pictured in Figure 89 B) harvested and the ascorbate content was monitored throughout storage. As would be expected, the leaves harvested during late stage were larger than those harvested during the early stage.

The initial ascorbate concentration of late stage spinach cultivars was marginally greater than that of early stage spinach leaves (Figure 89 A). However, the loss of ascorbate occurred more quickly in late stage spinach, with early stage spinach retaining more ascorbate over the 10-day storage period. After 3 days of storage the late stage spinach had lost the majority of its ascorbate, whereas the early stage spinach still retained more than half of the initial level of ascorbate.

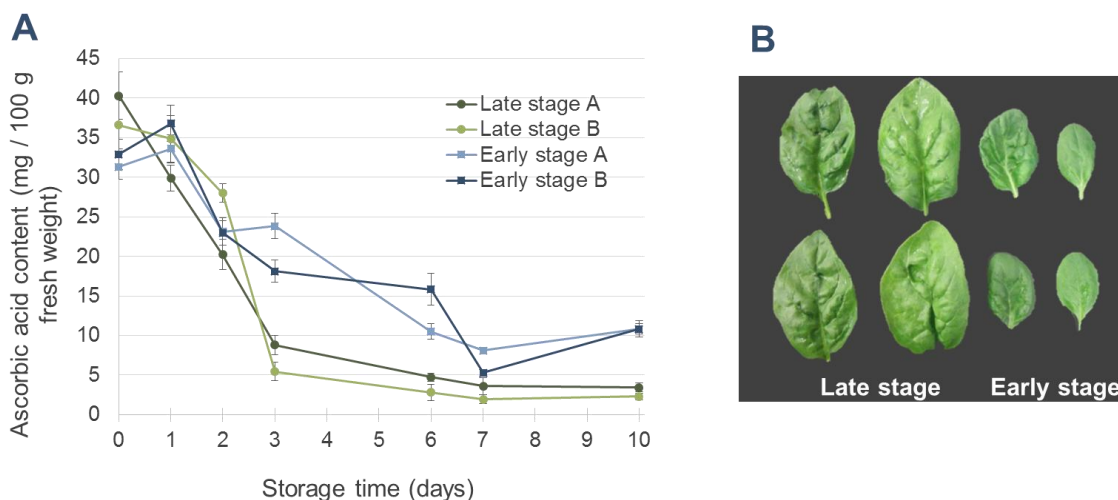


Figure 89: Ascorbic acid content in spinach at different growth stages. Two varieties of late stage spinach and two of early stage spinach (harvested from a farm that supplies Vitacress) were stored in the dark at 4°C for up to 10 days. At time intervals ascorbate was extracted from samples in 2% MPA, and the ascorbate content determined by the DCPIP titration method (A). Each point represents the mean of three individual samples of each variety ($n=3$, \pm SE). B shows the spinach leaves on day 0 of storage.

In conclusion, spinach leaves are more susceptible to ascorbate loss during the washing process than watercress or rocket leaves. The loss of ascorbate during the washing of spinach leaves seems to be due to the turbulent nature of the washing procedure, rather than merely submersion in spring water. Radiolabelled tracer experiments demonstrated that the major ascorbate degradation product formed during spinach washing was OxA, which is formed via oxidation reactions (section 3.3). Washing spinach leaves in spring water, as is the case at Vitacress, could reduce the ascorbate loss during washing when compared to washing in chlorinated water.

3.6.5 Degradation of ascorbate in watercress

Watercress has relatively high levels of ascorbic acid (Figure 80) but loses it substantially throughout storage (Figure 82 B).

The effect of the growth stage on the ascorbate content of watercress was investigated. Vitacress grows watercress from seedlings. These seedlings are planted in water beds and the mature watercress is generally harvested three weeks after planting. Seedlings are planted every week throughout the summer, meaning there was a variety of ages of watercress at any one time. For this experiment samples of various ages of watercress were taken (pictured in Figure 90 B and C). All these samples were taken at the same time, so were planted weeks apart. All the plants were stored in plastic bags at 4°C for the duration of the experiment (10 days). The ascorbate content of the watercress was assayed at various points throughout the storage time (Figure 90). After 10 days the watercress leaves showed signs of damage, including bruising and a loss of colour (Figure 90 C compared to B).

The ascorbate content varied with growth stage, with the 3-week old watercress showing the highest ascorbate levels over the 10 days' storage (Figure 90A). This suggests that the current practice of harvesting watercress at three weeks after planting is the optimum in terms of ascorbate content.

In general terms, the younger watercress (seedlings and 1 week and 2 weeks old) had lower ascorbate than the older watercress, 3 and 4 weeks old (Figure 90 A). In all the ages the ascorbate content remained fairly stable for the first 3 days of storage, before declining over the following 7 days.

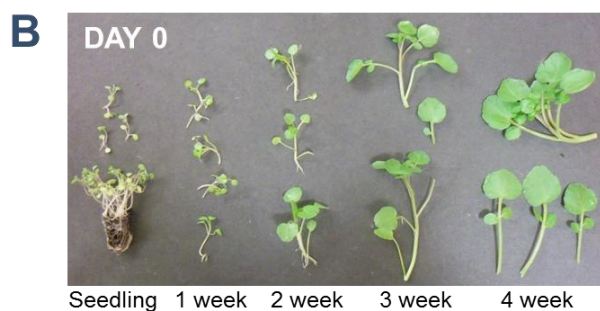
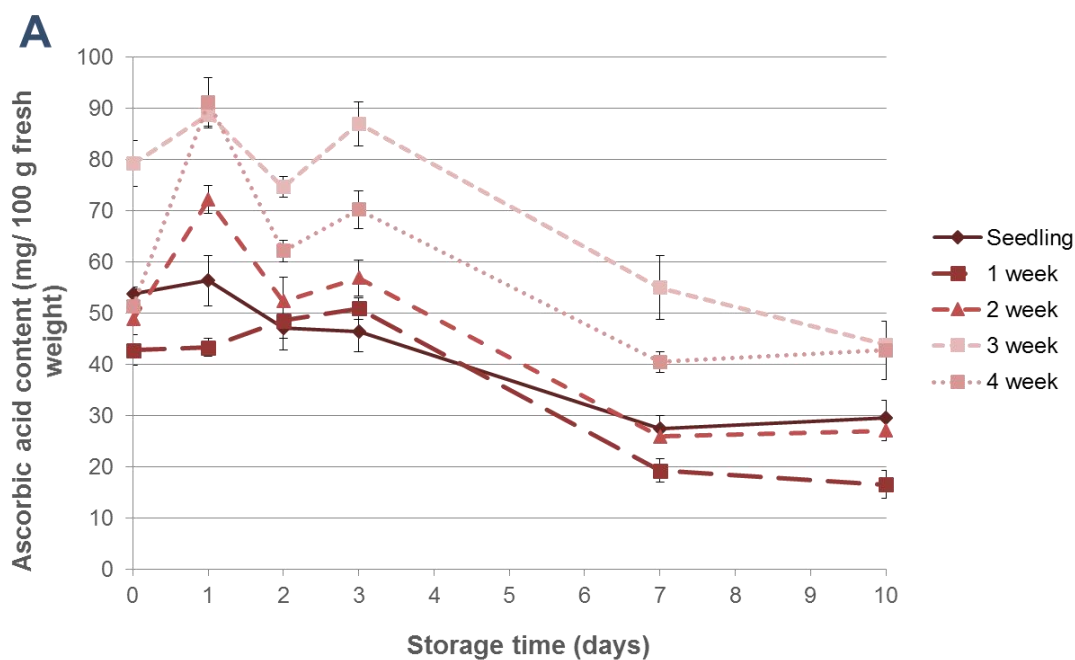


Figure 90: Ascorbic acid content of watercress at different growth stages. Various ages of watercress (seedling, 1 week, 2 weeks, 3 weeks and 4 weeks after planting) were stored in plastic bags in the dark at 4°C for up to 10 days. Examples of the watercress leaves are pictured on day 0 (**B**) and day 10 (**C**) of storage. At time intervals ascorbate was extracted from samples in 2% MPA, and the ascorbate content determined using the DCPIP titration method (**A**). Each point represents the average of three individual samples \pm SE.

Extracts of each age of watercress after 0 or 10 days' storage were run by HVPE at pH 2.0 (Figure 91). A compound with the same mobility as DKG was seen in all the samples, and at higher levels (as seen by the larger, more intense spot) in the older plant extracts. Compounds with similar mobilities to compounds C and E (discussed in section 3.1) were also present. Glc-6-P has the same mobility as compound C in this system, so it is possible that the spot running with compound C in the samples could also include Glc-6-P. However, when the samples were treated with a phosphatase prior to running by HVPE, the spot was still present, suggesting that this compound was not Glc-6-P (Figure 92).

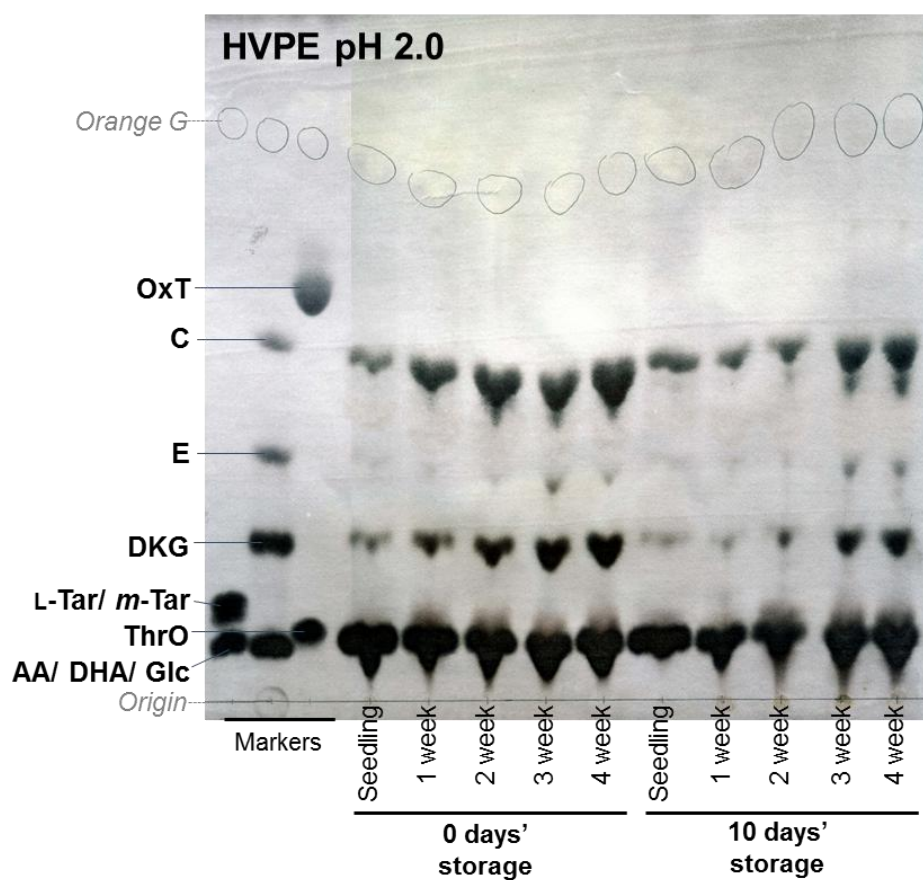


Figure 91: HVPE analysis of extracts from various growth stages of watercress. Extracts (100 μ l, in 0.5% oxalic acid, 5 ml per g FW) of the samples of various growth stages of watercress after 0 or 10 days of storage at 4°C, described in figure 11, were run by HVPE at pH 2.0. Compound C co-migrates with Glc-6-P (Figure 92), so the spot containing compound C also represents the position of Glc-6-P. The paper was then stained in silver nitrate. The position of the internal marker of orange G was marked with pencil circles.

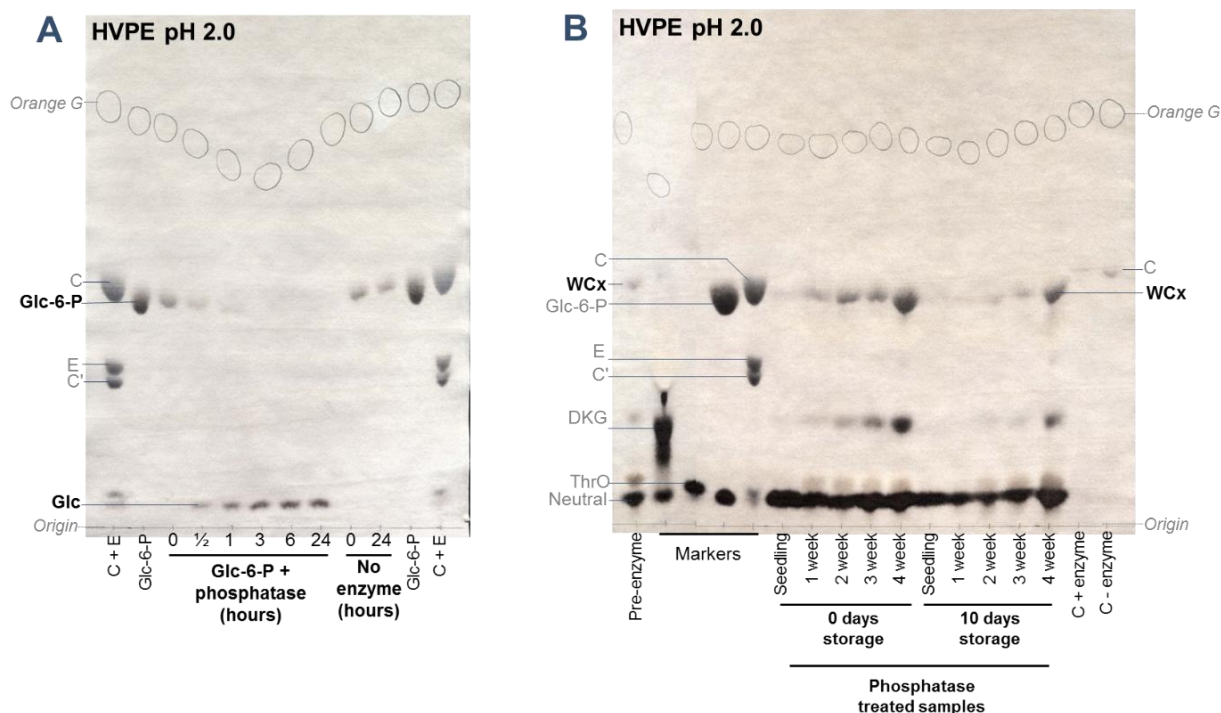


Figure 92: The compound co-migrating with Glc-6-P does not diminish upon phosphatase treatment. Samples of watercress extracts in 0.5% oxalic acid (adjusted to pH 5 with $\text{Ca}(\text{OH})_2$) were treated with phosphatase for 16 hours (B). The 'pre-enzyme' sample consists of an extract of 4 week watercress after 0 days of storage, without the addition of phosphatase. Samples of compound C with and without the phosphatase were also included. A positive control of Glc-6-P was incubated with the phosphatase for up to 24 hours (A) was also run. Samples were taken at time intervals and the reaction stopped with the addition of formic acid. The samples were run by HVPE at pH 2.0 and the papers stained in silver nitrate. C and C' are epimers of compound C (2-carboxy-l-xyloxolactone and 2-carboxy-l-lyxonolactone, discussed in section 3.1). The loading of the pre-enzyme samples was lower (half as much), so the spots are fainter, than the loadings of the phosphatase treated sample.

A selection of watercress samples (1 and 4 weeks old, after 0 and 10 days' storage) were run by HVPE at pH 6.5, and stained in either silver nitrate, to detect sugar-like compounds, or molybdate, to detect phosphorylated compounds (Figure 93).

The silver nitrate stained paper shows an unknown compound (referred to as WCx) running below orange G (labelled with WCx). The mobility of WCx shows that it has a lower charge : mass ratio than ascorbate. This could be achieved by being larger than ascorbate, maybe a di- or trisaccharide with a single negative charge.

WCx appears diminished after 10 days of storage, seemingly almost completely in the 1 week-old watercress, and partly in the 4 week-old samples (Figure 93). This suggests that this compound could potentially be used as an indicator of freshness of watercress

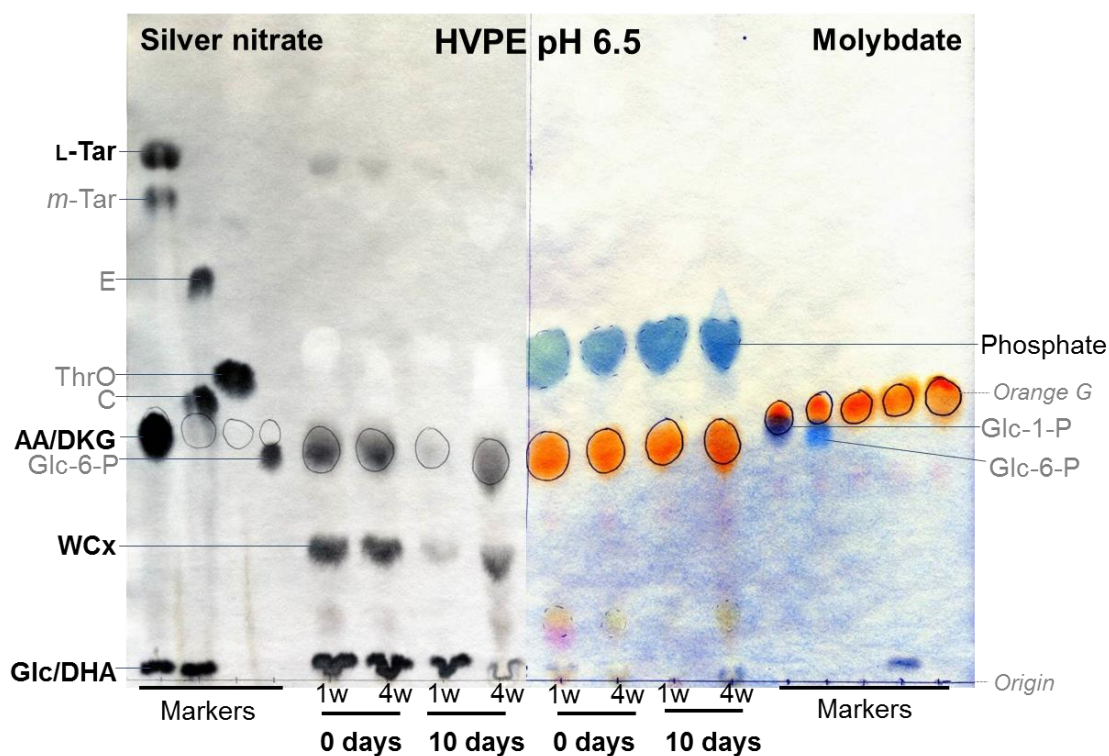


Figure 93: Analysis of a watercress extract by HVPE at pH 6.5. Samples of watercress extract (in 0.5% oxalic acid), from 1 week (1w) or 4 weeks (4w) after planting, stored for either 0 days or 10 days, were run by HVPE at pH 6.5. Duplicates of each sample were run and the paper cut in half after HVPE. One half of the paper was stained in silver nitrate and the other in molybdate. The position of the internal marker orange G was marked with pencil circles.

The silver nitrate stain (Figure 93) also shows a spot with the same mobility as L-Tar. This is known to be a degradation of ascorbate and to accumulate in certain plant species (76). The presence of L-Tar was less clear after HVPE at pH 2.0 (Figure 91) though there was a compound visible migrating just above the neutral compounds, which could potentially be identified as L-Tar. The large amount of neutral compounds present in the samples could have partially obscured the relatively low level of L-Tar present (as indicated by the fairly faint spot in Figure 93), as it migrates only slightly further than neutral compounds.

The silver nitrate stained spot running with orange G (Figure 93) is likely to contain DKG, as this compound was visible after HVPE at pH 2.0 (Figure 91). The spot could also contain ascorbate, as these two compounds have an identical mobility at pH 6.5. Ascorbate would be indistinguishable from neutral compounds by HVPE at pH 2.0.

There are no compounds visible in the region that compounds C and E would be expected to be migrating to, with m_{OG} values of 1.05 (compound C) and 1.32 (compound E) at pH 6.5. This suggests that the compounds visible co-migrating with C and E after HVPE at pH 2.0 (Figure 91) are not in fact compounds C and E. These unknown compounds co-migrating with compound C and E must have a very low pKa to migrate so quickly at pH 2.0.

An extract of watercress known to contain WCx (4-week grown watercress, 0 days storage)

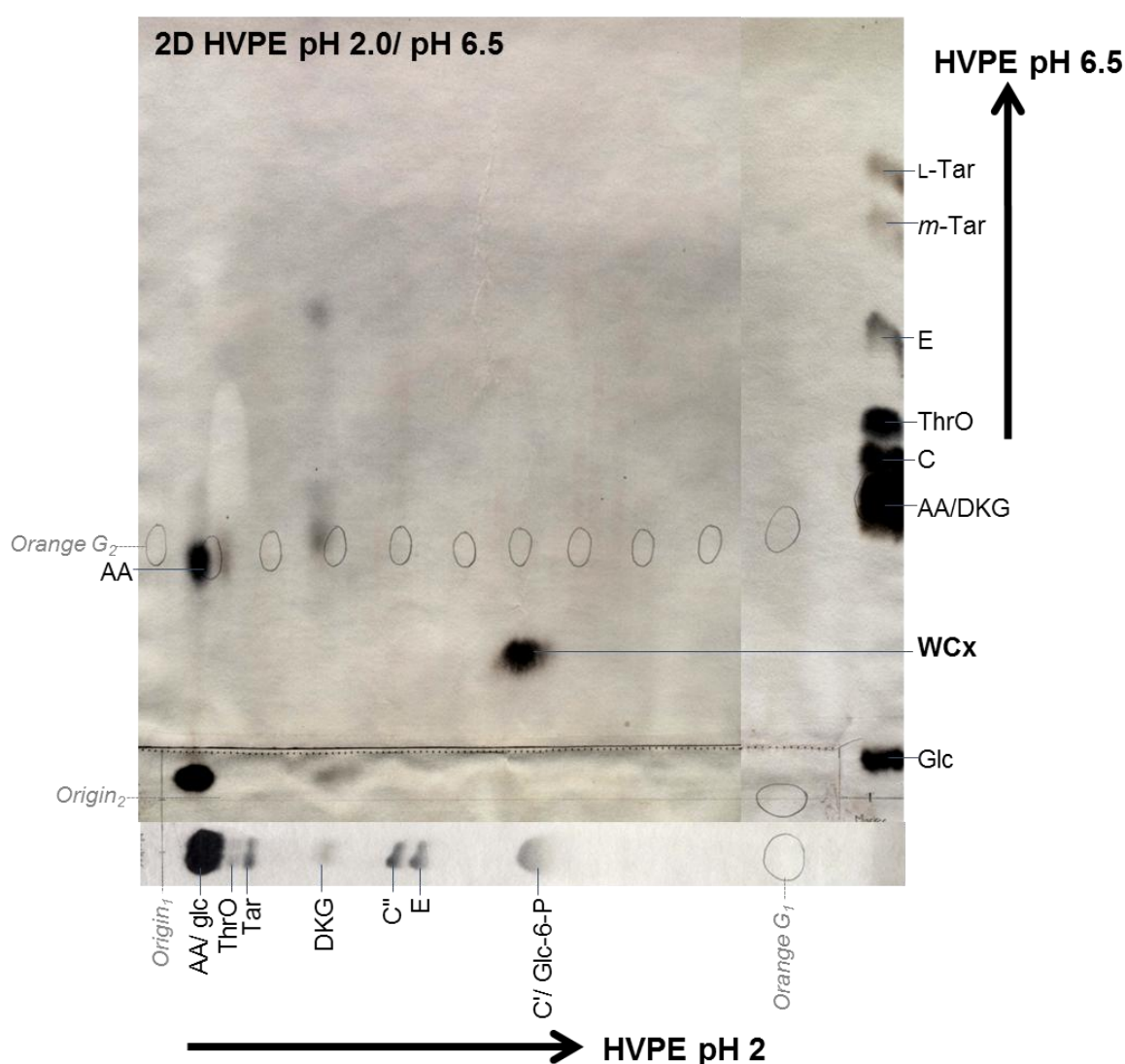


Figure 94: 2D HVPE of a watercress extract. An extract (in 0.5% oxalic acid) from 4-week-old watercress, stored for 0 days was run by HVPE at pH 2.0. The lane containing the watercress sample was carefully cut out and sewn onto the origin of a fresh sheet of paper. A lane containing markers was stained in silver nitrate. The new paper, including a lane containing markers, was run by HVPE at pH 6.5. The new paper was stained in silver nitrate. The position of the new origin and orange G after the first run at pH 2.0 are marked with '1' and their positions after the second run at pH 6.5 are marked with '2'.

was subjected to 2D HVPE at pH 2.0 followed by pH 6.5 (Figure 94).

The 2D HVPE showed that the unknown compound (WCx) detected after HVPE at pH 6.5 is the compound that co-migrates with compound C and Glc-6-P in HVPE at pH 2.0 (Figure 94). This serves as further evidence that this compound is not compound C.

The spot corresponding the DKG after HVPE at pH 2.0, shows the migration expected for DKG at pH 6.5 too, providing further evidence that this compound can be identified as DKG, the hydrolysis product of DHA. Compounds C and E can be seen in the lane containing DKG after HVPE at pH 6.5. As these compounds had not separated from DKG during HVPE at pH 2.0, it is assumed that they have been produced on the paper in the time between running at pH 2.0 and running at pH 6.5, and did not originate from the watercress sample itself.

The presence of L-Tar after 2D HVPE was unclear. The region where L-Tar would be expected to be, the top left-hand side of the paper, does not clearly show a distinct spot. However, the level of L-Tar present was fairly low (as in Figure 93), and there is a pale streak visible in the lane where L-Tar would be expected (Figure 94) which could potentially have caused the distortion of any L-Tar present.

3.6.6 Characterisation of WCx, a compound from watercress that indicates freshness

Further characterisation of WCx required the scaling up and purification of the compound. Watercress purchased from the supermarket was used to achieve this. Interestingly, WCx was not present in watercress that was grown in Portugal (Figure 95 C and D). Vitacress imports salads from Portugal during the winter months.

The watercress grown in Portugal is the same variety as that grown in UK, but the Portuguese-grown watercress is then transported to the UK by road, meaning that the leaves could have been harvested more than a week before arriving in the supermarket, compared to just a couple of days with the UK-grown watercress. This further supports the usefulness of this compound as an indicator of freshness, or time since harvesting. WCx was present in watercress obtained directly from farms in Hampshire that had not been through the washing process in the factory (as in Figure 91 and Figure 93) as well as in watercress purchased from the supermarket, that had been grown in UK and had undergone the washing process

(Figure 95 A and B).). It was also present in wild watercress collected from a stream in the Pentland Hills, near Edinburgh (Figure 95 A and B).

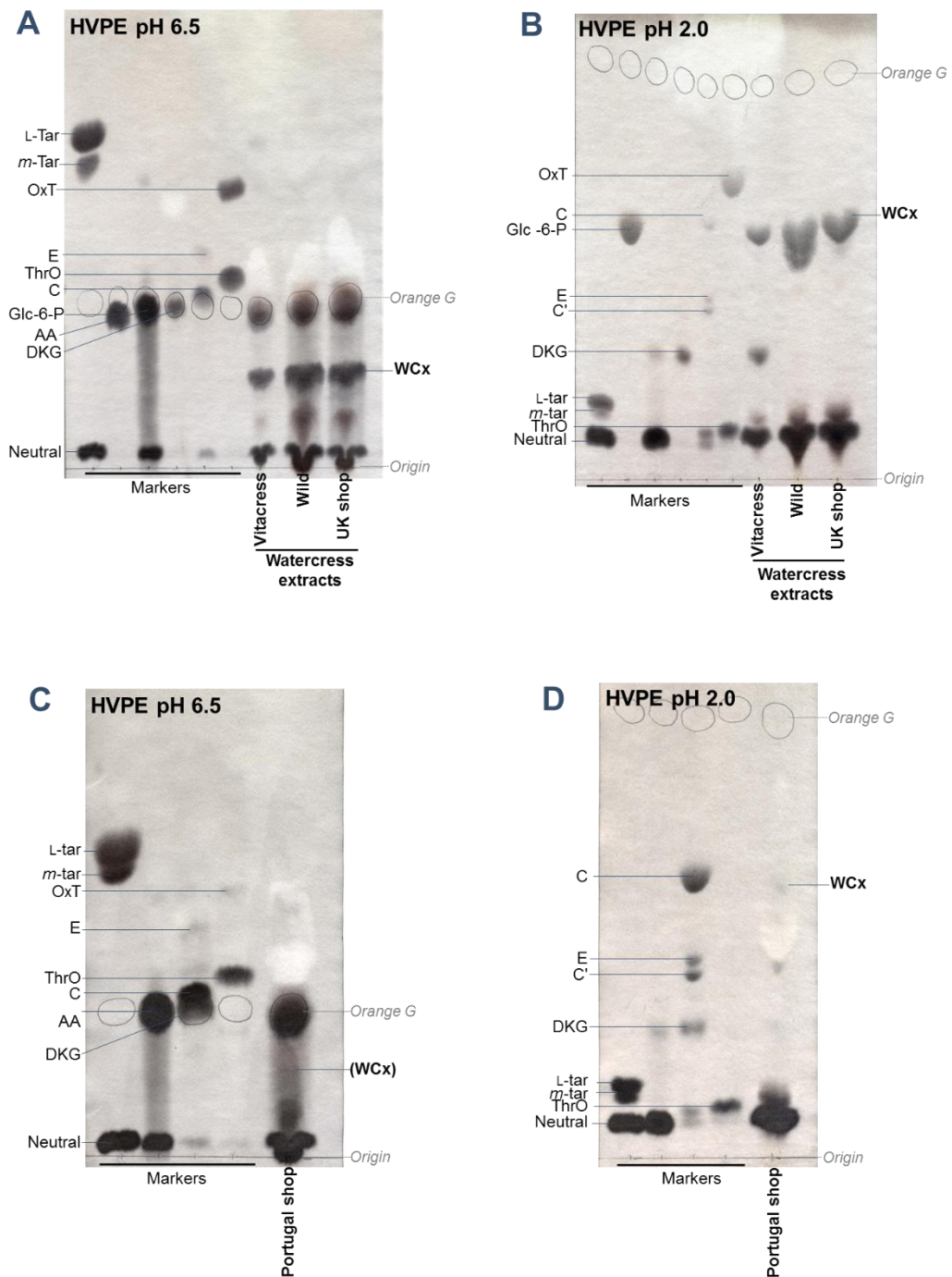


Figure 95: WCx is present in UK-grown watercress extracts but not Portuguese-grown watercress extracts. Extracts of watercress in 0.5% formic acid (1 g in 5 ml) were taken from unwashed watercress harvested from **Vitacress**, **wild** watercress harvested from a local stream, and watercress purchased from a local supermarket, that was grown in the UK (**UK shop**). Samples (100 μ l) were run by HVPE at pH 6.5 (**A**) and pH 2.0 (**B**). Extracts of watercress purchased from a local supermarket that was grown in Portugal was also analysed by HVPE at pH 6.5 (**C**) and at pH 2.0 (**D**). All the papers were stained in silver nitrate and the position of the internal marker orange G was marked with pencil circles.

The compound of interest (WCx) was purified by preparative HVPE from both wild watercress and UK-grown shop-bought watercress. The compound was eluted from paper, and re-run analytically by HVPE to ensure the purity of WCx (Figure 96). Silver nitrate staining revealed the purified preparations of WCx to be relatively pure and free of other compounds.

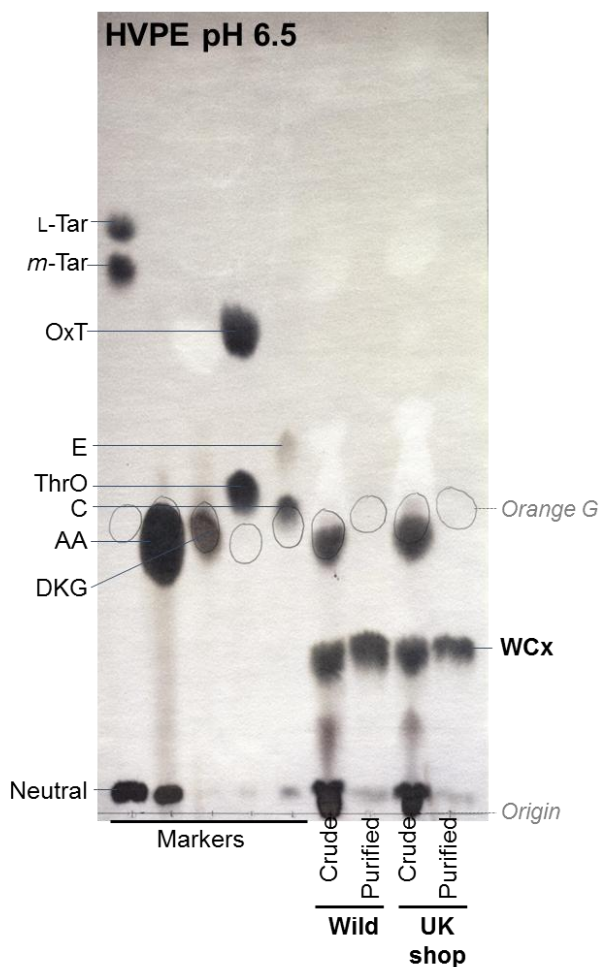


Figure 96: HVPE of purified WCx. Samples of watercress extract (in 0.5% formic acid) were run preparatively by HVPE at pH 6.5. The position of WCx was determined by the use of silver nitrate stained marker lanes, and the WCx was eluted from the paper in water. Samples of the crude extract and of the purified WCx from both wild watercress and shop-bought watercress, grown in UK were run by HVPE at pH 6.5. The paper was stained in silver nitrate and the position of orange G marked with pencil circles.

Samples of the purified WCx were run analytically by HVPE in pH 6.5 and pH 2.0 and stained in both silver nitrate and Wilson's dip (Figure 97). Wilson's dip stains reducing sugars, and a non-reducing, so non-staining, marker of Lb acid (lactobionic acid, a disaccharide of galactose and gluconic acid) was included (blank lanes labelled Lb acid in the markers sections, Figure 97). Wilson's dip did not stain WCx (as seen by the blank lanes labelled WCx stained in Wilson's dip in Figure 97). This shows that WCx is not a reducing sugar.

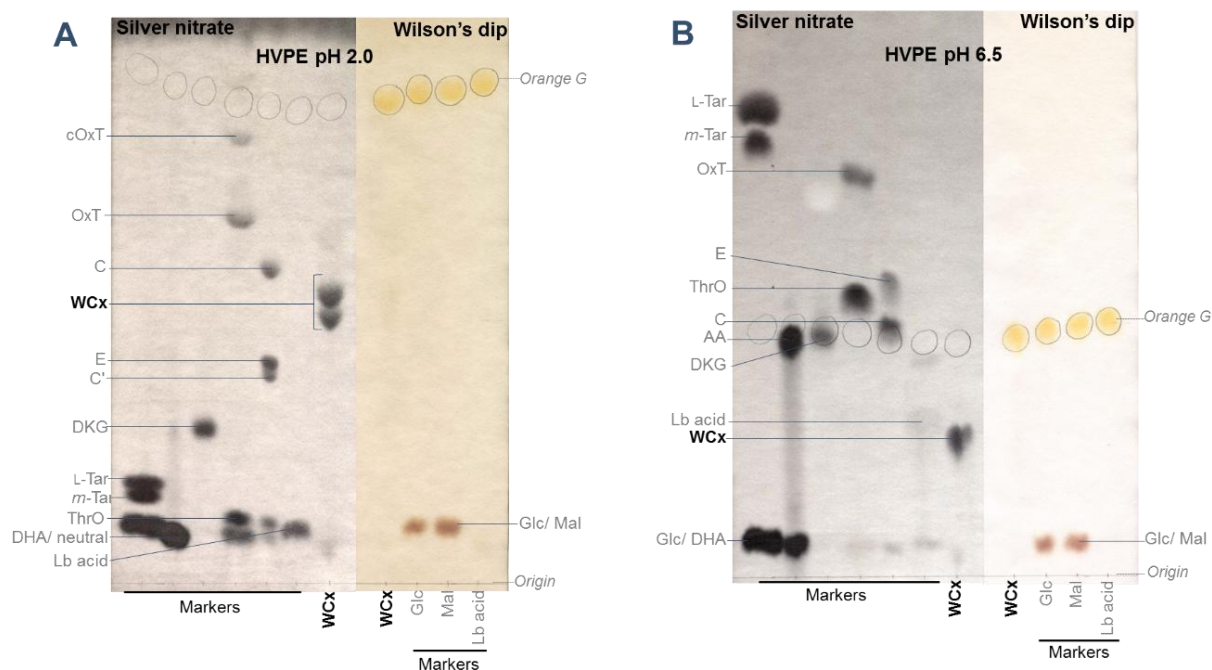


Figure 97: Wilson's dip staining of WCx. Purified (as described in Figure 96) samples of WCx (from shop-bought watercress) were run by HVPE at pH 2.0 (A) and at pH 6.5 (B). Duplicate samples of WCx were loaded onto each paper. One section of each paper was stained in silver nitrate, and the other section in Wilson's dip. The position of the internal marker orange G was marked with pencil circles. Mal=maltose and Lb acid=lactobionic acid.

HVPE at pH 2.0 revealed that the sample of WCx contained two distinct compounds, as seen by the two silver nitrate stained spots (Figure 97 A). The spot corresponding to WCx on the paper run by HVPE at pH 6.5 appears to show just one silver nitrate stained spot (Figure 97 B). However, HVPE at pH 6.5 was run for a shorter time than HVPE at pH 2.0. A sample of WCx was run by HVPE at pH 6.5 for a longer time to allow the potential two compounds the greatest chance to separate. Two distinct compounds were seen after an extended run by HVPE at pH 6.5 (Figure 98). The mobility of these compounds remains the same when run at pH 2.0 and pH 6.5, with m_{OG} values of 0.53 and 0.57.

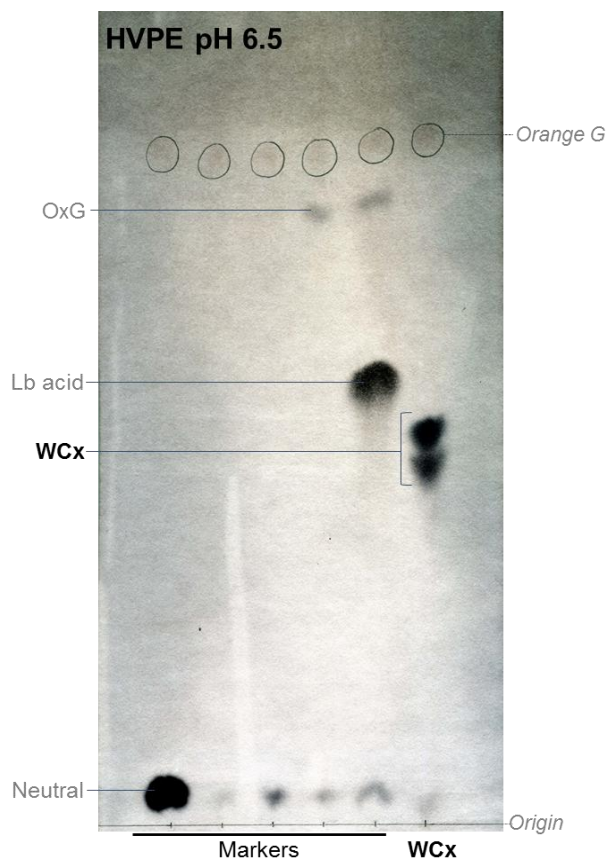


Figure 98: WCx separates into two compounds after HVPE at pH 6.5. WCx was purified from an extract of wild watercress by preparative HVPE followed by elution from the paper in water. A sample of purified WCx was run by HVPE at 6.5 for an extended length of time, until the internal marker of orange G (marked with pencil circles) had travelled $\frac{3}{4}$ the length of the paper. The paper was then stained in silver nitrate.

The negative charge of WCx was due to the presence of an acidic group, such as an oxalyl or sulphate group, which could be bound to a sugar moiety via an ester bond. Ester bonds are unstable in alkali, so in order to test for the presence of an ester bond within the compound, WCx was treated with NaOH, and the products analysed by HVPE at pH 2.0 (Figure 99).

Staining in silver nitrate revealed that WCx was diminished upon NaOH treatment, but not in the control treated with HOAc. Intriguingly, there were no obvious silver nitrate stained spots present in the lane containing the sample treated with NaOH to indicate what WCx had broken down into. Interestingly, the faster moving WCx spot (*mOG* of 0.57) seemed to remain stable in the presence of HOAc, whereas the slower moving compound (*mOG* of 0.53) had vanished upon HOAc treatment.

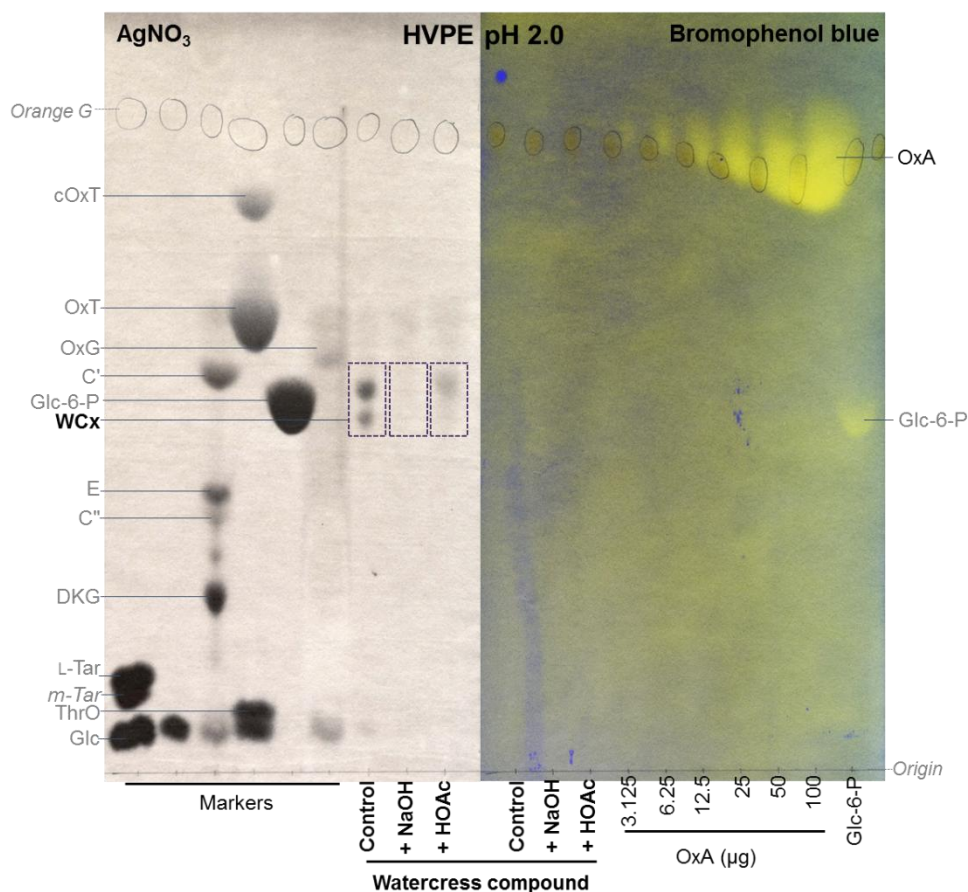


Figure 99: Saponification of WCx. Purified WCx samples were incubated with NaOH (0.1 M), HOAc (0.2 M) or neither (control) for 16 hours at 20°C. The samples were neutralised before running by HVPE at pH 2.0. Duplicate samples were loaded onto the paper. One half of the paper was stained in silver nitrate, and the other half in bromophenol blue. The position of orange G was marked with pencil circles.

Duplicate samples of WCx were stained in bromophenol blue, a pH indicator in which acidic compounds would be visible as yellow spots, as seen by the markers of OxA and Glc-6-P (Figure 99). No acidic compounds at all in any of the WCx samples (either the control or the NaOH and HOAc treated samples) were detected using this stain. It is possible that the

bromophenol blue stain was not sensitive enough to detect any acidic moieties present in the WCx samples, although OxA was detectable down to 3.125 µg.

Purified samples of WCx were run by TLC and stained in a selection of reagents (Figure 100). Molybdate is a general stain, and sensitive to most functional groups, whereas thymol stains sugars. A band from WCx was visible on the TLC sections stained in molybdate and thymol (labelled WCx a; Figure 100). Interestingly, staining in ninhydrin revealed a band at a different position (labelled WCx b), suggesting that one of the compounds contains an amine group. A band at the corresponding place in the TLC sections stained in thymol and molybdate was not present.

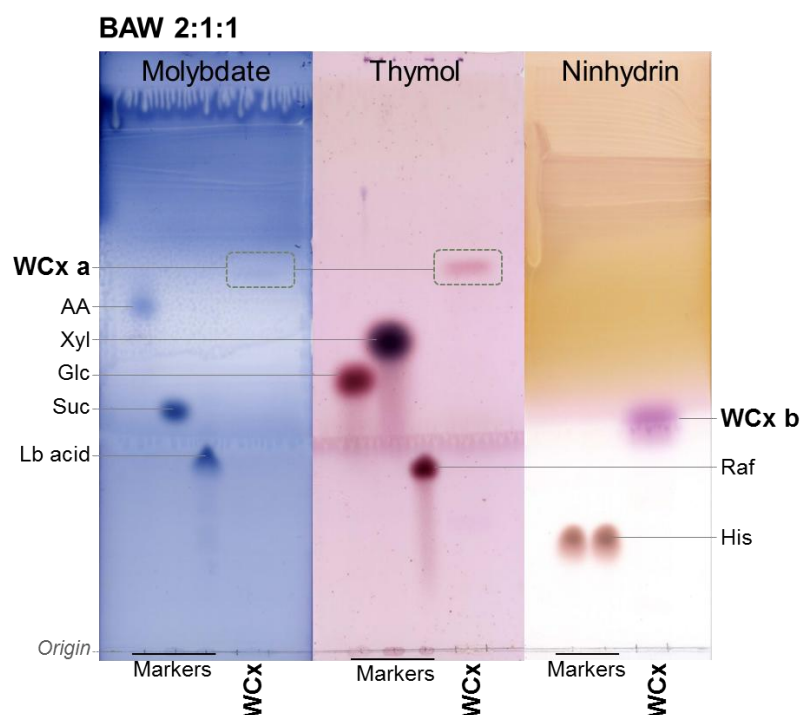


Figure 100: TLC analysis of WCx stained in thymol, molybdate and ninhydrin. Purified samples of WCx (10 µl) were loaded onto a silica-gel TLC plate. The TLC plate was developed in a solvent containing BuOH:HOAc:H₂O (in a ratio of 2:1:1). The plate was then sliced into three sections, each containing WCx and a selection of marker compounds. One section of the plate was stained in molybdate, one in thymol and one in ninhydrin.

WCx (purified by preparative HVPE and subsequently eluted from the paper in EtOH) was analysed by negative ion electrospray mass spectroscopy. The spectrum obtained contained numerous peaks with *m/z* values ranging from 311.2 to 492.1 (Figure 101). The number of peaks in this spectrum could be due to contaminating compounds present in the sample, for

instance compounds from the paper that were co-eluted with WCx. The numerous peaks could also represent fragments of WCx that have been broken down either during extraction from watercress itself, or during the analysis.

In terms of the elemental make-up of WCx, previous experiments have demonstrated that the compound(s) contain a sugar-like moiety, as deduced by staining in silver nitrate and thymol, and perhaps the presence of an amine group in one WCx compound, as demonstrated by staining with ninhydrin. Although WCx is known to be an acidic compound (evidenced by its mobility during HVPE), staining with bromophenol blue did not reveal any acidic moieties. However, the loading could have been below the level of detection for this stain.

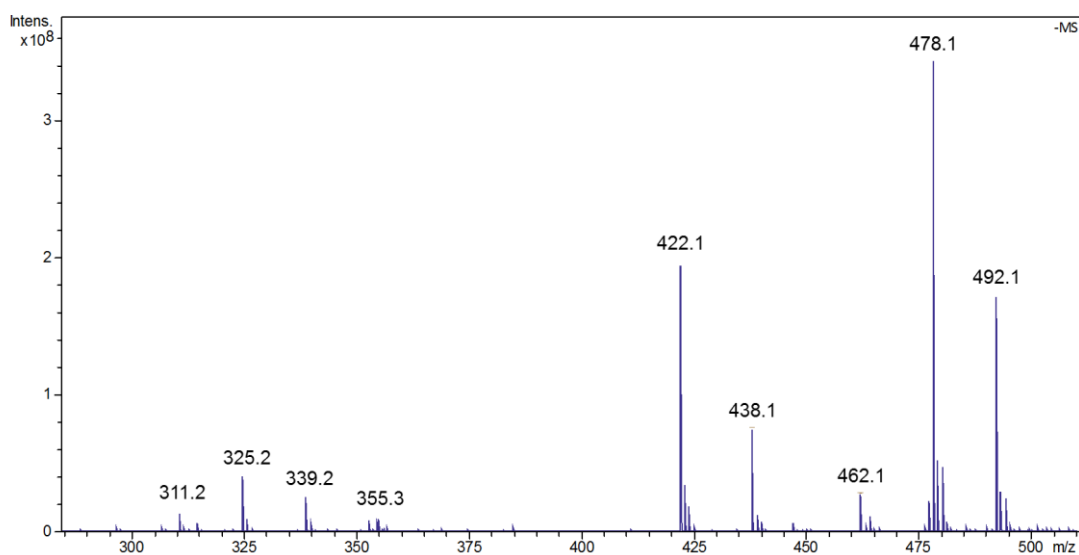


Figure 101: MS analysis of purified WCx. A sample of WCx, purified by preparative HVPE at pH 6.5, followed by elution from paper in EtOH, was analysed by negative ion electrospray mass spectroscopy. The m/z value for each peak is displayed.

Watercress, among other members of the Brassicaceae, is known to contain high levels of glucosinolates. These are a group of organic compounds containing a glucose moiety, linked to a sulphate group via sulphur and nitrogen (Figure 102) (273). One possible identity of WCx, from numerous other possibilities, could maybe be a glucosinolate; the sulphate group present in glucosinolates could account for the mobility of WCx when analysed by HVPE.

Glucosinolates are known to degrade into isothiocyanate compounds, catalysed by the enzyme myrosinase (274). There are hundreds of glucosinolates and related compounds already identified from plants (274,275). The most common glucosinolate in watercress seeds, though not necessarily leaves, is gluconasturtiin (276), so-called because of its initial discovery in watercress (*Nasturtium officinale*).

The mass of gluconasturtiin (Figure 102 C) is 423, so the peak with an m/z value of 422 (Figure 101) could potentially correspond to this compound (277). The peak at 438 (Figure 101) could maybe be attributable to glucobarbarin (278) (Figure 102 B), another glucosinolate known to be present in samples of watercress (279), although this glucosinolate is less common than gluconasturtiin, so glucobarbarin is not very likely to be present at high levels in WCx, if at all. Glucobarbarin differs from gluconasturtiin by a mass of 16, corresponding to the replacement of a hydrogen with a hydroxyl group (Figure 102).

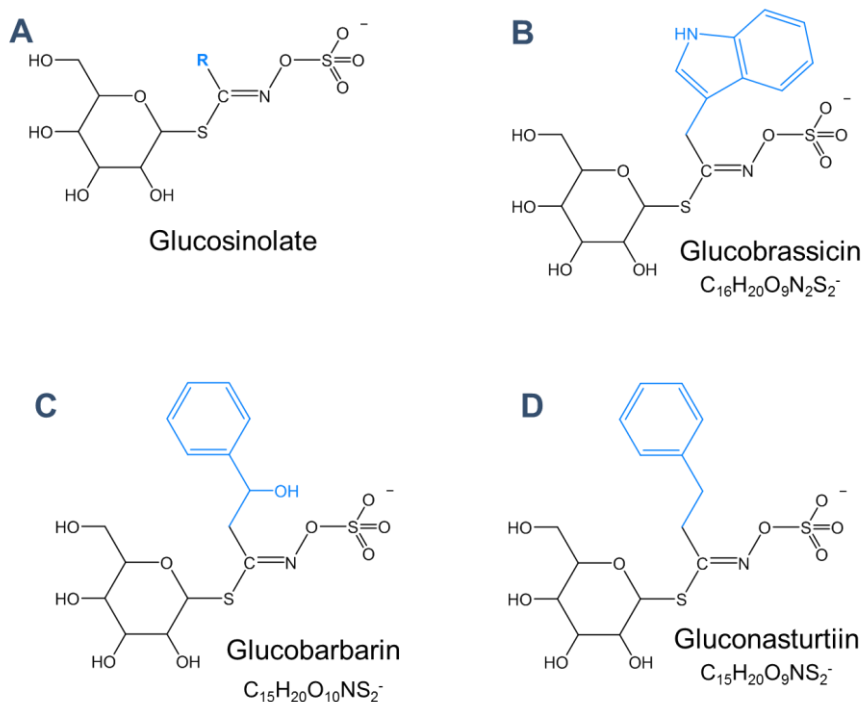


Figure 102: Structures of glucosinolates. The general structure of glucosinolates is shown (A) with R representing a variable side chain. The structures and chemical formula of three glucosinolates, glucobarbarin (B), gluconasturtiin (C) and gluconasturtiin (D) are shown, with the side chains indicated in blue.

The rest of the peaks present on the spectrum (Figure 101) did not correspond to any reported m/z values for compounds isolated from watercress, including other glucosinolates such as glucobrassicin (Figure 102 B), which has a mass of 448, so an expected m/z value of 447.

TLC analysis of WCx revealed a compound containing an amine group, which resolved from a compound containing a sugar group (Figure 100). Glucobrassicin contains an amine group, which would be visible when stained with ninhydrin (Figure 102 B). There is a small possibility that WCx contained a compound derived from glucobrassicin. Derivatives of glucobrassicin are known from watercress, such as 4-methoxy-glucobrassicin and 4-hydroxy-glucobrassicin, with predicted m/z values of 477 and 464 respectively (280). Although neither of these compounds correspond with the m/z values obtained during MS analysis (Figure 101), it is possible that WCx contains a compound related to glucobrassicin, which was able to be stained by ninhydrin. Equally, the ninhydrin stained spot after TLC could correspond to a completely different compound containing an amine group and not be a glucosinolate at all.

Previous studies reported a glucosinolate compound from another member of the Brassicaceae (woad, *Isatis tinctoria* L.) that had the same mobility after HVPE at both pH 7.0 and pH 2.0 (281), much like the compound(s) currently studied, albeit at pH 6.5 and pH 2.0. Several glucosinolate compounds isolated from *Redea media*, also a member of the Brassicaceae, were found to migrate towards the anode during HVPE at pH 6.5, and were detected by silver nitrate staining (282), similarly to WCx.

To summarise, watercress has high levels of ascorbate, but this diminishes relatively quickly upon post-harvest storage, including undergoing hydrolysis to DKG via DHA, as detected by silver nitrate staining after HVPE.

An unknown compound(s) (WCx) of high abundance in fresh watercress samples, but which diminishes upon storage and was absent from imported watercress, could serve as an indicator of freshness. Further analysis of WCx hinted to the possibility that it could be a glucosinolate-related compound. This is supported by the electrophoretic mobility of WCx, as well as its ability to be stained in silver nitrate, thymol and ninhydrin. The m/z values obtained from MS analysis suggest that WCx may include gluconasturtiin and glucobarbarin (although this is fairly unlikely to be present at such high concentration), and potentially further as yet unidentified glucosinolate-related compounds. Alternatively, WCx may not be a glucosinolate compound at all, but it could belong to a completely different class of

compounds. Further experiments would be needed to before making any conclusive statements about the identity of WCx. NMR analysis of the compounds was attempted, but the preparation proved too impure, so no meaningful data could be obtained (data not shown).

Discussion

4.1 Overview

Ascorbate is a very well-known and much studied compound, but the degradation pathways of this important antioxidant have yet to be fully elucidated. In-depth knowledge of the degradation pathways of ascorbate is vital, as there is much interest in increasing vitamin C content of foods (283), and this could be achieved by preventing its degradation. Furthermore, several derivatives of AA have been detected but have yet to be identified, and some of these, such as PxI (discussed in the current study), which has been shown to inhibit peroxidase activity (84), have been shown to have important biological roles. It is plausible that other AA derivatives are also biologically relevant, for instance the potential role of OxT and cOxT in the modification of cell wall components and sugars has been reported in the current study.

This project has added valuable knowledge on ascorbate degradation, including the characterisation and identification of previously uncharacterised compounds. More in-depth information about the oxidation pathways of DHA and DKG with a variety of different ROS has also been gained. A novel enzyme activity involving the transfer of oxalyl groups from OxT, a major oxidation product of both DHA and DKG, to sugar acceptor substrates has been identified, as well as the addition of oxalyl groups to cell wall material *in vivo*.

In addition to this, the degradation of ascorbate has been monitored in salad leaves throughout the industrial washing process and subsequent post-harvest storage. Spinach leaves were more susceptible to the loss of ascorbate than other leaves tested, and certain stages of the washing process were found to cause significant ascorbate loss. This is of commercial interest, as ascorbate has been reported to have numerous health benefits (reviewed in (13) and (284)), and so increasing the vitamin C content of salads is desirable. Increasing the ascorbate content of salads could be achieved by increasing the biosynthesis or decreasing the catabolism of ascorbate. This could be achieved by genetic modification, but the commercial production of genetically modified crops is not currently permitted in the UK. Therefore, altering either growth conditions or post-harvest processes represent a more feasible means of increasing ascorbate content of salads. The current study focussed on the degradation of ascorbate during post-harvest processing and storage of salads, with the aim of identifying particular processes contributing to the degradation of ascorbate, which could be altered in future to reduce this loss within salads.

The plant apoplast is an oxidising environment, and the site of production of H₂O₂ from numerous sources, including NADPH oxidases. This H₂O₂ may require detoxification to protect the plant cell, and ascorbate as the predominant low-molecular weight antioxidant present in the apoplast acts to do this. The present study has added valuable knowledge of the oxidative pathways of AA degradation products DHA and DKG under apoplastic conditions in the presence of various different ROS, which could be present in the apoplast. A signature of AA oxidation products for each different ROS has been described, potentially allowing the deduction of the major ROS acting to oxidise DHA or DKG. The major product detected was OxT, which has previously only been demonstrated to occur in the apoplast of rose cell-suspension culture, whereas in this study it was detected *in planta*, in spinach leaves, for the first time. Oxidative pathways were found to predominate, compared to hydrolysis, during the commercial washing of salad leaves, with the oxidation product OxA being the major product from the loss of AA. Mechanical stress, leading to oxidation was found to be a major contributor to the loss of AA during the industrial washing process, therefore a more gentle approach to washing salad leaves, especially spinach, would be advised.

The current study has also described a biological role for OxT; a novel acyltransferase activity localised to the cell wall was found to transfer the oxalyl group from OxT to sugar compounds such as glucose, and could potentially have a role in the modification of cell wall components by adding oxalyl side-groups.

As well as oxidation, DHA can also undergo hydrolysis, initially forming DKG. DKG can then be further degraded, under non-oxidative conditions to form newly identified compounds carboxy-l-xylonate and carboxy-l-xylonolactone. Although these compounds have been demonstrated to be formed *in vivo*, they do not serve an obvious biological role, and remain in the apoplast.

Overall this study has added valuable knowledge on the degradation of AA in the apoplast and whole salad leaves, and highlighted novel enzyme activities associated with AA degradation products.

4.2 The oxidation of DHA and DKG

The initial degradation steps of AA, oxidation to DHA and subsequent hydrolysis to DKG, are well characterised (33,71,253). However, the further oxidation of both of these compounds (DHA and DKG) had not been fully elucidated, and the fate of these compounds in the presence of ROS other than H_2O_2 had not been previously studied.

The DHA oxidation products, OxT, cOxT and OxA had previously been reported to be formed in a ratio of 6:1:1 (1). However that study used H_2O_2 as the oxidising reagent, and the current study showed that the ratio of the oxidation compounds alters with different ROS. The reaction of DHA with $\text{O}_2^{\cdot-}$ produces very little cOxT, but much more OxA (necessarily with the production of ThrO). The amount of $\cdot\text{OH}$ present in the reaction with DHA also affected the ratio of cOxT to ThrO.

Interestingly, earlier studies had noted that there are at least two, if not three, interconverting isomers of OxT, with the 4-OxT epimer dominating at equilibrium (2); however, it has now been shown that different ROS seem to lead to a different predominant isomer of OxT. This was determined by HVPE at pH 2.0, which separates the isomers. Incubation of DHA with H_2O_2 produced more of the fastest-moving isomer of OxT (presumed to be 4-OxT), whereas incubation with $\text{O}_2^{\cdot-}$ favoured the slowest-moving isomer (presumed to be 3-OxT). 4-OxT is presumed to be more mobile than 3-OxT during HVPE at pH 2.0 because the two potential negative charges are further apart in 4-OxT, and the closer the charges, the more one will suppress the ionisation of the other (Figure 103). The third isomer of OxT, 2-OxT, is presumed to be less stable than the other isomers, because of the proximity of the two negatively charged groups, thus 2-OxT is expected to convert to the other isomers rapidly in solution (2). The reason for the difference is unclear, but speculatively it could be due to different ROS forcing DHA down slightly differing oxidative pathways, resulting in varying oxidation products.

Singlet oxygen, the only non-radical ROS tested in this study, showed the most divergent oxidation profile of products derived from DHA, including an unknown compound with a mobility slightly below that of ThrO when analysed by HVPE at pH 6.5. Analysis of these samples by HVPE at pH 2.0 showed the compound moving in the same region as a compound previously reported to be a derivative of DKG, known as compound H (2). Compound H has been suggested to originate from DKG, so it is likely that during the present study compound H also originated from DKG rather than DHA. This could have occurred because of the long incubation time of this particular experiment (up to 24 hours),

which allows time for the hydrolysis of DHA to occur, forming DKG, which may then potentially react with singlet oxygen generated from the photosensitiser dye in the presence of light.

Some oxidation products were found to only occur when the starting substrate was DHA, such as cOxT, and some only from DKG, such as compound H, mentioned previously (Figure 103). DHA, an oxidation product of AA itself, is presumably more likely to occur in an oxidising environment than DKG, as DKG is produced by the hydrolysis of DHA and DHA is unlikely to undergo hydrolysis in an oxidising environment, as the DHA would be preferentially oxidised. This would suggest that the oxidation products arising from DHA are perhaps more likely to occur more frequently and in greater quantities *in vivo* than the products arising from DKG. However, as the plant cell is an aqueous environment, some hydrolysis of DHA to DKG would be expected, and DKG has been demonstrated to be formed in cauliflower (285) and in the apoplast of rose cell-suspension cultures (72). The presence of DKG within the apoplast, as well as other cellular compartments, would provide an opportunity for DKG oxidation, should ROS be generated in the vicinity of DKG.

Further elucidation of the separate oxidation pathways of DHA and DKG has been achieved, including the novel observation that the degradation pathways of DHA and DKG vary depending on the type of ROS present. This could potentially have applications indicating the nature of oxidative stress that a plant is experiencing, based on the signature of the oxidation products formed from DHA. For example high levels of cOxT *in vivo* may indicate oxidation of DHA by H₂O₂; equally, high levels of compound H may indicate the oxidation of DKG by O₂^{•-}. *In vivo* ROS generally occur together, and many ROS react to form other ROS, such as the production of ¹O₂ from ozone (152), and •OH from H₂O₂ and O₂^{•-} (110). This can create uncertainty in experimental settings as to which ROS is contributing to the oxidative stress *in vivo*, so analysis of AA oxidation products in this situation could help to shed light on this valuable information.

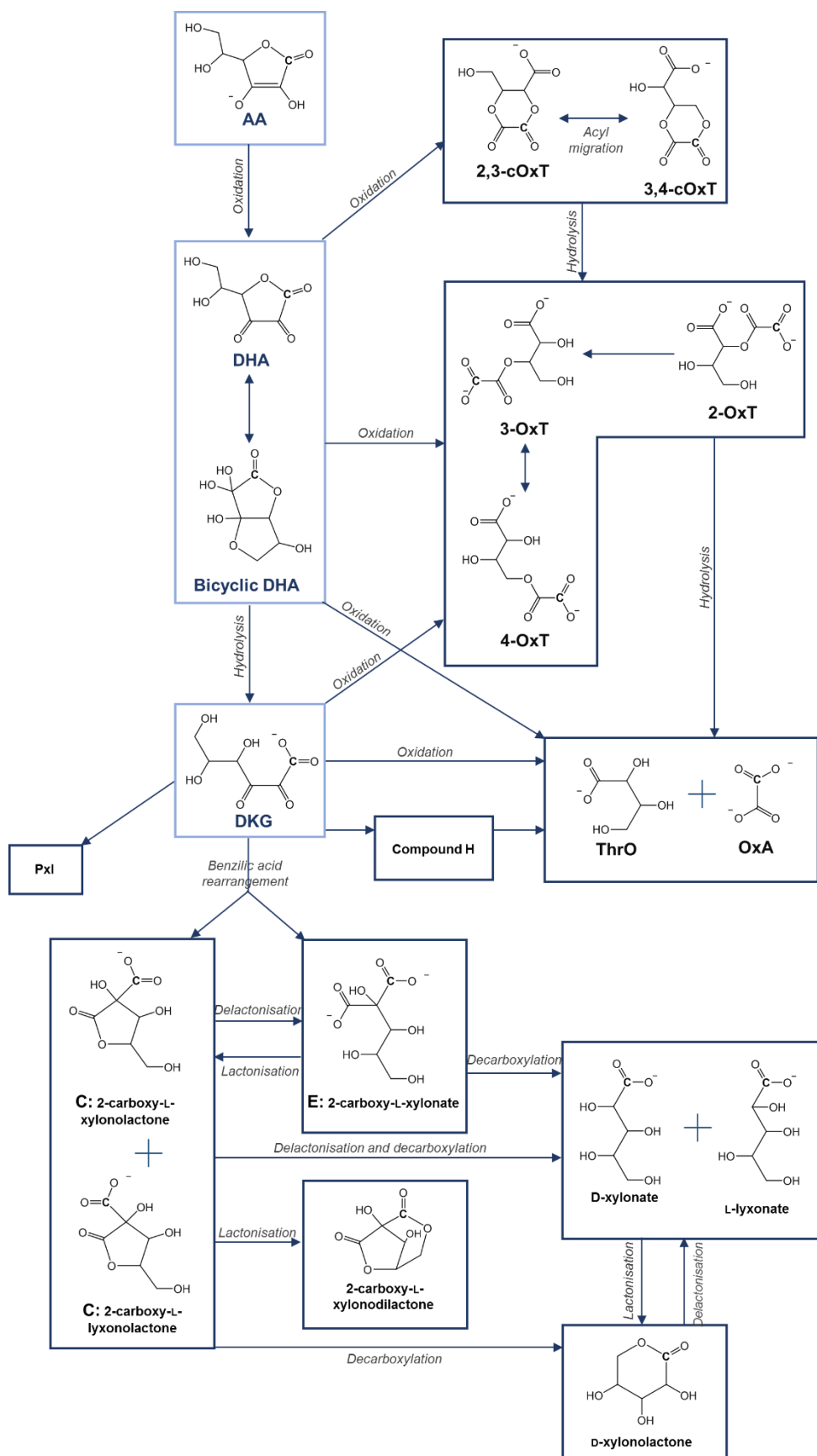


Figure 103: Proposed degradation pathways of ascorbate *in vitro*. The type of reaction is written above or beside each arrow. The reactions forming compound H and Pxl are unknown, so these arrows are not labelled. The carbon corresponding to the C-1 of the original AA is labelled with a bold C.

4.3 Characterisation of non-oxidative derivatives of DKG

Two derivatives of DKG (compounds C and E) were originally identified during the degradation of [^{14}C]AA in rose cell-suspension culture (72). Further work determined that these compounds were interconverting, with compound C representing a stable end-product of DKG catabolism *in vivo* (1). Hypothetical structures for both compounds C and E were proposed (1) and these structures have been confirmed in the current study, by MS and NMR spectroscopy. Compound E was identified as 2-carboxy-L-xylonate, and compound C was determined to be a mixture of two epimers, 2-carboxy-L-xylonolactone and 2-carboxy-L-lyxonolactone (Figure 103).

HVPE at pH 2.0 revealed the existence of previously undetected compounds along with the original C and E among the products of DKG formed by alkali treatment of DHA *in vitro*, including the separation of the two epimers of compound C. Xylonic acid (or potentially lyxonic acid, as these compounds are presumably indistinguishable by HVPE owing to their identical charge : mass ratios) was found to be present in preparations of compounds C and E. Xylonic acid and lyxonic acid are known to be produced from DKG in rat kidneys (4), but are not known to be produced by plant cells. Further investigation would be required to determine whether xylonic or lyxonic acid are ascorbate derivatives in plant cells rather than *in vitro* as in the current study. Xylonolactone is a precursor of xylonic acid in bacteria (*Pseudomonas fragi*), and this conversion is catalysed by an enzyme, xylonolactonase (286). Delactonisation of compound C (carboxy-L-xylonolactone) to compound E (carboxy-L-xylonate), followed by decarboxylation would produce xylonic acid along with CO_2 , thus suggesting that compounds C and E can act as precursors to xylonic acid.

The compound formerly named C*, and since characterised as xylonic (or lyxonic) acid was originally detected by silver nitrate staining, but was also found to be present in preparations of radiolabelled C and E. The labelled carbon corresponds to C-1 of the ascorbate molecule from which these compounds originated. The presence of radiolabelled xylonic acid demonstrates that the C-1 of ascorbate is still present in this derivative. If compound E were the precursor of xylonic/lyxonic acid, then there would be an equal chance of either of the two COO^- groups being lost during decarboxylation and released as CO_2 . As only one of the groups was labelled, the yield of [^{14}C]xylonic acid would be perhaps half of the true yield, as if the other COO^- group were removed, [^{14}C] CO_2 would be lost and the remaining xylonic acid not detectable.

A neutral compound was also detected among the products of DKG degradation formed by alkali treatment of DHA, both with silver nitrate staining, and in experiments with radiolabelled precursors. The presence of the radiolabelled neutral compound strongly suggests that this compound is in fact a derivative of DKG, and not merely an artefact of purification by elution from paper. A hypothetical identity for this neutral compound is proposed as being a dilactone of compound C. MS analysis did not detect a compound with the appropriate theoretical mass (of 174). The inability to detect this mass could be due to the very low amounts of this compound that were able to be purified. It is also likely that a preparation of this compound could contain contaminants of neutral compounds, such as sugars co-eluted from paper in a previous purification step. A further possible identity of a neutral compound arising from the degradation of DKG could be xylonolactone, a precursor of xylonic acid in bacteria (286), as mentioned previously. Xylonolactone could be formed from the decarboxylation of compound C (carboxy-L-xylonolactone), and in fact NaOH treatment (which favours delactonisation) of the neutral C and E-related compound produced a compound with the same mobility as xylonic acid, suggesting this could be the identity of this compound.

Further degradation products of DKG, separated by HPLC, were previously shown to inhibit peroxidase activity, as well as produce H_2O_2 (84). One particular fraction as separated by HPLC was demonstrated to inhibit peroxidase activity (A. Kärkönen and S.C. Fry, unpublished). Steps were taken to purify and characterise this unknown DKG-derivative (named PxI). Unfortunately, the compound proved too unstable, and NMR spectroscopy was unsuccessful in identifying this compound. The possibility that the identity of PxI could be compound C or E was tested, but the HPLC profiles of compounds C and E differed greatly from the profile of PxI, suggesting PxI is not in fact compound C or E.

If PxI could be stabilised e.g. by reducing the possibility for reactions that may be causing the degradation of this compound (such as oxidation) or by eluting the compound in a buffer found to provide optimum stability, then the characterisation may be more successful, and as this compound has been shown to have biological activity then this would warrant further investigation in the future.

4.4 The fate of ascorbate oxidation products *in vitro* and *in vivo*

OxT, a major oxidation product of both DHA and DKG degradation *in vitro*, was shown to remain in the apoplastic space of spinach cell-suspension cultures rather than be transported into the cells as DHA has been demonstrated to do (258). OxT was also fairly stable in the medium of spinach cell culture, representing the apoplast, and not hydrolysed to OxA, suggesting that spinach cells do not secrete an oxalyl esterase into their apoplast. This was not the case in *Arabidopsis*, as OxT was quickly hydrolysed forming OxA, and ThrO in cell cultures. Rose cell-suspension cultures have also been demonstrated to contain an oxalyl esterase in the apoplast (72).

Evidence was obtained for the transacylation of the oxalyl group from OxT to components of the cell wall (Figure 104). The incubation of spinach cell cultures with [¹⁴C]OxT resulted in the formation of radiolabelled cell wall material, in the form of AIR. The radiolabelled moiety was released in the form of free [¹⁴C]OxA upon saponification, suggesting it was originally bound to the cell wall material via an ester bond. Further investigations into the nature of the acceptor substrate for the oxalyl group within the cell wall material proved unsuccessful, as the oxalyl ester appeared to be unstable; a radiolabelled compound (presumably [¹⁴C]OxA) was released with or without the treatment of cell wall-degrading enzymes, so the *in vivo* acceptor substrate for the acyltransferase was unable to be identified. The addition of an oxalyl side-chain onto cell wall material represents a novel modification of cell wall components, adding to the already numerous modifications that cell wall polysaccharides, especially pectins, undergo, such as methylation and methylesterification (287,288).

As the donor substrate for this transacylation was OxT, containing only one activated oxalyl ester group, then only one oxalyl ester linkage could be formed with cell wall components, resulting in the addition of an oxalyl side-chain. If the donor substrate was cOxT instead of

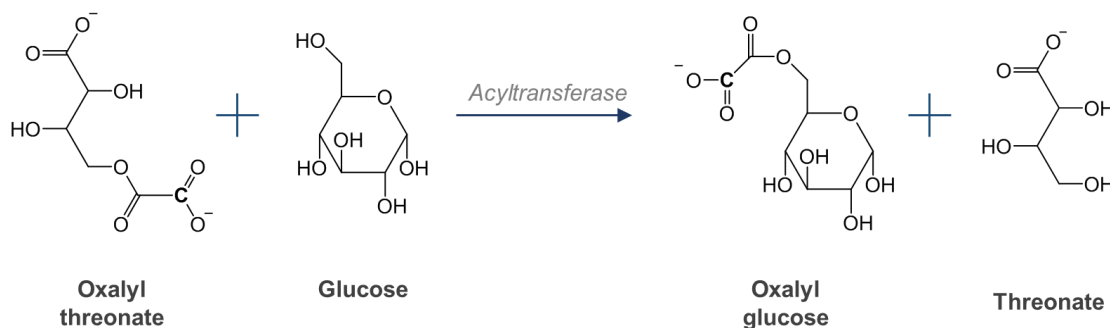


Figure 104: Example of oxalyl sugar formation via acyltransferase activity. The radiolabelled carbon (C-1 from the original [¹⁴C]AA used to purify [¹⁴C]OxT) is shown by a bold C.

OxT this would theoretically allow the formation of oxalyl diester cross-links between two cell wall components, for example polysaccharides. However, difficulties were encountered when attempting to purify cOxT, as the compound was not stable during the elution process, and a considerable proportion of the original cOxT was converted to the non-cyclic OxT form. However, if an improved method of purifying cOxT could be developed then testing for the formation of oxalyl cross-links formed from this compound within cell walls would be very valuable. The preparation containing a mixture of cOxT and OxT used in the current study formed the same products (mainly OxG) as a preparation of pure OxT, therefore it is likely that OxT, rather than cOxT, is the preferred substrate for the acyltransferase, and this could be determined using a purified cOxT preparation.

Spinach cell cultures incubated with [¹⁴C]OxT and an excess of sugar were found to form [¹⁴C]oxalyl sugars (Figure 104), identified by their specific electrophoretic mobilities. Oxalyl sugars were not formed in spent culture medium, suggesting that the enzyme (an acyltransferase) responsible for this activity was bound to the cell walls rather than free in the apoplast. An extract of ionically-bound cell wall material from spinach cell cultures showed high acyltransferase activity, determined by the formation of radiolabelled oxalyl sugars from [¹⁴C]OxT and non-radiolabelled sugars. This demonstrates that the enzyme was ionically rather than covalently bound to the cell wall.

The preferred acceptor substrates for the acyltransferase reaction seemed to be small molecules such as monosaccharides and disaccharides. Amines and polyamines did not seem to be suitable acceptors, and the product formed from the reaction of [¹⁴C]OxT with GlcN suggested that the oxalyl group was transferred onto C-6 of GlcN, rather than the amine group itself. Acceptor substrates with readily accessible primary OH groups, e.g. on C-6 of Glc, proved to be the most favoured by the acyltransferase.

It was originally thought that this acyltransferase could be responsible for the transfer of oxalyl groups onto cell wall components, as discussed previously. However, when the partially purified acyltransferase extract was tested with various polysaccharides, no acyltransferase activity was detected. This could be simply due to the methods used, rather than the enzyme not acting on these acceptor substrates. In fact, experiments that used hemicellulose–cellulose complexes as acceptor substrates for acyltransferase initially showed high activity, but this activity was negligible in further experiments with more rigorous controls. On the other hand, another reason the later experiments showed lower acyltransferase activity could be that the enzyme was slowly denatured during storage, losing

the acyltransferase activity. The tantalising results obtained in the initial polysaccharide–cellulose complex experiments suggest that this would be interesting to follow up.

Numerous acyltransferases have been identified from plants (206), but the transfer of an oxalyl group via the action of an acyltransferase (Figure 104) has not been reported, and thus represents a novel enzyme activity. Acyltransferases serve wide-ranging functions in plants, for example secondary modifications of phenolic compounds such as anthocyanins (213), modifications of lignin (220) and in the growth of root hairs, in which they modify the hydrophobicity of proteins, controlling their membrane associations (219). Acyl sugars, a product of an acyltransferase reaction, have been previously reported to be formed in plants, by the esterification of sugars and fatty acids, and act to protect the plant from herbivory (215,289).

The products (oxalyl sugars) of this novel acyltransferase activity have also not been reported, and so are novel compounds themselves. Oxalyl glucose (Figure 104) was found to be fairly stable in spinach cell culture, remaining in the apoplast, but the role of such compounds *in vivo* is not yet certain and warrants further investigation.

4.5 The degradation of ascorbate in salad leaves

The post-harvest storage of salad leaves, in terms of nutritional factors such as ascorbate, has been fairly extensively studied, but the loss of ascorbate during the washing process itself has been much less characterised.

Spinach leaves were found to be more susceptible to the loss of ascorbate during post-harvest processing than watercress or rocket leaves. Although cutting has been shown to negatively impact the ascorbate content of spinach (223,290), the rest of the washing and packing process had not been investigated in terms of ascorbate retention. Many studies into post-harvest processing of spinach have involved the effect of storage temperature and storage time.

Experiments have shown that the mechanical stress experienced by spinach leaves during washing led to a significant loss of ascorbate, whereas mere submersion of the leaves did not significantly affect the ascorbate content. Further investigation demonstrated that ascorbate undergoes oxidation during spinach washing, producing OxA. Spinach leaves are known to accumulate OxA (176), and OxA can act as an anti-nutrient, as it binds to calcium, potentially leading to calcium deficiency and to the formation of kidney stones (177,291,292).

The oxidative stress within leaves is known to be increased with mechanical stress and by processes such as cutting prior to the washing procedure (290). OxA is known to be produced from AA during the reaction with ROS, as demonstrated in section 3.3 (Figure 103), although *in vitro* OxA was a fairly minor product, compared to being the major product as observed in spinach leaves. The specific ROS present in the spinach leaves during washing is not known, so it may be interesting to investigate the nature of the oxidative stress during the washing of salad leaves.

Pre-harvest factors, such as the growth stage at harvest can also effect the ascorbate content of salad leaves (223). This was verified in the current study in which spinach leaves harvested at earlier growth stages showed an increased retention of ascorbate during a 10-day post-harvest storage period. Younger leaves are known to have higher ascorbate levels, potentially reflecting the role of ascorbate in plant growth (229). Although the initial levels of ascorbate did not differ between the early and late-stage spinach cultivars, it is possible that the younger leaves were more efficient at recycling ascorbate, thereby less prone to losing it.

Late-stage watercress leaves did not show a greater loss of ascorbate than early-stage leaves; on the contrary, the 3-week old watercress leaves showed the highest levels of initial ascorbate, but all the growth stages tested lost ascorbate at the same rate throughout storage. This represents the stage at which watercress is routinely harvested, so suggests that this harvest time is optimum in terms of ascorbate content.

The washing process used by Vitacress Ltd is unusual in the pre-packaged salad business as it does not use any chlorine, ozone or other anti-microbial agent; instead the leaves are washed only in spring water. Such antimicrobial agents (ozone and chlorine) have been previously shown to negatively affect the ascorbate content of salad leaves, including rocket, iceberg lettuce and spinach (240-242). The experiments described in section 3.6 on the effect of chlorinated water on ascorbate loss in spinach leaves during washing indicate that washing in chlorine does not lead to a greater loss of ascorbate.

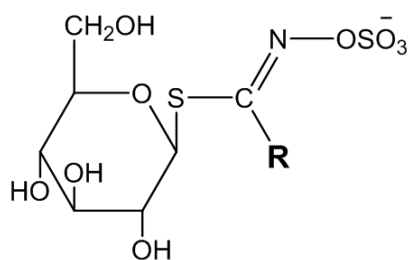
Attempts were made to detect degradation products of ascorbate in salad sample extracts. Silver nitrate staining was not particularly successful in this venture, as salad extracts contained numerous compounds that could be stained, and it was not possible to distinguish which of them originated from ascorbate. Also, the extracts contained relatively low amounts of AA, and presumably its derivatives, so heavy loadings were required, causing some distortion of the mobilities of the compounds present. However, the use of radiolabelled ascorbate fed to spinach leaves, which was then monitored throughout the washing process, allowed the detection of oxidation products OxT and OxA from ascorbate. It was well known that spinach accumulates OxA, and this study provides more evidence for this. Although the OxT levels did not alter with the different washing treatments, the presence of OxT is still noteworthy, as this is the first demonstration of the presence, or formation, of OxT *in planta*. OxT had previously been found to be produced from radiolabelled ascorbate in rose cell-suspension culture.

4.6 Compound from watercress that serves as an indicator of freshness

Samples of watercress extracts run by HVPE showed an abundance of an unknown compound, which appeared to decrease during storage. The compound was also absent from extracts of watercress imported from Portugal, which would have had a much longer time between harvest and being available in the shop than its UK-grown counterparts, providing further evidence for the presence of this compound acting as an indicator of freshness. This compound was mobile during HVPE at pH 2.0, indicating it must have a very low pK_a , which is fairly unusual among plant-derived compounds.

Species within the Brassicaceae, including watercress, are known to contain high levels of glucosinolates (274). Glucosinolates are compounds containing a glucopyranose group linked via a sulphur atom to a central carbon atom, itself linked via a nitrogen atom to a

A Glucosinolate (GSL)



B Examples of common glucosinolates (R groups)

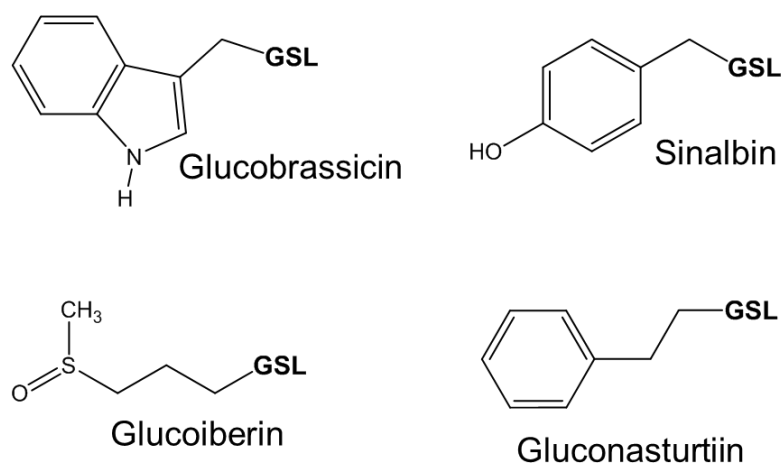


Figure 105: Structure of glucosinolates. The generalised structure for glucosinolates is shown (A). The R group represents a variable side chain usually derived from amino acids. Examples of the variable groups of some common glucosinolates are shown (B). GSL represents the generalised glucosinolate structure.

sulphate group, along with a variable side chain (Figure 105 A). The side chain can be aliphatic (glucoiberin, Figure 105 B) or aromatic (gluconasturtiin and sinalbin, Figure 105 B) including indolic side chains (glucobrassicin, Figure 105 B). The side chains can also be categorised according to the amino from which they derive. Aliphatic glucosinolates are generally methionine-derived, aromatic structures are mainly phenylalanine-derived and indolic side chains are tryptophan-derived (275).

Over a hundred different glucosinolate compounds have been isolated from plant species (275). Within the plant glucosinolates (and their isothiocyanate derivatives) serve protective roles, deterring potential herbivores (293,294). However, isothiocyanates can also act as attractants for some insect species (295). The distinctive flavour of watercress is due to the presence of glucosinolates, such as gluconasturtiin (phenylethyl glucosinolate, Figure 105 B) (296,297). Glucosinolates are also known to show considerable health benefits in humans (298-300). For instance, glucosinolate-derivatives have been shown to have anti-cancer properties, and protect against neurological diseases (298,301).

The compound(s) known as WCx in the current study has been very tentatively identified as a glucosinolate (Figure 105) or related compounds. Rocket (another Brassicaceae species) extracts also showed a compound co-migrating with WCx, so it is possible that other salad samples contain this same compound that may serve as an indicator of freshness.

MS analysis showed several peaks with m/z values varying from 311 to 492. Two of these peaks correspond to the expected m/z values of glucosinolates known to occur in watercress, gluconasturtiin (Figure 105) and glucobarbarin (277-279), suggesting that WCx possibly includes, most likely among other compounds, these two glucosinolates.

The m_{OG} of WCx was identical at pH 6.5 and pH 2.0, showing that it has a strongly acidic component, which could be due to a sulphate group (Figure 105). This was also the case with a previously identified glucosinolate which was found to have identical mobilities when analysed by HVPE at pH 7.0 and pH 2.0 (281). This indole compound, identified as 1-sulpho-3-indolyl-methyl glucosinolate, was also detected by staining in silver nitrate, as with WCx.

The side chains of glucosinolates are derived from amino acids (302). TLC analysis of WCx showed a ninhydrin-stained band separated from the thymol-stained bands. It is plausible that an amino acid-derived side chain could have been cleaved from the main glucosinolate structure during the extraction process, thus resulting in a differently mobile compound appearing after TLC analysis. Alternatively, the side chain of glucobrassicin (Figure 105) for

example would stain with ninhydrin, whilst retaining the acidic sulphate group ensuring its mobility during HVPE, so it is possible, although by no means certain, that a component of WCx is a glucosinolate with a similar side chain to glucobrassicin.

The extraction methods, in 0.5% formic acid or 0.5% oxalic acid, used in the current study were not optimal for the extraction of glucosinolates, rather they were optimised for the extraction of ascorbate, so it is not clear whether glucosinolate compounds would have been stable during the extraction process. It is known that glucosinolates are broken down into glucose, sulphate and isothiocyanates via myrosinase enzymes (303); however, enzymes are very unlikely to still be active in formic acid, so it is unlikely that any potential degradation of WCx, whether or not it is a glucosinolate, would have occurred via enzyme activity. Equally, extraction in dilute cold acid would be unlikely to contribute to the degradation of a glucosinolate.

With this knowledge, further investigations could be conducted to discover if WCx is in fact a glucosinolate compound, such as treating WCx with myrosinase, which should produce a negatively charged isothiocyanate, which would be easy to determine by HVPE analysis, and glucose. It would be interesting to investigate this compound further, both because of its apparent indication of freshness, and because of the potential health benefits of glucosinolates. Equally it is likely that WCx comprises a compound unrelated to glucosinolates and further experiments would be required to make a more informed prediction of the identity of WCx.

4.7 Summary

Overall, this project has illuminated the many-pronged degradation pathways of ascorbate. The oxidation pathways as affected by ROS and starting substrate (DHA or DKG) have been more thoroughly elucidated. Equally, the hydrolysis pathway of DHA, via DKG, has been further defined, including by the characterisation of compounds C and E, now known to be 2-carboxy-L-xylonolactone (and its epimer 2-carboxy-L-lyxonolactone) and 2-carboxy-L-xylonate respectively. Other C and E-related compounds are proposed to be xylonic (or lyxonic) acid, and potentially either xylonolactone or carboxy-xylonodilactone.

The fate of the major oxidation product of DHA, OxT, was studied *in vivo*. This led to the discovery of a novel acyltransferase activity, which was able to be eluted from spinach cell walls. The addition of oxalyl groups onto sugar molecules produced novel metabolites, which may have important roles within the plant, potentially as signalling molecules or acting to protect the plant from herbivory, as is the role of already characterised acyl sugars. The role of the novel oxalyl sugars in the plant requires further study.

Within salad plants, spinach leaves were found to be most susceptible to ascorbate loss during commercial washing practices. This loss of ascorbate was mainly due to mechanical damage, which potentially increases oxidative stress within the leaf, leading to an increase in the OxA produced from AA. Modifying the washing process to reduce the mechanical damage of spinach leaves would be advisable, and likely to lead to an increase in ascorbate content of the spinach leaves throughout post-harvest storage.

A further interesting finding was that of a compound (WCx) whose levels within leaves corresponded to the 'freshness' of watercress. Attempts to identify this compound were not completely successful, but there is a small possibility that it belongs to the glucosinolate group of compounds, and WCx preparations are likely to include gluconasturtiin and glucobarbarin. These compounds themselves have considerable health benefits, so further investigation into these compounds would be very valuable.

Overall the current study has added valuable insights into the degradation, both oxidative and non-oxidative, of ascorbate *in vitro* and in harvested salad plants, providing useful information for both basic research and industrial applications. Intriguing novel functions of ascorbate oxidation products have also been proposed, further highlighting the role of ascorbate in plant growth and metabolism.

References

1. Parsons, H. T., Yasmin, T., and Fry, S. C. (2011) Alternative pathways of dehydroascorbic acid degradation in vitro and in plant cell cultures: novel insights into vitamin C catabolism. *Biochemical Journal* **440**, 375-383
2. Parsons, H. T., and Fry, S. C. (2012) Oxidation of dehydroascorbic acid and 2,3-diketogulonate under plant apoplastic conditions. *Phytochemistry* **75**, 41-49
3. Hancock, R. D., and Viola, R. (2005) Biosynthesis and catabolism of L-ascorbic acid in plants. *Critical Reviews in Plant Sciences* **24**, 167-188
4. Kanfer, J., Ashwell, G., and Burns, J. J. (1960) Formation of L-lyxonic and L-xylonic acids from L-ascorbic acid in rat kidney. *Journal of Biological Chemistry* **235**, 2518-2521
5. Fry, S. C. (2011) High-voltage paper electrophoresis (HVPE) of cell-wall building blocks and their metabolic precursors. in *Plant Cell Wall: Methods and Protocols* (Popper, Z. A. ed.), Springer. pp 55-80
6. Du, J., Cullen, J. J., and Buettner, G. R. (2012) Ascorbic acid: Chemistry, biology and the treatment of cancer. *Biochimica Et Biophysica Acta-Reviews on Cancer* **1826**, 443-457
7. Lazaro, J. J., Jimenez, A., Camejo, D., Iglesias-Baena, I., del Carmen Marti, M., Lazaro-Payo, A., Barranco-Medina, S., and Sevilla, F. (2013) Dissecting the integrative antioxidant and redox systems in plant mitochondria. Effect of stress and S-nitrosylation. *Frontiers in Plant Science* **4**, 1-20
8. Bradshaw, M. P., Barril, C., Clark, A. C., Prenzler, P. D., and Scollary, G. R. (2011) Ascorbic acid: a review of its chemistry and reactivity in relation to a wine environment. *Critical Reviews in Food Science and Nutrition* **51**, 479-498
9. Valpuesta, V., and Botella, M. A. (2004) Biosynthesis of L-ascorbic acid in plants: new pathways for an old antioxidant. *Trends in Plant Science* **9**, 573-577
10. Burns, J. J. (1957) Missing step in man, monkey and guinea pig required for the biosynthesis of L-ascorbic acid. *Nature* **180**, 553
11. Noctor, G., and Foyer, C. H. (1998) Ascorbate and glutathione: Keeping active oxygen under control. *Annual Review of Plant Physiology and Plant Molecular Biology* **49**, 249-279
12. Stewart, M. L., McDonald, J. T., Levy, A. S., Schucker, R. E., and Henderson, D. P. (1985) Vitamin mineral supplement use - a telephone survey of adults in the United States. *Journal of the American Dietetic Association* **85**, 1585-1590
13. Naidu, K. A. (2003) Vitamin C in human health and disease is still a mystery? An overview. *Nutrition journal* **2**, 7-7
14. Wheeler, G. L., Jones, M. A., and Smirnoff, N. (1998) The biosynthetic pathway of vitamin C in higher plants. *Nature* **393**, 365-369
15. Gould, B. S., and Woessner, J. F. (1957) Biosynthesis of collagen - the influence of ascorbic acid on the proline, hydroxyproline, glycine, and collagen content of regenerating guinea pig skin. *Journal of Biological Chemistry* **226**, 289-300
16. Mandl, J., Szarka, A., and Banhegyi, G. (2009) Vitamin C: update on physiology and pharmacology. *British Journal of Pharmacology* **157**, 1097-1110
17. Ames, B. N., Shigenaga, M. K., and Hagen, T. M. (1993) Oxidants, antioxidants, and the degenerative diseases of aging. *Proceedings of the National Academy of Sciences of the United States of America* **90**, 7915-7922
18. Smirnoff, N., and Wheeler, G. L. (2000) Ascorbic acid in plants: Biosynthesis and function. *Critical Reviews in Plant Sciences* **19**, 267-290
19. Davey, M. W., Van Montagu, M., Inze, D., Sanmartin, M., Kanellis, A., Smirnoff, N., Benzie, I. J. J., Strain, J. J., Favell, D., and Fletcher, J. (2000) Plant L-ascorbic

- acid: chemistry, function, metabolism, bioavailability and effects of processing. *Journal of the Science of Food and Agriculture* **80**, 825-860
20. Lind, J. (1753) *A treatise on the scurvy: in three parts*, Third edition ed., Edinburgh
 21. Magiorkinis, E., Beloukas, A., and Diamantis, A. (2011) Scurvy: Past, present and future. *European Journal of Internal Medicine* **22**, 147-152
 22. Szent-Gyorgyi, A. (1928) Observations on the function of peroxidase systems and the chemistry of the adrenal cortex. Description of a new carbohydrate derivative. *Biochemical Journal* **22**, 1387-1409
 23. Harris, L. J., and Ray, S. N. (1933) Specificity of hexuronic (ascorbic) acid as anti-scorbutic factor. *Biochemical Journal* **27**
 24. Funk, C. (1975) Etiology of deficiency diseases - beriberi, polyneuritis in birds, epidemic dropsy, scurvy, experimental scurvy in animals, infantile scurvy, ship beriberi, pellagra. *Nutrition Reviews* **33**, 176-177
 25. Szent-Gyorgyi, A. (1931) On the function of hexuronic acid in the respiration of the cabbage leaf. *Journal of Biological Chemistry* **90**, 385-393
 26. King, C. G., and Waugh, W. A. (1932) The chemical nature of vitamin C. *Science* **75**, 357-358
 27. Linster, C. L., and Van Schaftingen, E. (2007) Vitamin C - Biosynthesis, recycling and degradation in mammals. *Febs Journal* **274**, 1-22
 28. Ault, R. G., Baird, D. K., Carrington, H. C., Haworth, W. N., Herbert, R., Hirst, E. L., Percival, E. G. V., Smith, F., and Stacey, M. (1933) Synthesis of D- and of L-ascorbic acid and of analogous substances. *Journal of the Chemical Society*, 1419-1423
 29. Ball, E. G. (1937) Studies on oxidation-reduction XXIII. Ascorbic acid. *Journal of Biological Chemistry* **118**, 219-239
 30. Khan, M. M. T., and Martell, A. E. (1967) Metal ion and metal chelate catalysed oxidation of ascorbic acid by molecular oxygen .I. cupric and ferric ion catalysed oxidation. *Journal of the American Chemical Society* **89**, 4176-4185
 31. Hossain, M. A., Nakano, Y., and Asada, K. (1984) Monodehydroascorbate reductase in spinach-chloroplasts and its participation in regeneration of ascorbate for scavenging hydrogen-peroxide. *Plant and Cell Physiology* **25**, 385-395
 32. Deutsch, J. C. (1998) Ascorbic acid oxidation by hydrogen peroxide. *Analytical Biochemistry* **255**, 1-7
 33. Deutsch, J. C. (2000) Dehydroascorbic acid. *Journal of Chromatography A* **881**, 299-307
 34. Murakawa, S., and Takahashi, T. (1977) Biosynthesis of a new ascorbic acid analog by D-gluconolactone dehydrogenase of *Penicillium cyaneo-fulvum*. *Agricultural and Biological Chemistry* **41**, 2103-2104
 35. Margolis, S. A., and Schapira, R. M. (1997) Liquid chromatographic measurement of L-ascorbic acid and D-ascorbic acid in biological samples. *Journal of Chromatography B* **690**, 25-33
 36. Goldman, H. M., Gould, B. S., and Munro, H. N. (1981) The anti-scorbutic action of l-ascorbic acid and d-isoascorbic acid (erythorbic acid) in the guinea pig. *American Journal of Clinical Nutrition* **34**, 24-33
 37. Huh, W. K., Lee, B. H., Kim, S. T., Kim, Y. R., Rhie, G. E., Baek, Y. W., Hwang, C. S., Lee, J. S., and Kang, S. O. (1998) D-Erythroascorbic acid is an important antioxidant molecule in *Saccharomyces cerevisiae*. *Molecular Microbiology* **30**, 895-903
 38. Loewus, F. A. (1999) Biosynthesis and metabolism of ascorbic acid in plants and of analogs of ascorbic acid in fungi. *Phytochemistry* **52**, 193-210
 39. Shao, Y. Y., Seib, P. A., Kramer, K. J., and Vangalen, D. A. (1993) Synthesis and properties of D-erythroascorbic acid and its vitamin-C activity in the tobacco

- hornworm (*Manduca sexta*). *Journal of Agricultural and Food Chemistry* **41**, 1391-1396
40. Jackel, S. S., Mosbach, E. H., Burns, J. J., and King, C. G. (1950) The synthesis of L-ascorbic acid by the albino rat. *Journal of Biological Chemistry* **186**, 569-579
 41. Horowitz, H. H., Doerschuk, A. P., and King, C. G. (1952) The origin of L-ascorbic acid in the albino rat. *Journal of Biological Chemistry* **199**, 193-198
 42. Isherwood, F. A., Chen, Y. T., and Mapson, L. W. (1954) Synthesis of L-ascorbic acid in plants and animals. *Biochemical Journal* **56**, 1-15
 43. Kar, N. C., Chatterjee, I. B., Ghosh, N. C., and Guha, B. C. (1962) Further observations on intracellular location and mechanism of action of liver enzymes catalysing synthesis of L-ascorbic acid. *Biochemical Journal* **84**, 16-25
 44. Loewus, F. A., Kelly, S., and Neufeld, E. F. (1962) Metabolism of myo-inositol in plants - conversion to pectin, hemicellulose, D-xylose, and sugar acids. *Proceedings of the National Academy of Sciences of the United States of America* **48**, 421-425
 45. Loewus, F. A. (1963) Tracer studies on ascorbic acid formation in plants. *Phytochemistry* **2**, 109-128
 46. Mapson, L. W., and Isherwood, F. A. (1956) Biological synthesis of ascorbic acid - conversion of derivatives of D-galacturonic acid into L-ascorbic acid by plant extracts. *Biochemical Journal* **64**, 13-22
 47. Oba, K., Ishikawa, S., Nishikawa, M., Mizuno, H., and Yamamoto, T. (1995) Purification and properties of L-galactono-gamma-lactone dehydrogenase, a key enzyme for ascorbic-acid biosynthesis, from sweet-potato roots. *Journal of Biochemistry* **117**, 120-124
 48. Loewus, F. A., and Loewus, M. W. (1987) Biosynthesis and metabolism of ascorbic acid in plants. *Crc Critical Reviews in Plant Sciences* **5**, 101-119
 49. Roberts, R. M., and Harrer, E. (1973) Determination of L-galactose in polysaccharide material. *Phytochemistry* **12**, 2679-2682
 50. Smirnoff, N. (2000) Ascorbic acid: metabolism and functions of a multi-facetted molecule. *Current Opinion in Plant Biology* **3**, 229-235
 51. Conklin, P. L., Norris, S. R., Wheeler, G. L., Williams, E. H., Smirnoff, N., and Last, R. L. (1999) Genetic evidence for the role of GDP-mannose in plant ascorbic acid (vitamin C) biosynthesis. *Proceedings of the National Academy of Sciences of the United States of America* **96**, 4198-4203
 52. Veljovic-Jovanovic, S. D., Pignocchi, C., Noctor, G., and Foyer, C. H. (2001) Low ascorbic acid in the vtc-1 mutant of *Arabidopsis* is associated with decreased growth and intracellular redistribution of the antioxidant system. *Plant Physiology* **127**, 426-435
 53. Lukowitz, W., Nickle, T. C., Meinke, D. W., Last, R. L., Conklin, P. L., and Somerville, C. R. (2001) *Arabidopsis* cyt1 mutants are deficient in a mannose-1-phosphate guanylyltransferase and point to a requirement of N-linked glycosylation for cellulose biosynthesis. *Proceedings of the National Academy of Sciences of the United States of America* **98**, 2262-2267
 54. Barth, C., Moeder, W., Klessig, D. F., and Conklin, P. L. (2004) The timing of senescence and response to pathogens is altered in the ascorbate-deficient *Arabidopsis* mutant vitamin c-1. *Plant Physiology* **134**, 1784-1792
 55. Conklin, P. L., Gatzek, S., Wheeler, G. L., Dowdle, J., Raymond, M. J., Rolinski, S., Isupov, M., Littlechild, J. A., and Smirnoff, N. (2006) *Arabidopsis thaliana* VTC4 encodes L-galactose-1-P phosphatase, a plant ascorbic acid biosynthetic enzyme. *Journal of Biological Chemistry* **281**, 15662-15670
 56. Linster, C. L., Gomez, T. A., Christensen, K. C., Adler, L. N., Young, B. D., Brenner, C., and Clarke, S. G. (2007) *Arabidopsis* VTC2 encodes a GDP-L-galactose phosphorylase, the last unknown enzyme in the Smirnoff-Wheeler pathway to ascorbic acid in plants. *Journal of Biological Chemistry* **282**, 18879-18885

57. Dowdle, J., Ishikawa, T., Gatzek, S., Rolinski, S., and Smirnoff, N. (2007) Two genes in *Arabidopsis thaliana* encoding GDP-L-galactose phosphorylase are required for ascorbate biosynthesis and seedling viability. *Plant Journal* **52**, 673-689
58. Gao, Y., Badejo, A. A., Shibata, H., Sawa, Y., Maruta, T., Shigeoka, S., Page, M., Smirnoff, N., and Ishikawa, T. (2011) Expression analysis of the VTC2 and VTC5 genes encoding GDP-L-galactose phosphorylase, an enzyme involved in ascorbate biosynthesis, in *Arabidopsis thaliana*. *Bioscience Biotechnology and Biochemistry* **75**, 1783-1788
59. Smirnoff, N., and Wheeler, G. L. (2000) Ascorbic acid in plants: Biosynthesis and function. *Critical Reviews in Biochemistry and Molecular Biology* **35**, 291-314
60. Badejo, A. A., Wada, K., Gao, Y., Maruta, T., Sawa, Y., Shigeoka, S., and Ishikawa, T. (2012) Translocation and the alternative D-galacturonate pathway contribute to increasing the ascorbate level in ripening tomato fruits together with the D-mannose/L-galactose pathway. *Journal of Experimental Botany* **63**, 229-239
61. Lorence, A., Chevone, B. I., Mendes, P., and Nessler, C. L. (2004) *myo*-inositol oxygenase offers a possible entry point into plant ascorbate biosynthesis. *Plant Physiology* **134**, 1200-1205
62. Wolucka, B. A., and Van Montagu, M. (2003) GDP-mannose 3',5'-epimerase forms GDP-L-gulose, a putative intermediate for the de novo biosynthesis of vitamin C in plants. *Journal of Biological Chemistry* **278**, 47483-47490
63. Levandoski, N. G., Baker, E. M., and Canham, J. E. (1964) Monodehydro form of ascorbic acid in autoxidation of ascorbic acid to dehydroascorbic acid. *Biochemistry* **3**, 1465-1469
64. Fox, F. W., and Levy, L. F. (1936) Experiments confirming the antiscorbutic activity of dehydroascorbic acid and a study of its storage and that of ascorbic acid by the guinea-pig at different levels of intake. *Biochemical Journal* **30**, 211-217
65. May, J. M., Qu, Z. C., and Morrow, J. D. (2001) Mechanisms of ascorbic acid recycling in human erythrocytes. *Biochimica Et Biophysica Acta-General Subjects* **1528**, 159-166
66. Retsky, K. L., Freeman, M. W., and Frei, B. (1993) Ascorbic acid oxidation product(s) protect human low-density-lipoprotein against atherogenic modification - antioxidant rather than prooxidant activity of vitamin-C in the presence of transition-metal ions. *Journal of Biological Chemistry* **268**, 1304-1309
67. Foyer, C. H., and Halliwell, B. (1977) Purification and properties of dehydroascorbate reductase from spinach leaves. *Phytochemistry* **16**, 1347-1350
68. de Pinto, M. C., Francis, D., and De Gara, L. (1999) The redox state of the ascorbate-dehydroascorbate pair as a specific sensor of cell division in tobacco BY-2 cells. *Protoplasma* **209**, 90-97
69. Sanmartin, M., Drogoudi, P. D., Lyons, T., Pateraki, I., Barnes, J., and Kanellis, A. K. (2003) Over-expression of ascorbate oxidase in the apoplast of transgenic tobacco results in altered ascorbate and glutathione redox states and increased sensitivity to ozone. *Planta* **216**, 918-928
70. Penney, J. R., and Zilva, S. S. (1943) The chemical behaviour of dehydro-L-ascorbic acid in vitro and in vivo. *Biochemical Journal* **37**, 403-417
71. Penney, J. R., and Zilva, S. S. (1943) The determination of 2 : 3-diketo-L-gulonic acid. *Biochemical Journal* **37**, 39-44
72. Green, M. A., and Fry, S. C. (2005) Vitamin C degradation in plant cells via enzymatic hydrolysis of 4-O-oxalyl-L-threonate. *Nature* **433**, 83-87
73. Deutsch, J. C., Santhoshkumar, C. R., Hassell, K. L., and Kolhouse, J. F. (1994) Variation in ascorbic acid oxidation routes in H₂O₂ and cupric ion solution as determined by GC/MS. *Analytical Chemistry* **66**, 345-350

74. Bendich, A., Machlin, L. J., Scandurra, O., Burton, G. W., and Wayner, D. D. M. (1986) The antioxidant role of vitamin C. *Advances in Free Radical Biology and Medicine* **2**, 419-444
75. Green, M. A., and Fry, S. C. (2005) Apoplastic degradation of ascorbate: Novel enzymes and metabolites permeating the plant cell wall. *Plant Biosystems* **139**, 2-7
76. DeBolt, S., Cook, D. R., and Ford, C. M. (2006) L-Tartaric acid synthesis from vitamin C in higher plants. *Proceedings of the National Academy of Sciences of the United States of America* **103**, 5608-5613
77. Hancock, R. D., Walker, P. G., Pont, S. D. A., Marquis, N., Vivera, S., Gordon, S. L., Brennan, R. M., and Viola, R. (2007) L-Ascorbic acid accumulation in fruit of *Ribes nigrum* occurs by in situ biosynthesis via the L-galactose pathway. *Functional Plant Biology* **34**, 1080-1091
78. DeBolt, S., Melino, V., and Ford, C. M. (2007) Ascorbate as a biosynthetic precursor in plants. *Annals of Botany* **99**, 3-8
79. Wechtersbach, L., Polak, T., Ulrih, N. P., and Cigic, B. (2011) Stability and transformation of products formed from dimeric dehydroascorbic acid at low pH. *Food Chemistry* **129**, 965-973
80. Penney, J. R., and Zilva, S. S. (1945) The isolation of barium and calcium diketo-L-gulonates and the biological significance of 2,3-diketo-L-gulonic acid. *Biochemical Journal* **39**, 1-4
81. Deutsch, J. C., and SanthoshKumar, C. R. (1996) Dehydroascorbic acid undergoes hydrolysis on solubilization which can be reversed with mercaptoethanol. *Journal of Chromatography A* **724**, 271-278
82. Kagawa, Y. (1962) Enzymatic studies on ascorbic acid catabolism in animals. 1. Catabolism of 2,3-diketo-L-gulonic acid. *Journal of Biochemistry* **51**, 134-144
83. Banhegyi, G., Braun, L., Csala, M., Puskas, F., and Mandl, J. (1997) Ascorbate metabolism and its regulation in animals. *Free Radical Biology and Medicine* **23**, 793-803
84. Karkonen, A., and Fry, S. C. (2006) Effect of ascorbate and its oxidation products on H₂O₂ production in cell-suspension cultures of *Picea abies* and in the absence of cells. *Journal of Experimental Botany* **57**, 1633-1644
85. Hancock, J. T., Desikan, R., Clarke, A., Hurst, R. D., and Neill, S. J. (2002) Cell signalling following plant/pathogen interactions involves the generation of reactive oxygen and reactive nitrogen species. *Plant Physiology and Biochemistry* **40**, 611-617
86. Karkonen, A., and Kuchitsu, K. (2015) Reactive oxygen species in cell wall metabolism and development in plants. *Phytochemistry* **112**, 22-32
87. Quan, L.-J., Zhang, B., Shi, W.-W., and Li, H.-Y. (2008) Hydrogen peroxide in plants: A versatile molecule of the reactive oxygen species network. *Journal of Integrative Plant Biology* **50**, 2-18
88. Grodzinski, B., and Butt, V. S. (1976) Hydrogen-peroxide production and release of carbon-dioxide during glycollate oxidation in lead peroxisomes. *Planta* **128**, 225-231
89. Harkin, J. M., and Obst, J. R. (1973) Lignification in trees - indication of exclusive peroxidase participation. *Science* **180**, 296-298
90. Elstner, E. F., and Heupel, A. (1976) Formation of hydrogen-peroxide by isolated cell-walls from horseradish (*Amaracia lapathifolia* gilib). *Planta* **130**, 175-180
91. Karkonen, A., Warinowski, T., Teeri, T. H., Simola, L. K., and Fry, S. C. (2009) On the mechanism of apoplastic H₂O₂ production during lignin formation and elicitation in cultured spruce cells-peroxidases after elicitation. *Planta* **230**, 553-567
92. Moller, S. G., and McPherson, M. J. (1998) Developmental expression and biochemical analysis of the *Arabidopsis* atao1 gene encoding an H₂O₂-generating diamine oxidase. *Plant Journal* **13**, 781-791

93. Foyer, C. H., LopezDelgado, H., Dat, J. F., and Scott, I. M. (1997) Hydrogen peroxide- and glutathione-associated mechanisms of acclimatory stress tolerance and signalling. *Physiologia Plantarum* **100**, 241-254
94. Neill, S., Desikan, R., and Hancock, J. (2002) Hydrogen peroxide signalling. *Current Opinion in Plant Biology* **5**, 388-395
95. Low, P. S., and Merida, J. R. (1996) The oxidative burst in plant defense: Function and signal transduction. *Physiologia Plantarum* **96**, 533-542
96. Doke, N. (1985) NADPH-dependent O₂ generation in membrane-fractions isolated from wounded potato-tubers inoculated with *Phytophthora infestans*. *Physiological Plant Pathology* **27**, 311-322
97. Apostol, I., Heinstejn, P. F., and Low, P. S. (1989) Rapid stimulation of an oxidative burst during elicitation of cultured plant-cells - role in defense and signal transduction. *Plant Physiology* **90**, 109-116
98. Doke, N., Miura, Y., Sanchez, L. M., Park, H. J., Noritake, T., Yoshioka, H., and Kawakita, K. (1996) The oxidative burst protects plants against pathogen attack: Mechanism and role as an emergency signal for plant bio-defence - A review. *Gene* **179**, 45-51
99. Levine, A., Tenhaken, R., Dixon, R., and Lamb, C. (1994) H₂O₂ from the oxidative burst orchestrates the plant hypersensitive disease resistance response. *Cell* **79**, 583-593
100. Bradley, D. J., Kjellbom, P., and Lamb, C. J. (1992) Elicitor-induced and wound-induced oxidative cross-linking of a proline-rich plant-cell wall protein - a novel, rapid defense response. *Cell* **70**, 21-30
101. Sagi, M., and Fluhr, R. (2006) Production of reactive oxygen species by plant NADPH oxidases. *Plant Physiology* **141**, 336-340
102. Marino, D., Dunand, C., Puppo, A., and Pauly, N. (2012) A burst of plant NADPH oxidases. *Trends in Plant Science* **17**, 9-15
103. Leto, T. L., and Geiszt, M. (2006) Role of Nox family NADPH oxidases in host defense. *Antioxidants & Redox Signaling* **8**, 1549-1561
104. Yun, B.-W., Feechan, A., Yin, M., Saidi, N. B. B., Le Bihan, T., Yu, M., Moore, J. W., Kang, J.-G., Kwon, E., Spoel, S. H., Pallas, J. A., and Loake, G. J. (2011) S-nitrosylation of NADPH oxidase regulates cell death in plant immunity. *Nature* **478**, 264-U161
105. Foreman, J., Demidchik, V., Bothwell, J. H. F., Mylona, P., Miedema, H., Torres, M. A., Linstead, P., Costa, S., Brownlee, C., Jones, J. D. G., Davies, J. M., and Dolan, L. (2003) Reactive oxygen species produced by NADPH oxidase regulate plant cell growth. *Nature* **422**, 442-446
106. Ishibashi, Y., Tawaratsumida, T., Zheng, S.-H., Yuasa, T., and Iwaya-Inoue, M. (2010) NADPH oxidases act as key enzyme on germination and seedling growth in barley (*Hordeum vulgare* L.). *Plant Production Science* **13**, 45-52
107. Sutherland, M. W. (1991) The generation of oxygen radicals during host plant-responses to infection. *Physiological and Molecular Plant Pathology* **39**, 79-93
108. Chance, B., Sies, H., and Boveris, A. (1979) Hydroperoxide metabolism in mammalian organs. *Physiological Reviews* **59**, 527-605
109. Asada, K. (2006) Production and scavenging of reactive oxygen species in chloroplasts and their functions. *Plant Physiology* **141**, 391-396
110. Van Breusegem, F., Vranova, E., Dat, J. F., and Inze, D. (2001) The role of active oxygen species in plant signal transduction. *Plant Science* **161**, 405-414
111. Bielski, B. H. J., Cabelli, D. E., Arudi, R. L., and Ross, A. B. (1985) Reactivity of H₂O₂/ O₂ radicals in aqueous solution. *Journal of Physical and Chemical Reference Data* **14**, 1041-1100

112. Vianello, A., and Macri, F. (1991) Generation of superoxide anion and hydrogen-peroxide at the surface of plant-cells. *Journal of Bioenergetics and Biomembranes* **23**, 409-423
113. Apel, K., and Hirt, H. (2004) Reactive oxygen species: Metabolism, oxidative stress, and signal transduction. *Annual Review of Plant Biology* **55**, 373-399
114. Lamb, C., and Dixon, R. A. (1997) The oxidative burst in plant disease resistance. *Annual Review of Plant Physiology and Plant Molecular Biology* **48**, 251-275
115. Richards, S. L., Wilkins, K. A., Swarbreck, S. M., Anderson, A. A., Habib, N., Smith, A. G., McAinsh, M., and Davies, J. M. (2015) The hydroxyl radical in plants: from seed to seed. *Journal of Experimental Botany* **66**, 37-46
116. Gutteridge, J. M. C., Halliwell, B., Treffry, A., Harrison, P. M., and Blake, D. (1983) Effect of ferritin-containing fractions with different iron loading on lipid-peroxidation. *Biochemical Journal* **209**, 557-560
117. Aruoma, O. I., and Halliwell, B. (1987) Superoxide-dependent and ascorbate-dependent formation of hydroxyl radicals from hydrogen peroxide in the presence of iron - are lactoferrin and transferrin promoters of hydroxyl radical generation. *Biochemical Journal* **241**, 273-278
118. Fridovich, I. (1997) Superoxide anion radical (O₂ radical anion), superoxide dismutases, and related matters. *Journal of Biological Chemistry* **272**, 18515-18517
119. Chen, S. X., and Schopfer, P. (1999) Hydroxyl-radical production in physiological reactions - A novel function of peroxidase. *European Journal of Biochemistry* **260**, 726-735
120. Pospisil, P., Arato, A., Krieger-Liszkay, A., and Rutherford, A. W. (2004) Hydroxyl radical generation by photosystem II. *Biochemistry* **43**, 6783-6792
121. Bowler, C., Slooten, L., Vandenbranden, S., Derycke, R., Botterman, J., Sybesma, C., Vanmontagu, M., and Inze, D. (1991) Manganese superoxide dismutase can reduce cellular damage mediated by oxygen radicals in transgenic plants. *Embo Journal* **10**, 1723-1732
122. Giulivi, C., Boveris, A., and Cadenas, E. (1995) Hydroxyl radical generation during mitochondrial electron-transfer and the formation of 8-hydroxydeoxyguanosine in mitochondrial DNA. *Archives of Biochemistry and Biophysics* **316**, 909-916
123. Fry, S. C. (1998) Oxidative scission of plant cell wall polysaccharides by ascorbate-induced hydroxyl radicals. *Biochemical Journal* **332**, 507-515
124. Dumville, J. C., and Fry, S. C. (2003) Solubilisation of tomato fruit pectins by ascorbate: a possible non-enzymic mechanism of fruit softening. *Planta* **217**, 951-961
125. Triantaphylides, C., Krischke, M., Hoeberichts, F. A., Ksas, B., Gresser, G., Havaux, M., Van Breusegem, F., and Mueller, M. J. (2008) Singlet oxygen is the major reactive oxygen species involved in photooxidative damage to plants. *Plant Physiology* **148**, 960-968
126. Krieger-Liszkay, A., Fufezan, C., and Trebst, A. (2008) Singlet oxygen production in photosystem II and related protection mechanism. *Photosynthesis Research* **98**, 551-564
127. DeRosa, M. C., and Crutchley, R. J. (2002) Photosensitized singlet oxygen and its applications. *Coordination Chemistry Reviews* **233**, 351-371
128. op den Camp, R. G. L., Przybyla, D., Ochsenbein, C., Laloi, C., Kim, C. H., Danon, A., Wagner, D., Hideg, E., Gobel, C., Feussner, I., Nater, M., and Apel, K. (2003) Rapid induction of distinct stress responses after the release of singlet oxygen in *Arabidopsis*. *Plant Cell* **15**, 2320-2332
129. Wagner, D., Przybyla, D., Camp, R. O. D., Kim, C., Landgraf, F., Lee, K. P., Wursch, M., Laloi, C., Nater, M., Hideg, E., and Apel, K. (2004) The genetic basis of singlet oxygen-induced stress responses of *Arabidopsis thaliana*. *Science* **306**, 1183-1185

130. Vellosillo, T., Vicente, J., Kulasekaran, S., Hamberg, M., and Castresana, C. (2010) Emerging complexity in reactive oxygen species production and signaling during the response of plants to pathogens. *Plant Physiology* **154**, 444-448
131. Flors, C., and Nonell, S. (2006) Light and singlet oxygen in plant defense against pathogens: Phototoxic phenalenone phytoalexins. *Accounts of Chemical Research* **39**, 293-300
132. Flors, C., Ogilby, P. R., Luis, J. G., Grillo, T. A., Izquierdo, L. R., Gentili, P. L., Bussotti, L., and Nonell, S. (2006) Phototoxic phytoalexins. Processes that compete with the photosensitized production of singlet oxygen by 9-phenylphenalenones. *Photochemistry and Photobiology* **82**, 95-103
133. Luis, J. G., Echeverri, F., Quinones, W., Brito, I., Lopez, M., Torres, F., Cardona, G., Aguiar, Z., Pelaez, C., and Rojas, M. (1993) Irenolone and emenolone - 2 new types of phytoalexin from *Musa paradisiaca*. *Journal of Organic Chemistry* **58**, 4306-4308
134. Berenbaum, M. R., and Larson, R. A. (1988) Flux of singlet oxygen from leaves of phototoxic plants. *Experientia* **44**, 1030-1032
135. Njus, D., and Kelley, P. M. (1991) Vitamin-C and vitamin-E donate single hydrogen-atoms in vivo. *Febs Letters* **284**, 147-151
136. Zechmann, B., Stumpe, M., and Mauch, F. (2011) Immunocytochemical determination of the subcellular distribution of ascorbate in plants. *Planta* **233**, 1-12
137. Vanacker, H., Carver, T. L. W., and Foyer, C. H. (1998) Pathogen-induced changes in the antioxidant status of the apoplast in barley leaves. *Plant Physiology* **117**, 1103-1114
138. Takahama, U., and Oniki, T. (1992) Regulation of peroxidase-dependent oxidation of phenolics in the apoplast of spinach leaves by ascorbate. *Plant and Cell Physiology* **33**, 379-387
139. Kollist, H., Moldau, H., Mortensen, L., Rasmussen, S. K., and Jorgensen, L. B. (2000) Ozone flux to plasmalemma in barley and wheat is controlled by stomata rather than by direct reaction of ozone with cell wall ascorbate. *Journal of Plant Physiology* **156**, 645-651
140. Takahama, U. (1993) Redox state of ascorbic-acid in the apoplast of stems of *Kalanchoe-daigremontiana*. *Physiologia Plantarum* **89**, 791-798
141. Burkey, K. O., Eason, G., and Fiscus, E. L. (2003) Factors that affect leaf extracellular ascorbic acid content and redox status. *Physiologia Plantarum* **117**, 51-57
142. Castillo, F. J., Miller, P. R., and Greppin, H. (1987) Extracellular biochemical markers of photochemical oxidant air-pollution damage to Norway spruce. *Experientia* **43**, 111-115
143. Castillo, F. J., and Greppin, H. (1988) Extracellular ascorbic acid and enzyme-activities related to ascorbic acid metabolism in *Sedum album* leaves after ozone exposure. *Environmental and Experimental Botany* **28**, 231-238
144. Pignocchi, C., and Foyer, C. H. (2003) Apoplastic ascorbate metabolism and its role in the regulation of cell signalling. *Current Opinion in Plant Biology* **6**, 379-389
145. Polle, A., Wieser, G., and Havranek, W. M. (1995) Quantification of ozone influx and apoplastic ascorbate content in needles of Norway spruce (*Picea abies* L.) at high-altitude. *Plant Cell and Environment* **18**, 681-688
146. Conklin, P. L., Williams, E. H., and Last, R. L. (1996) Environmental stress sensitivity of an ascorbic acid-deficient *Arabidopsis* mutant. *Proceedings of the National Academy of Sciences of the United States of America* **93**, 9970-9974
147. Zheng, Y. B., Lyons, T., Ollerenshaw, J. H., and Barnes, J. D. (2000) Ascorbate in the leaf apoplast is a factor mediating ozone resistance in *Plantago major*. *Plant Physiology and Biochemistry* **38**, 403-411

148. Gill, S. S., and Tuteja, N. (2010) Reactive oxygen species and antioxidant machinery in abiotic stress tolerance in crop plants. *Plant Physiology and Biochemistry* **48**, 909-930
149. Gullner, G., and Dodge, A. D. (2000) Effect of singlet oxygen generating substances on the ascorbic acid and glutathione content in pea leaves. *Plant Science* **154**, 127-133
150. May, M. J., Vernoux, T., Sanchez-Fernandez, R., Van Montagu, M., and Inze, D. (1998) Evidence for posttranscriptional activation of gamma-glutamylcysteine synthetase during plant stress responses. *Proceedings of the National Academy of Sciences of the United States of America* **95**, 12049-12054
151. May, M. J., and Leaver, C. J. (1993) Oxidative stimulation of glutathione synthesis in *Arabidopsis thaliana* suspension-cultures. *Plant Physiology* **103**, 621-627
152. Kanofsky, J. R., and Sima, P. (1991) Singlet oxygen production from the reactions of ozone with biological molecules. *Journal of Biological Chemistry* **266**, 9039-9042
153. Esaka, M., Fujisawa, K., Goto, M., and Kisu, Y. (1992) Regulation of ascorbate oxidase expression in pumpkin by auxin and copper. *Plant Physiology* **100**, 231-237
154. Lin, L. S., and Varner, J. E. (1991) Expression of ascorbic acid oxidase in zucchini squash (*Cucurbita-pepo* l). *Plant Physiology* **96**, 159-165
155. Pignocchi, C., Fletcher, J. M., Wilkinson, J. E., Barnes, J. D., and Foyer, C. H. (2003) The function of ascorbate oxidase in tobacco. *Plant Physiology* **132**
156. Kerk, N. M., Jiang, K. N., and Feldman, L. J. (2000) Auxin metabolism in the root apical meristem. *Plant Physiology* **122**, 925-932
157. Foyer, C. H., and Noctor, G. (2005) Redox homeostasis and antioxidant signaling: A metabolic interface between stress perception and physiological responses. *Plant Cell* **17**, 1866-1875
158. Pignocchi, C., Kiddle, G., Hernandez, I., Foster, S. J., Asensi, A., Taybi, T., Barnes, J., and Foyer, C. H. (2006) Ascorbate oxidase-dependent changes in the redox state of the apoplast modulate gene transcript accumulation leading to modified hormone signaling and orchestration of defense processes in tobacco. *Plant Physiology* **141**, 423-435
159. Fotopoulos, V., Sanmartin, M., and Kanellis, A. K. (2006) Effect of ascorbate oxidase over-expression on ascorbate recycling gene expression in response to agents imposing oxidative stress. *Journal of Experimental Botany* **57**, 3933-3943
160. Halliwell, B., and Foyer, C. H. (1976) Ascorbic-acid, metal ions and superoxide radical. *Biochemical Journal* **155**, 697-700
161. Jimenez, A., Hernandez, J. A., delRio, L. A., and Sevilla, F. (1997) Evidence for the presence of the ascorbate-glutathione cycle in mitochondria and peroxisomes of pea leaves. *Plant Physiology* **114**, 275-284
162. Meyer, A. J. (2008) The integration of glutathione homeostasis and redox signaling. *Journal of Plant Physiology* **165**, 1390-1403
163. Nakano, Y., and Asada, K. (1981) Hydrogen-peroxide is scavenged by ascorbate-specific peroxidase in spinach-chloroplasts. *Plant and Cell Physiology* **22**, 867-880
164. Foyer, C. H., and Halliwell, B. (1976) Presence of glutathione and glutathione reductase in chloroplasts - proposed role in ascorbic acid metabolism. *Planta* **133**, 21-25
165. Noctor, G., Mhamdi, A., Chaouch, S., Han, Y., Neukermans, J., Marquez-Garcia, B., Queval, G., and Foyer, C. H. (2012) Glutathione in plants: an integrated overview. *Plant Cell and Environment* **35**, 454-484
166. Noctor, G., Arisi, A. C. M., Jouanin, L., Kunert, K. J., Rennenberg, H., and Foyer, C. H. (1998) Glutathione: biosynthesis, metabolism and relationship to stress tolerance explored in transformed plants. *Journal of Experimental Botany* **49**, 623-647

167. Mehlhorn, H., Lelandais, M., Korth, H. G., and Foyer, C. H. (1996) Ascorbate is the natural substrate for plant peroxidases. *Febs Letters* **378**, 203-206
168. Shamsi, I. H., Jiang, S., Hussain, N., Lin, X., and Jiang, L. (2010) Coordinate role of ascorbate-glutathione in response to abiotic stresses. *Ascorbate-Glutathione Pathway and Stress Tolerance in Plants*, 323-336
169. Chen, Z., and Gallie, D. R. (2005) Increasing tolerance to ozone by elevating foliar ascorbic acid confers greater protection against ozone than increasing avoidance. *Plant Physiology* **138**, 1673-1689
170. Lee, S.-H., Ahsan, N., Lee, K.-W., Kim, D.-H., Lee, D.-G., Kwak, S.-S., Kwon, S.-Y., Kim, T.-H., and Lee, B.-H. (2007) Simultaneous overexpression of both CuZn superoxide dismutase and ascorbate peroxidase in transgenic tall fescue plants confers increased tolerance to a wide range of abiotic stresses. *Journal of Plant Physiology* **164**, 1626-1638
171. Kotchoni, S. O., Larrimore, K. E., Mukherjee, M., Kempinski, C. F., and Barth, C. (2009) Alterations in the endogenous ascorbic acid content affect flowering time in *Arabidopsis*. *Plant Physiology* **149**, 803-815
172. de Pinto, M. C., and De Gara, L. (2004) Changes in the ascorbate metabolism of apoplastic and symplastic spaces are associated with cell differentiation. *Journal of Experimental Botany* **55**, 2559-2569
173. Hidalgo, A., Gonzalezreyes, J. A., and Navas, P. (1989) Ascorbate free-radical enhances vacuolization in onion root-meristems. *Plant Cell and Environment* **12**, 455-460
174. Potters, G., Horemans, N., Caubergs, R. J., and Asard, H. (2000) Ascorbate and dehydroascorbate influence cell cycle progression in a tobacco cell suspension. *Plant Physiology* **124**, 17-20
175. Kato, N., and Esaka, M. (2000) Expansion of transgenic tobacco protoplasts expressing pumpkin ascorbate oxidase is more rapid than that of wild-type protoplasts. *Planta* **210**, 1018-1022
176. Yang, J. C., and Loewus, F. A. (1975) Metabolic conversion of L-ascorbic acid to oxalic-acid in oxalate-accumulating plants. *Plant Physiology* **56**, 283-285
177. Franceschi, V. R., and Nakata, P. A. (2005) Calcium oxalate in plants: Formation and function. *Annual Review of Plant Biology* **56**, 41-71
178. Keates, S. E., Tarlyn, N. M., Loewus, F. A., and Franceschi, V. R. (2000) L-ascorbic acid and L-galactose are sources for oxalic acid and calcium oxalate in *Pistia stratiotes*. *Phytochemistry* **53**, 433-440
179. Saito, K., and Kasai, Z. (1969) Tartaric acid synthesis from L-ascorbic acid-1-¹⁴C in grape berries. *Phytochemistry* **8**, 2177-2182
180. Bellincampi, D., Cervone, F., and Lionetti, V. (2014) Plant cell wall dynamics and wall-related susceptibility in plant-pathogen interactions. *Frontiers in plant science* **5**, 228-228
181. Bashline, L., Lei, L., Li, S., and Gu, Y. (2014) Cell wall, cytoskeleton, and cell expansion in higher plants. *Molecular Plant* **7**, 586-600
182. Scheller, H. V., and Ulvskov, P. (2010) Hemicelluloses. *Annual Review of Plant Biology*, Vol 61 **61**, 263-289
183. Cosgrove, D. J. (2005) Growth of the plant cell wall. *Nature Reviews Molecular Cell Biology* **6**, 850-861
184. Roberts, A. W., and Roberts, E. (2004) Cellulose synthase (CesA) genes in algae and seedless plants. *Cellulose* **11**, 419-435
185. Fry, S. C., Nesselrode, B. H. W. A., Miller, J. G., and Mewburn, B. R. (2008) Mixed-linkage (1 -> 3,1 -> 4)-beta-D-glucan is a major hemicellulose of *Equisetum* (horsetail) cell walls. *New Phytologist* **179**, 104-115
186. Hayashi, T., and Kaida, R. (2011) Functions of xyloglucan in plant cells. *Molecular Plant* **4**, 17-24

187. Zhou, Q., Rutland, M. W., Teeri, T. T., and Brumer, H. (2007) Xyloglucan in cellulose modification. *Cellulose* **14**, 625-641
188. Mohnen, D. (2008) Pectin structure and biosynthesis. *Current Opinion in Plant Biology* **11**, 266-277
189. Caffall, K. H., and Mohnen, D. (2009) The structure, function, and biosynthesis of plant cell wall pectic polysaccharides. *Carbohydrate Research* **344**, 1879-1900
190. Popper, Z. A., and Fry, S. C. (2008) Xyloglucan-pectin linkages are formed intraprotoplasmically, contribute to wall-assembly, and remain stable in the cell wall. *Planta* **227**, 781-794
191. Fry, S. C. (1986) Cross-linking of matrix polymers in the growing cell-walls of angiosperms. *Annual Review of Plant Physiology and Plant Molecular Biology* **37**, 165-186
192. Ishii, T. (1997) Structure and functions of feruloylated polysaccharides. *Plant Science* **127**, 111-127
193. Fujino, T., Sone, Y., Mitsuishi, Y., and Itoh, T. (2000) Characterization of cross-links between cellulose microfibrils, and their occurrence during elongation growth in pea epicotyl. *Plant and Cell Physiology* **41**, 486-494
194. Marry, M., Roberts, K., Jopson, S. J., Huxham, I. M., Jarvis, M. C., Corsar, J., Robertson, E., and McCann, M. C. (2006) Cell-cell adhesion in fresh sugar-beet root parenchyma requires both pectin esters and calcium cross-links. *Physiologia Plantarum* **126**, 243-256
195. O'Neill, M. A., Ishii, T., Albersheim, P., and Darvill, A. G. (2004) Rhamnogalacturonan II: Structure and function of a borate cross-linked cell wall pectic polysaccharide. *Annual Review of Plant Biology* **55**, 109-139
196. Perez, S., Rodriguez-Carvajal, M. A., and Doco, T. (2003) A complex plant cell wall polysaccharide: rhamnogalacturonan II. A structure in quest of a function. *Biochimie* **85**, 109-121
197. Fleischer, A., O'Neill, M. A., and Ehwald, R. (1999) The pore size of non-graminaceous plant cell walls is rapidly decreased by borate ester cross-linking of the pectic polysaccharide rhamnogalacturonan II. *Plant Physiology* **121**, 829-838
198. Chormova, D., Messenger, D. J., and Fry, S. C. (2014) Rhamnogalacturonan-II cross-linking of plant pectins via boron bridges occurs during polysaccharide synthesis and/or secretion. *Plant signaling & behavior* **9**, e28169-e28169
199. Chormova, D., Messenger, D. J., and Fry, S. C. (2014) Boron bridging of rhamnogalacturonan-II, monitored by gel electrophoresis, occurs during polysaccharide synthesis and secretion but not post-secretion. *Plant Journal* **77**, 534-546
200. Burr, S. J., and Fry, S. C. (2009) Feruloylated arabinoxylans are oxidatively cross-linked by extracellular maize peroxidase but not by horseradish peroxidase. *Molecular Plant* **2**, 883-892
201. Fry, S. C., Willis, S. C., and Paterson, A. E. J. (2000) Intraprotoplasmic and wall-localised formation of arabinoxylan-bound diferulates and larger ferulate coupling-products in maize cell-suspension cultures. *Planta* **211**, 679-692
202. Harris, P. J., and Trethewey, J. A. K. (2010) The distribution of ester-linked ferulic acid in the cell walls of angiosperms. *Phytochemistry Reviews* **9**, 19-33
203. Barros-Rios, J., Malvar, R. A., Jung, H.-J. G., Bunzel, M., and Santiago, R. (2012) Divergent selection for ester-linked diferulates in maize pith stalk tissues. Effects on cell wall composition and degradability. *Phytochemistry* **83**, 43-50
204. Buanafina, M. M. d. O., and Fescemyer, H. W. (2012) Modification of esterified cell wall phenolics increases vulnerability of tall fescue to herbivory by the fall armyworm. *Planta* **236**, 513-523
205. D'Auria, J. C. (2006) Acyltransferases in plants: a good time to be BAHD. *Current Opinion in Plant Biology* **9**, 331-340

206. St-Pierre, B., and De Luca, V. (2000) Evolution of acyltransferase genes: Origin and diversification of the BAHD superfamily of acyltransferases involved in secondary metabolism. *Evolution of Metabolic Pathways* **34**, 285-315
207. Dudareva, N., D'Auria, J. C., Nam, K. H., Raguso, R. A., and Pichersky, E. (1998) Acetyl-CoA : benzylalcohol acetyltransferase - an enzyme involved in floral scent production in *Clarkia breweri*. *Plant Journal* **14**, 297-304
208. Fujiwara, H., Tanaka, Y., Yonekura-Sakakibara, K., Fukuchi-Mizutani, M., Nakao, M., Fukui, Y., Yamaguchi, M., Ashikari, T., and Kusumi, T. (1998) cDNA cloning, gene expression and subcellular localization of anthocyanin 5-aromatic acyltransferase from *Gentiana triflora*. *Plant Journal* **16**, 421-431
209. Yang, Q., Reinhard, K., Schiltz, E., and Matern, U. (1997) Characterization and heterologous expression of hydroxycinnamoyl/benzoyl-CoA : anthranilate N-hydroxycinnamoyl/benzoyltransferase from elicited cell cultures of carnation, *Dianthus caryophyllus* L. *Plant Molecular Biology* **35**, 777-789
210. St-Pierre, B., Laflamme, P., Alarco, A. M., and De Luca, V. (1998) The terminal O-acetyltransferase involved in vindoline biosynthesis defines a new class of proteins responsible for coenzyme A-dependent acyl transfer. *Plant Journal* **14**, 703-713
211. Yeats, T. H., Martin, L. B. B., Viart, H. M. F., Isaacson, T., He, Y., Zhao, L., Matas, A. J., Buda, G. J., Domozych, D. S., Clausen, M. H., and Rose, J. K. C. (2012) The identification of cutin synthase: formation of the plant polyester cutin. *Nature Chemical Biology* **8**, 609-611
212. Cheynier, V., Comte, G., Davies, K. M., Lattanzio, V., and Martens, S. (2013) Plant phenolics: Recent advances on their biosynthesis, genetics, and ecophysiology. *Plant Physiology and Biochemistry* **72**, 1-20
213. Luo, J., Nishiyama, Y., Fuell, C., Taguchi, G., Elliott, K., Hill, L., Tanaka, Y., Kitayama, M., Yamazaki, M., Bailey, P., Parr, A., Michael, A. J., Saito, K., and Martin, C. (2007) Convergent evolution in the BAHD family of acyl transferases: identification and characterization of anthocyanin acyl transferases from *Arabidopsis thaliana*. *Plant Journal* **50**, 678-695
214. Zhou, L.-Z., Li, S., Feng, Q.-N., Zhang, Y.-L., Zhao, X., Zeng, Y.-l., Wang, H., Jiang, L., and Zhang, Y. (2013) PROTEIN S-ACYL TRANSFERASE10 is critical for development and salt tolerance in *Arabidopsis*. *Plant Cell* **25**, 1093-1107
215. Weinhold, A., and Baldwin, I. T. (2011) Trichome-derived O-acyl sugars are a first meal for caterpillars that tags them for predation. *Proceedings of the National Academy of Sciences of the United States of America* **108**, 7855-7859
216. Chortyk, O. T., Kays, S. J., and Teng, Q. (1997) Characterization of insecticidal sugar esters of Petunia. *Journal of Agricultural and Food Chemistry* **45**, 270-275
217. Schillmiller, A. L., Charbonneau, A. L., and Last, R. L. (2012) Identification of a BAHD acetyltransferase that produces protective acyl sugars in tomato trichomes. *Proceedings of the National Academy of Sciences of the United States of America* **109**, 16377-16382
218. Qi, B., Doughty, J., and Hooley, R. (2013) A Golgi and tonoplast localized S-acyl transferase is involved in cell expansion, cell division, vascular patterning and fertility in *Arabidopsis*. *New Phytologist* **200**, 443-454
219. Hemsley, P. A., Kemp, A. C., and Grierson, C. S. (2005) The TIP GROWTH DEFECTIVE1 S-acyl transferase regulates plant cell growth in *Arabidopsis*. *Plant Cell* **17**, 2554-2563
220. Bartley, L. E., Peck, M. L., Kim, S.-R., Ebert, B., Manisseri, C., Chiniquy, D. M., Sykes, R., Gao, L., Rautengarten, C., Vega-Sanchez, M. E., Benke, P. I., Canlas, P. E., Cao, P., Brewer, S., Lin, F., Smith, W. L., Zhang, X., Keasling, J. D., Jentoff, R. E., Foster, S. B., Zhou, J., Ziebell, A., An, G., Scheller, H. V., and Ronald, P. C. (2013) Overexpression of a BAHD acyltransferase, OsAt10, alters rice cell wall

- hydroxycinnamic acid content and saccharification. *Plant Physiology* **161**, 1615-1633
221. Mitchell, R. A. C., Dupree, P., and Shewry, P. R. (2007) A novel bioinformatics approach identifies candidate genes for the synthesis and feruloylation of arabinoxylan. *Plant Physiology* **144**, 43-53
 222. Beisson, F., Li, Y., Bonaventure, G., Pollard, M., and Ohlrogge, J. B. (2007) The acyltransferase GPAT5 is required for the synthesis of suberin in seed coat and root of *Arabidopsis*. *Plant Cell* **19**, 351-368
 223. Lee, S. K., and Kader, A. A. (2000) Preharvest and postharvest factors influencing vitamin C content of horticultural crops. *Postharvest Biology and Technology* **20**, 207-220
 224. Liu, R. H. (2013) Dietary bioactive compounds and their health implications. *Journal of Food Science* **78**, A18-A25
 225. Mackenzie, B., and Garrick, M. D. (2005) Iron imports. II. Iron uptake at the apical membrane in the intestine. *American Journal of Physiology-Gastrointestinal and Liver Physiology* **289**, G981-G986
 226. McCance, R. A., and Widdowson, E. M. (1991) McCance and Widdowson's the composition of food-5th Edition. (Agency, F. S. ed.), 5th revised and extended edition Ed., Royal Society of Chemistry (Great Britain) and Ministry of Agriculture, Fisheries and Food, London. pp
 227. Hodges, D. M., and Forney, C. F. (2003) Postharvest ascorbate metabolism in two cultivars of spinach differing in their senescence rates. *Journal of the American Society for Horticultural Science* **128**, 930-935
 228. Koh, E., Charoenprasert, S., and Mitchell, A. E. (2012) Effect of organic and conventional cropping systems on ascorbic acid, vitamin C, flavonoids, nitrate, and oxalate in 27 Varieties of spinach (*Spinacia oleracea* L.). *Journal of Agricultural and Food Chemistry* **60**, 3144-3150
 229. Bergquist, S. A. M., Gertsson, U. E., and Olsson, M. E. (2006) Influence of growth stage and postharvest storage on ascorbic acid and carotenoid content and visual quality of baby spinach (*Spinacia oleracea* L.). *Journal of the Science of Food and Agriculture* **86**, 346-355
 230. Bartoli, C. G., Yu, J. P., Gomez, F., Fernandez, L., McIntosh, L., and Foyer, C. H. (2006) Inter-relationships between light and respiration in the control of ascorbic acid synthesis and accumulation in *Arabidopsis thaliana* leaves. *Journal of Experimental Botany* **57**, 1621-1631
 231. Toledo, M. E. A., Ueda, Y., Imahori, Y., and Ayaki, M. (2003) L-ascorbic acid metabolism in spinach (*Spinacia oleracea* L.) during postharvest storage in light and dark. *Postharvest Biology and Technology* **28**, 47-57
 232. Liu, J. D., Goodspeed, D., Sheng, Z., Li, B., Yang, Y., Kliebenstein, D. J., and Braam, J. (2015) Keeping the rhythm: light/dark cycles during postharvest storage preserve the tissue integrity and nutritional content of leafy plants. *Bmc Plant Biology* **15**, 92
 233. Kiyota, M., Numayama, N., and Goto, K. (2006) Circadian rhythms of the L-ascorbic acid level in *Euglena* and spinach. *Journal of Photochemistry and Photobiology B-Biology* **84**, 197-203
 234. Seljasen, R., Kristensen, H. L., Lauridsen, C., Wyss, G. S., Kretzschmar, U., Birlouez-Aragone, I., and Kahl, J. (2013) Quality of carrots as affected by pre- and postharvest factors and processing. *Journal of the Science of Food and Agriculture* **93**, 2611-2626
 235. Ezell, B. D., and Wilcox, M. S. (1959) Vegetable vitamins - loss of vitamin-C in fresh vegetables as related to wilting and temperature. *Journal of Agricultural and Food Chemistry* **7**, 507-509

236. Barry-Ryan, C., and O'Beirne, D. (1999) Ascorbic acid retention in shredded iceberg lettuce as affected by minimal processing. *Journal of Food Science* **64**, 498-500
237. Sun, D. W., and Zheng, L. Y. (2006) Vacuum cooling technology for the agri-food industry: Past, present and future. *Journal of Food Engineering* **77**, 203-214
238. He, S. Y., Feng, G. P., Yang, H. S., Wu, Y., and Li, Y. F. (2004) Effects of pressure reduction rate on quality and ultrastructure of iceberg lettuce after vacuum cooling and storage. *Postharvest Biology and Technology* **33**, 263-273
239. Garrido, Y., Tudela, J. A., and Gil, M. I. (2015) Comparison of industrial precooling systems for minimally processed baby spinach. *Postharvest Biology and Technology* **102**, 1-8
240. Martinez-Sanchez, A., Allende, A., Bennett, R. N., Ferreres, F., and Gil, M. I. (2006) Microbial, nutritional and sensory quality of rocket leaves as affected by different sanitizers. *Postharvest Biology and Technology* **42**, 86-97
241. Kenny, O., and O'Beirne, D. (2009) The effects of washing treatment on antioxidant retention in ready-to-use iceberg lettuce. *International Journal of Food Science and Technology* **44**, 1146-1156
242. Karaca, H., and Velioglu, Y. S. (2014) Effects of ozone treatments on microbial quality and some chemical properties of lettuce, spinach, and parsley. *Postharvest Biology and Technology* **88**, 46-53
243. Gomez-Lopez, V. M., Marin, A., Medina-Martinez, M. S., Gil, M. I., and Allende, A. (2013) Generation of trihalomethanes with chlorine-based sanitizers and impact on microbial, nutritional and sensory quality of baby spinach. *Postharvest Biology and Technology* **85**, 210-217
244. Gil, M. I., Ferreres, F., and Tomas-Barberan, F. A. (1999) Effect of postharvest storage and processing on the antioxidant constituents (flavonoids and vitamin C) of fresh-cut spinach. *Journal of Agricultural and Food Chemistry* **47**, 2213-2217
245. Agar, I. T., Streif, J., and Bangerth, F. (1997) Effect of high CO₂ and controlled atmosphere (CA) on the ascorbic and dehydroascorbic acid content of some berry fruits. *Postharvest Biology and Technology* **11**, 47-55
246. Gil, M. I., Ferreres, F., and Tomas-Barberan, F. A. (1998) Effect of modified atmosphere packaging on the flavonoids and vitamin C content of minimally processed Swiss chard (*Beta vulgaris* subspecies *cycla*). *Journal of Agricultural and Food Chemistry* **46**, 2007-2012
247. Hancock, R. D., and Viola, R. (2005) Improving the nutritional value of crops through enhancement of L-ascorbic acid (vitamin C) content: Rationale and biotechnological opportunities. *Journal of Agricultural and Food Chemistry* **53**, 5248-5257
248. Chen, Z., Qin, C., Lin, L., Zeng, X., Zhao, Y., He, S., Lu, S., and Guo, Z. (2015) Overexpression of yeast arabinono-1,4-lactone oxidase gene (ALO) increases tolerance to oxidative stress and Al toxicity in transgenic tobacco plants. *Plant Molecular Biology Reporter* **33**, 806-818
249. Tokunaga, T., Miyahara, K., Tabata, K., and Esaka, M. (2005) Generation and properties of ascorbic acid-overproducing transgenic tobacco cells expressing sense RNA for L-galactono-1,4-lactone dehydrogenase. *Planta* **220**, 854-863
250. Murashige, T., and Skoog, F. (1962) A revised medium for rapid growth and bio assays with tobacco tissue cultures. *Physiologia Plantarum* **15**, 473-497
251. Eshdat, Y., and Mirelman, D. (1972) Improved method for recovery of compounds from paper chromatograms. *Journal of Chromatography* **65**, 458-459
252. Ponting, J. D. (1943) Extraction of ascorbic acid from plant materials - Relative suitability of various acids. *Industrial and Engineering Chemistry-Analytical Edition* **15**, 389-391
253. Kagawa, Y. (1962) Enzymatic studies on ascorbic acid catabolism in animals. 1. Catabolism of 2,3-diketo-L-gulonic acid. *Journal of Biochemistry* **51**

254. Otsuka, M., Kurata, T., and Arakawa, N. (1986) Isolation and characterization of an intermediate product in the degradation of 2,3-diketo-L-gulononic acid. *Agricultural and Biological Chemistry* **50**, 531-533
255. Slesak, I., Libik, M., Karpinska, B., Karpinski, S., and Miszalski, Z. (2007) The role of hydrogen peroxide in regulation of plant metabolism and cellular signalling in response to environmental stresses. *Acta Biochimica Polonica* **54**, 39-50
256. DeRosa, M. C., and Crutchley, R. J. (2002) Photosensitized singlet oxygen and its applications. *Coordination Chemistry Reviews* **233**
257. Huang, R., Choe, E., and Min, D. B. (2004) Kinetics for singlet oxygen formation by riboflavin photosensitization and the reaction between riboflavin and singlet oxygen. *Journal of Food Science* **69**, C726-C732
258. Horemans, N., Szarka, A., De Bock, M., Raeymaekers, T., Potters, G., Levine, M., Banhegyi, G., and Guisez, Y. (2008) Dehydroascorbate and glucose are taken up into *Arabidopsis thaliana* cell cultures by two distinct mechanisms. *Febs Letters* **582**, 2714-2718
259. Fry, S. C. (2011) High-voltage paper electrophoresis (HVPE) of cell-wall building blocks and their metabolic precursors. in *Plant Cell Wall: Methods and Protocols* (Popper, Z. A. ed.), Springer. pp
260. Otte, O., and Barz, W. (1996) The elicitor-induced oxidative burst in cultured chickpea cells drives the rapid insolubilization of two cell wall structural proteins. *Planta* **200**, 238-246
261. Kieliszewski, M. J., and Lamport, D. T. A. (1994) Extensin - repetitive motifs, functional sites, posttranslational coded, and phylogeny. *Plant Journal* **5**, 157-172
262. Bouchereau, A., Aziz, A., Larher, F., and Martin-Tanguy, J. (1999) Polyamines and environmental challenges: recent development. *Plant Science* **140**, 103-125
263. Chormova, D., and Fry, S. C. (2015) Boron bridging of rhamnogalacturonan-II is promoted by cationic chaperones, including polyhistidine and wall glycoproteins. *New Phytologist* [in press]
264. Cassab, G. I., and Varner, J. E. (1988) Cell-wall proteins. *Annual Review of Plant Physiology and Plant Molecular Biology* **39**, 321-353
265. Bolin, D. W., and Book, L. (1947) Oxidation of ascorbic acid to dehydroascorbic acid. *Science* **106**, 451-451
266. Ragaert, P., Verbeke, W., Devlieghere, F., and Debevere, J. (2004) Consumer perception and choice of minimally processed vegetables and packaged fruits. *Food Quality and Preference* **15**, 259-270
267. Vidal, L., Ares, G., and Gimenez, A. (2013) Projective techniques to uncover consumer perception: Application of three methodologies to ready-to-eat salads. *Food Quality and Preference* **28**, 1-7
268. Pagani, M., Vittuari, M., and Falasconi, L. (2015) Does packaging matter? Energy consumption of pre-packed salads. *British Food Journal* **117**, 1961-1980
269. Martinez-Sanchez, A., Gil-Izquierdo, A., Gil, M. I., and Ferreres, F. (2008) A comparative study of flavonoid compounds, vitamin C, and antioxidant properties of baby leaf Brassicaceae species. *Journal of Agricultural and Food Chemistry* **56**, 2330-2340
270. Degl'Innocenti, E., Pardossi, A., Tognoni, F., and Guidi, L. (2007) Physiological basis of sensitivity to enzymatic browning in lettuce, escarole and rocket salad when stored as fresh-cut products. *Food Chemistry* **104**, 209-215
271. Fry, S. C. (1988) Separation and identification of degradation products. in *The growing plant cell wall: chemical and metabolic analysis*, The Blackburn Press, New Jersey, U.S.A. pp 153-184
272. Zheng, Y., Yang, C., Pu, W., and Zhang, J. (2009) Determination of oxalic acid in spinach with carbon nanotubes-modified electrode. *Food Chemistry* **114**, 1523-1528

273. Aires, A., Carvalho, R., Rosa, E. A. S., and Saavedra, M. J. (2013) Phytochemical characterization and antioxidant properties of baby-leaf watercress produced under organic production system. *Cyta-Journal of Food* **11**, 343-351
274. Fahey, J. W., Zalcmann, A. T., and Talalay, P. (2001) The chemical diversity and distribution of glucosinolates and isothiocyanates among plants. *Phytochemistry* **56**, 5-51
275. Agerbirk, N., and Olsen, C. E. (2012) Glucosinolate structures in evolution. *Phytochemistry* **77**, 16-45
276. Williams, D. J., Critchley, C., Pun, S., Chaliha, M., and O'Hare, T. J. (2009) Differing mechanisms of simple nitrile formation on glucosinolate degradation in *Lepidium sativum* and *Nasturtium officinale* seeds. *Phytochemistry* **70**, 1401-1409
277. Ares, A. M., Nozal, M. J., Bernal, J. L., and Bernal, J. (2014) Optimized extraction, separation and quantification of twelve intact glucosinolates in broccoli leaves. *Food Chemistry* **152**, 66-74
278. Bianco, G., Agerbirk, N., Losito, I., and Cataldi, T. R. I. (2014) Acylated glucosinolates with diverse acyl groups investigated by high resolution mass spectrometry and infrared multiphoton dissociation. *Phytochemistry* **100**, 92-102
279. Agerbirk, N., Olsen, C. E., Cipollini, D., Orggaard, M., Linde-Laursen, I., and Chew, F. S. (2014) Specific glucosinolate analysis reveals variable levels of epimeric glucobarbarins, dietary precursors of 5-phenyloxazolidine-2-thiones, in watercress types with contrasting chromosome numbers. *Journal of Agricultural and Food Chemistry* **62**, 9586-9596
280. Kopsell, D. A., Barickman, T. C., Sams, C. E., and McElroy, J. S. (2007) Influence of nitrogen and sulfur on biomass production and carotenoid and glucosinolate concentrations in watercress (*Nasturtium officinale* R. Br.). *Journal of Agricultural and Food Chemistry* **55**, 10628-10634
281. Elliott, M. C., and Stowe, B. B. (1970) A novel sulphonated natural indole. *Phytochemistry* **9**, 1629-1632
282. Olsen, O., and Sorensen, H. (1980) Glucosinolates and amines in *Reseda-media*. *Phytochemistry* **19**, 1783-1787
283. Gallie, D. R. (2013) Increasing vitamin C content in plant foods to improve their nutritional value-successes and challenges. *Nutrients* **5**, 3424-3446
284. Chambial, S., Dwivedi, S., Shukla, K. K., John, P. J., and Sharma, P. (2013) Vitamin C in disease prevention and cure: an overview. *Indian journal of clinical biochemistry : IJCB* **28**, 314-328
285. Tewari, C. P., and Krishnan, P. S. (1960) Enzymatic transformation of dehydroascorbic acid to diketogulonic acid. *Nature* **188**, 144-144
286. Buchert, J., and Viikari, L. (1988) The role of xylonolactone in xylonic acid production by *Pseudomonas fragi*. *Applied Microbiology and Biotechnology* **27**, 333-336
287. Schmelter, T., Wientjes, R., Vreeker, R., and Klaffke, W. (2002) Enzymatic modifications of pectins and the impact on their rheological properties. *Carbohydrate Polymers* **47**, 99-108
288. Pettolino, F. A., Walsh, C., Fincher, G. B., and Bacic, A. (2012) Determining the polysaccharide composition of plant cell walls. *Nature Protocols* **7**, 1590-1607
289. Puterka, G. J., Farone, W., Palmer, T., and Barrington, A. (2003) Structure-function relationships affecting the insecticidal and miticidal activity of sugar esters. *Journal of Economic Entomology* **96**, 636-644
290. Cocetta, G., Baldassarre, V., Spinardi, A., and Ferrante, A. (2014) Effect of cutting on ascorbic acid oxidation and recycling in fresh-cut baby spinach (*Spinacia oleracea* L.) leaves. *Postharvest Biology and Technology* **88**, 8-16
291. Libert, B., and Franceschi, V. R. (1987) Oxalate in crop plants. *Journal of Agricultural and Food Chemistry* **35**, 926-938

292. Noonan, S. C., and Savage, G. P. (1999) Oxalate content of foods and its effect on humans. *Asia Pacific journal of clinical nutrition* **8**, 64-74
293. Lambrix, V., Reichelt, M., Mitchell-Olds, T., Kliebenstein, D. J., and Gershenzon, J. (2001) The *Arabidopsis* epithiospecifier protein promotes the hydrolysis of glucosinolates to nitriles and influences *Trichoplusia ni* herbivory. *Plant Cell* **13**, 2793-2807
294. Mithoefer, A., and Boland, W. (2012) Plant defense against herbivores: chemical aspects. *Annual Review of Plant Biology*, Vol 63 **63**, 431-450
295. Redovnikovic, I. R., Glivetic, T., Delonga, K., and Vorkapic-Furac, J. (2008) Glucosinolates and their potential role in plant. *Periodicum Biologorum* **110**, 297-309
296. Engelen-Eigles, G., Holden, G., Cohen, J. D., and Gardner, G. (2006) The effect of temperature, photoperiod, and light quality on gluconasturtiin concentration in watercress (*Nasturtium officinale* R. Br.). *Journal of Agricultural and Food Chemistry* **54**, 328-334
297. Halkier, B. A., and Gershenzon, J. (2006) Biology and biochemistry of glucosinolates. *Annual Review of Plant Biology* **57**, 303-333
298. Dinkova-Kostova, A. T., and Kostov, R. V. (2012) Glucosinolates and isothiocyanates in health and disease. *Trends in Molecular Medicine* **18**, 337-347
299. Traka, M., and Mithen, R. (2009) Glucosinolates, isothiocyanates and human health. *Phytochemistry Reviews* **8**, 269-282
300. Verkerk, R., Schreiner, M., Krumbein, A., Ciska, E., Holst, B., Rowland, I., De Schrijver, R., Hansen, M., Gerhaeuser, C., Mithen, R., and Dekker, M. (2009) Glucosinolates in Brassica vegetables: The influence of the food supply chain on intake, bioavailability and human health. *Molecular Nutrition & Food Research* **53**, S219-S265
301. Verhoeven, D. T. H., Verhagen, H., Goldbohm, R. A., vandenBrandt, P. A., and vanPoppel, G. (1997) A review of mechanisms underlying anticarcinogenicity by brassica vegetables. *Chemico-Biological Interactions* **103**, 79-129
302. Mithen, R., Bennett, R., and Marquez, J. (2010) Glucosinolate biochemical diversity and innovation in the Brassicales. *Phytochemistry* **71**, 2074-2086
303. Rask, L., Andreasson, E., Ekbom, B., Eriksson, S., Pontoppidan, B., and Meijer, J. (2000) Myrosinase: gene family evolution and herbivore defense in Brassicaceae. *Plant Molecular Biology* **42**, 93-113